

Purinergic Regulation of Acid/Base Transport in Human and Rat Biliary Epithelial Cell Lines

ÁKOS ZSEMBERY,¹ CARLO SPIRILI,^{1,3} ANNA GRANATO,¹ NICHOLAS F. LARUSSO,² LAJOS OKOLICSANYI,³ GAETANO CREPALDI,¹ AND MARIO STRAZZABOSCO¹

Biliary epithelial cells (cholangiocytes) are responsible for rapid regulation of bile volume and alkalinity. Secretin and other hormones raising intracellular cyclic adenosine monophosphate (cAMP) concentrations promote biliary HCO_3^- secretion by stimulating apical Cl^- channels and $\text{Cl}^-/\text{HCO}_3^-$ exchange (AE2). Cholangiocyte ion transport may also be stimulated by locally acting mediators; for example, adenosine 5'-triphosphate (ATP), a secretagogue that can be released into the bile by hepatocytes and cholangiocytes, activates Cl^- conductances and Na^+/H^+ exchange (NHE) in cholangiocyte cell lines. To further explore the role of extracellular ATP in the paracrine regulation of carrier mechanisms regulating cholangiocyte $\text{H}^+/\text{HCO}_3^-$ secretion, we investigated the effects of nucleotides on intracellular pH regulation (measured by microfluorimetry with 2',7'-bis(2-carboxyethyl)-5,6-carboxyfluorescein [BCECF]) in human (MZ-ChA-1) and rat (NRC-1) cholangiocyte cell lines. In MZ-ChA-1 cells, 10 mol/L ATP, uridine 5'-triphosphate (UTP), and ATPs significantly increased NHE activity. The pharmacological profile of agonists was consistent with that anticipated for receptors of the P2Y_2 class. ATP did not increase AE2 activity, but, when given to cells pretreated with agents raising intracellular cAMP, had a synergistic stimulatory effect that was

inhibited by amiloride. To assess the polarity of purinergic receptors, monolayers of NRC-1 cells were exposed to apical or basolateral nucleotides. Apical administration of purinergic agonists, but not adenosine, increased basolateral NHE activity ($\text{ATP}\gamma\text{S} > \text{UTP} > \text{ATP}$). Basolateral administration of purinergic agonists induced a weaker activation of NHE, which was instead strongly stimulated by adenosine and by adenosine receptor agonists ($\text{NECA} = \text{R-PIA} = \text{S-PIA}$). In conclusion, this study demonstrates that, consistent with the proposed role for biliary ATP in paracrine and autocrine control of cholangiocyte ion secretion, extracellular ATP stimulates cholangiocyte basolateral NHE activity through P2Y_2 receptors that are predominantly expressed at the apical cell membrane. (HEPATOLOGY 1998;28:914-920.)

Bile production requires the integrated function of hepatocytes and biliary epithelial cells (cholangiocytes). While hepatocytes secrete the major biliary constituents, such as bile acids, lipids and glutathione, the biliary epithelium represents the critical site for rapid regulation of bile volume and alkalinity.¹⁻³ Rates of ductular ion transport are regulated by gastrointestinal hormones able to modulate cyclic adenosine monophosphate (cAMP) concentrations: secretin⁴ and vasoactive intestinal peptide⁵ stimulate ductal choleresis, while somatostatin⁶ and gastrin⁷ inhibit ductal fluid secretion.

In intact organs, secretin induces the production of a HCO_3^- -enriched biliary fluid with a parallel decrease in biliary Cl^- concentration.⁸ At a cellular level, secretin stimulates two ion transporters located at the apical membrane of the biliary epithelial cell, the cystic fibrosis transmembrane conductance regulator (CFTR)^{9,10} and the AE2 isoform of $\text{Cl}^-/\text{HCO}_3^-$ exchanger¹¹⁻¹³ that mediate apical Cl^- and HCO_3^- excretion, respectively. Several lines of evidence suggest that secretin, via cAMP/protein kinase A (PKA), activates CFTR, resulting in Cl^- efflux from the cholangiocyte,¹⁴ and therefore increasing the gradient for HCO_3^- efflux via AE2. Bicarbonate efflux must be compensated by increased cellular HCO_3^- influx; basolateral Na^+/H^+ exchanger (NHE), acting in concert with carbonic anhydrase, accounts for electroneutral HCO_3^- uptake, as suggested by inhibition of secretin-stimulated choleresis by acetazolamide¹⁵ and by amiloride.¹⁶

Recent data indicate that cholangiocyte secretory function may also be controlled by local factors, such as acetylcholine that is released by intrahepatic parasympathetic terminations^{17,18} and by adenosine 5'-triphosphate (ATP), a potent autacoid substance able to stimulate secretory events in a number of epithelia.^{19,20} Extracellular ATP has been shown to

Abbreviations: cAMP, cyclic adenosine monophosphate; CFTR, cystic fibrosis transmembrane conductance regulator; AE2, $\text{Cl}^-/\text{HCO}_3^-$ exchanger isoform-2; NHE, Na^+/H^+ exchanger; ATP, adenosine 5'-triphosphate; DIDS, 4,4'-diisothiocyanatostilbene-2,2'-disulfonic acid; DBcAMP, $\text{N}^6,2'$ -O-dibutyryl-adenosine 3':5'-cyclic monophosphate; IBMX, 3-isobutyl-1-methyl-xanthine; ATP γS , adenosine 5'-O-(3-thiotriphosphate); UTP, uridine 5'-triphosphate; R-PIA, [R]- N^6 -[1-methyl-2-phenylethyl]adenosine; S-PIA, [S]- N^6 -[1-methyl-2-phenylethyl]adenosine; NECA, 5'-(N-ethylcarboxamido)-adenosine; XAC, xanthine amine congener; BCECF-AM, 2',7'-bis(2-carboxyethyl)-5,6-carboxyfluorescein-acetoxymethyl ester; pH_i, intracellular pH; β _i, cellular intrinsic buffering power; β _{tot}, total intracellular buffering power; JH⁺, transmembrane H⁺ flux.

From the ¹Institute of Internal Medicine and Azienda Ospedaliera di Padova, University of Padova, Padova, Italy; ²Mayo Clinic, Rochester, MN; and ³Chair of Gastroenterology, University of Parma, Parma, Italy.

Received December 23, 1997; accepted June 5, 1998.

Drs. Zsembery and Spirili contributed equally to different aspects of the work and should both be considered as first authors.

Presented in part at the 96th Annual Meeting of the American Association for the Study of Liver Diseases and published in abstract form in HEPATOLOGY 1996;24:225A.

Sponsored by grant 96.03440.04 from "Consiglio Nazionale delle Ricerche." The financial support of Telethon (grant E430) is gratefully acknowledged. Partially supported by a grant (DK 24031) from the National Institution of Health to Dr. LaRusso. Dr. Zsembery was the recipient of an International Fellowship from the University of Padova.

Address reprint requests to: Mario Strazzabosco, M.D., Ph.D., Institute of Internal Medicine, University of Padova, Via Giustiniani, 2, 35100 Padova, Italy. Fax: 39-49-8212151.

Copyright © 1998 by the American Association for the Study of Liver Diseases.

0270-9139/98/2804-0003\$3.00/0

stimulate Cl^- conductances²¹ and NHE^{22} in human cholangiocyte cell lines. ATP is present in micromolar concentrations into the bile,²³ where it can be released both by hepatocytes and cholangiocytes following anisotonic challenges²⁴ and mechanical stresses.²⁵ It has thus been suggested that ATP may be capable of paracrine/autocrine control of duct secretion.^{21,26,27} Through this local control, the liver may partly sustain bile flow,²⁶ even in conditions such as cystic fibrosis,^{28,29} in which mutated CFTR results in impaired electrolyte transport and chronic damage to a number of organs.^{30,31}

This study was designed to address the role of ATP in paracrine regulation of carriers mediating acid/base transport in the bile duct epithelium. Our results show that extracellular ATP, interacting with apical P2Y_2 purinergic receptors, stimulates basolateral Na^+/H^+ exchange and increases cellular HCO_3^- load, an effect that, in cells pretreated with cAMP, results in increased AE2 activity. These observations add strong evidence in favor of the proposed role for biliary ATP in paracrine stimulation of transepithelial $\text{H}^+/\text{HCO}_3^-$ transport in cholangiocytes.²⁷

MATERIALS AND METHODS

Materials. HEPES, amiloride, dimethylsulfoxide, nigericin, 4,4'-diisothiocyanatostilben-2,2'-disulfonic acid (DIDS), choline chloride, ammonium bicarbonate, epidermal growth factor, dexamethasone, triiodothyronine, high-activity collagenase, ethylenediaminetetraacetic acid, forskolin, $\text{N}^6,2'$ -O-dibutyryl-adenosine 3':5'-cyclic monophosphate (DBcAMP), 3-isobutyl-1-methyl-xanthine (IBMX), adenosine 5'-O-(3-thiotriphosphate) (ATP γ S), uridine 5'-triphosphate (UTP), [R]- N^6 -[1-methyl-2-phenylethyl]adenosine (R-PIA), [S]- N^6 -[1-methyl-2-phenylethyl]-adenosine (S-PIA), and 5'-(N-ethylcarboxamido)-adenosine (NECA) were purchased from Sigma Chemical Company (Milano, Italy). ATP was purchased from Boehringer Mannheim GmbH (Milano, Italy). Xanthine amine congener (XAC) was purchased from Amersham (Milano, Italy). 2',7'-bis(2-carboxyethyl)-5,6-carboxyfluorescein-acetoxymethyl ester (BCECF-AM) was purchased from Molecular Probes Inc. (Eugene, OR). Culture media (DMEM, HAM F12, MEM, fetal bovine serum, penicillin/streptomycin, MEM nonessential amino acids solution, GMS-S, chemically defined lipid concentrate, and MEM vitamin solutions) trypsin inhibitor soybean, gentamicin, trypsin/ethylenediaminetetraacetic acid, and glutamine were from GIBCO (Grand Island, NY). NuSerum and bovine pituitary extract were from Becton Dickinson S.p.A. (Milano, Italy). Membrane inserts were purchased from NUNC (Mascia Brunelli, Milano, Italy).

Cell Cultures. The human biliary cell line, MZ-ChA-1 (kindly provided by Dr. A. Knuth, Mainz University, Mainz, Germany), was cultured in MEM medium supplemented with 10% fetal calf serum and penicillin/streptomycin (100 U-0.1 mg/mL) in a humidified 95% air, 5% CO_2 atmosphere. Two to 3 days before the experiment, cells were suspended by washing with Ca^{2+} - Mg^{2+} -free phosphate-buffered saline containing 0.68 mmol/L ethylenediaminetetraacetic acid, plated over glass-coverslip fragments contained into tissue culture plastic wells (Falcon, Mascia Brunelli, Milano, Italy) and cultured with the same MEM medium, until subconfluent. The MZ-ChA-1 cell line³² was chosen because these cells have been extensively used as a model biliary cell line and are positive for the bile duct cell markers γ -glutamyl transpeptidase and cytokeratin 19³³; they have been shown to express CFTR¹⁰ and purinergic receptors,²² and to possess cAMP- and ATP-induced Cl^- efflux³³ and cholangiocyte-specific acid/base transporters, including NHE and AE2.¹²

The normal rat cholangiocyte cell line (NRC-1) was cultured on the top of rat tail collagen, as described.³⁴ Confluent monolayers of NRC-1 cells were resuspended and placed on the top of NUNC Anopore (0.2- μm pore) membrane inserts coated with a thin layer of collagen. When cultured in these conditions, NRC-1 cells develop

competent tight junctions, retain cholangiocyte phenotypic markers, such as apical γ -glutamyl transpeptidase, and cytoplasmic cytokeratin-7 and cytokeratin-19 expression and display morphological and functional polarity.³⁴ For example, the basolateral membrane expresses somatostatin receptors and NHE, while Cl^- conductances and $\text{Cl}^-/\text{HCO}_3^-$ exchange are present at the apical pole.^{27,34,35} Establishment of a confluent monolayer with competent tight junctions was routinely checked by measuring transepithelial resistance and membrane potential difference with a Millicell-ERS system (Millipore Co., Bedford, MA); only monolayers showing a transepithelial resistance above 800 Ωcm^2 were used for these experiments.

Intracellular pH Measurement. For intracellular pH (pHi) measurements, MZ-ChA-1 and NRC-1 cells were placed, respectively, on glass-coverslip fragments or on semipermeable membrane inserts. pHi was measured, essentially as previously described,^{4,11,12} using the fluorescent dye, BCECF, which was loaded into the cells by incubation for 10 to 20 minutes at 37°C (30 minutes in the case of NRC-1 cells) with its tetracetoxymethyl ester derivative (BCECF-AM) (12 $\mu\text{mol/L}$). At the end of the incubation period, to remove the extracellular dye, cells were washed for 10 minutes at 37°C in a BCECF-free medium. Cells easily took up the dye that showed an even distribution in the cytoplasm. At the end of the loading procedure, MZ-ChA-1 cells were transferred into a thermostated (37°C) perfusion chamber, placed on the stage of a NIKON TDM inverted microscope. In the case of NRC-1 cells, monolayers containing membrane inserts of proper resistance were transferred into thermostated (37°C) custom-made perfusion chambers allowing separate perfusion of the apical and basolateral aspects. All tubings were made by CO_2 -impermeant material; HEPES-buffered solutions were gassed with 100% O_2 , while a 95% $\text{O}_2/5\%$ CO_2 mixture was used for solutions containing 25 mmol/L HCO_3^- .

The microfluorimetric set-up has been previously described.¹² A NIKON 40 \times Fluor N.A. 1.3 objective was used for MZ-ChA-1 cells, while a NIKON 40 \times Achromat LWD was used in the case of NRC-1 cells. Experimental procedures were essentially as described.^{12,36} Signal-to-background ratio at 440 nm was approximately 110:1 in MZ-ChA-1 cells and 40:1 in NRC-1 cells. Fluorescence 495/440 ratio data were calibrated using the K^+/H^+ ionophore, nigericin (12 $\mu\text{mol/L}$),^{11,12} as described. Cellular intrinsic buffering power (β_i) was determined at different pHi, by exposing cells to stepwise-decreasing NH_4Cl concentrations, as described.^{11,12,36,37} The total intracellular buffering power (β_{tot}) in the presence of the open buffering system [$\text{H}_2\text{CO}_3/\text{CO}_2$] was then calculated from β_i as: $\beta_{\text{tot}} = \beta_i + 2.302 \times [\text{HCO}_3^-]_i$, where intracellular HCO_3^- concentration is derived from the measured pHi using the Henderson-Hasselbach equation. Rates of pHi changes in the alkaline or in the acid direction were measured as $\delta\text{pHi}/\delta t$ by hand-drawing a tangent from the experimental plot. Transmembrane H^+ fluxes (JH^+) were calculated from β_i and $\delta\text{pHi}/\delta t$ as $\text{JH}^+ = \beta_i \times \delta\text{pHi}/\delta t$.³⁸

Solutions. Buffers for pHi experiments were essentially as previously described.^{11,12} Briefly, bicarbonate-free ringers (HEPES) were buffered with HEPES at pH 7.4 and contained the following salts: 135 mmol/L NaCl, 4.7 mmol/L KCl, 1 mmol/L MgSO_4 , 1.2 mmol/L KH_2PO_4 , 1.5 mmol/L CaCl_2 , 10 mmol/L HEPES, 5 mmol/L glucose, and 1 mmol/L pyruvate, titrated to pH 7.4 with NaOH. Bicarbonate-buffered ringer (KRB) contained: 115 mmol/L NaCl, 4.7 mmol/L KCl, 1.2 mmol/L KH_2PO_4 , 1 mmol/L MgSO_4 , 1.5 mmol/L CaCl_2 , 25 mmol/L NaHCO_3 , 5 mmol/L glucose, and 1 mmol/L pyruvate, and was equilibrated with 5% CO_2 . In KRB and HEPES used to acid-load cells, 30 mmol/L NH_4Cl substituted equal amounts of NaCl. BCECF-AM was dissolved in dimethylsulfoxide as a 1-mmol/L stock solution. Amiloride was dissolved in dimethylsulfoxide as a 1-mmol/L stock solution, while nigericin was solubilized in ethanol.

Statistical Analysis. Results are shown as means \pm SD. Paired and unpaired *t* test analyses were performed using STATGRAPH software (STSC, Inc., Rockville, Maryland).

TABLE 1. Effects of Purinergic Nucleotides on NHE Activity in MZ-ChA-1 Cells

	JH ⁺ (mmol/L/min)	ΔpH/min	pHi nadir	n
Controls	5.25 ± 2.34	0.146 ± 0.065	6.5 ± 0.13	26
ATP (10 μmol/L)	20.04 ± 6.61†	0.557 ± 0.184	6.61 ± 0.11	5
ATP + amiloride	2.85 ± 0.67*	0.051 ± 0.01	6.32 ± 0.12	6
UTP (10 μmol/L)	30.41 ± 2.08†	0.845 ± 0.058	6.62 ± 0.15	4
ATPγS	26.71 ± 4.42†	0.742 ± 0.123	6.6 ± 0.13	4
ATP (10 μmol/L + XAC)	21.09 ± 1.04†	0.586 ± 0.029	6.67 ± 0.07	4

*P < .0001 vs. controls.

†P < .0005 vs. controls.

RESULTS

Effects of Extracellular ATP on H⁺/HCO₃⁻ Transport

Effects on NHE Activity. The effects of extracellular ATP on NHE were examined in MZ-ChA-1 cholangiocytes. Here, NHE activity was defined as the rate of pHi recovery from an acid-load in the nominal absence of HCO₃⁻, and acid-loading was achieved by transient exposure to 30 mmol/L NH₄Cl³⁸ (Table 1, Fig. 1A). In control conditions (n = 26), cells recovered from this acid-load by extruding protons at a rate (JH⁺) of 5.25 ± 2.34 mmol/L/min (ΔpHi/Δt: 0.146 ± 0.065/min, measured at pHi 6.6). Administration of 10 μmol/L ATP caused a striking increase in NHE activity (JH⁺: 20.04 ± 6.61 mmol/L/min; ΔpHi/Δt: 0.557 ± 0.184/min; n = 5, measured at pHi = 6.6; P < .001). These changes were inhibited by 1 mmol/L amiloride (JH⁺: 2.85 ± 0.67 mmol/L/min; ΔpHi/Δt: 0.051 ± 0.01; n = 6; P < .0001, at pHi 6.4). If H⁺ fluxes are plotted versus the corresponding pHi values (Fig. 2), a significant inverse linear correlation between acid fluxes and pHi (r² = .9443) is evident. As described for many agents activating NHE1,³⁹ ATP appears to shift to the right its activity versus the pHi curve, increasing the affinity of the regulatory site of NHE to protons.

In addition, UTP (10 μmol/L) and ATPγS (10 μmol/L), a nonhydrolyzable ATP derivative, increased NHE activity (JH⁺: 30.41 ± 2.08 mmol/L/min; ΔpHi/Δt: 0.845 ± 0.058/min; n = 4; and 26.71 ± 4.42 mmol/L/min; ΔpHi/Δt: 0.742 ± 0.123/min; n = 4, at pHi 6.6, respectively) (P < .005 with respect to controls). Pretreatment with the adenosine receptor blocker xanthine amine congener (XAC) (100 μmol/L), did not inhibit the effects of ATP on NHE (JH⁺: 21.09 ± 1.04 mmol/L/min; ΔpHi/Δt: 0.586 ± 0.029/min; n = 4; P = not significant, with respect to ATP alone), indicating that NHE activation was not mediated by ATP degradation products. These results are consistent with a previous report from Elsing et al.,²² and the pharmacological profile of nucleotide efficacy indicates that extracellular ATP activates NHE interacting with P2Y₂ purinergic receptors.

ATP administration resulted in higher baseline pHi both in the presence and in the absence of HCO₃⁻/CO₂ in the perfusion medium. In HEPES-buffered media, 10 μmol/L ATP increased baseline pHi from 6.96 ± 0.09 (n = 7) to 7.21 ± 0.11 (n = 7) (P < .001). When HCO₃⁻/CO₂ was present in the perfusion medium (KRB), ATP increased baseline pHi from 7.1 ± 0.1 (n = 9) to 7.24 ± 0.05 (n = 9) (P < .005). Changes induced by ATP were fully inhibited by pretreatment with amiloride (1 mmol/L), suggesting that ATP regulates resting pHi at a more alkaline level through activation of NHE.

Effects of ATP on Cl⁻/HCO₃⁻ Exchanger (AE2) Activity. Having shown that extracellular ATP promotes cellular HCO₃⁻ uptake via NHE, we then evaluated the effects of extracellular ATP on AE2 activity in MZ-ChA-1 cholangiocytes, following the protocol shown in Fig. 1B. Here, AE2 activity was defined as the rate of pHi recovery from an intracellular alkaline load. The alkaline load was induced by acute removal of HCO₃⁻/CO₂⁻ from the perfusion medium.⁴⁰⁻⁴² Because of the strict pHi dependence of Cl⁻/HCO₃⁻ exchange (Fig. 2), HCO₃⁻ efflux was measured in all groups at a common pHi (7.3). To evaluate the effects of ATP, cells were superfused with 10 μmol/L ATP for 3 minutes; after a new steady-state pHi was obtained, the alkaline load was induced. In these conditions (see Table 2), JH⁺ at 7.3 was not significantly different from controls (JH⁺: 7.12 ± 1.74 mmol/L/min; ΔpHi/Δt: 0.139 ± 0.034/min [n = 5] vs. JH⁺: 7.85 ± 2.29 mmol/L/min; ΔpHi/Δt: 0.157 ± 0.041/min [n = 47] in controls) (P = not significant). On the contrary to NHE, ATP did not change the activity versus pHi relationship of AE2 (Fig. 2).

On the contrary, administration of ATP to cells pretreated with agents raising intracellular cAMP levels (100 μmol/L DbcAMP + 100 μmol/L IBMX + 3 μmol/L forskolin) (cAMPmix)^{10,33,43,44} further increased AE2 activity (Table 2)

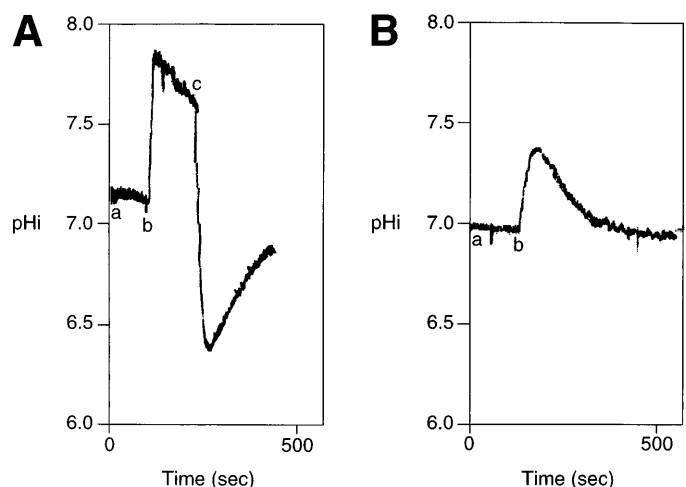


FIG. 1. Representative examples of pHi tracings illustrating the experimental protocols followed to assess the activity of Na⁺/H⁺ exchanger (A) and Cl⁻/HCO₃⁻ exchanger (B) in MZ-ChA-1 cells. (A) NHE activity was measured from the pHi recovery rates after intracellular acidification induced by administration (b) and withdrawal (c) of the permeant weak base, NH₄Cl, as described.^{11,12,35} pHi rises upon exposure to NH₄Cl as a result of the entry of the permeant NH₃ and its protonation to the impermeant NH₄⁺. After withdrawal of external NH₄Cl, NH₄⁺ releases the proton, thereby acidifying the cytoplasm and leaves the cell as NH₃. Cells rapidly recover to baseline by extruding protons. In nominally HCO₃⁻/CO₂-free HEPES-buffered media, this process is inhibited by amiloride and by extracellular Na⁺ removal, indicating that it is mediated by NHE. The rate at which this electroneutral exchange extrudes protons during the recovery phase is a measure of its activity; because this is characteristically inversely related to pHi, Na⁺/H⁺ activity in the different experimental groups was measured at a common pHi (see text and Tables). (B) Cl⁻/HCO₃⁻ exchange is the main alkali extruder in cholangiocytes; its activity was thus measured from the pHi recovery rates after intracellular alkalization induced by withdrawal (b) of extracellular HCO₃⁻/CO₂ at constant external pH.^{41,42} Exit of CO₂ from the cell creates an intracellular alkaline load from which MZ-ChA-1 cells recover by extruding HCO₃⁻ via a Cl⁻-dependent and DIDS-inhibitable mechanism. The rate at which this electroneutral exchange extrudes base equivalents during the recovery phase is a measure of its activity; because its activity is characteristically directly related to pHi, Cl⁻/HCO₃⁻ activity in the different experimental groups was measured at a common pHi (see text and Tables).

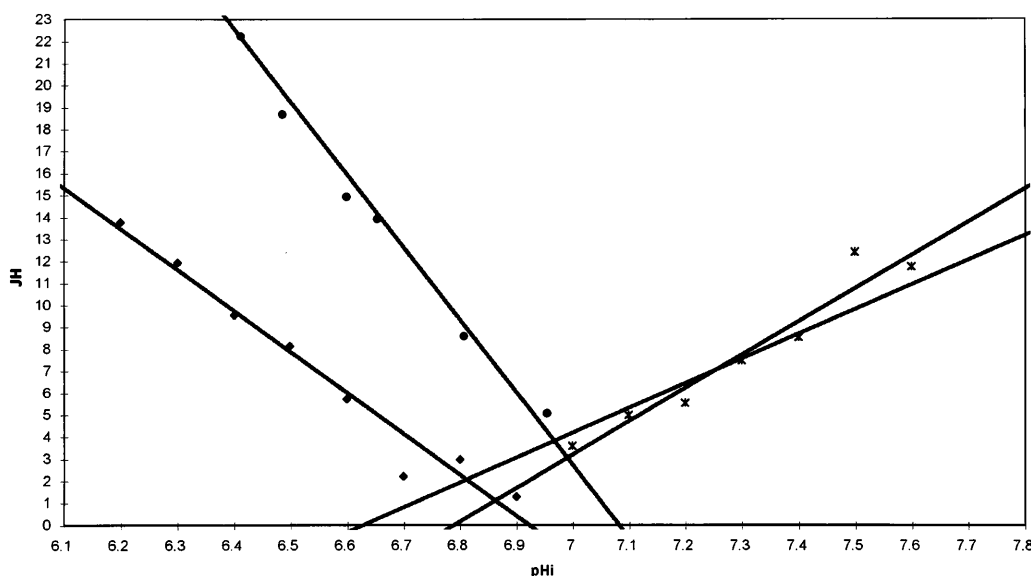


FIG. 2. Effects of ATP on activity versus pHi relationship of NHE (left tracings) and AE2 (right tracings). The graph shows plots of H^+ (left) or OH^- fluxes (right) measured during pHi recovery from an acid-load (left) or alkali-load (right) and their corresponding pHi values. All plots show significant correlation between acid base fluxes and pHi: (◆), NHE controls ($r^2 = .9646$); (●), NHE ATP 10 $\mu\text{mol/L}$ ($r^2 = .9443$); (*), AE2 controls ($r^2 = .9369$); (X), AE2 ATP 10 $\mu\text{mol/L}$ ($r^2 = .9641$). This figure demonstrates the following points: 1) indirect and direct relationships of acid and base fluxes mediated by NHE and Cl^-/HCO_3^- exchangers; 2) as described for many agents activating NHE1, the main effect of ATP on NHE1 is to increase the activity of the regulatory site to H^+ , thus changing its apparent "set point"; 3) ATP, when given alone, does not change AE2 kinetic parameters; however, 4) at the new steady state, i.e., the point at which acid-extrusion matches acid-loading (see the points at which the two linear regressions, with and without ATP, cross AE2 regression), AE2 base-extruding activity will be higher.

compared with cells treated with cAMPmix alone (JH^+ : 13.13 ± 2.5 mmol/L/min; $\delta pHi/\delta t$: 0.260 ± 0.05 [$n = 7$] vs. JH^+ : 10.16 ± 2.6 mmol/L/min; $\delta pHi/\delta t$: 0.198 ± 0.05 ; $n = 9$; $P < .01$). Interestingly, as also shown in Table 2, these effects, including those of cAMPmix alone, were inhibited by the NHE inhibitor, amiloride (1 mmol/L) (JH^+ in the presence of cAMPmix + ATP + amiloride was 7.72 ± 1.8 mmol/L/min; $\delta pHi/\delta t$: 0.160 ± 0.032 ; $n = 10$; $P =$ not significant with respect to controls; JH^+ in the presence of cAMPmix + amiloride was 7.30 ± 2.3 mmol/L/min; $\delta pHi/\delta t$: 0.143 ± 0.05 ; $n = 6$; $P =$ not significant with respect to controls), demonstrating that HCO_3^- uptake via functional NHE is also required for cAMP-mediated stimulation of HCO_3^- efflux.

Polarity of Purinergic Receptors

To investigate the membrane polarity of purinergic receptors involved in the stimulation of NHE by ATP, we studied the effects of apical and basolateral administration of nucleotides on NHE activity using a polarized rat cholangiocyte (NRC-1)³⁴ cell line that expresses basolateral NHE.³⁵ NRC-1 cells were cultured on collagen-coated tissue-culture inserts

until confluence, and then placed into a custom-made thermostated chamber allowing separate perfusion of the apical and basolateral aspects of the monolayer. Cells were acidified by perfusing the basolateral side with a Na^+ -free HEPES medium (substitution with choline), while the apical side was exposed to 1 mmol/L amiloride (Fig. 3). After Na^+ readmission, NRC-1 cells recovered to baseline pHi by way of an amiloride-inhibitable mechanism at a rate of JH^+ : 8.22 ± 2.96 mmol/L/min ($\delta pHi/\delta t$: 0.175 ± 0.074 /min at pHi 7.0; $n = 24$). Administration of 10 $\mu\text{mol/L}$ ATP on the apical surface of the cells caused a significant increase in NHE activity: JH^+ : 14.51 ± 6.6 mmol/L/min ($\delta pHi/\delta t$: 0.342 ± 0.150 /min at pHi = 7.0; $n = 6$; $P < .01$). The pharmacological profile of purinergic agonists (UTP 10 $\mu\text{mol/L}$ or ATP γ S 10 $\mu\text{mol/L}$) (Table 3) suggests that the effects of ATP are mediated via activation of $P2Y_2$ receptors, and are not caused by breakdown of ATP to adenosine, because preincubation with XAC (100 $\mu\text{mol/L}$) did not inhibit ATP effects (JH^+ : 16.7 ± 11.09 mmol/L/min; $\delta pHi/\delta t$: 0.46 ± 0.32 /min; $n = 5$; pHi = 7.0), and apical administration of adenosine (10 $\mu\text{mol/L}$) did not significantly increase NHE activity (JH^+ : 8.57 ± 2.31 mmol/L/min; $\delta pHi/\delta t$: 0.23 ± 0.08 /min at pHi 7.0; $n = 6$).

When administered from the basolateral aspect (Table 3), ATP and UTP induced a smaller increase in NHE activity (42% and 58% increase, respectively, vs. 76% and 100% after apical administration), suggesting that, although less represented, $P2Y_2$ receptors could also reside at the basolateral membrane.^{27,45} On the contrary to apical administration, basolateral adenosine (10 $\mu\text{mol/L}$) induced a potent stimulation of NHE activity (JH^+ : 19.72 ± 5.6 mmol/L/min; $\delta pHi/\delta t$: 0.402 ± 0.18 /min; $n = 8$; $P < .001$). XAC inhibited adenosine effects, while adenosine receptor agonists (NECA, R-PIA, S-PIA [10 $\mu\text{mol/L}$]) significantly stimulated NHE activity with similar rank order potency (Table 3), indicating

TABLE 2. Effect of ATP and cAMP on Cl^-/HCO_3^- Exchanger Activity

	JH^+ (mmol/L/min)	$\delta pHi/\delta t$ (min)	n
Controls	7.85 ± 2.29	0.157 ± 0.041	47
ATP (10 μmol)	7.12 ± 1.74	0.139 ± 0.034	5
cAMP	10.16 ± 2.6	0.198 ± 0.05	9
cAMP + ATP	13.13 ± 2.5	0.260 ± 0.05	7
cAMP + ATP + Amiloride	7.72 ± 1.8	0.160 ± 0.032	10
cAMP + Amiloride	7.30 ± 2.3	0.143 ± 0.05	6

NOTE. Controls vs. ATP: $P =$ not significant; controls vs. cAMP: $P < .002$; controls vs. cAMP + ATP: $P < .0005$; cAMP vs. cAMP + ATP: $P < .01$.

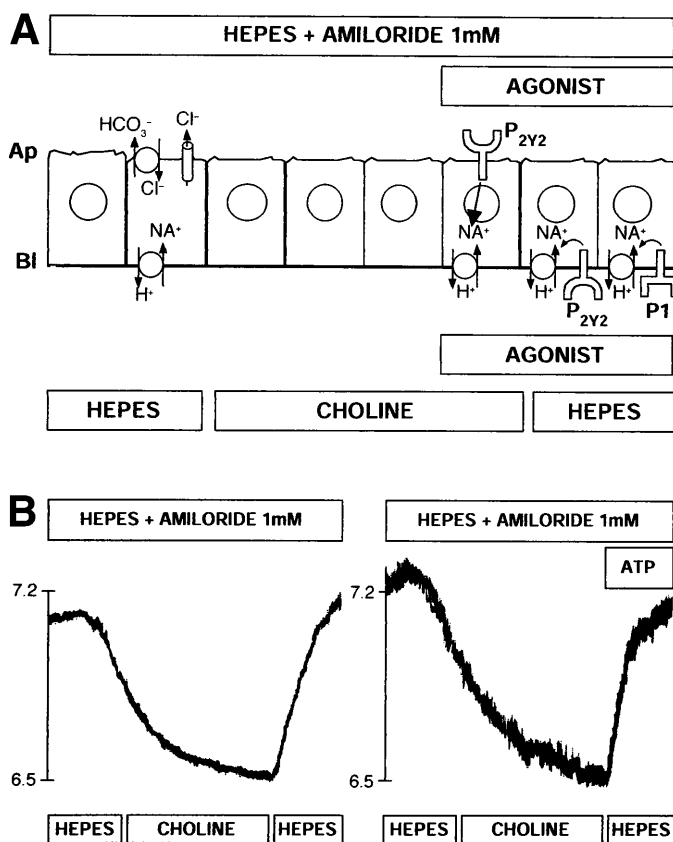


FIG. 3. To investigate the membrane polarity of purinergic receptors involved in the stimulation of NHE by ATP, the effects of apical and basolateral administration of nucleotides on NHE activity were assessed using a polarized rat cholangiocyte (NRC-1)³⁴ cell line that expressed basolateral NHE³⁵ (upper panel). NRC-1 cells were cultured on collagen-coated tissue-culture inserts until confluence, and then placed into a custom-made thermostated chamber allowing separate perfusion of the apical and basolateral aspects of the monolayer. Apical and basolateral solution changes during the representative experiment shown in the upper panel are illustrated in boxes above (apical) and below (basolateral) the cartoon of the monolayer. Cells were acidified by perfusing the basolateral side with a Na⁺-free HEPES medium (substitution with choline), while the apical side was exposed to 1 mmol/L amiloride (to inhibit the contribution of putative apical Na⁺ channels) (lower left panel). After Na⁺ readmission, NRC-1 cells recover to baseline pH_i by way of an amiloride-inhibitable basolateral NHE. Administration of 10 μmol/L ATP on the apical surface of the cells, before Na⁺ readmission, caused a significant increase in NHE activity (see lower right panel). A control experiment is shown in the lower left panel. Results of these experiments are shown in Table 3.

that P1 receptors are restricted at the basolateral membrane of NRC-1 cells.

DISCUSSION

The main findings of this study investigating the role of extracellular ATP on cholangiocyte acid/base transport are: 1) extracellular ATP stimulates NHE interacting with P2Y₂ receptors; 2) purinergic receptors able to stimulate basolateral NHE are polarized with P2Y₂ receptors mainly on the apical side and P1 receptors strictly restricted to the basolateral aspect of the epithelium; and 3) in the presence of cAMP, ATP administration results in increased activity of AE2, the carrier responsible for apical HCO₃⁻ efflux, indicating that local control via ATP may be relevant for cholangiocyte secretory function.

Consistent with a recent report,²² 10 μmol/L ATP induced a

dramatic increase in NHE activity, which resulted in a shift to the right of its activity versus pH_i relationship and in a higher baseline pH_i, even in the presence of HCO₃⁻/CO₂. Simultaneous administration of an adenosine receptor inhibitor (XAC) did not prevent activation of NHE by ATP, suggesting that this effect was not mediated by the ATP breakdown product, adenosine; the rank order of potency of ATP analogues (UTP > ATPγS > ATP) indicates that ATP-induced activation of NHE is mediated through P2Y₂ purinergic receptors. Several NHE isoforms have been described; in addition to the amiloride-sensitive, mitogen-activated isoform 1 (NHE1), mRNA for the amiloride-insensitive apical NHE2 isoforms has recently been detected in isolated rat cholangiocytes.⁴⁶ Our data showing that ATP activates basolateral NHE in NRC-1 cells, that its effects are inhibited by amiloride, and that ATP changes NHE set point, together with the reported sensitivity to cimetidine,²² strongly suggest that NHE1 is the isoform stimulated by purinergic nucleotides.

Given the basolateral location of NHE1, the question arises as to the side of action of extracellular ATP. Because MZ-ChA-1 cells are not polarized, to ascertain the localization of purinergic receptors, we have used a polarized cell line established from normal rat cholangiocytes (NRC-1). When grown over collagen-coated tissue-culture inserts, NRC-1 cells form a confluent polarized monolayer that allows the separate study of events taking place at the apical and basolateral aspect of the cell.³⁴ In this cell system, administration of 10 μmol/L ATP on the apical side of cholangiocytes significantly increased the basolateral NHE activity, with a pharmacological profile consistent with that anticipated for receptors of the P2Y₂ class. In line with the recently reported stimulation of Cl⁻-dependent currents in NRC-1 cells,²⁷ our findings demonstrate, in a polarized preparation of cholangiocytes, that biliary ATP, interacting with purinergic receptors localized at the apical membrane of the cholangiocyte, is able to increase cellular HCO₃⁻ load. Consistent with a report in isolated bile duct units,⁴⁵ we observed that P2Y₂ receptors are also expressed at the basolateral pole of the cell; however, response to basolateral ATP and UTP is smaller, suggesting that apical receptors contribute more importantly to local regulation of secretion. On the contrary to ATP, adenosine had no effect when administered apically, but it did increase NHE activity, when given from the basolateral side. Although the profile of adenosine receptor agonists (NECA = R-PIA = S-PIA) did not allow a pharmacological distinction between the different receptor subtypes, our findings clearly indicate that P1 receptors are restricted to the basolateral aspect of the epithelium. Given the rapid degradation of ATP to adenosine, absence of P1 receptors from the apical side further indicates an important regulatory role of ATP on the apical membrane; on the other hand, it is tempting to speculate that activation of NHE by basolateral adenosine may play a role in cellular response to ischemia, a condition in which adenosine is released in large quantities.

NHE1 fulfils several distinct physiological functions, which include control of intracellular pH_i, regulation of cell volume, facilitation of cell proliferation in response to growth factors, and transepithelial HCO₃⁻ transport.^{2,38,46} In fact, this basolateral acid extruder, in concert with carbonic anhydrase, provides intracellular HCO₃⁻ that is then excreted by Cl⁻/HCO₃⁻ exchange. Luminal HCO₃⁻ excretion in gastrointestinal epithelia is in fact mediated by the AE2 isoform of the Cl⁻/HCO₃⁻ exchanger. By increasing NHE activity, activating

TABLE 3. Effect of Apical or Basolateral Administration of Nucleotides on NHE Activity in NRC-1 Cells*

	Apical					Basolateral				
	JH ⁺ (mmol/L/min)	ΔpH/min	%	n	P	JH ⁺ (mmol/L/min)	ΔpH/min	%	n	P
Controls	8.22 ± 2.96	0.175 ± 0.074		24		8.22 ± 2.96	0.175 ± 0.074		24	
ATP	14.51 ± 6.6	0.342 ± 0.15	76	6	<.01	11.69 ± 6.3	0.275 ± 0.149	42	7	<.05
ATPγS	27.97 ± 7.15	0.662 ± 0.17	240	5	<.001	9.7 ± 3.7	0.228 ± 0.087	18	8	ns
UTP	16.51 ± 7.1	0.392 ± 0.164	100	8	<.01	13.00 ± 2.75	0.307 ± 0.065	58	7	<.01
ATP + XAC	16.7 ± 11.09	0.46 ± 0.32	103	5	<.01	10.02 ± 3.1	0.269 ± 0.08	22	5	ns
Adenosine	8.57 ± 2.31	0.23 ± 0.08	4	6	ns	19.72 ± 5.6	0.402 ± 0.18	140	8	<.001
Adenosine + XAC	—	—	—	—	—	12.85 ± 6.75	0.249 ± 0.009	40	7	<.05†
NECA	—	—	—	—	—	14.6 ± 4.43	0.341 ± 0.1	77	7	<.001
R-PIA	—	—	—	—	—	13.58 ± 6.75	0.320 ± 0.06	65	7	<.001
S-PIA	—	—	—	—	—	12.38 ± 5.28	0.292 ± 0.12	50	8	<.01

NOTE. Effect of apical and basolateral administration of nucleotides on NHE exchangers in NRC-1 cells. ATPγS, (adenosine 5'-O-(thiotriphosphate) is a nonhydrolyzable ATP analog. UTP interacts specifically with P2Y₂ receptors. XAC is an inhibitor of adenosine receptor that was administered together with ATP to rule out adenosine receptor activation caused by breakdown of ATP to adenosine by ectoATPase. R-PIA, S-PIA, and NECA are adenosine receptor agonists.

*See text for concentrations of different purinergic agonists and experimental details.

†P < .05 with respect to basolateral adenosine alone.

K⁺ channels,³³ and increasing Cl⁻ exit through Ca²⁺-dependent Cl⁻ channels,²¹ ATP would theoretically impose a combination of ionic gradients favoring AE2 operation. However, after administration of 10 μmol/L ATP, neither the rate of Cl⁻/HCO₃⁻ exchange at pHi 7.3, nor its pHi versus activity relationship were significantly changed (Fig. 2). Given the direct relationship between pHi and AE2 activity, at the new steady state (i.e., the pHi at which acid-loading matches acid-extrusion), AE2 activity is higher, but the ATP-dependent increase in baseline pHi clearly indicates the lack of a direct effect of ATP on AE2 activity.

On the other hand, our data clearly show that ATP further increases AE2 activity in cells pretreated with cAMP. In a number of epithelia, including hepatocytes, it is well established that the cAMP/protein kinase A system increases AE2 activity by activating Cl⁻ efflux and by cytoskeleton-mediated targeting of new transporter units to the plasma membrane.^{48,49} While the recently described synergistic effect of acetylcholine and secretin on AE2 activity is mediated by a calcineurin-dependent potentiation of cAMP production,¹⁷ in the case of extracellular ATP, the inhibitory effect of amiloride on agonist-stimulated AE2 activity suggests a major role for modulation of HCO₃⁻ uptake via NHE. It is well known that the activity of the apical anion exchanger not only depends on the out to in Cl⁻ gradient, but it is also directly related to pHi and HCO₃⁻ concentration, a feature that distinguishes AE2 from the AE1 isoform.^{47,50,51} The reported inhibition of secretin-stimulated HCO₃⁻ secretion by amiloride in perfused rat livers¹⁶ is consistent with this interpretation and further indicates that NHE1 plays a role in biliary HCO₃⁻ secretion.

In conclusion, our data are fully consistent with the proposed role of ATP in paracrine regulation of cholangiocyte ion transport.²²⁻²⁷ Binding of biliary ATP to P2Y₂ receptors present on the apical membrane of cholangiocytes stimulates a number of transport proteins, including basolateral NHE. The higher intracellular HCO₃⁻, in the presence of cAMP, provides a potent stimulus for Cl⁻/HCO₃⁻ exchanger, contributing to effective alkalinization of the bile. The physiological relevance of biliary ATP will depend on various parameters controlling the concentration of ATP in the bile, including the

amount of ATP delivered by hepatocytes and the activity of luminal ectoATPases. Because extracellular ATP is rapidly degraded to adenosine, which, from the apical side has no effect on NHE, a local increase in extracellular ATP concentration can provide a very effective autocrine/paracrine signal through apical P2Y₂ receptors. These findings provide a rationale for future studies aimed at modulating biliary ATP concentration in cholestatic conditions. In addition, the use of polarized cholangiocyte preparations such as those used here will greatly facilitate the study of pharmacological agents able to overcome the secretory defect in cystic fibrosis.

Acknowledgment: The authors are indebted to Jürg Graf, M.D., and Elena Ossi, M.D., for helpful discussion. Ákos Zsembery thanks Prof. László Rosivall for helpful discussion and his constant support.

REFERENCES

- Alpini G, Lenzi R, Zhai WR, Slott PA, Liu MH, Sarkozi L, Tavoloni N. Bile secretory function of intrahepatic biliary epithelium in the rat. *Am J Physiol* 1989;257:G124-G133.
- Strazzabosco M, Zsembery A, Fabris L. Electrolyte transport in bile ductular epithelial cells. *J Hepatol* 1996;24(Suppl 1):78-87.
- Boyer JL. Bile duct epithelium: frontiers in transport physiology. *Am J Physiol* 1996;270:G1-G5.
- Alvaro D, Cho WK, Mennone A, Boyer JL. Effect of secretin on pHi regulation in isolated rat bile duct epithelial cells. *J Clin Invest* 1993;92:1314-1325.
- Cho WK, Mennone A, Rudyberg SA, Boyer JL. VIP is a potent stimulus for of bicarbonate and fluid secretion in bile ducts [Abstract]. *HEPATOLOGY* 1996;22:294A.
- Tietz PS, Alpini G, Pham LD, LaRusso NF. Somatostatin inhibits secretin-induced ductal hyperchloresis and exocytosis by cholangiocytes. *Am J Physiol* 1995;269:G110-G118.
- Glaser SS, Rodgers R, Phinzy J, Robertson WE, Lasater J, Caligiuri A, Tretjak Z, et al. Gastrin inhibits secretin-induced ductal secretion by interaction with specific receptors on rat cholangiocytes. *Am J Physiol* 1997;273:G1061-G1070.
- Hardison WGM, Norman JC. Electrolyte composition of the secretin fraction of bile from the perfused pig liver. *Am J Physiol* 1968;214:758-763.
- Cohn JA, Strong TV, Picciotto MR, Nairn AC, Collins FS, Fitz JG. Localization of the cystic fibrosis transmembrane conductance regulator in human bile duct epithelial cells. *Gastroenterology* 1993;105:1857-1864.
- Fitz JG, Basavappa S, McGill J, Melhus O, Cohn JA. Regulation of

- membrane chloride currents in rat bile duct epithelial cells. *J Clin Invest* 1993;91:319-328.
11. Strazzabosco M, Mennone A, Boyer JL. Intracellular pH regulation in isolated rat bile duct epithelial cells. *J Clin Invest* 1991;87:1503-1512.
 12. Strazzabosco M, Joplin R, Zsembery A, Wallace L, Spirli C, Fabris L, Granato A, et al. Na^+ -dependent and -independent $\text{Cl}^-/\text{HCO}_3^-$ exchange mediate cellular HCO_3^- transport in cultured human intrahepatic bile duct cells. *HEPATOLOGY* 1997;25:976-985.
 13. Martinez-Ansò E, Castillo JE, Diaz J, Medina JE, Prieto J. Immunohistochemical detection of $\text{Cl}^-/\text{HCO}_3^-$ anion exchanger in human liver. *HEPATOLOGY* 1994;19:1400-1406.
 14. McGill JM, Basavappa S, Gettys TW, Fitz JG. Secretin activates Cl^- channels in bile duct epithelial cells through a cAMP-dependent mechanism. *Am J Physiol* 1994;266:G731-G736.
 15. Baunes T, Grotmol T, Veel T, Landsverk T, Ridderstrale Y, Reader MG. Importance of carbonic anhydrase for canalicular and ductular cholestasis in the pig. *Acta Physiol Scand* 1988;133:535-544.
 16. Renner EL, Heydtmann M. Amiloride, but not DIDS and NPPB, inhibit secretin (SEC)-induced cholestasis: evidence for a role of Na^+/H^+ , but not $\text{Cl}^-/\text{HCO}_3^-$ exchange and Cl^- channels, in ductular bile formation [Abstract]. *HEPATOLOGY* 1995;22:315A.
 17. Alvaro D, Alpini G, Jezequel AM, Bassotti C, Francia C, Fraioli F, Romeo R, et al. Role and mechanisms of action of acetylcholine in the regulation of rat cholangiocyte secretory functions. *J Clin Invest* 1997;100:1349-1362.
 18. Elsing C, Hubner C, Fitcher BA, Kassner A, Stremmel W. Muscarinic acetylcholine receptor stimulation of biliary epithelial cells and its effect on bile secretion in the isolated perfused rat liver. *HEPATOLOGY* 1997;25:804-813.
 19. Knowles MR, Clarke LL, Boucher RC. Activation by extracellular nucleotides of chloride secretion in the airway epithelial of patients with cystic fibrosis. *N Engl J Med* 1991;325:533-538.
 20. Dho S, Stewart K, Foskett JK. Purinergic receptor activation of Cl^- secretion in T84 cells. *Am J Physiol* 1992;262:C67-C74.
 21. McGill J, Basavappa S, Shimohura GH, Middleton JP, Fitz JG. ATP activates ion permeabilities in biliary epithelial cells. *Gastroenterology* 1994;107:236-243.
 22. Elsing C, Kassner A, Stremmel W. Sodium, Hydrogen antiporter activation by extracellular adenosine triphosphate in biliary epithelial cells. *Gastroenterology* 1996;111:1321-1332.
 23. Chari RS, Schutz SM, Haebig JE, Shimokura GH, Cotton PB, Fitz JG, Meyers WC. Adenosine nucleotides in bile. *Am J Physiol* 1996;270:G246-G252.
 24. Schlosser SE, Burgstahler AD, Nathanson MH. Isolated rat hepatocytes can signal to other hepatocytes and bile duct cells by release of nucleotides. *Proc Natl Acad Sci U S A* 1996;93:9948-9953.
 25. Roman RM, Wang Y, Fitz JG. Volume-sensitive biliary Cl^- channels: regulation by extracellular ATP and implications for biliary secretion [Abstract]. *HEPATOLOGY* 1997;26:261A.
 26. Fitz JG, Cohn JA. Biology and pathophysiology of CFTR and other Cl^- channels in biliary epithelial cells. In: Sirica AE, Longnecker DS, eds. *Biliary and Pancreatic Ductal Epithelia*. New York: Dekker, 1997:107-126.
 27. Schlenker T, Romac JM-J, Sharara AI, Roman RM, Kim SJ, LaRusso N, Liddle RA, et al. Regulation of bile secretion through apical purinergic receptors in cultured rat cholangiocytes. *Am J Physiol* 1997;273:G1108-G1117.
 28. Hogan DL, Crombie DL, Isemberg JJ, Svendsen P, Schaffalitzky de Muckadell OB, Ainsworth M. CFTR mediates cAMP and Ca_2^+ activated duodenal epithelial HCO_3^- secretion. *Am J Physiol* 1996;272:G872-G878.
 29. Kopelman H, Corey M, Gaskin K, Durie P, Weizman Z, Forstner G. Impaired chloride secretion, as well as bicarbonate secretion underlies the fluid secretory defect in the cystic fibrosis pancreas. *Gastroenterology* 1988;95:349-355.
 30. Marino CR, Gorelick FS. Scientific advances in cystic fibrosis. *Gastroenterology* 1992;103:681-693.
 31. Colombo C, Battezzati PM, Podda M. Hepatobiliary disease in cystic fibrosis. *Semin Liver Dis* 1994;14:259-269.
 32. Knuth A, Gabbert H, Dippold W, Klein O, Sachsse W, Bitter-Suermann D, Prellwitz W, et al. Biliary adenocarcinoma: characterization of three new human tumor cell lines. *J Hepatol* 1985;1:579-596.
 33. Basavappa S, Middleton J, Mangel AW, McGill JM, Cohn JA, Fitz JG. Cl^- and K^+ transport in human biliary cell lines. *Gastroenterology* 1993;104:1796-1805.
 34. Vroman B, LaRusso NF. Development and characterization of polarized primary cultures of rat intrahepatic bile duct epithelial cells. *Lab Invest* 1996;74:303-313.
 35. Spirli C, Granato A, Zsembery A, Okolicsanyi L, LaRusso NF, Strazzabosco M. Gene expression and polarized distribution of membrane acid/base carriers in a differentiated rat cholangiocyte cell line (NRC-1) [Abstract]. *J Hepatol* 1997;26:63A.
 36. Boyarsky G, Ganz MB, Sterzel RB, Boron WF. pH regulation in single glomerular mesangial cells I. Acid extrusion in absence and presence of HCO_3^- . *Am J Physiol* 1988;255:C844-C856.
 37. Wenzel E, Machen TE. Intracellular pH dependence of buffer capacity and anion exchange in the parietal cell. *Am J Physiol* 1989;257:G741-G747.
 38. Boron WF. Control of intracellular pH. In: Seldin DW, Giebisch G, eds. *The Kidney: Physiology and Pathophysiology*. 2nd ed. New York: Raven, 1992:219-263.
 39. Grinstein S, Rotin D, Mason MJ. Na^+/H^+ exchange and growth factor-induced cytosolic pH changes. Role in cellular proliferation. *Biochim Biophys Acta* 1989;988:73-97.
 40. Benedetti A, Strazzabosco M, Corasanti JC, Haddad P, Graf J, Boyer JL. $\text{Cl}^-/\text{HCO}_3^-$ exchanger in isolated rat hepatocytes: role in regulation of intracellular pH. *Am J Physiol* 1991;261:G512-G522.
 41. Putnam RW. pH regulatory transport systems in a smooth muscle-like cell line. *Am J Physiol* 1990;258:C470-C479.
 42. Shepherd RM, Williams GH, Quinn SJ. Regulation of intracellular pH in single rat zona glomerulosa cells. *Am J Physiol* 1992;262:C182-C190.
 43. Gray MA, Plant S, Argent BE. cAMP regulated whole cell chloride currents in pancreatic duct cells. *Am J Physiol* 1993;264:C591-C602.
 44. Gray MA, Winpenny JP, Porteous DJ, Dorin JR, Argent BE. CFTR and calcium-activated chloride currents in pancreatic duct cells of a transgenic CF mouse. *Am J Physiol* 1994;266:C213-C221.
 45. Nathanson MH, Burgstahler AD, Mennone A, Boyer JL. Characterization of cytosolic Ca_2^+ signaling in rat bile duct epithelia. *Am J Physiol* 1996;271:G86-G96.
 46. Marti U, Elsing C, Renner EL, Liechti-Gallati S, Reichen J. Differential expression of Na^+/H^+ antiporter mRNA in biliary epithelial cells and hepatocytes. *J Hepatol* 1996;24:498-502.
 47. Noel J, Pouyssegur J. Hormonal regulation, pharmacology and membrane sorting of vertebrate Na^+/H^+ exchanger isoforms. *Am J Physiol* 1995;268:C283-C269.
 48. Bruck R, Benedetti A, Strazzabosco M, Boyer JL. Intracellular alkalinization induces cholestasis and stimulates HCO_3^- and horseradish peroxidase excretion in isolated perfused rat liver by vesicular mediated exocytosis. *Am J Physiol* 1993;265:G347-G353.
 49. Benedetti A, Strazzabosco M, Ng OC, Boyer JL. Regulation of activity and apical targeting of the $\text{Cl}^-/\text{HCO}_3^-$ exchanger in rat hepatocytes. *Proc Natl Acad Sci U S A* 1994;91:792-796.
 50. Borgese F, Malapert B, Fievet B, Pouyssegur J, Motais R. The cytoplasmic domain of Na^+/H^+ exchanger dictates the nature of the hormonal response: behaviour of a chimeric human NHE1/trout-NHE antiporter. *Proc Natl Acad Sci U S A* 1994;89:6765-6769.
 51. Humphreys BD, Jiang L, Chernova MN, Alper SL. Hypertonic activation of AE2 anion exchanger in xenopus oocytes via NHE-mediated intracellular alkalinization. *Am J Physiol* 1995;268:C201-C209.

Ca²⁺-activated Cl⁻ channels can substitute for CFTR in stimulation of pancreatic duct bicarbonate secretion¹

ÁKOS ZSEMBERY,^{*,†,‡} MARIO STRAZZABOSCO,[†] AND JÜRG GRAF^{*,2}

^{*}Department of General and Experimental Pathology, University of Vienna, Vienna, Austria; [†]Istituto di Medicina Interna, Università ed Azienda Ospedaliera di Padova, Padua, Italy; and [‡]Department of Pathophysiology, Semmelweis University, Faculty of Medicine, Budapest, Hungary

ABSTRACT This study addresses the mechanisms by which a defect in CFTR impairs pancreatic duct bicarbonate secretion in cystic fibrosis. We used control (PANC-1) and CFTR-deficient (CFPAC-1; $\Delta F508$ mutation) cell lines and measured HCO_3^- extrusion by the rate of recovery of intracellular pH after an alkaline load and recorded whole cell membrane currents using patch clamp techniques. 1) In PANC-1 cells, cAMP causes parallel activation of Cl⁻ channels and of HCO_3^- extrusion by DIDS-sensitive and Na⁺-independent Cl⁻/HCO₃⁻ exchange, both effects being inhibited by Cl⁻ channel blockers NPPB and glibenclamide. 2) In CFPAC-1 cells, cAMP fails to stimulate Cl⁻/HCO₃⁻ exchange and Cl⁻ channels, except after promoting surface expression of $\Delta F508$ -CFTR by glycerol treatment. Instead, raising intracellular Ca²⁺ concentration to 1 $\mu\text{mol/l}$ or stimulating purinergic receptors with ATP (10 and 100 $\mu\text{mol/l}$) leads to parallel activation of Cl⁻ channels and HCO_3^- extrusion. 3) K⁺ channel function is required for coupling cAMP- and Ca²⁺-dependent Cl⁻ channel activation to effective stimulation of Cl⁻/HCO₃⁻ exchange in control and CF cells, respectively. It is concluded that stimulation of pancreatic duct bicarbonate secretion via Cl⁻/HCO₃⁻ exchange is directly correlated to activation of apical membrane Cl⁻ channels. Reduced bicarbonate secretion in cystic fibrosis results from defective cAMP-activated Cl⁻ channels. This defect is partially compensated for by an increased sensitivity of CF cells to purinergic stimulation and by alternative activation of Ca²⁺-dependent Cl⁻ channels, mechanisms of interest with respect to possible treatment of cystic fibrosis and of related chronic pancreatic diseases.—Zsembery, Á., Strazzabosco, M., Graf, J. Ca²⁺-activated Cl⁻ channels can substitute for CFTR in stimulation of pancreatic duct bicarbonate secretion. *FASEB J.* 14, 2345–2356 (2000)

Key Words: cystic fibrosis • anion exchange • purinergic stimulation • K⁺ channel function

CYSTIC FIBROSIS (CF) is the most common hereditary disorder among the Caucasian population (1, 2). The disease affects cAMP-dependent electrolyte

transport in a variety of organs resulting, as the most prominent manifestations of the disease, in progressive respiratory and pancreatic insufficiency. In the pancreas, obstruction of the ductal system is followed by cystic dilatation, fibrosis and atrophy of the gland (3). CF is caused by mutations in the gene that encodes for CFTR, the cystic fibrosis transmembrane conductance regulator (4, 5). Of more than 800 known mutations, the majority of patients (~70%) present with the homozygous $\Delta F508$ deletion. Furthermore, heterozygosis in the CFTR defect has been identified as a risk factor for chronic pancreatitis (6).

CFTR functions mainly as a low conductance cAMP/PKA-activated epithelial Cl⁻ channel (7, 8), but it may participate in trafficking of certain proteins (9) and in the regulation of other membrane transport mechanisms such as sodium- (ENaC) (10, 11), potassium- (12, 13) and cAMP-independent outwardly rectifying chloride channels (ORCC) (14, 15), water transport (16), and cellular secretion of ATP (15, 17), which could lead to autocrine activation of purinergic receptors. Furthermore, intracellular vesicle acidification (18) and regulation of intracellular pH (pH_i), including the activity of chloride/bicarbonate exchange, appear to be under the control of CFTR (19–21). However, the mechanistic links between CFTR and these ion transporters remain to be elucidated.

CFTR assumes different functions in various organs. In the pancreas, CFTR is expressed at high levels in the apical plasma membrane of duct cells (22, 23). In these cells, secretin promotes secretion of HCO_3^- via a mechanism that appears to involve three consecutive steps: 1) activation of the adenylate cyclase signal transduction pathway, 2) activation of basolateral K⁺ and apical Cl⁻ channels, and 3) stimulation of apical Cl⁻/HCO₃⁻ exchange that is driven by both a low intracellular Cl⁻ concentration

¹ Presented in part at the 99th Annual Meeting of the American Gastroenterological Association and published in abstract form in *Gastroenterology* (1998) vol. 114, p. 2092A.

² Correspondence: Department of General and Experimental Pathology, University of Vienna, Währinger Gürtel 18–20, 1090 Vienna, Austria. E-mail: juerg.graf@univie.ac.at

($[\text{Cl}^-]_i$) and high $[\text{HCO}_3^-]_i$ (24, 25). Pancreatic duct HCO_3^- secretion is impaired in the course of CF (26, 27), suggesting that CFTR is the Cl^- channel that cooperates with $\text{Cl}^-/\text{HCO}_3^-$ exchange to promote secretin/cAMP-dependent HCO_3^- secretion. Intracellular cAMP is also generated by other hormones [VIP (28), PHI (29), β -adrenergic agonists (30)] that may activate CFTR. In addition, measurements of short circuit current indicate that other agonists promote anion transport in pancreatic duct cells via Ca^{2+} signaling [purinergic agonists (31–33), cholinergic (34), angiotensin II (35), and histamine (36)]. However, it is unknown whether this alternative signal transduction pathway may sustain fluid and HCO_3^- secretion in CFTR-deficient cells and could thus be exploited for ameliorating the course of the disease in some patients affected by CF (37).

The aim of this study was to directly correlate cAMP- and Ca^{2+} -dependent activation of Cl^- channels with $\text{Cl}^-/\text{HCO}_3^-$ exchange activity in control and CFTR-deficient pancreatic duct cells. We used pancreatic duct cell lines derived from control and CFTR-deficient ($\Delta\text{F508}/\Delta\text{F508}$) ductal adenocarcinomas, PANC-1 and CFPAC-1, respectively (38, 39). The $\Delta\text{F508}/\Delta\text{F508}$ deletion present in CFPAC-1 cells belongs to a group of CFTR mutations that result in impaired targeting to the plasma membrane of the otherwise functional protein (40, 41). This defect can be restored by exposing the cells to chemical chaperons such as glycerol, resulting in proper expression at the plasma membrane of functional CFTR Cl^- channels (42, 43). Therefore, glycerol-treated CFPAC-1 cells were also used to test for the correlation between activation by cAMP of CFTR Cl^- channels and stimulation of $\text{Cl}^-/\text{HCO}_3^-$ exchange. We used the patch clamp technique to measure whole cell Cl^- and K^+ currents and fluorometric measurements of pH_i using BCECF to determine HCO_3^- extrusion from the rate of recovery of pH_i after an alkaline load. Interactions of Cl^- and K^+ currents with $\text{Cl}^-/\text{HCO}_3^-$ exchange activity were analyzed in both cell lines by studying the effects of 1) raising intracellular cAMP or Ca^{2+} concentration, 2) inhibition of Cl^- channels, 3) cell membrane depolarization, 4) ion substitution, and 5) purinergic receptor stimulation with ATP.

MATERIALS AND METHODS

Materials

N-2-hydroxyethylpiperazine-N'-2-ethanesulfonic acid (HEPES), dimethyl sulfoxide (DMSO), nigericin, 4,4-diisothiocyanatostilbene-2,2'-disulfonic acid (DIDS), ethylenediaminetetraacetic acid (EDTA), ethylene glycol-bis(β -aminoethyl ether) N, N,N',N'-tetraacetic acid (EGTA), gluconic acid, choline chloride, glycerol, forskolin, ionomycin, adenosine 3':5'-cyclic monophosphate (cAMP), N⁶,2'-O-dibutyryl-adenosine 3':5'-cyclic

monophosphate (DBcAMP), 3-isobutyl-1-methylxanthine (IBMX), glibenclamide, adenosine-5'-triphosphate magnesium salt, adenosine-5'-triphosphate sodium salt, tetramethylammonium hydroxide (TMA-OH) were from Sigma Chemical Company (St. Louis, Mo.); 2',7'-bis(2-carboxyethyl)-5(6)-carboxyfluorescein-acetoxymethylester (BCECF-AM) was from Lambda GmbH (Graz, Austria). 5-nitro-2-(3-phenylpropylamino)-benzoic acid (NPPB) was purchased from Calbiochem Chemical Company (La Jolla, Calif.). Culture media [Dulbecco's modified Eagle medium (DMEM), Iscove's modified Dulbecco's medium, and Leibowitz L-15 medium], fetal bovine serum (FBS), penicillin/streptomycin, and trypsin/EDTA were from Life Technologies, Inc. (Grand Island, N.Y.). A combination of 100 $\mu\text{mol/l}$ DBcAMP, 100 $\mu\text{mol/l}$ IBMX, and 3 $\mu\text{mol/l}$ forskolin ('cAMPmix') was used to increase intracellular cAMP concentration (44).

Cell cultures

PANC-1 and CFPAC-1 cells were obtained from the American Type Culture Collection (Rockville, Md.). PANC-1 cells were grown in DMEM supplemented with 10% FBS, penicillin (100 U/ml), and streptomycin (0.1 mg/ml). PANC-1 cells were used between passage 42 and 65. CFPAC-1 cells were grown in Iscove's modified Dulbecco's medium supplemented with 10% FBS, penicillin (100 U/ml), and streptomycin (0.1 mg/ml). These cells were studied between passage 23 and 38. Cultures were incubated at 37°C in 5% CO_2 95% air atmosphere. The cells were suspended by washing with Ca^{2+} - Mg^{2+} -free PBS solution containing 2 mmol/l EDTA and plated on glass coverslip fragments. Cells were transferred to bicarbonate-free Leibowitz L-15 medium 1 h before use in patch clamp experiments.

Glycerol-pretreated CFPAC-1 cells were prepared by incubation for 24 h in Iscove's modified Dulbecco's medium supplemented with 10% glycerol (v/v), and glycerol was removed by stepwise diluting the glycerol-containing medium with fresh medium over the course of 90 min.

Intracellular pH (pH_i) measurement

Intracellular pH was measured as described (45) using the fluorescent intracellular sensor BCECF. In brief, BCECF was loaded into the cells in the form of its tetraacetoxymethyl ester derivative (BCECF-AM) (12 μM) by incubation for 15–20 min at 37°C. After washing for 10 min at 37°C in a BCECF-free medium, the cells were transferred into a thermostated (37°C) perfusion chamber placed on the stage of an Axiovert (Zeiss, Jena, Germany) inverted microscope. The microscope was equipped with a microfluorometer (Photon Technological Instruments, Monmouth Junction, N.J.), allowing for continuous dual wavelength excitation photometry. Intracellular pH was measured in single cells as the ratio of emission intensities at 530 nm after excitation at 495 nm (pH_i and concentration sensitive) and 440 nm (only concentration sensitive), respectively. Data were collected at 50 Hz chopping frequency and averaged every 2 s. After each experiment, internal dye calibration was performed by superfusing the cells with a medium containing high $[\text{K}^+]$ and the K^+/H^+ ionophore nigericin (12 $\mu\text{mol/l}$) at pH 6.8 and 7.6.

Determination of intrinsic intracellular buffer capacity

The intrinsic buffer capacity (β_i) is defined as the sum of intracellular buffers other than $\text{CO}_2/\text{HCO}_3^-$. Testing for buffer capacity by measuring changes of pH_i after the intracellular addition or removal of acid or base requires that pH_i is not affected by cell membrane acid or base transporters

(45). We performed measurements of β_i in HEPES-buffered, HCO_3^- - and Na^+ -free solutions by exposing cells to NH_4Cl (30 mmol/l) to add base; after 3 min, we lowered external NH_4Cl concentration to 20 mmol/l to remove base. β_i was determined from calculated changes of $[\text{NH}_3 + \text{NH}_4^+]_i$ and the associated changes of pH_i (45).

Measurement of $\text{Cl}^-/\text{HCO}_3^-$ exchange activity

Cells were first superfused for 10 min with medium containing 25 mmol/l HCO_3^- and 5% CO_2 , which results in intracellular equilibration of $[\text{HCO}_3^-]_i$ according to pH_i . Acute removal of $\text{CO}_2/\text{HCO}_3^-$ from the superfusion medium by exposure to HEPES-buffered HCO_3^- -free medium (see solutions below) results in depletion of intracellular CO_2 and sudden intracellular alkalinization. Intracellular pH recovers from this alkaline load toward the initial value. To prove that this pH_i recovery is due to the activity of Na^+ -independent $\text{Cl}^-/\text{HCO}_3^-$ exchange, we monitored pH_i after an alkaline load in the absence of external Cl^- (replacement with gluconic acid) and in cells preincubated with 0.5 mmol/l DIDS for 40 min. Possible dependence on Na^+ of the base extrusion mechanism was evaluated after preincubation with Na^+ -free medium (replacement with choline). The rate of recovery from the intracellular alkaline load was determined by linear regression of the slope $\delta\text{pH}/\delta t$. For comparison between individual experiments, this slope was determined at the same range of pH_i (given in legends to Figs. 3 and 5). Experimental effects on $\text{Cl}^-/\text{HCO}_3^-$ exchange activity were studied by preincubation of the cells for 10 min with either 'cAMPmix', NPPB, glibenclamide, high external K^+ concentration, ATP, or ionomycin.

Whole cell current recording

Whole cell currents were measured 24–48 h after plating the cells using patch clamp recording techniques (46). Studies were performed at room temperature (22°C) using NaCl-rich extracellular solution with 1 mmol/l free $[\text{Ca}^{2+}]$. Recording pipettes were pulled from VC-H075P glass (Terumo, Japan) on a micropipette puller P-87 (Sutter Instrument Co., Novato, Calif.) and had a resistance of 4–7 M Ω . The pipettes were filled either with KCl-rich solution or CsCl-rich solution with free $[\text{Ca}^{2+}]$ adjusted to ≈ 100 nmol/l (0.4 mmol/l CaCl_2 and 1 mmol/l EGTA). Data were recorded with an EPC-9 amplifier and digitized (3 kHz), stored on hard disk, and analyzed using Pulse+PulseFit version 7.4 programs (HEKA Elektronik GmbH, Lambrecht, Germany). Whole cell currents were measured at the holding potential (–40 mV) and during 100 ms square pulses of the test potential (–100 mV to +100 mV) in 20 mV increments, with 5 s intervals (polarity given for cell interior). For control bath and KCl-rich pipette solutions, the equilibrium potentials for K^+ (E_K) and Cl^- (E_{Cl}) were –86 mV and –1.3 mV, respectively. Therefore, membrane currents near these clamping voltages were considered to represent Cl^- and K^+ currents, respectively. Current-voltage relations were obtained after currents had stabilized 30 ms after applying voltage pulses. Whole cell currents were normalized for unit cell surface area by division by the whole cell membrane capacitance that ranged between 25 and 40 pF. Accordingly, current is presented as pA/pF. Corrections for pipette to bath liquid junction potentials were applied when asymmetrical solutions (KCl/NaCl or CsCl/NaCl) were used (4 mV and 5 mV, respectively).

Solutions

Buffers for pH experiments

Bicarbonate-free bath solution (HEPES) contained (mmol/l): NaCl 135, KCl 4.7, MgSO_4 1, KH_2PO_4 1.2, CaCl_2 1.5, HEPES 10, glucose 5, titrated to pH 7.4 with NaOH. Bicarbonate buffered solution (KRB) contained (mmol/l): NaCl 115, KCl 4.7, KH_2PO_4 1.2, MgSO_4 1, CaCl_2 1.5, NaHCO_3 25, glucose 5, and was equilibrated with 5% CO_2 .

Solutions for patch clamp experiments

Control NaCl-rich bath solution (mmol/l): NaCl 150, KCl 5, MgCl_2 2, CaCl_2 1, HEPES 10, glucose 5, titrated to pH 7.4 with NaOH, osmolality: 310–320 mosm/kg. Pipette solutions: KCl-rich solution contained (mmol/l): KCl 145, NaCl 5, MgCl_2 1, HEPES 10, CaCl_2 0.4, EGTA 1, MgATP 2, titrated to pH 7.2 with KOH, osmolality: 280–290 mosm/kg. CsCl-rich pipette solution contained (mmol/l): CsCl 150, MgCl_2 1, HEPES 10, CaCl_2 0.4, EGTA 1, MgATP 2, titrated to pH 7.2 with TMA-OH, osmolality: 280–290 mosm/kg. The osmotic difference between the pipette and bath solution was applied in order to prevent activation of volume-activated currents (47). With pipette solutions containing ATP, the efflux of ATP from the pipette could have stimulated purinergic membrane receptors when approaching the cell. This was avoided by first filling the pipette tip by dipping into an ATP-free pipette solution, followed by filling the pipette with the ATP-containing solution from the back. Stock solutions of NPPB, glibenclamide, forskolin and BCECF-AM were prepared in DMSO at 1000-fold the desired concentration. Nigericin was dissolved in ethanol.

Data analysis and statistics

We noticed some variation in electrical current and the rate of HCO_3^- extrusion between individual preparations that we could not attribute to the passage number or time after seeding. To avoid systematic errors in comparing one experimental condition with control or two different experimental conditions with each other, we performed the respective experiments on the same day, from one set of cell cultures and in random order. Data are acquired from single cells and given as mean values \pm SE (n =number of cells). Differences between grouped experiments from one day are evaluated by the unpaired t test and are considered significant if $P < 0.05$.

RESULTS

Intracellular pH and $\text{Cl}^-/\text{HCO}_3^-$ exchange activity in PANC-1 and CFPAC-1 cells

Under control conditions, pH_i was higher in CFPAC-1 cells (7.34 ± 0.02 ; $n=16$) than in control PANC-1 cells (7.16 ± 0.05 ; $n=10$) ($P < 0.005$). To test whether the high pH_i in CF cells may result from reduced HCO_3^- extrusion, we determined $\text{Cl}^-/\text{HCO}_3^-$ exchange activity in both cell lines by measuring the rate of pH_i recovery after intracellular alkalinization. In both cell lines, pH_i recovered to baseline levels. Bicarbonate extrusion was Cl^- dependent, Na^+ independent, and inhibited by DIDS,

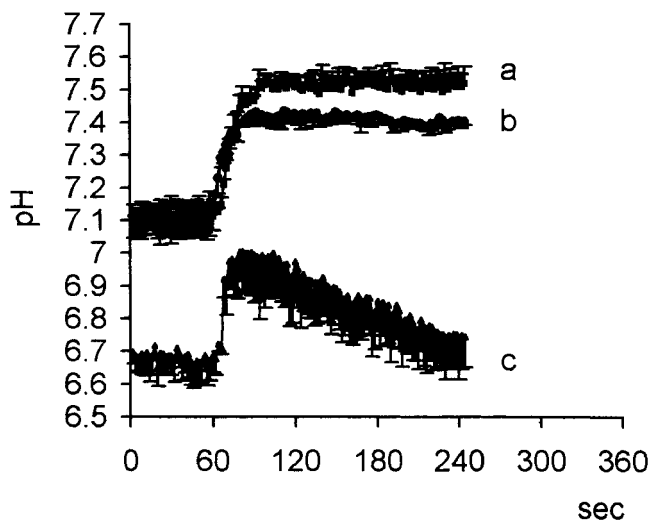


Figure 1. Measurement of pH_i in PANC-1 cells in order to test for the mechanism of base extrusion after an intracellular alkaline load. At 60 s, intracellular alkalization was obtained by removal of HCO_3^- and CO_2 from the superfusion solution. a) No significant recovery of pH_i is obtained when extracellular Cl^- is also removed at the time of intracellular alkalization. b) No significant recovery of pH_i is obtained when cells were preincubated for 40 min with 0.5 mmol/l DIDS. c) pH_i recovers at a normal rate toward baseline values in the absence of Na^+ (extracellular Na^+ being removed 40 min prior to alkalization and absent throughout the experiment). Note low baseline pH_i in this condition. Data are presented as means \pm SE, $n=3$ for a–c. Compare also Fig. 2.

consistent with Cl^-/HCO_3^- exchange (Fig. 1) as previously demonstrated in rat pancreatic duct cells (48, 49). The basal activity of this exchanger was higher in PANC-1 than in CFPAC-1 cells ($\delta pH/\delta t=0.119 \pm 0.02/\text{min}$; $n=7$ vs. $\delta pH/\delta t=0.078 \pm 0.01/\text{min}$; $n=7$; measured at $pH=7.6$; $P<0.05$).

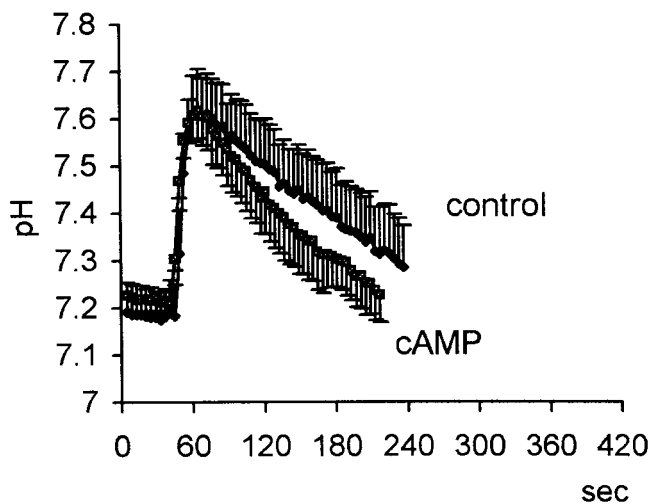


Figure 2. Measurement of pH_i in PANC-1 cells. Intracellular alkalization was obtained by removal of HCO_3^- and CO_2 from the superfusion solution (at 50 s). The activity of Cl^-/HCO_3^- exchange was assessed from the rate of pH recovery under control condition ($n=7$) and after increasing intracellular cAMP concentration ($n=6$). Data are presented as means \pm SE.

To compare rates of $\delta pH/\delta t$ in the two cell lines, we measured intracellular buffer capacity (β_i) using the NH_4Cl technique (45). Intracellular alkalization was first obtained by exposing cells to 30 mmol/l NH_4Cl . Reducing external NH_4Cl from 30 to 20 mmol/l caused a sudden decrease of pH_i from 7.57 ± 0.10 to 7.45 ± 0.10 ($n=5$) and from 7.60 ± 0.06 to 7.47 ± 0.06 ($n=4$) corresponding to a β_i of 22.0 ± 3.6 mM/pH and 18.6 ± 1.8 mM/pH in PANC-1 and CFPAC-1 cells, respectively. The two values were not significantly different.

Increasing intracellular levels of cAMP and activating protein kinase A by administration of cAMPmix (44) led to a significant increase of Cl^-/HCO_3^- exchange activity in PANC-1 cells (Fig. 2 and Fig. 3). In contrast, HCO_3^- extrusion can be stimulated in CFPAC-1 cells by an increase of $[Ca^{2+}]_i$ (Fig. 4, see below), whereas cAMPmix had no effect in these cells (Fig. 5). Because these two cell lines could differ in transport properties not related to differences in CFTR expression we also studied effects of cAMP in CFPAC-1 cells after induction by glycerol treatment

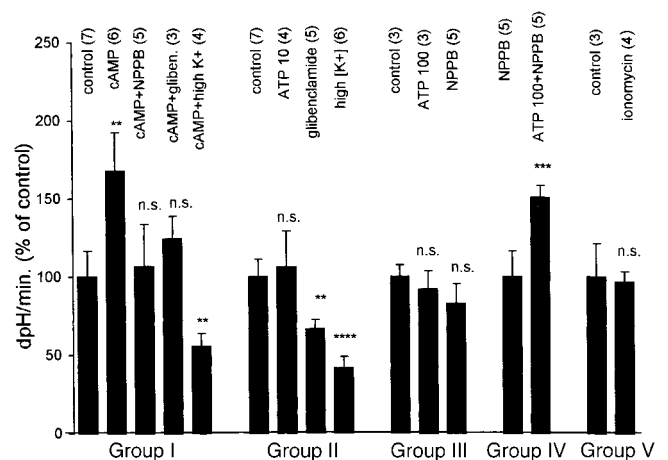


Figure 3. Cl^-/HCO_3^- exchange activity in PANC-1 cells is presented as the rate of recovery of pH_i after an alkaline load. Data from five groups of experiments are shown, each group with reference to the control rate (100%). Group I shows activation of Cl^-/HCO_3^- exchange by increasing intracellular cAMP and inhibition of the effect by the Cl^- channel blockers NPPB (10 $\mu\text{mol/l}$) and glibenclamide (100 $\mu\text{mol/l}$) and by exposure to high K^+ concentration (control value at $pH_i=7.55$; $\delta pH/\delta t=0.119 \pm 0.02/\text{min}$). Group II shows lack of effect of 10 $\mu\text{mol/l}$ ATP and inhibition of basal activity by glibenclamide (100 $\mu\text{mol/l}$) and by exposure to high $[K^+]_o$ (control value at $pH=7.55$; $\delta pH/\delta t=0.173 \pm 0.02/\text{min}$). Group III: no significant effects of ATP (100 $\mu\text{mol/l}$) and NPPB (10 $\mu\text{mol/l}$) are seen for basal activity (control value at $pH_i=7.25$; $\delta pH/\delta t=0.145 \pm 0.011/\text{min}$). Group IV: ATP (100 $\mu\text{mol/l}$) activates anion exchange in presence of NPPB (control value at $pH_i=7.40$; $\delta pH/\delta t=0.085 \pm 0.014/\text{min}$). Group V: ionomycin did not increase the anion exchange activity (control value at $pH_i=7.55$; $\delta pH/\delta t=0.173 \pm 0.037/\text{min}$). Data are presented as means \pm SE. Number of cells is shown in parentheses for each group. * $P<0.05$; ** $P<0.025$; *** $P<0.01$; **** $P<0.005$.

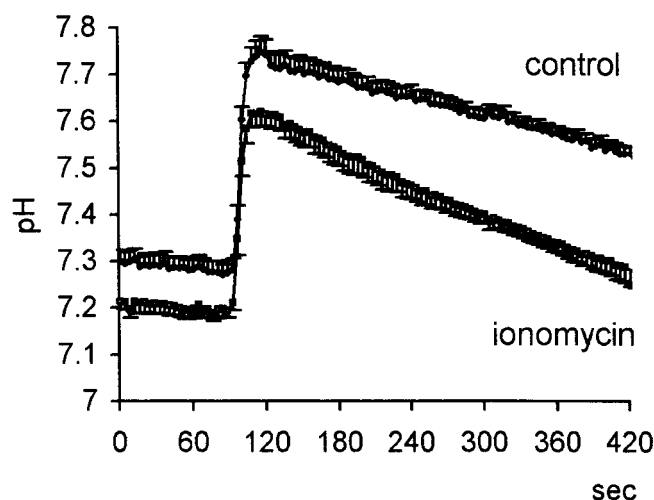


Figure 4. Measurement of pH_i in CFPAC-1 cells, experimental conditions as in Fig. 1. Note that basal pH_i is higher than in PANC-1 cells in control conditions ($n=7$) and that application of ionomycin (1 $\mu\text{mol/l}$) ($n=6$) reduces control pH_i and accelerates the rate of pH_i recovery after the alkaline load. Data are presented as means \pm SE.

of plasma membrane expression of $\Delta F508\text{-CFTR}$ (42, 43). After glycerol pretreatment, CFPAC-1 cells assumed cAMP-induced HCO_3^- extrusion, $\delta p\text{H}/\delta t$ increasing by ~ 2.5 -fold by application of cAMPmix (Fig. 5). These data confirm that expression of CFTR in the plasma membrane is a prerequisite for stimulation of $\text{Cl}^-/\text{HCO}_3^-$ exchange by cAMP.

To correlate $\text{Cl}^-/\text{HCO}_3^-$ exchange activity in PANC-1 cells with simultaneous Cl^- flux via conductive pathways, we studied the effect of NPPB and glibenclamide, Cl^- channel blockers that inhibit CFTR at low concentration (28, 51, 52). Furthermore, we depolarized the membrane potential by exposing the cells to high extracellular K^+ concentration ($[\text{K}^+]_o=70$ mmol/l) with the aim to inhibit Cl^- efflux. As shown in Fig. 3, NPPB (10 $\mu\text{mol/l}$), glibenclamide (100 $\mu\text{mol/l}$), and application of high $[\text{K}^+]_o$ abolished the effect of cAMPmix on $\text{Cl}^-/\text{HCO}_3^-$ exchange activity. In addition, 100 $\mu\text{mol/l}$ glibenclamide and high $[\text{K}^+]_o$ reduced the basal bicarbonate output as well (Fig. 3). In accordance with measurements of membrane currents (see below), these data show that cAMP stimulates $\text{Cl}^-/\text{HCO}_3^-$ exchange in PANC-1 cells by activation of NPPB- and glibenclamide-sensitive Cl^- channels. These channels allow for continuous recycling of Cl^- that is taken up by $\text{Cl}^-/\text{HCO}_3^-$ exchange. Furthermore, the activation of these channels will render the $[\text{Cl}^-]_i$ dependent on the membrane potential; i.e., $[\text{Cl}^-]_i$ will be reduced on hyperpolarization, which in turn provides a steeper out-to-in Cl^- concentration gradient to activate $\text{Cl}^-/\text{HCO}_3^-$ exchange.

To test whether Ca^{2+} -stimulated Cl^- efflux could provide another pathway for Cl^- recycling and for activation of the $\text{Cl}^-/\text{HCO}_3^-$ exchanger, we studied the effects of purinergic receptor activation by appli-

cation of ATP and of the calcium ionophore ionomycin (extracellular $[\text{Ca}^{2+}]$ being buffered to 1 $\mu\text{mol/l}$). In PANC-1 cells, application of ATP (10 and 100 $\mu\text{mol/l}$) had no significant effect on the high basal rate of anion exchange activity under control conditions, indicating a minor role of an additional ATP-activated Cl^- exit pathway in this cell line. Significant activation of base extrusion by ATP was seen only in the presence of NPPB, which is thought to inhibit basal activity of cAMP-dependent Cl^- channels, although inhibition of basal rate of base extrusion by NPPB remained below the level of significance (Fig. 3). In contrast, the basal $\text{Cl}^-/\text{HCO}_3^-$ exchange activity in CFPAC-1 cells was highly activated by ATP at concentrations of 10 $\mu\text{mol/l}$ and 100 $\mu\text{mol/l}$; increasing $[\text{Ca}^{2+}]_i$ by application of ionomycin (1 $\mu\text{mol/l}$) also doubled the rate of cell acidification (Figs. 4 and 5). This latter effect was inhibited by application of high $[\text{K}^+]_o$ but not by NPPB (10 $\mu\text{mol/l}$) (Fig. 5). These data indicate that both control and CF cells express Ca^{2+} -dependent Cl^- channels, but their activation stimulates the basal bicarbonate secretion through

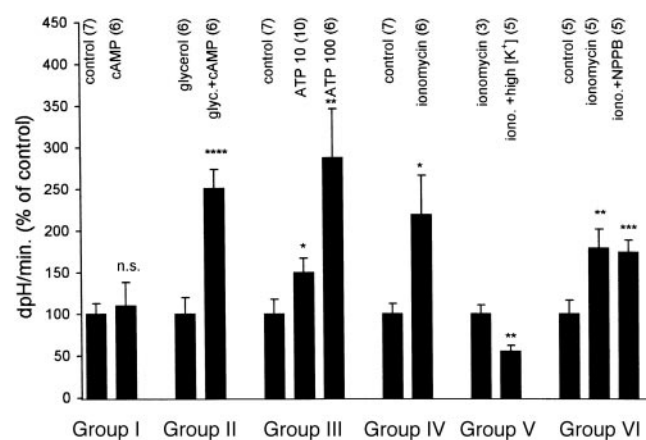


Figure 5. $\text{Cl}^-/\text{HCO}_3^-$ exchange activity in CFPAC-1 cells is presented as the rate of recovery of pH_i after an alkaline load. Data from four groups of experiments are shown, each group with reference to the control value (100%). Group I shows that administration of cAMP had no effect on the $\text{Cl}^-/\text{HCO}_3^-$ exchange activity (control value at $pH_i=7.55$: $\delta p\text{H}/\delta t=0.078\pm 0.011/\text{min}$). Group II: glycerol pretreatment restored cAMP effect on anion exchange (control value at $pH_i=7.55$: $\delta p\text{H}/\delta t=0.035\pm 0.007/\text{min}$). Group III shows that both 10 $\mu\text{mol/l}$ and 100 $\mu\text{mol/l}$ ATP significantly stimulated the anion exchange activity (control value at $pH_i=7.75$: $\delta p\text{H}/\delta t=0.048\pm 0.009/\text{min}$). Group IV: administration of 1 $\mu\text{mol/l}$ ionomycin significantly increased the HCO_3^- secretion (control value at $pH_i=7.6$: $\delta p\text{H}/\delta t=0.042\pm 0.005/\text{min}$). Group V: exposure to high extracellular $[\text{K}^+]_o$ inhibits the stimulatory effects of ionomycin (control value at $pH_i=7.55$: $\delta p\text{H}/\delta t=0.123\pm 0.013/\text{min}$). Group VI: NPPB (10 $\mu\text{mol/l}$) had no effect on ionomycin stimulated HCO_3^- secretion. (control value at $pH_i=7.5$: $\delta p\text{H}/\delta t=0.114\pm 0.019/\text{min}$). Data are presented as means \pm SE. Number of cells is shown in parentheses for each group. * $P<0.05$; ** $P<0.025$; *** $P<0.01$; **** $P<0.005$.

TABLE 1. Patch clamp whole cell recordings in PANC-1 cells^a

	Control (KCl) (10)	cAMP (KCl) (7)	High [Ca ²⁺] _i (KCl) (4)
−85 mV	−2.49 ± 0.28	−6.3 ± 1.2***	−6.0 ± 1.42*
0 mV	+1.27 ± 0.22	+2.18 ± 0.73 ns	+3.33 ± 0.92 ns
+80 mV	+29.4 ± 4.4	+64.3 ± 13.91**	+28.4 ± 5.75 ns
Rev. pot.	−25.2 ± 3.9	−15.8 ± 1.9**	−29.7 ± 7.4 ns
	Glibenclamide (KCl) (7)	cAMP + glibenclamide (KCl) (4)	
−85 mV	−2.58 ± 0.61	−2.04 ± 0.46 ns	
0 mV	+1.88 ± 0.54	+1.12 ± 0.19 ns	
+80 mV	+42.6 ± 5.67	+52.6 ± 9.8 ns	
Rev. pot.	−30.1 ± 4.2	−29.0 ± 2.1 ns	
	Control (CsCl) [#] (6)	cAMP (CsCl) (5)	cAMP + NPPB (CsCl) (4)
−85 mV	−2.91 ± 0.48 ns	−4.37 ± 0.36**	−2.22 ± 0.8 ns
0 mV	+0.77 ± 0.22 ns	+1.09 ± 0.28 ns	+0.85 ± 0.23 ns
+80 mV	+4.13 ± 0.71****	+7.3 ± 0.46****	+3.7 ± 0.5 ns
Rev. pot.	−15.8 ± 4.4 ns	−17.1 ± 3.4 ns	−33.1 ± 9.5 ns

^a Currents: pA/pF; positive values = outward current; reversal potential: mV; inside with respect to outside; KCl: KCl-rich pipette solution; CsCl: CsCl-rich pipette solution. Data represent the means ± SE. Number of cells is shown in parentheses. (ns = not significant; * $P < 0.05$; ** $P < 0.025$; *** $P < 0.005$; **** $P < 0.001$); [#] controls (CsCl) are compared to controls (KCl).

Cl[−]/HCO₃[−] exchange predominantly in CFTR-deficient CFPAC-1 cells.

Whole cell membrane Cl[−] and K⁺ currents in PANC-1 and CFPAC-1 cells

The experiments shown above indicate that activation of Cl[−] currents by cAMP or Ca²⁺ stimulate Cl[−]/HCO₃[−] exchange in PANC-1 or CFPAC-1 cells, respectively, PANC-1 cells being responsive to cAMP with little effect of increasing [Ca²⁺]_i, whereas CFPAC-1 cells respond to an increase of [Ca²⁺]_i only (except after pretreatment with glycerol). We used the patch clamp technique to correlate these effects of cAMP and [Ca²⁺]_i on HCO₃[−] secretion with changes in whole cell membrane currents. Current/voltage (I/V) correlations were obtained using standard pipette (intracellular) solution with high KCl concentration, ~ 100 nmol/l free [Ca²⁺] and 2 mmol/l ATP, and a NaCl-rich bath (extracellular) solution. Application of these solutions determines the K⁺ and Cl[−] equilibrium potentials, E_K and E_{Cl} respectively, and clamping the membrane potential (V_m) to chosen values allows to obtain a measure of K⁺ current (I_K) at V_m = 0 mV (near E_{Cl}, where the driving force for Cl[−] current is absent; V_m − E_{Cl} = 0) and of Cl[−] current (I_{Cl}) at V_m = −85 (near E_K where K⁺ current is absent; V_m − E_K = 0). At the current reversal potential (V_m = V_{rev}) outward I_K (I_K = g_K * (V_m − E_K)) and inward I_{Cl} (I_{Cl} = g_{Cl} * (V_m − E_{Cl})) are of equal magnitude resulting in zero total membrane current and, depending on the relative values of membrane K⁺ and Cl[−] conductance, g_K and g_{Cl} respectively, V_{rev} will be close to E_K if g_K ≫ g_{Cl} or close to E_{Cl} if g_{Cl} ≫ g_K. It may be noted that Cl[−]

inward current reflects conductive Cl[−] efflux. In addition to I_{Cl} at V_m = −85 mV and to I_K at V_m = 0 mV, **Table 1** and **Table 2** also give the current reversal potentials as a measure of relative K⁺ and Cl[−] conductances together with the current at +80 mV, which in PANC-1 cells is predominated by an outwardly rectifying component of K⁺ current (see below). In some experiments, intracellular KCl was completely replaced by CsCl. Thus, whole cell current is dominated by Cl[−] over the entire voltage range.

Figure 6 shows the basal I/V relationship in PANC-1 cells and **Table 1** gives the corresponding parameters for Cl[−] and K⁺ currents. A large outwardly rectifying current is observed at membrane voltages > +20 mV. This latter current component was suppressed by replacing K⁺ with Cs⁺ in the pipette solution which results in a near linear I/V relation, thus indicating the presence of outwardly rectifying K⁺ channels in PANC-1 cells (**Table 1**).

In CFPAC-1 cells, the I/V relation was near linear over the entire voltage range studied (**Fig. 7**), current at −85 mV was small as compared to PANC-1 cells (−1.44 ± 0.21 pA/pF; n = 4 vs. −2.49 ± 0.28 pA/pF; n = 10, respectively) ($P < 0.01$), and the reversal potential was more negative (−40.9 ± 5.8 mV; n = 4 vs. −25.2 ± 3.9 mV; n = 10, respectively) ($P < 0.05$). Replacing K⁺ with Cs⁺ in the pipette solution resulted in a shift of the reversal potential toward E_{Cl} and reduced the current near E_{Cl}, demonstrating inhibition of K⁺ current (**Table 2**). These data show that CFPAC-1 cells lack an outwardly rectifying component of K⁺ current and that basal Cl[−] current is smaller than in PANC-1 cells.

Figure 6 shows activation by intracellular cAMP of

TABLE 2. Patch clamp whole cell recordings in CFPAC-1 cells^a

	Control (KCl) (4)	cAMP (KCl) (4)	High [Ca ²⁺] _i (KCl) (5)
-85 mV	-1.44 ± 0.21	-1.55 ± 0.59 ns	-6.25 ± 0.6****
0 mV	+1.73 ± 0.5	+0.98 ± 0.24 ns	+3.74 ± 1.12 ns
+80 mV	+5.49 ± 0.66	+3.77 ± 1.35 ns	+15.2 ± 2.54***
Rev. pot.	-40.9 ± 5.8	-34.5 ± 6.1 ns	-28.2 ± 5.1 ns
	ATP (10 μM) (KCl) (4)	Glycerol (KCl) (4)	Glycerol + cAMP (KCl) (4)
-85 mV	-3.64 ± 0.24****	-1.10 ± 0.13	-3.2 ± 0.36****
0 mV	+3.42 ± 0.87 ns	+1.41 ± 0.22	+2.92 ± 0.96 ns
+80 mV	+13.3 ± 0.7***	+5.0 ± 0.33	+14.8 ± 2.94**
Rev. pot.	-35.4 ± 6.5 ns	-39.1 ± 6.9	-28 ± 8.1 ns
	Control (CsCl) [#] (4)	High [Ca ²⁺] _i (CsCl) (4)	High [Ca ²⁺] _i + NPPB (CsCl) (5)
-85 mV	-3.50 ± 0.98 ns	-8.90 ± 1.58**	-14.9 ± 0.9****
0 mV	+0.24 ± 0.06*	+0.83 ± 0.11****	+1.4 ± 0.18****
+80 mV	+4.48 ± 0.72 ns	+10.0 ± 1.2***	+16.0 ± 1.65***
Rev. pot.	-6.0 ± 1.3****	-7.9 ± 0.9 ns	-7.9 ± 1.5 ns

^a Currents: pA/pF; positive values = outward current; reversal potential: mV; inside with respect to outside; KCl: KCl-rich pipette solution; CsCl: CsCl-rich pipette solution. Data represent the means ± SE. Number of cells is shown in parentheses. (ns = not significant; * $P < 0.05$; ** $P < 0.025$; *** $P < 0.005$; **** $P < 0.001$); [#] controls (CsCl) are compared to controls (KCl).

Cl⁻ and K⁺ currents in PANC-1 cells: including 400 μmol/l cAMP into the pipette solution resulted in a significant increase of Cl⁻ current and of outwardly rectifying K⁺ current (Table 1). Activation of Cl⁻ current by cAMP remained unaffected when the outward K⁺ current was blocked by substituting intracellular K⁺ by Cs⁺ (Table 1), but additional application of NPPB (10 μmol/l) inhibited cAMP-activated Cl⁻ currents also (Table 1). Furthermore, application of glibenclamide (25 μmol/l) prevented the activation by cAMP of both Cl⁻ and K⁺ currents (Table 1). In CFPAC-1 cells, intracellular application of cAMP had no effect on either Cl⁻ or K⁺ currents (Table 2). However, after pretreatment of CFPAC-1

cells with glycerol, application of cAMP nearly tripled Cl⁻ current at -85 mV while K⁺ current did not change significantly (Table 2).

In association with the experiments that showed stimulation of Cl⁻/HCO₃⁻ exchange by an increase of [Ca²⁺]_i (see above), we tested for the presence of Ca²⁺-activated membrane currents in PANC-1 and CFPAC-1 cells. We included Ca²⁺ in the pipette solution to raise [Ca²⁺]_i to a free concentration of ~1 μmol/l; in addition, we studied activation of membrane currents through stimulation of purinergic receptors by extracellular application of ATP.

Raising [Ca²⁺]_i resulted in an increase of Cl⁻

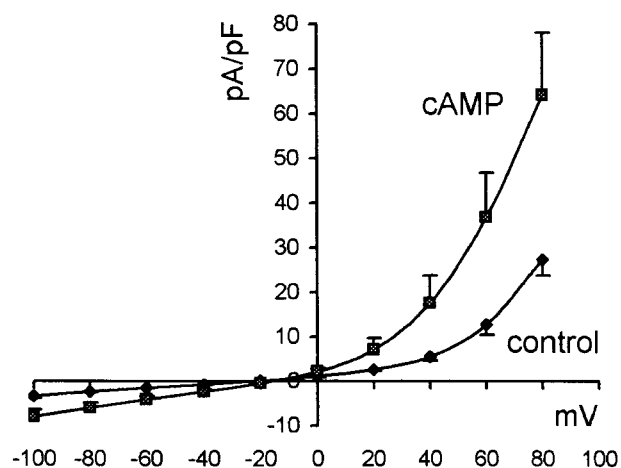


Figure 6. Whole cell patch clamp analysis of PANC-1 cells. Current-voltage relationships obtained under basal conditions ($n=10$) and after inclusion of 400 μmol/l cAMP in the patch pipettes ($n=7$). Data are presented as means ± SE.

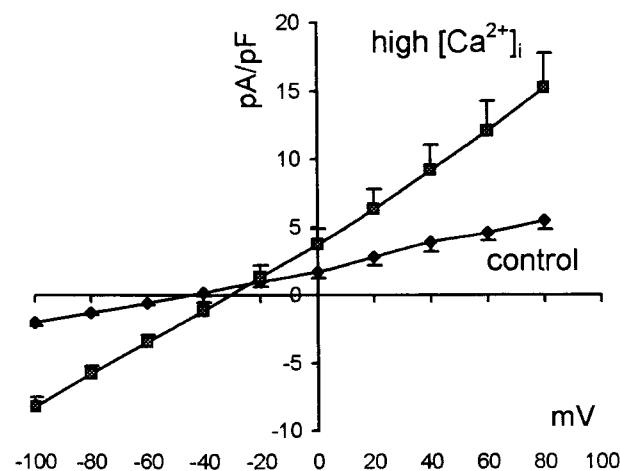


Figure 7. Whole cell patch clamp analysis of CFPAC-1 cells. Current-voltage relationships obtained under basal conditions ($n=4$) and after inclusion of 1 μmol/l Ca²⁺ in the patch pipettes ($n=5$). Note that the reversal potential is shifted toward E_{Cl} . Data are presented as means ± SE.

current in both cell lines (Tables 1 and 2). With respect to the basal level, the increase of Cl^- current by raising $[\text{Ca}^{2+}]_i$ was more pronounced in CFPAC-1 cells (Fig. 7). This increase of Cl^- current became particularly apparent when K^+ outward currents were suppressed by replacing intracellular K^+ by Cs^+ (Table 2). NPPB (10 $\mu\text{mol/l}$) was ineffective to inhibit this Ca^{2+} -activated Cl^- current. Similar to raising $[\text{Ca}^{2+}]_i$, extracellular application of 10 $\mu\text{mol/l}$ ATP led to a substantial increase of the Cl^- current in CFPAC-1 cells (Table 2).

DISCUSSION

Pancreatic duct cells secrete a bicarbonate-rich fluid in response to secretin and other gastrointestinal hormones (25). The initial step for HCO_3^- secretion is the uptake of HCO_3^- ions into the epithelial cells, a process that can occur either by direct transport of HCO_3^- on $\text{Na}^+:\text{HCO}_3^-$ cotransporters or by diffusion of CO_2 into the duct cells, followed by its hydration to H_2CO_3 and extrusion of protons via Na^+/H^+ exchangers or vacuolar H^+ -ATPases (53). HCO_3^- ions are then secreted across the apical membrane by an electroneutral $\text{Cl}^-/\text{HCO}_3^-$ exchanger. At a given pH_i , the rate at which this exchanger cycles will depend on the out-to-in Cl^- concentration gradient, where intracellular Cl^- concentration in turn depends on Cl^- efflux provided by opening of cAMP-activated apical Cl^- channels. Therefore, regulation of these channels appears to represent the main control point in the secretory mechanism.

In agreement with this concept, epithelial HCO_3^- secretion is reduced in patients with CF (26, 27). However, so far no study has directly addressed the relationships between CFTR deficiency and HCO_3^- secretion in the pancreatic duct epithelium. This study was therefore designed to directly compare $\text{Cl}^-/\text{HCO}_3^-$ exchange activity and Cl^- conductance in two human pancreatic cell lines, one possessing functional CFTR (PANC-1) and the other being homozygous for ΔF508 (CFPAC-1). This mutation is characterized by impediment of surface expression of CFTR, a defect that can be overcome by chaperoning expression by glycerol treatment (42, 43).

These two cell lines appeared to represent useful models to study parallel activation of Cl^- channels and $\text{Cl}^-/\text{HCO}_3^-$ exchange. The PANC-1 cell line retains a variety of normal differentiated epithelial cell characteristics, including expression of carbonic anhydrase (38) together with both cAMP- and Ca^{2+} -activated Cl^- conductance (54). The CFPAC-1 cell line is widely used as a model of CFTR-deficient cells (34, 35, 55–57). These cells have been shown to exhibit a high pH_i (56) but, as shown by short circuit

current measurements, retain the ability of anion secretion on purinergic stimulation (33).

Both these cell lines exhibit $\text{Cl}^-/\text{HCO}_3^-$ exchange activity that is dependent on extracellular Cl^- , independent of Na^+ , and inhibited by DIDS. We show that elevation of intracellular cAMP increases HCO_3^- extrusion in PANC-1 cells, an effect that we could also observe after glycerol treatment of ΔF508 -CFTR expressing cells. Purinergic stimulation was poorly effective in PANC-1 cells and detectable only in presence of NPPB. In contrast, HCO_3^- secretion was effectively stimulated in CFPAC-1 cells by both purinergic receptor occupancy and elevation of intracellular $[\text{Ca}^{2+}]_i$.

In interpreting these data we were faced with different concepts (proposed previously): 1) the 'classical' view that electrogenic release of Cl^- through Cl^- channels and lowering of $[\text{Cl}^-]_i$ is a prerequisite of HCO_3^- secretion via $\text{Cl}^-/\text{HCO}_3^-$ exchange (49). For this, cAMP-activated CFTR Cl^- channels could provide the necessary Cl^- conductance themselves or, alternatively, CFTR may activate other outwardly rectifying Cl^- channels (ORCC) that support $\text{Cl}^-/\text{HCO}_3^-$ exchange (15), 2) CFTR is directly responsible for HCO_3^- secretion without involving $\text{Cl}^-/\text{HCO}_3^-$ exchange (58, 59), and 3) regulation of $\text{Cl}^-/\text{HCO}_3^-$ exchange by CFTR is independent of CFTR operating as a Cl^- channel (21).

To discriminate between these possibilities, we first showed that $\text{Cl}^-/\text{HCO}_3^-$ exchange is the major if not the only mechanism of HCO_3^- extrusion in PANC-1 cells: this mechanism is dependent on extracellular Cl^- , independent of Na^+ , and inhibited by DIDS. In addition, AE2 isoform is expressed in human fetal pancreatic ducts (60). We proceeded with studying 1) the effects of inhibiting CFTR Cl^- conductance with NPPB or glibenclamide (48, 52) on HCO_3^- extrusion, 2) effects of cell depolarization by high extracellular $[\text{K}^+]$ to identify electrogenic transport components, and 3) effects on ion currents of elevating intracellular cAMP, intracellular $[\text{Ca}^{2+}]_i$, and of application of Cl^- channel blockers.

In all conditions tested, we find that activation or inhibition of HCO_3^- secretion is associated with a parallel increase or decrease of Cl^- conductance, respectively: raising intracellular cAMP lead to activation of Cl^- channels and HCO_3^- extrusion in PANC-1 cells and application of NPPB or glibenclamide inhibited both the cAMP-activated Cl^- conductance and cAMP-activated HCO_3^- extrusion. In addition, enabling ΔF508 -CFTR expression in CFPAC-1 cells by glycerol treatment restored stimulatory effects of cAMP on both Cl^- conductance and HCO_3^- secretion. In CFPAC-1 cells, stimulation of HCO_3^- extrusion by raising $[\text{Ca}^{2+}]_i$ or by purinergic stimulation with ATP were both paralleled by an increase of Cl^- conductance. Neither Ca^{2+} -activated

Cl^- -conductance nor Ca^{2+} -activated HCO_3^- extrusion was affected by NPPB. cAMP-activated HCO_3^- extrusion in PANC-1 cells and Ca^{2+} -activated HCO_3^- extrusion in CFPAC-1 cells were both abolished by cell depolarization. In addition, raising intracellular cAMP activated an outwardly rectifying current in PANC-1 cells. This current was suppressed by replacing K^+ with Cs^+ and inhibited by glibenclamide, indicating the presence of cAMP-activated K^+ channels but absence of ORCC. We therefore conclude that stimulation of $\text{Cl}^-/\text{HCO}_3^-$ exchange depends on increase of Cl^- conductance, the latter being provided by CFTR in PANC-1 cells and by Ca^{2+} -activated Cl^- channels in CFPAC-1 cells, respectively. Thus, the lack of cAMP-mediated stimulation of HCO_3^- secretion in CFTR-deficient CFPAC-1 cells is compensated for by Ca^{2+} -activated Cl^- channels that are amenable to purinergic stimulation.

Our results also point to a specific role for K^+ channels in stimulation of HCO_3^- secretion: as noted above, PANC-1 cells exhibit a large outwardly rectifying K^+ current that is further activated by cAMP together with the increase of Cl^- conductance. These observations are in accordance with previous studies on isolated pancreatic ducts that showed that stimulation by secretin and VIP leads to sequential activation of K^+ and Cl^- currents, resulting in transient membrane hyperpolarization and followed by depolarization (24, 34). Note that expression of epithelial K^+ channels may be under the control of CFTR as shown in pancreas (13) and in kidney tubular cells (12). In CFTR-deficient CFPAC-1 cells, cAMP failed to activate both Cl^- and K^+ currents. However, glycerol treatment of these cells restored cAMP-dependent Cl^- conductance without effect on K^+ current. Notwithstanding, Lous-sourn et al. have shown that transfection of CFPAC-1 cells with wild-type CFTR induced a cAMP-dependent K^+ current (13), possibly, suggesting that the ΔF508 mutation is less efficient in supporting K^+ channel expression. On the other hand, CFPAC-1 cells exhibited a large K^+ current in the presence of extracellular ATP or at high $[\text{Ca}^{2+}]_i$ that was significantly suppressed by replacing intracellular K^+ with Cs^+ (Table 2). This current appeared sufficient to provide for charge neutralization for Cl^- efflux through Ca^{2+} -activated channels.

In Fig. 8 we have summarized the proposed roles of Cl^- and K^+ channels in supporting bicarbonate secretion via $\text{Cl}^-/\text{HCO}_3^-$ exchange. The apical membrane is shown on the top, including electroneutral $\text{Cl}^-/\text{HCO}_3^-$ exchange together with cAMP-activated (CFTR; left) and Ca^{2+} -activated Cl^- channels, as found in PANC-1 and CFPAC-1 cells, respectively. Activation of these channels serves for recycling of Cl^- that enters the cell through $\text{Cl}^-/\text{HCO}_3^-$ exchange, thus permitting for HCO_3^- secretion at a high rate. Channels and

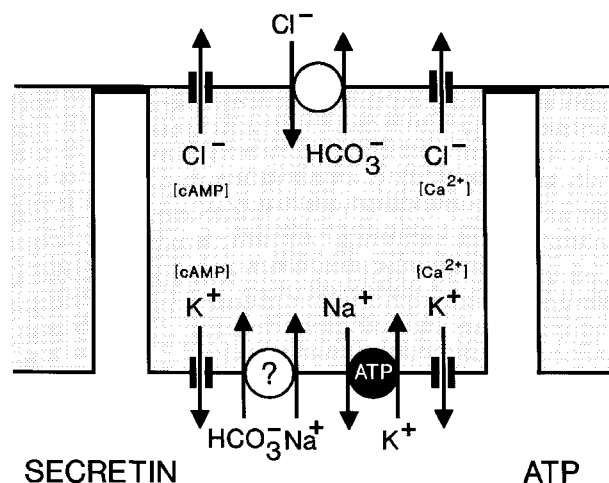


Figure 8. Model of pancreatic duct cell to show apical membrane bicarbonate secretion (upper part) by interaction of Cl^- and K^+ channels and apical $\text{Cl}^-/\text{HCO}_3^-$ exchange. The basal membrane (lower part) contains the Na^+/K^+ -pump that establishes an out-to-in Na^+ concentration gradient that serves as a driving force for intracellular accumulation of HCO_3^- via $\text{Na}^+:\text{HCO}_3^-$ symport or Na^+/H^+ exchange. Stimulation of bicarbonate secretion by secretin (left) and ATP (right) is shown. Secretin activates K^+ and Cl^- channels via generation of intracellular cAMP. Activation of basolateral K^+ channels hyperpolarizes the cell favoring apical Cl^- efflux through cAMP-activated Cl^- channels (CFTR). These channels allow for recycling of Cl^- that is taken up into the cell by $\text{Cl}^-/\text{HCO}_3^-$ exchange. ATP acts via purinergic receptors (not shown) resulting in activation of Ca^{2+} -dependent K^+ and Cl^- channels. Activation of Ca^{2+} -dependent Cl^- channels can substitute in sustaining $\text{Cl}^-/\text{HCO}_3^-$ exchange if CFTR is inoperative.

transporters of the basolateral membrane are shown in the lower part. K^+ channels play a significant role in the activation of $\text{Cl}^-/\text{HCO}_3^-$ exchange: activation of a K^+ efflux will tend to hyperpolarize the membrane potential, which, as a consequence, stimulates Cl^- efflux through apical Cl^- channels, thus reducing $[\text{Cl}^-]_i$ and providing a steeper Cl^- concentration gradient as the driving force for electroneutral $\text{Cl}^-/\text{HCO}_3^-$ exchange. Viewed differently, K^+ outward current will provide charge neutralization for efflux of Cl^- through apical Cl^- channels, which is required for recycling of Cl^- that enters the cell through $\text{Cl}^-/\text{HCO}_3^-$ exchange (61). Furthermore, in this interplay between channels and carriers, basolateral Na^+/K^+ -ATPase will serve as the primary pump to refuel intracellular K^+ . Simultaneously, the pump will maintain intracellular Na^+ concentration at a low level and thus provide the driving force for stimulation of either Na^+/H^+ exchange or $\text{Na}^+:\text{HCO}_3^-$ symport mechanisms that lead to accumulation or generation of intracellular HCO_3^- . The latter transporter exhibits reduced activity in CF (20). In this integrated view, stimulation of HCO_3^- secretion will result in simultaneous conductive apical Cl^- efflux (inward current) and basolateral K^+ efflux. Combined, these ion fluxes result in an apical-to-basolateral transcellular current

that is the basis for assessing secretion by short circuit current measurements.

In Fig. 8, secretin is depicted as the classical agonist for cAMP-mediated stimulation of HCO_3^- secretion. This mechanism is the prevailing one if CFTR is present in the apical cell membrane (data presented for PANC-1 cells). For CFTR-deficient pancreatic duct cells (CFPAC-1), our results show that Ca^{2+} -dependent apical Cl^- channels provide an alternative mechanism of stimulating apical $\text{Cl}^-/\text{HCO}_3^-$ exchange. We also show that this mechanism is activated by purinergic stimulation. This alternative activation of cAMP and Ca^{2+} -dependent Cl^- channels appears analogous to the recent observation that the decrease of cAMP-dependent Cl^- flux in gallbladder epithelium of CF patients is compensated by reciprocal increase of ATP-dependent flux (62).

This Ca^{2+} -dependent mechanism of Cl^- channel activation is of considerable interest. CFTR appears to modulate ATP secretion from the cells (15, 17) whereby extracellular ATP could serve as an autocrine purinergic agonist to stimulate Ca^{2+} -dependent transport. Furthermore, purinergic receptor agonists have been shown to enhance Cl^- transport by increasing $[\text{Ca}^{2+}]_i$ in a number of epithelia such as airway epithelial cells (63), bile duct cells (64), gallbladder (62), and pancreatic duct cells deficient in CFTR (65). In the biliary system, apical purinergic receptors have been identified and ATP is present in bile in micromolar concentrations, perhaps explaining why cholestatic symptoms of CF are delayed in their appearance (66). Trials using UTP and ATP for treatment of pulmonary complications of CF have been promising (67). The demonstration of Ca^{2+} -activated Cl^- channels in freshly isolated human pancreatic duct cells (68) and of P_{2Y_2} receptors in both CFPAC-1 cells (57) and dog pancreatic duct cells (31) suggests that similar strategies can be considered for treatment of pancreatic disease in CF.

In conclusion, our data confirm the presence of cAMP- and Ca^{2+} -activated Cl^- transport in PANC-1 and CFPAC-1 cells, respectively, and we show that stimulation of HCO_3^- secretion via $\text{Cl}^-/\text{HCO}_3^-$ exchange is linked to activation of the respective Cl^- channels. Ca^{2+} -dependent Cl^- channels and HCO_3^- secretion in CFTR deficient cells can be activated by purinergic stimulation, a mechanism that could be exploited by devising pharmacological strategies to bypass the secretory defect in cystic fibrosis and related pancreatic diseases (6). **[FJ]**

We are grateful to Dr. Carlo Spirli for skillful help in the cell culture. The technical assistance by Leszek Gajdzik is gratefully acknowledged. Á.Z. thanks Prof. László Rosivall for helpful discussions and constant support. This work was supported by grants from Telethon, Italy, E430 and E873 from MURST 1998, Italy, n. 9806210866 (to M. S.), and fellowships from the European Association for the Study of the Liver (EASL-Knoll fellowship and EASL research fellow-

ship) and from the Hungarian Foundation for Higher Education and Research (to Á.Z.).

REFERENCES

1. Marino, C. R., and Gorelick, F. S. (1992) Scientific advances in cystic fibrosis. *Gastroenterology* **103**, 681–693
2. Fuller, C. M., and Benos, D. J. (1992) CFTR! *Am. J. Physiol.* **263**, C267–C286
3. Durie, P. R., and Forstner, G. G. (1989) Pathophysiology of the exocrine pancreas in cystic fibrosis. *J. R. Soc. Med.* **82**, 2–10
4. Riordan, J. R., Rommens, J. M., Kerem, B., Alon, N., Rozmahel, R., Grzelczak, Z., Zielenski, J., Lok, S., Plavsic, N., Chou, J., Drumm, M. L., Iannuzzi, M. C., Collins, F. S., and Tsui, L. (1989) Identification of the cystic fibrosis gene: cloning and characterization of complementary DNA. *Science* **245**, 1066–1073
5. Welsh, M. J., Tsui, L. C., Boat, T. F., and Beaudet, A. L. (1995) Cystic fibrosis. In *The Metabolic Basis of Inherited Diseases* (Scriver, C., Beaudet, A., Sly, W., and Valle, D., eds) 7th Ed, pp. 3799–3876, McGraw-Hill, New York
6. Sharer, N., Schwarz, M., Malone, G., Howarth, A., Painter, J., Super, M., and Braganza, J. (1998) Mutation of the cystic fibrosis gene in patients with chronic pancreatitis. *N. Engl. J. Med.* **339**, 645–652
7. Anderson, M. P., Gregory, R. J., Thomson, S., Souza, D. W., Paul, S., Mulligan, R. C., Smith, A. E., and Welsh, M. J. (1991) Demonstration that CFTR is a chloride channel by alteration of its anion selectivity. *Science* **253**, 202–205
8. Bear, C. E., Li, C., Kartner, N., Bridges, R. J., Jensen, T. J., Ramjessingh, M., and Riordan, J. R. (1992) Purification and functional reconstitution of the cystic fibrosis transmembrane conductance regulator (CFTR). *Cell* **68**, 809–818
9. Bradbury, N. A., Jilling, T., Berta, G., Sorscher, E. J., Bridges, M. J., and Kirk, K. L. (1992) Regulation of plasma membrane recycling by CFTR. *Science* **271**, 530–531
10. Stutts, M. J., Canessa, C. M., Olsen, J. C., Hamrick, M., Cohn, J. A., Rossier, B. C., and Boucher, R. C. (1995) CFTR as a cAMP-dependent regulator of sodium channels. *Science* **269**, 847–850
11. Ismailov, I. I., Awayda, M. S., Jorov, B., Berdiev, B. K., Fuller, C. M., Dedman, J. R., Kaetzel, M., and Benos, D. J. (1996) Regulation of epithelial sodium channels by the cystic fibrosis transmembrane conductance regulator. *J. Biol. Chem.* **271**, 4725–4732
12. McNicholas, C. M., Guggino, W. B., Schwiebert, E. M., Hebert, S. C., Giebisch, G., and Egan, M. E. (1996) Sensitivity of a renal K^+ channel (ROMK2) to the inhibitory sulphonylurea compound glibenclamide is enhanced by coexpression with the ATP-binding cassette transporter cystic fibrosis transmembrane regulator. *Proc. Natl. Acad. Sci. USA* **93**, 8083–8088
13. Loussour, G., Demolombe, S., Mohammad-Panah, R., Escande, D., and Baro, I. (1996) Expression of CFTR controls cAMP-dependent activation of epithelial K^+ currents. *Am. J. Physiol.* **271**, C1565–C1573
14. Egan, M., Flotte, T., Afione, S., Solov, R., Zeitlin, P. L., Carter, B. J., and Guggino, W. B. (1992) Defective regulation of outwardly rectifying Cl^- channels by protein kinase A corrected by insertion of CFTR. *Nature (London)* **358**, 581–584
15. Schwiebert, E. M., Egan, M. E., Hwang, T. H., Fulmer, S. B., Allen, S. S., Cutting, G. R., and Guggino, W. B. (1995) CFTR regulates outwardly rectifying chloride channels through an autocrine mechanism involving ATP. *Cell* **81**, 1063–1073
16. Schreiber, R., Greger, R., Nitschke, R., and Kunzelmann, K. (1997) Cystic fibrosis transmembrane conductance regulator activates water conductance in *Xenopus* oocytes. *Pfluegers Arch.* **434**, 841–847
17. Al-Awqati, Q. (1995) Regulation of ion channels by ABC transporters that secrete ATP. *Science* **269**, 805–806
18. Barasch, J., Kiss, B., Prince, A., Saiman, L., Gruenert, D., and Al-Awqati, Q. (1991) Defective acidification of intracellular organelles in cystic fibrosis. *Nature (London)* **352**, 70–73
19. Casavola, V., Turner, R. J., Guay-Broder, C., Jacobson, K. A., Eidelman, O., and Pollard, H. B. (1995) CPX, a selective Al

- adenosine-receptor antagonist regulates intracellular pH in cystic fibrosis cells. *Am. J. Physiol.* **269**, C226–C233
20. Shumaker, H., Amlal, H., Frizzel, R., Ulrich, C. D., and Soilemani, M. (1999) CFTR drives $\text{Na}^+/\text{nHCO}_3^-$ cotransport in pancreatic duct cell: a basis for defective HCO_3^- secretion in CF. *Am. J. Physiol.* **276**, C16–C25
21. Lee, M. G., Wigley, W. C., Zeng, W. Z., Noel, L. E., Marino, C. R., Thomas, P. J., and Muallem, S. (1999) Regulation of $\text{Cl}^-/\text{HCO}_3^-$ exchange by cystic fibrosis transmembrane conductance regulator expressed in NIH 3T3 and HEK 293 cells. *J. Biol. Chem.* **274**, 3414–3421
22. Marino, C. R., Matovcik, L. M., Gorelick, F. S., and Cohn, J. A. (1991) Localization of the cystic fibrosis transmembrane conductance regulator in pancreas. *J. Clin. Invest.* **88**, 712–716
23. Zeng, W., Lee, M. G., Yan, M., Diaz, J., Benjamin, I., Marino, C. R., Kopito, R., Freedman, S., Cotton, C., Muallem, S., and Thomas, P. (1997) Immuno and functional characterization of CFTR in submandibular and pancreatic acinar and duct cells. *Am. J. Physiol.* **273**, C442–C455
24. Novak, I., and Pahl, C. (1993) Effect of secretin and inhibitors of $\text{HCO}_3^-/\text{H}^+$ transport on the membrane voltage of rat pancreatic duct cells. *Pfluegers Arch.* **425**, 272–279
25. Argent, B. E., and Case, R. M. (1994) Pancreatic ducts. Cellular mechanism and control of bicarbonate secretion. In *Physiology of the Gastrointestinal Tract* (Johnson, L. R., ed) 3rd Ed, pp. 1473–1497, New York
26. Gaskin, K. J., Durie, P., Corey, M., Wei, P., and Forstner, G. G. (1982) Evidence for a primary defect of pancreatic HCO_3^- secretion in cystic fibrosis. *Pediatr. Res.* **16**, 554–557
27. Kopelman, H. R., Corey, M., Gaskin, K. J., Durie, P., and Forstner, G. G. (1988) Impaired chloride secretion, as well as bicarbonate secretion, underlies the fluid and secretory defect in the cystic fibrosis pancreas. *Gastroenterology* **98**, 349–355
28. Jiang, S., Kopras, E., McMichael, M., Bell, R. H., and Ulrich, C. D. (1997) Vasoactive intestinal peptide (VIP) stimulates in vitro growth of VIP-1 receptor-bearing human pancreatic adenocarcinoma-derived cells. *Cancer Res.* **57**, 1475–1480
29. Slimak, G. G., Stark, H. A., Egan, J. J., Jensen, R. T., and Gardner, J. D. (1993) Effect of verapamil on the cAMP-mediated pathway for amylase secretion in rat pancreatic acini. *Pancreas* **8**, 212–219
30. Al-Nakkash, L., Simmons, N. L., Lingard, J. M., and Argent, B. E. (1996) Adenylate cyclase activity in human pancreatic adenocarcinoma cell lines. *Int. J. Pancreatol.* **19**, 39–47
31. Nguyen, T. D., Moody, M. W., Savard, C. E., and Lee, S. P. (1998) Secretory effects of ATP on nontransformed dog pancreatic duct epithelial cells. *Am. J. Physiol.* **275**, G104–G113
32. Chan, H. C., Cheung, W. T., Leung, P. Y., Wu, L. J., Cheng, S. B., Ko, W. H., and Wong, P. Y. (1996) Purinergic regulation of anion secretion by cystic fibrosis pancreatic duct cells. *Am. J. Physiol.* **271**, C469–C477
33. Galletta, L. J., Zegarra, M. O., Mastrocola, T., Wohrle, C., Rugolo, M., and Romeo, G. (1994) Activation of Ca^{2+} -dependent K^+ and Cl^- currents by UTP and ATP in CFPAC-1 cells. *Pfluegers Arch.* **426**, 534–541
34. Pahl, C., and Novak, I. (1993) Effect of vasoactive intestinal peptide, carbachol and other agonists on the membrane voltage of pancreatic duct cells. *Pfluegers Arch.* **424**, 315–320
35. Chan, H. C., Law, S. H., Leung, P. S., Fu, L. X., and Wong, P. Y. (1997) Angiotensin II receptor type I-regulated anion secretion in cystic fibrosis pancreatic duct cells. *J. Membr. Biol.* **156**, 241–249
36. Nguyen, T. D., Okolo, C. N., and Moody, M. W. (1998) Histamine stimulates ion transport by dog pancreatic duct epithelial cells through H_1 receptors. *Am. J. Physiol.* **275**, G76–G84
37. Veeze, H. J., Halley, D. J., Bijman, J., de Jongste, J. C., de Jonge, H. R., and Sinaasappel, M. (1994) Determinants of mild clinical symptoms in cystic fibrosis patients. Residual chloride secretion measured in rectal biopsies in relation to the genotype. *J. Clin. Invest.* **93**, 461–466
38. Madden, M. E., and Sarraz, M. P. (1988) Morphological and biochemical characterization of a human pancreatic ductal cell line (PANC-1). *Pancreas* **5**, 512–528
39. Schoumacher, R. A., Ram, J., Ianuzzi, N. A., Bradbury, N. A., Wallace, R. W., Hon, C. T., Kelly, D. R., Schmid, S. M., Gelder, F. B., Rado, T. A., and Frizzel, R. A. (1990) A cystic fibrosis pancreatic adenocarcinoma cell line. *Proc. Natl. Acad. Sci. USA* **87**, 4012–4016
40. Ward, C. L., Omura, S., and Kopito, R. R. (1995) Degradation of CFTR by the ubiquitin-proteasome pathway. *Cell* **83**, 121–127
41. Rubenstein, R. C., and Zeitlin, P. L. (1998) Use of protein repair therapy in the treatment of cystic fibrosis. *Curr. Opin. Pediatr.* **10**, 250–255
42. Brown, C. R., Hong-Brown, L. Q., Biwersi, J., Verkman, A. S., and Welch, W. J. (1996) Chemical chaperones correct the mutant phenotype of the deltaF508 cystic fibrosis transmembrane conductance regulator protein. *Cell Stress Chaperones* **1**, 117–125
43. Sato, S., Ward, C. L., Krouse, M. E., Wine, J. J., and Kopito, R. R. (1996) Glycerol reverses the misfolding phenotype of the most common cystic fibrosis mutation. *J. Biol. Chem.* **271**, 635–638
44. Gray, M. A., Winpenny, J. P., Porteous, D. J., Dorin, J. R., and Argent, B. E. (1994) CFTR and calcium-activated chloride currents in pancreatic duct cells of a transgenic CF mouse. *Am. J. Physiol.* **266**, C213–C221
45. Boyarsky, G., Ganz, M. B., Sterzel, R. B., and Boron, W. F. (1988) pH regulation in single glomerular mesangial cells. I. Acid extrusion in absence and presence of HCO_3^- . *Am. J. Physiol.* **255**, C844–C855
46. Hamill, O. P., Marty, A., Neher, E., Sakmann, B., and Sigworth, F. J. (1981) Improved patch clamp techniques for high resolution current recording from cells and cell-free membrane patches. *Pfluegers Arch.* **391**, 85–100
47. Worrell, R. T., Butt, A. G., Cliff, W. H., Frizzell, R. A. (1989) A volume-sensitive chloride conductance in human colonic cell line T84. *Am. J. Physiol.* **256**, C1111–C1119
48. Novak, I., and Greger, R. (1988) Properties of the luminal membrane of isolated perfused rat pancreatic ducts. Effect of cyclic AMP and blockers of chloride transport. *Pfluegers Arch.* **411**, 58–68
49. Zhao, H., Star, R. A., and Muallem, S. (1994) Membrane localization of H^+ and HCO_3^- transporters in the rat pancreatic duct. *J. Gen. Physiol.* **104**, 57–85
50. Boron, W. F. (1992) Control of intracellular pH. In *The Kidney: Physiology and Pathophysiology* (Seldin, D. W., and Giebisch, G., eds) 2nd Ed, pp. 219–263, New York
51. Tauc, M., Bidet, M., and Poujeol, P. (1996) Chloride currents activated by calcitonin and cAMP in primary cultures of rabbit distal convoluted tubule. *J. Membr. Biol.* **150**, 255–273
52. Sheppard, D. N., and Welsh, M. J. (1993) Inhibition of CFTR by ATP-sensitive K^+ channel regulators. *Ann. N.Y. Acad. Sci.* **707**, 275–284
53. Villanger, O., Veel, T., and Reader, M. G. (1995) Secretin causes $\text{H}^+/\text{HCO}_3^-$ secretion from pig pancreatic ductules by vacuolar-type H^+ -adenosine triphosphatase. *Gastroenterology* **108**, 850–859
54. Kopelman, H., Gauthier, C., and Bornstein, M. (1993) Antisense oligonucleotide to the cystic fibrosis transmembrane conductance regulator inhibits cyclic AMP-activated but not calcium activated cell volume reduction in a human pancreatic duct cell line. *J. Clin. Invest.* **91**, 1253–1257
55. Chao, A. C., Kouyama, K., Heist, E. K., Dong, Y., and Gardner, P. (1995) Calcium and CaMKII-dependent chloride secretion induced by the microsomal Ca^{2+} -ATPase inhibitor 2,5-Di-(tert-butyl)-1,4-hydroquinone in cystic fibrosis pancreatic epithelial cells. *J. Clin. Invest.* **96**, 1794–1801
56. Elgavish, A. (1991) High intracellular pH in CFPAC: A pancreas cell line from patient with cystic fibrosis is lowered by retrovirus mediated CFTR gene transfer. *Biochem. Biophys. Res. Commun.* **180**, 342–348
57. O'Reilly, C. M., O'Farrell, A. M., and Ryan, M. P. (1998) Purinoceptor activation of chloride transport in cystic fibrosis and CFTR-transfected pancreatic cell lines. *Br. J. Pharmacol.* **124**, 1597–1606
58. Poulsen, J. H., and Machen, T. E. (1996) HCO_3^- -dependent pH_i regulation in tracheal epithelial cells. *Pfluegers Arch.* **432**, 546–554
59. Hogan, D. L., Crombie, D. L., Isenberg, J. I., Svendsen, P., Schaffalitzky-de-Muckadell, O. B., and Ainsworth, M. A. (1997) CFTR mediates cAMP- and Ca^{2+} -activated duodenal epithelial HCO_3^- secretion. *Am. J. Physiol.* **272**, G872–G878
60. Hyde, K., Harrison, D., Hollingsworth, M. A., and Harris, A. (1999) Chloride-Bicarbonate exchangers in the human fetal pancreas. *Bioch. Biophys. Res. Commun.* **263**, 315–321

61. Barò, I., Roch, B., Hongre, A. S., and Escande, D. (1994) Concomitant activation of Cl^- and K^+ currents by secretory stimulation in human epithelial cells. *J. Physiol.* **478**, 469–482
62. Dray-Charier, N., Paul, A., Scoazec, J. Y., Veissière, D., Mergey, M., Capeau, J., Soubrane, O., and Housset, C. (1999) Expression of delta F508 cystic fibrosis transmembrane conductance regulator protein and related chloride transport properties in the gallbladder epithelium from cystic fibrosis patients. *Hepatology* **29**, 1624–1634
63. Rugolo, M., Mastrocola, T., Whorle, C., Rasola, A., Gruenert, D. C., Romeo, G., and Galletta, L. J. (1993) ATP and A1 adenosine receptor agonists mobilize intracellular Ca^{2+} and activate K^+ and Cl^- currents in normal and cystic fibrosis airway epithelial cells. *J. Biol. Chem.* **268**, 24779–24784
64. McGill, J., Basavappa, S., Shimohura, G. H., Middleton, J. P., and Fitz, J. G. (1996) ATP activates ion permeabilities in biliary epithelial cells. *Gastroenterology* **107**, 236–243
65. Warth, R., and Greger, R. (1993) The ion conductance of CFPAC-1 cells. *Cell Physiol.* **3**, 2–16
66. Lindblad, A., Glaumann, H., and Strandvik, B. (1998) A two-year prospective study of the effect of ursodeoxycholic acid on urinary bile acid excretion and liver morphology in cystic fibrosis-associated liver disease. *Hepatology* **27**, 166–174
67. Bennett, W. D., Olivier, K. N., Zeman, K. L., Hohneker, K. W., Boucher, R. C., and Knowles, M. R. (1996) Effect of uridine 5'-triphosphate plus amiloride on mucociliary clearance in adult cystic fibrosis. *Am. J. Resp. Crit. Care Med.* **153**, 1796–1801
68. Winpenny, J. P., Harris, A., Hollingsworth, M. A., Argent, B. E., and Gray, M. A. (1998) Calcium-activated chloride conductance in a pancreatic adenocarcinoma cell line of ductal origin (HPAF) and in freshly isolated human pancreatic duct cells. *Pfluegers Arch.* **435**, 796–803

Received for publication May 12, 1999.

Revised for publication May 8, 2000.

Correction of CFTR Malfunction and Stimulation of Ca^{2+} -Activated Cl^- Channels Restore HCO_3^- Secretion in Cystic Fibrosis Bile Ductular Cells

Ákos Zsembery,^{1,2,3} Wolfgang Jessner,¹ Gerlinde Sitter,¹ Carlo Spirli,² Mario Strazzabosco,^{2,4} and Jürg Graf¹

In view of the occurrence of hepatobiliary disorders in cystic fibrosis (CF) this study addresses the role of the cystic fibrosis transmembrane conductance regulator (CFTR) and of Ca^{2+} -activated Cl^- channels in promoting HCO_3^- secretion in bile ductular cells. Human cholangiocytes were isolated from control livers and from 1 patient with CF ($\Delta\text{F508}/\text{G542X}$ mutations). Single channel and whole cell currents were analyzed by patch clamp techniques, and HCO_3^- secretion was determined by fluorometric analysis of the rate of recovery of intracellular pH following alkaline loading. In control cholangiocytes, both cyclic adenosine monophosphate (cAMP) and protein kinase A (PKA) catalytic subunit, activated CFTR Cl^- channels that exhibited a nonrectifying conductance of 8 pS and appeared in clusters. Activation of Cl^- current by cAMP was associated with an increase in the rate of HCO_3^- secretion. The basal rate of HCO_3^- secretion was lower in CF than in control cholangiocytes. In both control and CF cholangiocytes, raising intracellular Ca^{2+} concentrations with ionomycin led to a parallel activation of Cl^- current and HCO_3^- secretion. Consistent with reports that premature stop codon mutations (class I; e.g., G542X) can be read over by treatment with aminoglycoside antibiotics, exposure of CF cholangiocytes to gentamicin restored activation by cAMP of Cl^- current and HCO_3^- secretion. The observation that activation of Ca^{2+} -dependent Cl^- channels can substitute for cystic fibrosis transmembrane conductance regulator (CFTR) in supporting HCO_3^- secretion and the efficacy of gentamicin in restoring CFTR function and HCO_3^- secretion in class I mutations are of potential clinical interest. (HEPATOLOGY 2002;35:95-104.)

Abbreviations: CF, cystic fibrosis; cAMP, cyclic adenosine monophosphate; CFTR, cystic fibrosis transmembrane conductance regulator; PKA, protein kinase A; DMSO, dimethyl sulfoxide; EDTA, ethylenediaminetetraacetic acid; EGTA, ethylene glycol-bis(β -aminoethyl ether)N,N,N',N'-tetraacetic acid; DB-cAMP, N⁶,2'-O-dibutyryl-adenosine 3':5'-cyclic monophosphate; IBMX, 3-isobutyl-1-methylxanthine; TMA-OH, tetramethyl-ammonium hydroxide; BCECF-AM, 2',7'-bis(2-carboxyethyl)-5(6)-carboxyfluorescein-acetoxymethyl ester; NPPB, 5-nitro-2-(3-phenylpropylamino)-benzoic acid; DMEM, Dulbecco's modified Eagle medium; hHGF, human hepatocyte growth factor; pH_i, intracellular pH; hBDC, human bile duct cells; CFhBDC, cystic fibrosis human bile duct cells; DIDS, 4,4'-diisothiocyano-2,2'-disulfonic acid.

From the ¹Department of Pathophysiology, University of Vienna, Vienna, Austria; ²Department of Medical and Surgical Sciences, University of Padua, Padua, Italy; ³Department of Pathophysiology, Semmelweis University, Budapest, Hungary; and ⁴Division of Gastroenterology, Ospedali Riuniti di Bergamo, Bergamo, Italy.

Received April 16, 2001; accepted October 22, 2001.

Presented in part at the 34th Annual Meeting of the European Association of the Study of the Liver and published in abstract form in *J Hepatol* 1999;30:141A.

Supported by grants from Telethon, Italy, E430 and E873, from MURST 1998, n. 9806210866 and MURST 2000, n. MM06215421 (to M.S.), from Hungarian grants OTKA 29260, FKFP 316 and ETT 226/2000 (to A.Z.) and the scientific and technical cooperation Austria-Hungary (A-8/99). M.S. and C.S. thank the Istituto Veneto di Medicina Molecolare and Fondazione per la Ricerca Biomedica Avanzata for support. Á.Z. gratefully acknowledges research fellowships from EASL and from the Hungarian Foundation for Higher Education and Research.

Address reprint requests to: Jürg Graf, M.D., Department of Pathophysiology, University of Vienna, Währinger Gürtel 18-20, 1090 Vienna, Austria. E-mail: juerg.graf@univie.ac.at; fax: (43) 1 40400 5130.

Copyright © 2002 by the American Association for the Study of Liver Diseases.

0270-9139/02/3501-0014\$35.00/0

doi:10.1053/jhep.2002.30423

Cystic fibrosis (CF) is one of the most common hereditary disorders among the white population.^{1,2} The disease impairs cyclic adenosine monophosphate (cAMP)-dependent electrolyte transport in a variety of organs. CF results from genetic defects in the cystic fibrosis transmembrane conductance regulator (CFTR), which functions as a cAMP/protein kinase A (PKA)-activated epithelial Cl^- channel.^{3,4}

In addition to operating as a low conductance chloride channel, CFTR plays an important role in the regulation of other transport mechanisms such as epithelial sodium channels, potassium channels, cAMP-independent outwardly rectifying chloride channels, ATP release, and water transport.⁵⁻⁷ In CF patients impaired HCO_3^- transport results in production of a viscous secretion in pancreas and intestine, which has been attributed to disturbed interaction of the CFTR Cl^- channel with electroneutral $\text{Cl}^-/\text{HCO}_3^-$ anion exchange mechanism.⁸⁻¹⁰ Both CFTR and anion exchange are present in the apical membrane of human and rat intrahepatic bile duct cells,¹¹⁻¹⁴ and their dysfunction likely accounts for the hepatobiliary complications that are seen more frequently with increased survival of CF patients and affect their life quality and expectancy.¹⁵

Bile duct cells (cholangiocytes) fulfil a variety of transport functions that determine the rate of secretion and the final composition of bile. The biliary secretion of electrolytes and water from the biliary epithelium is under the control of various gastrointestinal hormones.¹⁶ In intrahepatic bile duct cells, secretin and vasoactive intestinal peptide promote secretion of bicarbonate via a mechanism that appears to involve 3 consecutive steps: (1) activation of

the adenylate cyclase signal transduction pathway, (2) opening of apical Cl^- channels¹⁷, and (3) stimulation of apical $\text{Cl}^-/\text{HCO}_3^-$ exchange,^{12,18} which is driven by the outside to inside transmembrane Cl^- concentration ($[\text{Cl}^-]$) gradient at relatively high intracellular bicarbonate concentration ($[\text{HCO}_3^-]_i$).¹³ Although never directly tested in primary cultures of CF human cholangiocytes, this regulatory mechanism may be altered in CF and lead to impaired hydration and alkalinization of bile and to chronic liver damage.

In addition to cAMP-stimulated Cl^- channels, Ca^{2+} -activated Cl^- conductances have also been described in both murine^{19,20} and human biliary epithelial cells,^{21,22} but their relationship to HCO_3^- secretion and their function in CFTR-deficient cells are unknown. We studied these relationships in both control and CFTR-deficient human bile duct cells. In addition, the CF cells available to us were heterozygous at the CFTR locus, carrying the ΔF508 trafficking mutation (class II²³) on one allele and the G542X premature stop codon mutation (class I²³) on the other. These latter mutations have been shown to be amenable to "protein repair" by treatment with certain aminoglycoside antibiotics.²⁴⁻²⁶ Therefore, we also studied whether treatment with gentamycin could restore CFTR function and bicarbonate secretion in CF cholangiocytes.

Materials and Methods

Materials

HEPES, dimethylsulfoxide (DMSO), 4,4'-diisothiocyanatostilbene-2,2'-disulfonic acid, glibenclamide, nigericin, ethylenediaminetetraacetic acid (EDTA), ethylene glycol-bis(β -aminoethyl ether) N,N,N',N'-tetraacetic acid (EGTA), cholera toxin, insulin, epidermal growth factor, triiodothyronine, hydrocortisone, forskolin, ionomycin, adenosine 3':5'-cyclic monophosphate (cAMP), N⁶,2'-O-dibutyryladenosine 3':5'-cyclic monophosphate (DBcAMP), 3-isobutyl-1 methylxanthine (IBMX), adenosine-5'-triphosphate magnesium salt, adenosine-5'-triphosphate sodium salt, and tetramethyl-ammonium hydroxide (TMA-OH) were from Sigma Chemical Company (St. Louis, MO). 2',7'-Bis(2-carboxyethyl)-5(6)-carboxyfluorescein acetoxymethylester (BCECF-AM) was from Lambda GmbH (Graz, Austria). 5-Nitro-2-(3-phenylpropylamino)-benzoic acid (NPPB) was purchased from Calbiochem Chemical Co. Culture media (Dulbecco's modified Eagle medium [DMEM], HAMF 12 medium and Leibowitz L-15 medium), fetal bovine serum, gentamycin, penicillin/streptomycin and trypsin/EDTA were from GIBCO (Grand Island, NY). Percoll was purchased from Pharmacia (Cologno Monzese, Italy). The human hepatocyte growth factor (hHGF) was obtained from the Mitsubishi Corporation (Yokohama, Japan). The mouse monoclonal antibody against human epithelial antigen (HEA 125) was purchased from Progen Biotechnik GmbH (Heidelberg, Germany), and Dynabeads were from Unipax (Milano, Italy). A combination of 100 $\mu\text{mol/L}$ DBcAMP, 100 $\mu\text{mol/L}$ IBMX, and 3 $\mu\text{mol/L}$ forskolin ("cAMPmix") was used to increase intracellular cAMP concentration.²⁷

Cell Isolation and Culture

Human cholangiocytes were isolated from fragments of one liver used for reduced size orthotopic transplantation or from livers

explanted for alcohol-induced liver disease (3 patients) or CF (1 patient) as previously described^{12,28,29} and approved by the Padua University Ethical Committee. Briefly, after mincing and digesting the approximately 30 g of liver tissue with collagenase, nonparenchymal liver cells were separated by filtration and centrifugation on a discontinuous Percoll gradient and then purified by immunomagnetic separation with a monoclonal antibody directed against a 34-kd membrane glycoprotein (HEA 125), which, in the liver, is only expressed in cholangiocytes.²⁸ CF cholangiocytes were isolated by the same methods from a patient affected with CF who underwent liver transplantation for end-stage CF-related liver disease. Cholangiocytes were cultured in Falcon plastic flasks at 37°C in a humidified 95% air and 5% CO_2 atmosphere. The cells were incubated with DMEM and HAMF 12 medium containing 10 ng/mL of hHGF²⁹, fetal calf serum 5%, epidermal growth factor 10 ng/mL, hydrocortisone 0.4 $\mu\text{g/mL}$, cholera toxin 10 ng/mL, transferrin 5 $\mu\text{g/mL}$, tri-iodothyronine 2 nmol/L, insulin 5 $\mu\text{g/mL}$ and penicillin (100 U/mL)/streptomycin (0.1 mg/mL). The cells were suspended by trypsin/EDTA solution and plated on glass coverslip fragments. For patch clamp experiments, cells were used after 24 to 48 hours, whereas pH measurements were performed 3 to 4 days after plating. Cells were transferred to bicarbonate free Leibowitz L-15 medium 1 hour before use in patch clamp experiments. Gentamycin-pretreated CF cholangiocytes were prepared by incubation for 18 hours in DMEM and HAMF 12 medium supplemented with 200 $\mu\text{g/mL}$ gentamycin.

Intracellular pH

Intracellular pH (pH_i) was measured as described³⁰ by using the fluorescent intracellular sensor BCECF. In brief, BCECF was loaded into the cells in form of its tetraacetoxymethylester (BCECF-AM) (12 $\mu\text{mol/L}$) by incubation for 15 to 20 minutes at 37°C. After washing for 10 minutes at 37°C in a BCECF-free medium the cells were transferred into a temperature controlled (37°C) perfusion chamber placed on the stage of an Axiovert (Zeiss, Jena, Germany) inverted microscope. The microscope was equipped with a microfluorometer (Photon Technological Instruments, Monmouth Junction, NJ) allowing for continuous dual wavelength excitation photometry. pH_i was measured in single cells as the ratio of emission intensities at 530 nm after excitation at 495 nm (pH and concentration sensitive) and 440 nm (only concentration sensitive), respectively. Data were collected at 50 Hz chopping frequency and were averaged every 2 seconds. After each experiment internal dye calibration was performed by superfusing the cells with a medium containing high $[\text{K}^+]$ and the K^+/H^+ ionophore nigericin³¹ (12 $\mu\text{mol/L}$) at pH 6.8 and 7.6.^{9,13}

To measure HCO_3^- secretion, cells were first superfused for 10 minutes with medium containing 25 mmol/L HCO_3^- and 5% CO_2 , which results in intracellular equilibration of $[\text{HCO}_3^-]$ according to the pH_i and CO_2 concentration. Acute removal of $\text{CO}_2/\text{HCO}_3^-$ from the superfusion medium by exposure to HEPES-buffered HCO_3^- free medium (see solutions below) results in depletion of intracellular CO_2 and sudden intracellular alkalinization. pH_i recovers from this alkaline load towards the initial value. Our previous data, obtained by using both primary culture of human cholangiocytes¹² and a cholangiocarcinoma cell line (MZ-ChA-1)¹⁸ indicated that this pH_i recovery was due to the activation of Na^+ -independent $\text{Cl}^-/\text{HCO}_3^-$ exchange. The rate of

recovery from the intracellular alkaline load was determined by linear regression analysis of the slope $\delta\text{pH}/\delta t$. For comparison between individual experiments, this slope was determined at the same range of pH_i between 7.35 and 7.45, except where noted otherwise. Experimental effects on HCO_3^- secretion were studied by preincubation of the cells for 10 minutes with either cAMPmix, NPPB, high external K^+ concentration, ATP, or ionomycin. Gentamycin (200 $\mu\text{g}/\text{mL}$) was applied by preincubation for 18 hours.

Whole Cell and Single Channel Current Recordings

Whole cell configuration of the patch clamp technique was used, and single channel currents were studied by using both inside-out and cell-attached membrane patches.³² Studies were done at room temperature (22°C) using NMDG-Cl-rich and NaCl-rich extracellular solution both with 1 mmol/L free $[\text{Ca}^{2+}]$ in inside-out and whole-cell configuration, respectively. To avoid exposure of the internal surface of the plasma membrane to high $[\text{Ca}^{2+}]$ (1 mmol/L) during formation of inside-out patches we reduced free $[\text{Ca}^{2+}]$ of the bath to 100 nmol/L (0.4 mmol/L CaCl_2 + 1 mmol/L EGTA) after formation of the "giga-seal" but prior to excision of membrane patches. Recording pipettes were pulled from VC-H075P glass (Terumo, Japan) on a P-87 micropipette puller (Sutter Instrument Corp., Novato, CA) and had resistances of 2–5 M Ω . In experiments using inside-out membrane patches pipettes were filled with the NMDG-Cl-rich solution (free $[\text{Ca}^{2+}]$ = 1 mmol/L). For whole cell recordings pipettes were filled either with KCl-rich solution or CsCl-rich solution with free $[\text{Ca}^{2+}]$ adjusted to 100 nmol/L. Single channel and whole cell data were recorded with an EPC-9 amplifier and digitized (5 kHz) and stored on hard disk and analyzed by using Pulse + PulseFit version 7.4 programs (HEKA Elektronik GmbH, Lambrecht, Germany). Single channel currents were measured at clamp potentials ranging between –100 mV and +100 mV. For analysis, the analog signal was passed through a Bessel filter with the corner frequency set at 800 Hz. Whole cell currents were measured at the holding potential (–40 mV) and during 100 ms square pulses of the test potential (–100 mV to +80 mV) in 20-mV increments, with 2-second intervals (polarity given for cell interior). For control bath and KCl-rich pipette solutions the equilibrium potentials for K^+ (E_K) and Cl^- (E_{Cl}) were –86 mV and –1.3 mV, respectively. Therefore, membrane currents near these clamping voltages were considered to represent Cl^- and K^+ current, respectively. Values at –85 mV were calculated by linear interpolation between data obtained at –80 mV and –100 mV. Current-voltage relations were obtained after currents had stabilized 30 ms after applying voltage pulses. Whole cell currents were normalized for unit cell surface area by division by the whole cell membrane capacitance that ranged between 25 and 40 pF. Accordingly, current is presented as pA/pF. Corrections for pipette to bath liquid junction potentials were applied when asymmetrical solutions (KCl/NaCl or CsCl/NaCl) were used (4 mV and 5 mV, respectively).

Solutions

Buffers for pH Experiments. Bicarbonate-free bath solution (HEPES) contained the following (mmol/L): NaCl 135, KCl 4.7, MgSO_4 1, KH_2PO_4 1.2, CaCl_2 1.5, HEPES 10, glucose 5, titrated to pH 7.4 with NaOH. Bicarbonate buffered solution (KRB) con-

tained the following (mmol/L): NaCl 115, KCl 4.7, KH_2PO_4 1.2, MgCl_2 1, CaCl_2 1.5, NaHCO_3 25, glucose 5, and was equilibrated with 5% CO_2 .

Solution for Whole Cell Recordings. Control NaCl-rich bath solution contained the following (mmol/L): NaCl 150, KCl 5, MgCl_2 2, CaCl_2 1, HEPES 10, glucose 5, titrated to pH 7.4 with NaOH; osmolality, 310–320 mosm/kg. KCl-rich pipette solution contained the following (mmol/L): KCl 145, NaCl 5, MgCl_2 1, HEPES 10, CaCl_2 0.4, EGTA 1, MgATP 2, titrated to pH 7.2 with KOH; osmolality: 280–290 mosm/kg. CsCl-rich pipette solution contained the following (mmol/L): CsCl 150, MgCl_2 1, HEPES 10, CaCl_2 0.4, EGTA 1, MgATP 2, titrated to pH 7.2 with TMA-OH; osmolality: 280–290 mosm/kg.

The osmotic difference between the pipette and bath solution was applied to prevent activation of volume-activated currents.³³ With pipette solutions containing ATP, the efflux of ATP from the pipette could have stimulated purinergic membrane receptors when approaching the cell. This was avoided by first filling the pipette tip by dipping into an ATP-free pipette solution followed by filling the pipette with the ATP-containing solution from the back.

Solutions for Single Channel Recordings in Inside-Out Configuration. NMDG-Cl rich bath solution contained the following (mmol/L): NMDG-Cl 150, MgCl_2 2, CaCl_2 1.25, HEPES 10, adjusted to pH 7.3 with HCl. After seal formation and before obtaining inside-out configuration, free $[\text{Ca}^{2+}]$ of the bath solution was changed to approximately 100 nmol/L (CaCl_2 0.4 + EGTA 1). Solutions osmolality was 300 to 310 mosm/kg. Pipette solution contained the following (mmol/L): NMDG-Cl 150, MgCl_2 2, CaCl_2 1.25, HEPES 10, adjusted to pH 7.3 with HCl.

Stock solutions of NPPB, forskolin, glibenclamide, and BCECF-AM were prepared in DMSO at 1,000 times the desired concentration. Gentamycin was dissolved in water. Nigericin was dissolved in ethanol.

Statistics

Data are given as mean values \pm SEM (n = number of cells). Differences between control and experimental conditions were evaluated from the same preparation by using the unpaired one-sided Mann-Whitney test and are considered significant if $P < .05$.

Results

CFTR Is Functionally Active in Cultured Human Bile Duct Cells

The presence of functional CFTR Cl^- channels has not yet been shown in cultured human cholangiocytes. Single channel recordings were thus performed in the excised membrane patches in "inside-out" configuration and in "cell attached" mode. In excised membrane patches we used symmetrical bath/pipette solutions containing Cl^- as the only permeable ion. As shown in Fig. 1, combined administration of PKA catalytic subunit (50 U/mL) and Mg_2ATP (2 mmol/L) to the cytoplasmic face of the membrane patch activated low conductance Cl^- channels. These channels displayed a linear current-voltage relationships (I/V) with a reversal potential at 0 mV and showed a single channel conductance of approximately 8 pS. In addition, we observed flickering current when channels were open at negative membrane potentials. In

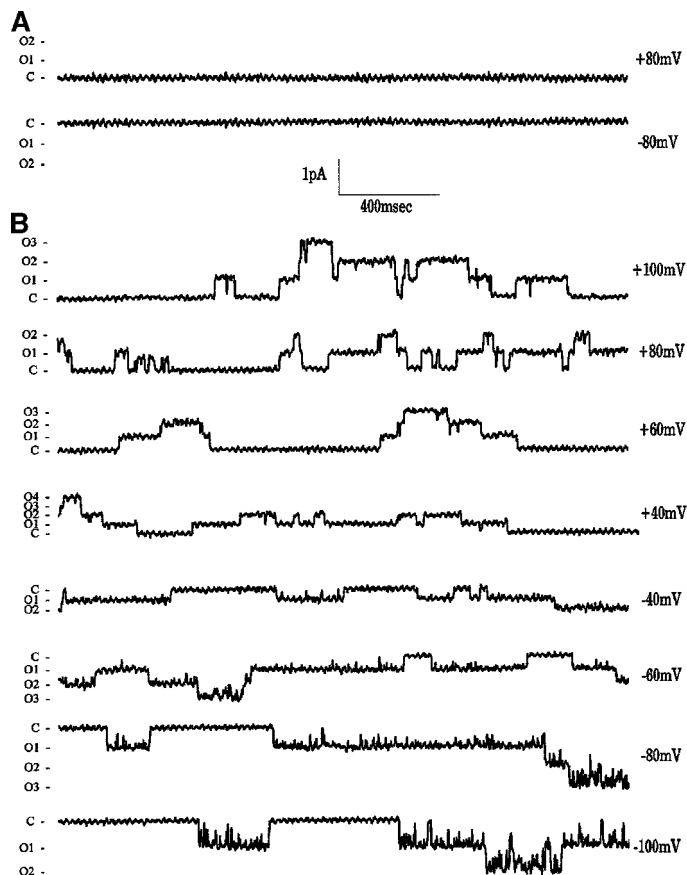


Fig. 1. Patch clamp recording in control human bile ductular cell (hBDC). Cl^- channel activity in excised inside-out configuration is shown at symmetrical NMDG-Cl concentrations. (A) No channel activity is observed under control conditions at ± 80 mV. (B) Administration of protein kinase A (50 U/mL) and Mg_2ATP (2 mmol/L) to the cytoplasmic face of the plasma membrane results in activation of up to 4 CFTR Cl^- channels. Channel currents reversed at 0 mV and channel activity displayed no voltage dependence. Note flickering current characteristics at negative clamping voltages (cytoplasmic face vs. outside). Closed and open levels are indicated.

cell-attached configuration, patches were obtained that exhibited spontaneous openings of single low-conductance channels (Fig. 2A). Application of DBcAMP (100 $\mu\text{mol/L}$) and forskolin (5 $\mu\text{mol/L}$) caused further openings with up to 5 identical channels being open at the same time (Fig. 2B). Taken together, these electrophysiologic characteristics are identical with CFTR Cl^- channels studied in other cell types.^{34,35}

HCO₃⁻ Efflux in Normal and CF Human Cholangiocytes

Microfluorometric and patch clamp experiments were made with similar experimental protocols to allow direct comparison of the rates of HCO_3^- secretion with whole cell Cl^- and K^+ currents (see below). Experiments were performed in control human bile duct cells (hBDC) and in cholangiocytes isolated from a patient with cystic fibrosis (CFhBDC). Previous studies had shown that pH recovery after intracellular alkalinization is Cl^- dependent and DIDS-inhibitable consistent with $\text{Cl}^-/\text{HCO}_3^-$ exchange activity.^{12,18} Therefore, HCO_3^- secretion, was measured by the rate of recovery of pH_i following intracellular alkalinization. Basal rates of HCO_3^- secretion (dpH/min) in different preparations ranged from 0.103 ± 0.012 to 0.222 ± 0.015 .

Raising intracellular cAMP activated HCO_3^- secretion in hBDC (Figs. 3 and 4A). DIDS (0.5 mmol/L) inhibited basal HCO_3^- secretion and prevented its stimulation by cAMP (Fig. 3). Since DIDS has no inhibitory effect on CFTR³⁶ these data support the notion that $\text{Cl}^-/\text{HCO}_3^-$ exchange is a requisite of cAMP-stimulated HCO_3^- secretion in hBDC. In contrast to hBDC, increasing intracellular cAMP in CFhBDC failed to stimulate HCO_3^- exit above the basal values ($\text{dpH}/\text{min} = 0.061 \pm 0.06$) (Fig. 5). To show that activation of HCO_3^- secretion by cAMP in hBDC was due to parallel activation of Cl^- efflux, we studied the effect of NPPB and glibenclamide, Cl^- channel blockers that are known to inhibit CFTR.^{13,37} Furthermore, we exposed the cells to high $[\text{K}^+]_o$ to depolarize the cell membrane and to inhibit Cl^- efflux. As shown in Fig. 3, high $[\text{K}^+]_o$, glibenclamide, and NPPB inhibited the stimulatory effects of cAMP on HCO_3^- efflux in hBDC.

To test whether Ca^{2+} -stimulated Cl^- channels could provide an alternative pathway for Cl^- efflux and possibly support $\text{Cl}^-/\text{HCO}_3^-$ exchange we studied the effects of raising intracellular Ca^{2+} concentration with the calcium ionophore ionomycin³⁸ (extracellular $[\text{Ca}^{2+}]$ being buffered to 1 $\mu\text{mol/L}$) and of purinergic receptor activation by ATP (100 $\mu\text{mol/L}$). Increasing $[\text{Ca}^{2+}]_i$ by ionomycin caused a significant stimulation in HCO_3^- extrusion in both hBDC (determined in the pH range between 7.4 and 7.5) (Figs. 3 and 6A) and CFhBDC (Figs. 5 and 6C). If present throughout the experiment ATP failed to activate HCO_3^- secretion in both hBDC (Fig. 3) and CFhBDC (Fig. 5). As noted below,

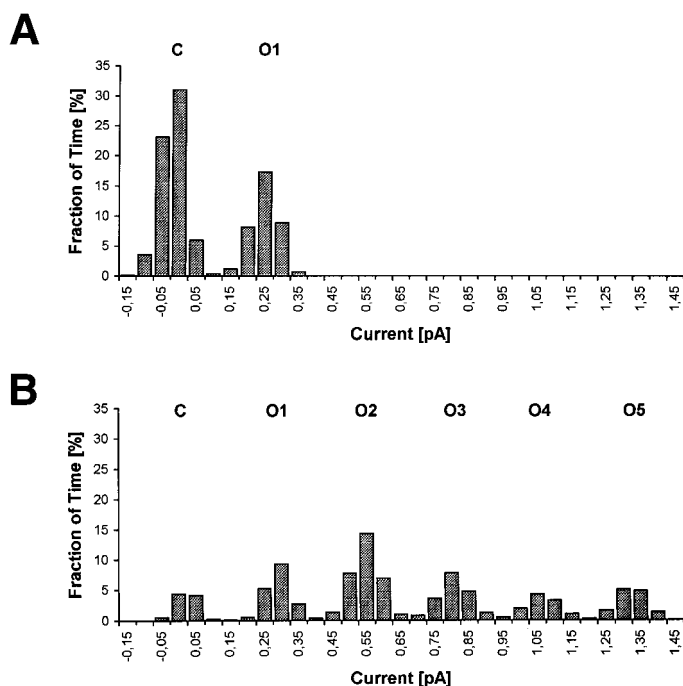


Fig. 2. (A) Amplitude histogram of CFTR channel current in cell-attached configuration under control conditions in hBDC. Time fraction of only one open state is 0.36. (B) In the same patch, increasing intracellular cAMP concentration (100 $\mu\text{mol/L}$ DBcAMP + 5 $\mu\text{mol/L}$ forskolin), activated additional channels with up to 5 channels being open simultaneously. Time fractions for 0, 1, 2, 3, 4, and 5 channels being open are 0.09, 0.18, 0.32, 0.18, 0.10, and 0.13, respectively. Clamping voltage was + 80 mV (pipette negative) and bin width for sampling was 0.05 pA. Closed and open levels are indicated.

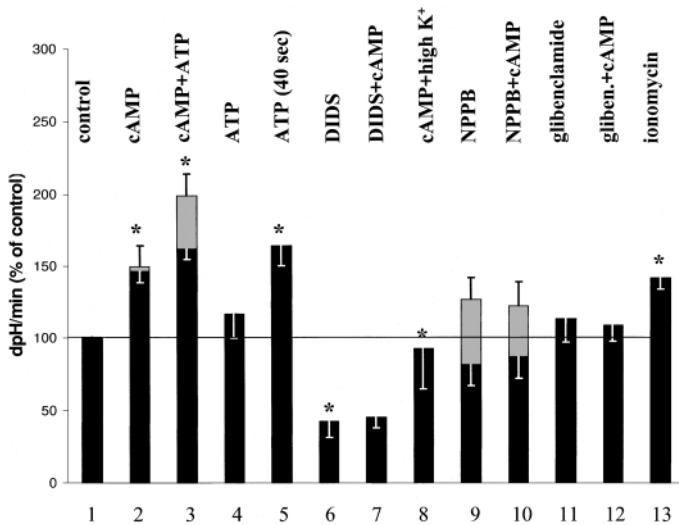


Fig. 3. HCO_3^- secretion in hBDC: HCO_3^- secretion was assessed by the rates of recovery of intracellular pH after an alkaline load. Experimental values are shown with reference to control rates obtained from the same preparation. Note: (1) stimulation of HCO_3^- extrusion by raising intracellular cAMP (column 2), which was further augmented in the presence of extracellular ATP (column 3); (2) lack of effect of continuous presence of ATP alone but stimulation of HCO_3^- extrusion immediately after application of ATP (columns 4 and 5, respectively); (3) inhibition of both basal and cAMP-stimulated HCO_3^- secretion by DIDS (columns 6 and 7, respectively); (4) inhibition of cAMP-stimulated HCO_3^- extrusion by membrane depolarization (column 8) or in the presence of CFTR channel inhibitors NPPB (columns 9 and 10) or glibenclamide (columns 11 and 12); and (5) activation of HCO_3^- extrusion by raising intracellular Ca^{2+} concentration with ionomycin (column 13). Experiments shown in columns 2, 3, 9, and 10 were repeated in 2 different preparations. Statistics (* $P < .05$): 2 vs. 1, $P < .005$ ($n = 5$) and $P < .01$ ($n = 14$); 3 vs. 2, $P < .05$ ($n = 4$) and not significant (NS) ($n = 4$); 4 vs. 1, NS ($n = 6$); 5 vs. 1, $P < .05$ ($n = 6$); 6 vs. 1, $P < .025$ ($n = 8$); 7 vs. 6, NS ($n = 6$); 8 vs. 2, $P < .05$ ($n = 5$); 9 vs. 1, NS ($n = 5$) and NS ($n = 6$); 10 vs. 9, NS ($n = 5$) and NS ($n = 6$); 11 vs. 1, NS ($n = 5$); 12 vs. 11, NS ($n = 11$); and 13 vs. 1, $P < .05$ ($n = 4$).

application of ATP in hBDC resulted only in a short lasting stimulation of ionic currents consistent with its transient effect on $[\text{Ca}^{2+}]_i$.³⁹ Therefore we administered ATP 40 seconds after alkaline loading, which resulted in an abrupt acceleration of the rate of

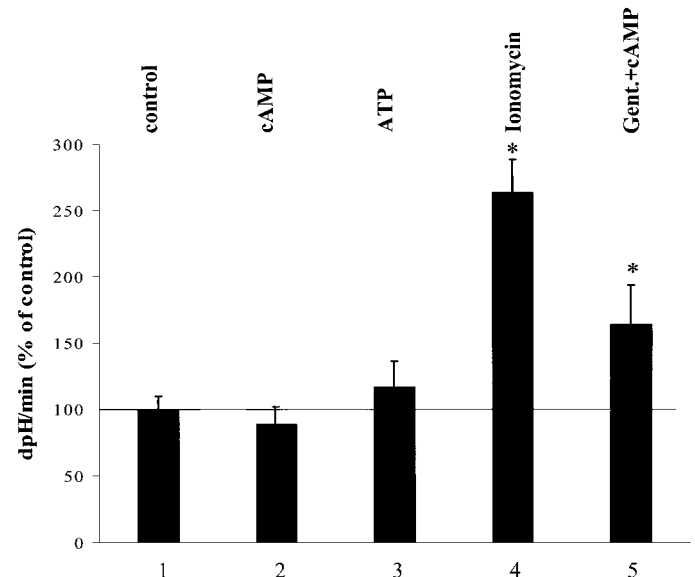


Fig. 5. HCO_3^- secretion in CFhBDC: HCO_3^- secretion was assessed by the rates of recovery of intracellular pH after an alkaline load. Experimental values are shown with reference to control rates. Note: (1) Absence of effect of raising intracellular cAMP (column 2) and of the continuous presence of extracellular ATP (column 3); (2) large activation of HCO_3^- extrusion by raising intracellular Ca^{2+} concentration with ionomycin (column 4); and (3) unveiling of cAMP-stimulated HCO_3^- secretion by restoring translation of CFTR-G542X with gentamycin (column 5). Statistics (* $P < .05$): 2 vs. 1, NS ($n = 6$); 3 vs. 1, NS ($n = 5$); 4 vs. 1, $P < .005$ ($n = 4$); and 5 vs. 2, $P < .05$ ($n = 6$).

HCO_3^- extrusion from $(\text{dpH}/\text{min}) 0.154 \pm 0.017$ to 0.253 ± 0.021 ($n = 6$; data obtained in the pH range from 7.45 to 7.30) (Fig. 3). As shown previously¹⁸ increasing intracellular cAMP and simultaneous presence of extracellular ATP resulted in an additive effect in stimulating HCO_3^- extrusion (Fig. 3).

Ca²⁺ and cAMP-Dependent Cl⁻ Currents in Normal and CF Cholangiocytes

We used whole cell recordings to correlate effects of cAMP and $[\text{Ca}^{2+}]_i$ on HCO_3^- secretion with changes of whole cell membrane

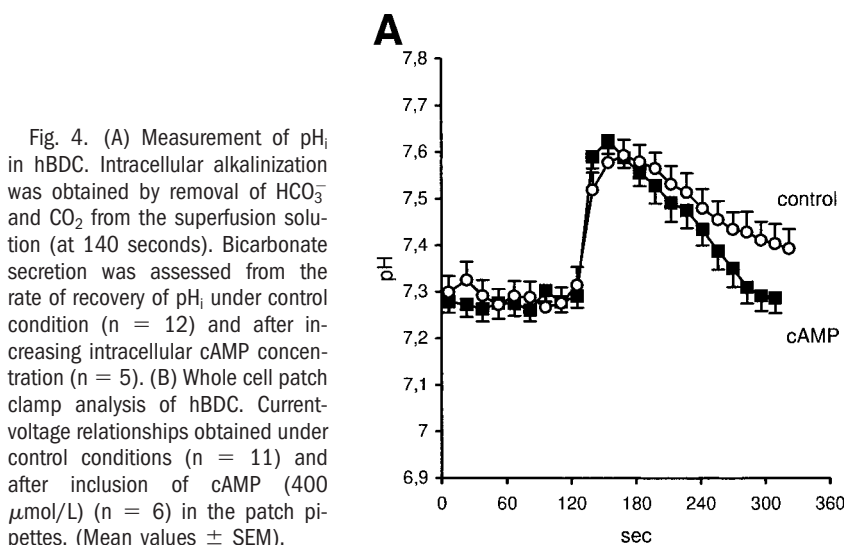
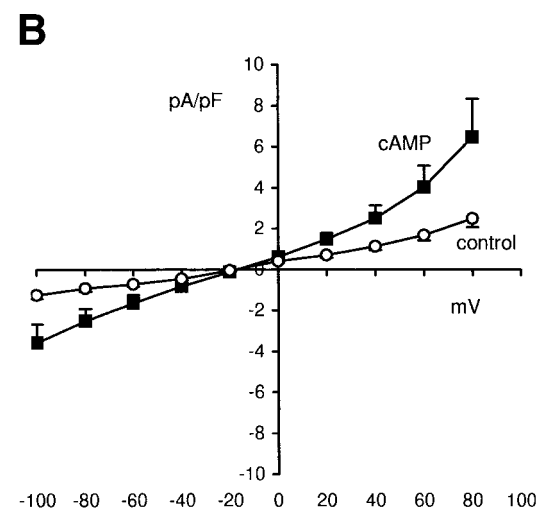


Fig. 4. (A) Measurement of pH_i in hBDC. Intracellular alkalinization was obtained by removal of HCO_3^- and CO_2 from the superfusion solution (at 140 seconds). Bicarbonate secretion was assessed from the rate of recovery of pH_i under control condition ($n = 12$) and after increasing intracellular cAMP concentration ($n = 5$). (B) Whole cell patch clamp analysis of hBDC. Current-voltage relationships obtained under control conditions ($n = 11$) and after inclusion of cAMP (400 $\mu\text{mol/L}$) ($n = 6$) in the patch pipettes. (Mean values \pm SEM).



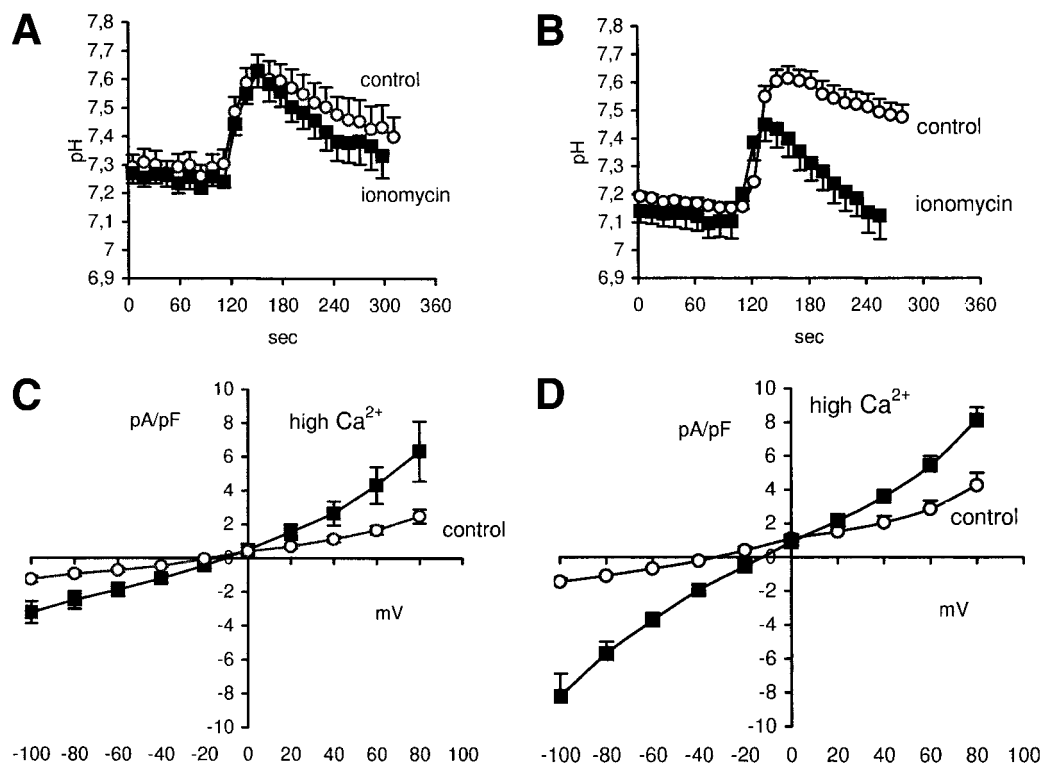


Fig. 6. (A) Measurement of pH_i in hBDC. Bicarbonate secretion was assessed from the rate of recovery of pH_i as in Fig. 4A under control condition (n = 12) and after application of ionomycin (n = 4). (B) Whole cell patch clamp analysis of hBDC. Current-voltage relationships obtained under control conditions (n = 8) and after inclusion of 1 μ mol/L Ca²⁺ (n = 8) in the patch pipettes. (C) Measurement of recovery of pH_i in CFhBDC, under control condition (n = 6) and after increasing [Ca²⁺]_i by application of ionomycin (n = 4). Note that the rate of HCO₃⁻ secretion in CFhBDC under control conditions is lower than in hBDC but pH recovery was complete after approximately 10 minutes. (D) Whole cell patch clamp analysis of CFhBDC. Current-voltage relationships obtained under control conditions (n = 14) and after inclusion of 1 μ mol/L Ca²⁺ (n = 4) in the patch pipettes. Mean values \pm SEM.

currents. Similar to a previous study performed in pancreatic duct cells,⁹ current/voltage (I/V) relations were obtained by using standard KCl-rich pipette solution and NaCl-rich bath solution. Application of these solutions allows us to obtain a measure of K⁺ current at 0 mV (near E_{Cl} where the driving force for Cl⁻ current is absent) and of Cl⁻ current at -85 mV (near E_K where K⁺ current is absent). It may be noted that Cl⁻ inward current reflects conductive Cl⁻ efflux. In addition to these parameters, Tables 1 and 2 give also the current reversal potentials (V_{rev}) where outward I_K (I_K = gK * (V_m - E_K)) and inward I_{Cl} (I_{Cl} = gCl * (V_m - E_{Cl})) are of equal magnitude resulting in zero total membrane current. Depending on the relative values of membrane K⁺ and Cl⁻ conductance, gK and gCl, respectively, the reversal potential will be close to E_K if gK >> gCl or close to E_{Cl} if gCl >> gK. Outward currents at +80 mV may consist of both, K⁺ and Cl⁻ components. Figure 4B shows I/V relationships in control hBDC cells, and Table 1 gives the corresponding parameters for Cl⁻ and K⁺ cur-

rents. In these cells, intracellular application of 400 μ mol/L cAMP resulted in a 3.3-fold increase of Cl⁻ current (measured at E_K), whereas K⁺ current (measured at E_{Cl}) was stimulated 1.8-fold. In CFhBDC, intracellular application of cAMP had no effect on either Cl⁻ or K⁺ currents (Table 2). In association with the experiments that showed stimulation of HCO₃⁻ extrusion by an increase of [Ca²⁺]_i (see above) we tested for the presence of Ca²⁺-activated membrane currents in both control and CF cells: we studied activation of currents by raising [Ca²⁺]_i to a free concentration of approximately 1 μ mol/L and after stimulation of purinergic receptors by extracellular application of ATP (100 μ mol/L). Elevation of [Ca²⁺]_i increased Cl⁻ current 2.7- and 5.2-fold in hBDC (Fig. 6B and Table 1) and in CFhBDC (Fig. 6D and Table 2), respectively. No effects of [Ca²⁺]_i on K⁺ currents were observed (Figs. 6B and 6D and Tables 1 and 2). Effects of ATP were studied with standard intracellular K⁺ concentrations at clamping voltages of 0 and -85 mV to explore the time course of activation of K⁺ and Cl⁻ currents by ATP: 10 seconds after application of ATP K⁺ current (measured at 0 mV) increased in an amazingly wide range (up to 100-fold), whereas Cl⁻ current increased up to 13-fold. This current stimulation was transient and current returned towards control values within 1 minute (data not shown).^{22,39}

Table 1. Patch Clamp Whole Cell Recordings in hBDC

	Control (KCl) (n = 11)	cAMP (KCl) (n = 6)	High [Ca ²⁺] _i (KCl) (n = 8)
-85 mV	-0.93 \pm 0.15	-3.00 \pm 0.68*	-2.48 \pm 0.56†
0 mV	+0.41 \pm 0.08	+0.74 \pm 0.11‡	+0.50 \pm 0.28 NS
+80 mV	+2.49 \pm 0.42	+6.69 \pm 1.54*	+6.34 \pm 1.91‡
Reversal potential	-18.6 \pm 2.4	-15.7 \pm 1.3 NS	-9.6 \pm 2.6‡

NOTE. Currents are pA/pF; positive values = outward current; reversal potential (mV), inside with respect to outside. Values are mean \pm SEM; number of cells is shown in parentheses.

Abbreviations: KCl, KCl-rich pipette solution; NS, not significant.

*P < .005.

†P < .025.

‡P < .05.

Correction of Cl⁻ and HCO₃⁻ Secretory Defect in CFhBDC by Gentamicin

Class I mutations of CFTR, which result in premature stop codons (e.g., G542X) can be corrected with certain aminoglycoside antibiotics.²⁴⁻²⁶ We pretreated CFhBDC with 200 μ g/mL gentamicin for 18 hours and measured HCO₃⁻ extrusion in the presence of cAMPmix. As shown in Figs. 5 and 7A gentamicin-treated CFhBDC regained cAMP-stimulated HCO₃⁻ secretory activity. In CFhBDC cells pretreated with gentamicin we also studied the

Table 2. Patch Clamp Whole Cell Recordings in CFhBDC

	Control (KCl) (n = 14)	cAMP (KCl) (n = 7)	High $[Ca^{2+}]_i$ (KCl) (n = 4)	cAMP (CsCl) (n = 4)	cAMP + Gentamycin (CsCl) (n = 4)
-85 mV	-1.10 ± 0.13	-1.27 ± 0.25 NS	-5.72 ± 0.83*	-0.67 ± 0.1	-1.85 ± 0.33†
0 mV	+1.10 ± 0.25	+0.87 ± 0.14 NS	+0.90 ± 0.12 NS	+0.34 ± 0.08	+0.34 ± 0.06 NS
+80 mV	+4.27 ± 0.76	+3.59 ± 0.59 NS	+8.13 ± 0.87†	+1.24 ± 0.19	+3.20 ± 0.41‡
Reversal potential	-31.4 ± 4.2	-21.1 ± 3.6 NS	-12.4 ± 0.6†	-19.6 ± 5.7	-13.7 ± 0.8 NS

NOTE. Currents are pA/pF; positive values = outward current; reversal potential (mV), inside with respect to outside. Values are mean ± SEM.

Abbreviations: KCl, KCl-rich pipette solution; CsCl, CsCl-rich pipette solution; NS, not significant.

* $P < .001$.

† $P < .05$.

‡ $P < .025$.

effects of cAMPmix on whole cell Cl^- currents substituting K^+ by Cs^+ in the pipette solution to eliminate outward K^+ currents. The data show that gentamicin pretreated cells regained cAMP-stimulated Cl^- currents measured at -80 mV and +80 mV (Fig. 7B and Table 2). Thus, activation by cAMP of Cl^- currents and HCO_3^- secretion could both be restored in CF cholangiocytes carrying the premature stop codon mutation (G542X).

Discussion

In CF, electrolyte transport is impaired in various epithelia, including pancreatic ducts in which both Cl^- and HCO_3^- secretion is compromised.^{9,40} In the liver, CFTR is specifically expressed in the biliary epithelium.¹⁹ A major function of cholangiocytes is the secretion of HCO_3^- , which is stimulated by secretin via the cAMP-PKA signal transduction pathway.^{13,41} Hepatobiliary disease in patients with CF primarily affects intrahepatic bile ductular cells rather than hepatocytes.^{15,42} However, the effects of defective CFTR on biliary cells secretory function have not been studied as yet. We have addressed this issue in primary cultures of intrahepatic bile ductular cells isolated from control livers and from 1 patient with CF.

Intrahepatic bile ductular cells secrete HCO_3^- across the apical membrane by Cl^-/HCO_3^- exchange.¹²⁻¹⁴ This anion exchange is driven by the out-to-in Cl^- concentration gradient where $[Cl^-]_i$ is

maintained low by electrogenic efflux across apical Cl^- channels. CFTR has been localized at the apical membrane⁴³ and its hormonal activation could allow for rapid Cl^- recycling during stimulated HCO_3^- secretion. Using patch clamp techniques we show that human cholangiocytes express a cAMP-PKA activated Cl^- channel that exhibits a nonrectifying conductance of approximately 8 pS, features that are characteristic for CFTR Cl^- channels.^{34,35} In excised inside-out membrane patches the channel was completely inactive but was activated after administration of catalytic subunit of PKA in the presence of ATP. In control cells without stimulation, low basal CFTR channel activity was observed in the cell-attached configuration (Fig. 2A). This basal channel activity could explain why HCO_3^- extrusion rate is higher in control cells than in CF cells (see below). In both configurations, either none or multiple channels were observed. This observation is in accordance with the notion that CFTR chloride channels are expressed in clusters on the plasma membrane.⁴⁴

In this study we show that cAMP activates HCO_3^- output and Cl^- conductance only in control but not in CF cholangiocytes. Thus, regulation of cAMP-PKA-dependent Cl^- channels seems to represent the main control point in HCO_3^- secretory mechanism. We have recently shown that cAMP stimulates whole-cell Cl^- conductance and Cl^-/HCO_3^- exchange in a pancreatic adenocarcinoma cell line (PANC-1).⁹ In contrast, in a CFTR-deficient

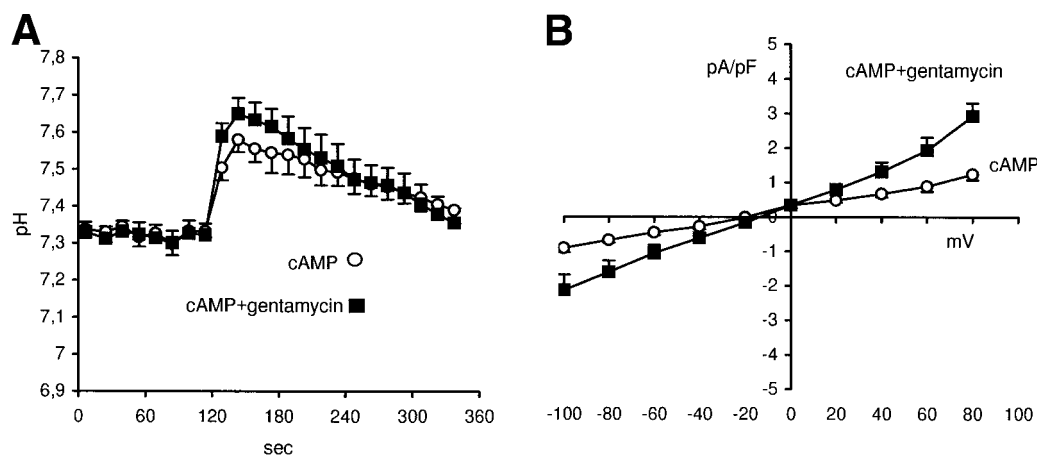


Fig. 7. (A) Measurement of recovery of pH_i in CFhBDC. Experimental maneuver was as in Fig. 4A. Bicarbonate secretion was assessed after increasing intracellular cAMP concentration by application of cAMPmix without pretreatment (n = 6) and after preincubation of CFhBDC with gentamicin (200 μ g/mL) for 18 hours (n = 6). (B) Whole cell patch clamp analysis of CFhBDC. Patch pipette solutions contained CsCl. Current-voltage relationships were obtained in the presence of 400 μ mol/L cAMP in the patch pipettes without pretreatment (n = 4) and in cells preincubated in the presence of gentamicin (200 μ g/mL) for 18 hours (n = 4). Mean values ± SEM.

cell line (CFPAC-1) cAMP failed to stimulate both whole cell Cl^- conductance and $\text{Cl}^-/\text{HCO}_3^-$ exchange activity.⁹ To test the concept of whether Cl^- channel function could support cAMP-stimulated HCO_3^- secretion in hBDC we inhibited electrogenic Cl^- efflux by either NPPB and glibenclamide or by cell membrane depolarization. Application of 10 $\mu\text{mol/L}$ NPPB, or 100 $\mu\text{mol/L}$ glibenclamide concentrations sufficient to block CFTR,^{13,37} inhibited HCO_3^- transport. It is noticed that these data do not confirm those of a previous study in which inhibition by NPPB of cAMP-stimulated HCO_3^- secretion could not be shown.¹² A similar inhibition was obtained following membrane depolarization by application of high extracellular K^+ concentration. Inhibition of HCO_3^- extrusion by these maneuvers allows for a dual explanation: (1) inhibition of electrogenic HCO_3^- efflux through CFTR Cl^- channels or (2) inhibition of electrogenic Cl^- efflux that prevents Cl^- from recycling, which is required to support electroneutral $\text{Cl}^-/\text{HCO}_3^-$ exchange.

It has been proposed that the CFTR Cl^- channel may itself provide for HCO_3^- efflux.⁴⁵⁻⁴⁸ However, in the presence of DIDS, cAMP failed to stimulate HCO_3^- extrusion in hBDC indicating that $\text{Cl}^-/\text{HCO}_3^-$ exchange is likely the major, if not the only mechanism of cAMP-dependent HCO_3^- extrusion.^{12,18} It is noted, though, that basal HCO_3^- extrusion was not completely inhibited by DIDS (Fig. 3) or by omission of extracellular Cl^- (data not shown). It appears possible that anion channels that allow for Cl^- current in nonstimulated cells (Fig. 4B and Table 1) may also provide a means for basal HCO_3^- efflux.

In aggregate these data provide the first direct evidence that cAMP-dependent Cl^- and HCO_3^- transport are both impaired in CFTR-deficient cholangiocytes. The resulting reduced hydration and alkalinity of bile could precipitate a series of events able to damage the biliary epithelium. Thus retention of bile acids and cytotoxic xenobiotics¹⁵ and a reduction in natural defense against microbial pathogens^{49,50} may finally lead to the typical focal biliary cirrhosis. Therefore, amelioration of Cl^- and particularly of HCO_3^- ^{51,52} secretion should prevent the progression of the disease.

Stimulation of Ca^{2+} -activated Cl^- conductance present in biliary epithelial cells,²² could provide an alternative pathway for stimulation of HCO_3^- secretion. The supplemental role of non-CFTR Cl^- channels in bile ductular secretion is also supported by the finding that over-expression of Ca^{2+} -activated Cl^- channels in CFTR (-/-) knockout mice could be responsible for lack of cystic fibrosis bile duct lesions.⁵³ To test whether Cl^- channels other than CFTR could support HCO_3^- secretion we studied activation of Cl^- conductances by raising $[\text{Ca}^{2+}]_i$. We show that application of ionomycin stimulated both Cl^- current and HCO_3^- secretion. Although cAMP failed to activate HCO_3^- secretion in CF cholangiocytes this Ca^{2+} -dependent mechanism was not only preserved but even more pronounced in CF cells. Purinergic nucleotides are present in bile in concentrations sufficient to activate purinergic receptors.⁵⁴ Stimulation of these receptors may promote anion transport both in biliary^{18,21,22} and pancreatic⁵⁵ duct epithelial cells, at least transiently.^{19,20} Interestingly, ATP stimulated HCO_3^- secretion only in the presence of elevated intracellular cAMP as previously shown.¹⁸ In both control and CF cholangiocytes continuous presence of ATP (100 $\mu\text{mol/L}$) alone had no

stimulatory effect on the basal rate of HCO_3^- secretion (Figs. 3 and 5). This observation could be explained by the transient nature of the ATP effect on $[\text{Ca}^{2+}]_i$ and by the short-lasting and irregular activation of K^+ and Cl^- currents.^{22,39} Indeed, ATP administered during the course of pH recovery after alkalization immediately accelerated the rate of HCO_3^- extrusion in hBDC (Fig. 3). Unfortunately no more cells were available to conduct this experiment in CFhBDC. Nevertheless, our data obtained with ionomycin indicate that the alternative Ca^{2+} -dependent signal transduction pathway is able to support fluid secretion in CFTR-deficient cells and could possibly be used for ameliorating the organ damage in CF.^{56,57}

Other strategies for restoration of CFTR function in CF are conceptualized as "protein repair" therapies that aim at correcting abnormal function in a specific mutation. More than 800 mutations in the CFTR gene have been identified and classified in 5 groups.²³ Many patients are double heterozygous in these mutations. The CFTR-deficient cells used in this study were heterozygous exhibiting the $\Delta\text{F508}/\text{G542X}$ alleles, mutations belonging to class II and class I groups, respectively. Class I mutations lead to defects in the synthesis of the full-length CFTR protein, class II mutations are characterized by the abnormal targeting of the protein from the endoplasmic reticulum to the surface membrane.²³ It has been shown that the defect in type I mutations can be corrected by certain aminoglycoside antibiotics (such as gentamicin but not streptomycin) that are able to bind the decoding site in ribosomal RNA and to suppress premature terminations of CFTR translation.^{24-26,58} Accordingly, in a small number of CF patients with class I mutations, application of gentamicin increases transport rates in the nasal mucosa.⁵⁹ Following the experimental protocol of Bedwell et al.²⁵ we could show that pretreatment of CF cholangiocytes with gentamicin promoted the appearance of both cAMP-activated Cl^- current and cAMP-stimulated HCO_3^- secretion. However, in contrast to the study by Bedwell et al.²⁵ in a bronchial epithelial cell line (IB3-1), the Cl^- current activated in cholangiocytes by gentamicin did not exhibit a significant outwardly rectifying component. The other allele in our CF cells carried the ΔF508 mutation (class II). We had previously shown that chaperoning with glycerol leads to proper surface membrane targeting of CFTR- ΔF508 , which restored cAMP-dependent HCO_3^- transport in CF pancreatic ductular cells.⁹ Unfortunately, no more $\Delta\text{F508}/\text{G542X}$ cholangiocytes were available and analogous experiments to restore CFTR function in bile ductular cells could not be performed.

In conclusion, this study in primary culture of human cholangiocytes shows activation by cAMP-PKA of CFTR at the level of single ion channels. We show that human CF cholangiocytes lack both cAMP-stimulated Cl^- and HCO_3^- secretion, however in these cells Ca^{2+} -activated Cl^- channels are able to support HCO_3^- secretion. Finally, in case of a class I mutation, gentamicin is able to promote expression of a functional CFTR protein. Taken together our observations that activation of Ca^{2+} -dependent Cl^- channels and gentamicin-induced expression of CFTR Cl^- channels can restore HCO_3^- secretion in CF cholangiocytes may be of clinical interest.

Acknowledgment: The authors are grateful to Drs. Carla Colombo and Maria Luisa Melzi (Cystic Fibrosis Center, Milan,

Italy) for providing the CF liver specimen and to the members of the Laboratory of Genetics, Istituti Clinici di Perfezionamento, Milan, Italy, for diagnosis of the mutations. The technical assistance by Leszek Gajdzik is gratefully acknowledged. Ákos Zsembery thanks Dr. László Rosivall for helpful discussion and his constant support.

References

- Marino CR, Gorelick FS. Scientific advances in cystic fibrosis. *Gastroenterology* 1992;103:681-693.
- Fuller CM, Benos DJ. CFTR! *Am J Physiol* 1992;263:C267-C286.
- Riordan JR, Rommens JM, Kerem B, Alon N, Rozmahel R, Grzelczak Z, Zielenski J, et al. Identification of the cystic fibrosis gene: cloning and characterization of complementary DNA. *Science* 1989;245:1066-1073.
- Welsh MJ, Tsui LC, Boat TF, Beaudet AL. Cystic fibrosis. In: Scriver C, Beaudet A, Sly W, Valle D, eds. *The Metabolic Basis of Inherited Diseases*. 7th ed. New York: McGraw-Hill, 1995;3799-3876.
- Schwiebert EM, Benos DJ, Egan ME, Stutts MJ, Guggino WB. CFTR is a conductance regulator as well as a Cl^- channel. *Physiol Rev* 1999;79(Suppl):145-166.
- Braunstein GM, Roman RM, Clancy JP, Kudlow BA, Taylor AL, Shylonsky VG, et al. Cystic fibrosis transmembrane conductance regulator facilitates ATP release by stimulating a separate ATP release channel for autocrine control of cell volume regulation. *J Biol Chem* 2001;276:6621-6630.
- Schreiber R, Greger R, Nitschke R, Kunzelmann K. Cystic fibrosis transmembrane conductance regulator activates water conductance in *Xenopus* oocytes. *Pflügers Arch* 1997;434:841-847.
- Lee MG, Wigley WC, Zeng W, Noel LE, Marino CR, Thomas PJ, Muallem S. Regulation of $\text{Cl}^-/\text{HCO}_3^-$ exchange by cystic fibrosis transmembrane conductance regulator expressed in NIH 3T3 and HEK 293 cells. *J Biol Chem* 1999;274:3414-3421.
- Zsembery Á, Strazzabosco M, Graf J. Ca^{2+} -activated Cl^- channels can substitute for CFTR in stimulation of pancreatic duct bicarbonate secretion. *FASEB J* 2000;14:2345-2356.
- Lee MG, Choi JY, Luo X, Strickland E, Thomas PJ, Muallem S. Cystic fibrosis transmembrane conductance regulator regulates luminal $\text{Cl}^-/\text{HCO}_3^-$ exchange in mouse submandibular and pancreatic ducts. *J Biol Chem* 1999;274:14670-14677.
- Basavappa S, Middleton J, Mangel AW, McGill JM, Cohn JA, Fitz JG. Cl^- and K^+ transport in human biliary cell lines. *Gastroenterology* 1993;104:1796-1805.
- Strazzabosco M, Joplin R, Zsembery Á, Wallace L, Spirli C, Fabris L, Granato A, et al. Na^+ -dependent and -independent $\text{Cl}^-/\text{HCO}_3^-$ exchange mediate cellular HCO_3^- transport in cultured human intrahepatic bile duct cells. *HEPATOLOGY* 1997;25:976-985.
- Alvaro D, Cho WK, Mennone A, Boyer JL. Effect of secretin on intracellular pH regulation in isolated rat bile duct epithelial cells. *J Clin Invest* 1993;92:1314-1325.
- Martinez-Anso E, Castillo JE, Diez J, Medina JF, Prieto J. Immunohistochemical detection of chloride/bicarbonate anion exchangers in human liver. *HEPATOLOGY* 1994;19:1400-1406.
- Colombo C, Battezzati PM, Strazzabosco M, Podda M. Liver and biliary problems in cystic fibrosis. *Sem Liv Dis* 1998;18:227-235.
- Baiocchi L, LeSage G, Glaser S, Alpini G. Regulation of cholangiocyte bile secretion. *J Hepatol* 1999;31:179-191.
- McGill JM, Basavappa S, Gettys TW, Fitz JG. Secretin activates Cl^- channels in bile duct epithelial cells through a cAMP-dependent mechanism. *Am J Physiol* 1994;266:G731-G736.
- Zsembery Á, Spirli C, Granato A, LaRusso NF, Okolicsányi L, Crepaldi C, Strazzabosco M. Purinergic regulation of acid/base transport in human and rat biliary epithelial cell lines. *HEPATOLOGY* 1998;28:914-920.
- Fitz JG, Basavappa S, McGill JM, Melhus O, Cohn JA. Regulation of membrane chloride currents in rat bile duct epithelial cells. *J Clin Invest* 1993;91:319-328.
- Gruber AD, Gandhi R, Pauli BU. The murine calcium-sensitive chloride channel (mCaCC) is widely expressed in secretory epithelia and in other select tissues. *Histochem Cell Biol* 1998;110:43-49.
- Chinet T, Fouassier L, Charier ND, Ghali MI, Morel H, Mergey M, Doussert B, et al. Regulation of electrogenic anion secretion in normal and cystic fibrosis gallbladder mucosa. *HEPATOLOGY* 1999;29:5-13.
- McGill JM, Basavappa S, Shimokura GH, Middleton JP, Fitz JG. ATP activates ion permeabilities in biliary epithelial cells. *Gastroenterology* 1994;107:236-243.
- Zeitlin PM. Novel pharmacologic therapies for cystic fibrosis. *J Clin Invest* 1999;103:447-452.
- Howard M, Frizzell RA, Bedwell DM. Aminoglycoside antibiotics restore CFTR function by overcoming premature stop mutations. *Nat Med* 1996;2:467-469.
- Bedwell DM, Kaenjak A, Benos DJ, Bebek Z, Bubien JK, Hong J, Tousson A, et al. Suppression of a CFTR premature stop mutation in a bronchial epithelial cell line. *Nat Med* 1997;3:1280-1284.
- Kaufman RJ. Correction of genetic disease by making sense from nonsense. *J Clin Invest* 1999;104:367-368.
- Gray MA, Winpenny JP, Porteous DJ, Dorin JR, Argent BE. CFTR and calcium-activated chloride currents in pancreatic duct cells of a transgenic CF mouse. *Am J Physiol* 1994;266:C213-C221.
- Joplin R, Strain AJ, Neuberger JM. Immunolocalization and culture of biliary epithelial cells from normal human liver. *In Vitro Cell Dev Biol* 1989;25:1189-1192.
- Joplin R, Hishida T, Tsubouchi H, Daikuhara Y, Ayres R, Neuberger JM, Strain AJ. Human intrahepatic biliary epithelial cells proliferate in vitro in response to human hepatocyte growth factor. *J Clin Invest* 1992;90:1284-1289.
- Boyarsky G, Ganz MB, Sterzel RB, Boron WF. pH regulation in single glomerular mesangial cells. I. Acid extrusion in absence and presence of HCO_3^- . *Am J Physiol* 1988;255:C844-C855.
- Thomas JA, Buchsbaum RN, Zimniak A, Racker E. Intracellular pH measurements in Ehrlich ascites tumor cells utilizing spectroscopic probes generated in situ. *Biochemistry* 1979;18:2210-2218.
- Hamill OP, Marty A, Neher E, Sakmann B, Sigworth FJ. Improved patch clamp techniques for high resolution current recording from cells and cell-free membrane patches. *Pflügers Arch* 1981;391:85-100.
- Worrell RT, Butt AG, Cliff WH, Frizzell RA. A volume-sensitive chloride conductance in human colonic cell line T84. *Am J Physiol* 1989;256:C1111-C1119.
- Zeng W, Lee MG, Yan M, Diaz J, Benjamin I, Marino CR, Kopito R, et al. Immuno and functional characterization of CFTR in submandibular and pancreatic acinar and duct cells. *Am J Physiol* 1997;273:C442-C455.
- Fischer H, Machen TE. The tyrosine kinase p60c-src regulates the fast gate of the cystic fibrosis transmembrane conductance regulator chloride channel. *Biophys J* 1996;71:3073-3082.
- Ballard ST, Trout L, Bebek Z, Sorscher EJ, Crews A. CFTR involvement in chloride, bicarbonate, and liquid secretion by airway submucosal glands. *Am J Physiol* 1999;277:L694-L699.
- Sheppard DN, Welsh MJ. Inhibition of CFTR by ATP-sensitive K^+ channel regulators. *Ann N Acad Sci* 1993;707:275-284.
- Williams DA, Fay FS. Intracellular calibration of the fluorescent calcium indicator Fura-2. *Cell Calcium* 1990;11:75-83.
- Warth R, Greger R. The ion conductance of CFPAC-1 cells. *Cell Physiol* 1993;3:2-16.

40. Kopelman HR, Corey M, Gaskin KJ, Durie P, Forstner GG. Impaired chloride secretion, as well as bicarbonate secretion, underlies the fluid and secretory defect in the cystic fibrosis pancreas. *Gastroenterology* 1988;98:349-355.
41. Zsembery Á, Thalhammer T, Graf J. Bile formation: a concerted action of membrane transporters in hepatocytes and cholangiocytes. *News Physiol Sci* 2000;15:6-11.
42. Lindblad A, Glaumann H, Strandvik B. A two-year prospective study of the effect of ursodeoxycholic acid on urinary bile acid excretion and liver morphology in cystic fibrosis-associated liver disease. *HEPATOL-OGY* 1998;27:166-174.
43. Kinnman N, Lindblad A, Housset C, Buentke E, Scheynius A, Strandvik B, Hultcrantz R. Expression of cystic fibrosis conductance regulator in liver tissue from patients with cystic fibrosis. *HEPATOL-OGY* 2000;32:334-340.
44. Naren AP, Cormet-Boyaka E, Fu J, Villain M, Blalock JE, Quick MW, Kirk KL. CFTR chloride channel regulation by an interdomain interaction. *Science* 1999;286:544-548.
45. Illek B, Yankaskas JR, Machen TE. cAMP and genistein stimulate HCO_3^- conductance through CFTR in human airway epithelia. *Am J Physiol* 1997;272:L752-L761.
46. Hogan DL, Crombie DL, Isenberg JI, Svendsen P, Schaffalitzky OB, Muckadell D, Ainsworth MA. Acid-stimulated duodenal bicarbonate secretion involves a CFTR-mediated transport pathway in mice. *Gastroenterology* 1997;113:533-541.
47. Illek B, Tam AW, Fischer H, Machen TE. Anion selectivity of apical membrane conductance of Calu 3 human airway epithelium. *Pflügers Arch* 1999;437:812-822.
48. Devor DC, Singh AK, Lambert LC, DeLuca AJ, Frizzel RA, Bridges RJ. Bicarbonate and chloride secretion in Calu-3 human airway epithelial cells. *J Gen Physiol* 1999;113:743-760.
49. Bals R, Weiner DJ, Wilson JM. The innate immune system in cystic fibrosis lung diseases. *J Clin Invest* 1999;103:303-307.
50. Strazzabosco M, Spirli C, Okolicsanyi L. Pathophysiology of the intra-hepatic biliary epithelium. *J Gastroen Hepatol* 2000;15:244-253.
51. Choi JY, Muallem D, Kiselyov K, Lee MG, Thomas PJ, Muallem S. Aberrant CFTR-dependent HCO_3^- transport in mutations associated with cystic fibrosis. *Nature* 2001;410:94-97.
52. Quinton PM. The neglected ion: HCO_3^- . *Nat Med* 2001;7:292-293.
53. Clarke LL, Grubb BR, Yankaskas JR, Cotton CU, McKenzie A, Boucher RC. Relationship of a non-cystic fibrosis transmembrane conductance regulator-mediated chloride conductance to organ-level disease in *Cftr*(-/-) mice. *Proc Natl Acad Sci U S A* 1994;91:479-483.
54. Chari RS, Schutz SM, Haebig JE, Shimokura GH, Cotton PB, Fitz JG, Meyers WC. Adenosine nucleotides in bile. *Am J Physiol* 1996;270:G246-G252.
55. Nguyen TD, Moody MW, Savard CE, Lee SP. Secretory effects of ATP on nontransformed dog pancreatic duct epithelial cells. *Am J Physiol* 1998;275:G104-G113.
56. Cheung CY, Wang XF, Chan HC. Stimulation of HCO_3^- secretion across cystic fibrosis pancreatic duct cells by extracellular ATP. *Biol Sig Receptors* 1998;7:321-327.
57. Bennett WD, Olivier KN, Zeman KL, Hohnaker KW, Boucher RC, Knowles MR. Effect of uridine 5'-triphosphate plus amiloride on mucociliary clearance in adult cystic fibrosis. *Am J Respir Crit Care Med* 1996;153:1796-1801.
58. Schroeder R, Waldisch C, Wank H. Modulation of RNA function by aminoglycoside antibiotics. *EMBO J* 2000;19:1-9.
59. Wilschanski M, Fardini C, Blau H, Rivlin J, Augarten A, Avital A, Kerem B, et al. A pilot study of the effect of gentamycin on nasal potential difference measurements in cystic fibrosis patients carrying stop mutations. *Am J Respir Crit Care Med* 2000;161:860-865.

Review

Extracellular ATP as a signaling molecule for epithelial cells

Erik M. Schwiebert^{a,b,c,*}, Akos Zsembery^{a,c,d}^aDepartment of Physiology and Biophysics, University of Alabama at Birmingham, 1918 University Boulevard, Birmingham, AL 35294-0005, USA^bDepartment of Cell Biology, University of Alabama at Birmingham, 1918 University Boulevard, Birmingham, AL 35294-0005, USA^cGregory Fleming James Cystic Fibrosis Research Center, University of Alabama at Birmingham, 1918 University Boulevard, Birmingham, AL 35294-0005, USA^dHungarian Academy of Sciences and Semmelweis University Nephrology Research Group, Budapest, Hungary

Received 23 September 2002; received in revised form 8 April 2003; accepted 4 July 2003

Abstract

The charge of this invited review is to present a convincing case for the fact that cells release their ATP for physiological reasons. Many of our “purinergic” colleagues as well as ourselves have experienced resistance to this concept, because it is teleologically counter-intuitive. This review serves to integrate the three main tenets of extracellular ATP signaling: ATP release from cells, ATP receptors on cells, and ATP receptor-driven signaling within cells to affect cell or tissue physiology. First principles will be discussed in the Introduction concerning extracellular ATP signaling. All possible cellular mechanisms of ATP release will then be presented. Use of nucleotide and nucleoside scavengers as well as broad-specificity purinergic receptor antagonists will be presented as a method of detecting endogenous ATP release affecting a biological endpoint. Innovative methods of detecting released ATP by adapting luciferase detection reagents or by using “biosensors” will be presented.

Because our laboratory has been primarily interested in epithelial cell physiology and pathophysiology for several years, the role of extracellular ATP in regulation of epithelial cell function will be the focus of this review. For ATP release to be physiologically relevant, receptors for ATP are required at the cell surface. The families of P2Y G protein-coupled receptors and ATP-gated P2X receptor channels will be introduced. Particular attention will be paid to P2X receptor channels that mediate the fast actions of extracellular ATP signaling, much like neurotransmitter-gated channels versus metabotropic heptahelical neurotransmitter receptors that couple to G proteins. Finally, fascinating biological paradigms in which extracellular ATP signaling has been implicated will be highlighted. It is the goal of this review to convert and attract new scientists into the exploding field of extracellular nucleotide signaling and to convince the reader that extracellular ATP is indeed a signaling molecule.

© 2003 Elsevier B.V. All rights reserved.

Keywords: ATP; Extracellular nucleotide signaling; P2X receptor channel**1. Introduction**

To understand autocrine and paracrine ATP signaling, the “first principles” of extracellular nucleotide and nucleoside signaling must be presented. No other review in the past spoke to all of the issues germane to extracellular ATP signaling than the review by Gordon in 1986 [1]. This review is modeled after that treatise, having benefited from 16 additional years of productive research as well as the emergence of new ideas. The first evidence that extracellular

adenine compounds may have physiological activities was described by Drury and Szent-Gyorgyi in 1929 [2]. This early study opened a new field of cardiovascular research investigating effects of extracellular purine nucleotides and nucleosides in blood flow. However, more than 40 years passed before adenosine re-emerged as an important autocrine and paracrine mediator in extracellular signaling [3]. In 1972, Burnstock [4] postulated that ATP could act as an extracellular signal in nerve-mediated responses of the smooth muscles in the gastrointestinal tract and bladder. Initially, this concept was met with considerable skepticism. Today, we already know that extracellular signaling through purinoceptors is vital not only in excitable cells and tissues but also in non-excitable cells and tissues.

Newly synthesized ATP is first made and transported out of the mitochondrion via oxidative phosphorylation. The

* Corresponding author. Department of Physiology and Biophysics, University of Alabama at Birmingham, MCLM 740, 1918 University Boulevard, Birmingham, AL 35294-0005, USA. Tel.: +1-205-934-6234; fax: +1-205-934-1445.

E-mail address: eschwiebert@physiology.uab.edu (E.M. Schwiebert).

steady-state cytosolic concentration of ATP is 3–10 mM, the fuel for countless metabolic and enzymatic reactions. Because ATP is essential for metabolism, release of this precious energy substrate is met with some anxiety. Nevertheless, if one assumes that the steady-state extracellular ATP is approximately 10 nM under basal conditions and intracellular ATP is 10 mM, the gradient for ATP secretion or efflux is approximately 10^6 -fold. This gradient is 100-fold greater, yet opposite to, the gradient for calcium entry into cells. Naturally, if a pathway is activated or opened for ATP release, ATP would exit the cell down a very favorable chemical concentration gradient. However, it must be emphasized that only 1% or less of the intracellular ATP pool needs to be released to activate maximally any and all receptors. Thus, accomplishment of extracellular ATP signaling can occur without compromising cellular metabolism or essential enzymatic reactions.

Purinoreceptors are divided into two classes: P1 or adenosine receptors and P2, which recognize primarily extracellular ATP, ADP, UTP and UDP [5]. The P2 receptors are further subdivided into two subclasses. P2X receptors are extracellular ATP-gated calcium-permeable non-selective cation channels that are modulated by extracellular Ca^{2+} , Na^+ , Mg^{2+} , H^+ and metal ions, such as Zn^{2+} and/or Cu^{2+} [6]. P2Y receptors (with exception of P2Y₁₂ and P2Y₁₃) couple to heterotrimeric G proteins and phospholipases (primarily phospholipase C β) to raise intracellular free calcium concentration [7]. Once released, ATP is free to bind to P2X and P2Y receptors, on the same cell or neighboring cells. Alternatively, ADP, a metabolite, may also bind with high affinity to a subset of P2 receptors. UTP and UDP follow

similar chemistry and have their specific P2Y receptor subtypes; however, the intracellular concentration of UTP is micromolar rather than millimolar. The final metabolite of ATP, adenosine, is also biologically active and binds to P1 receptors. Once these receptors are activated, signal transduction begins and affects cell or tissue function. These “first principles” are illustrated in Fig. 1 in the context of three neighboring epithelial cells in a polarized epithelium.

Once ATP leaves the cell, it is also degraded rapidly; thus, it is thought of as a local mediator that acts in an autocrine or paracrine manner within tissues and tissue microenvironments to stimulate its receptors before it is chemically modified. Ecto-enzymes secreted into the extracellular milieu as a secreted protein or membrane-bound as an ecto-enzyme target ATP. Ecto-apyrases cleave the gamma- and beta-phosphates of ATP, yielding ADP and 5'-AMP. Ecto-ATPases and ADPases also subserve this function. Ecto-5'-nucleotidases can convert 5'-AMP into adenosine, a higher-affinity purinergic agonist than ATP for its own class of P1 G protein-coupled receptors. Like any biochemical reaction, these can occur in reverse to re-synthesize ATP. Secreted or membrane-bound ecto-kinases such as adenylate kinase or nucleoside monophospho- and diphosphokinases can phosphorylate nucleosides to remake 5'-AMP, ADP and, ultimately, the triphosphate nucleotide ATP [8].

In this review, we put particular emphasis on mechanisms by which ATP is released from the cells and purinergic receptors and signaling in epithelial cells that transduce that extracellular ATP signal.

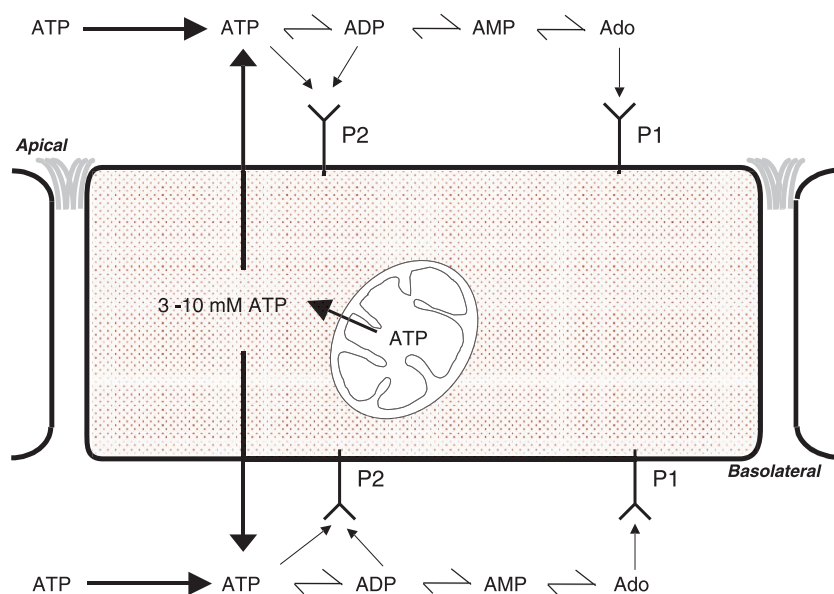


Fig. 1. The first principles of extracellular ATP signaling. This epithelial cell model illustrates the first principles of extracellular ATP signaling in the apical and basolateral spaces. Intracellular ATP generated by the mitochondria creates a large intracellular pool and an enormous gradient for ATP efflux, secretion, or release. Nevertheless, only 1% or less of this cytosolic ATP pool is required to be released to stimulate P2 receptors and stimulate signal transduction in the same cell or in a neighboring cell. Not every cell in the epithelium needs to release its ATP; it can diffuse from a neighboring cell that released it.

2. Mechanisms of ATP release into the extracellular milieu

Driven by the very favorable chemical concentration gradient for ATP secretion out of the cell, many possible ATP release mechanisms have been postulated. Considerable evidence has been amassed that adenosine is transported across the membrane by concentrative nucleoside transporters (CNTs) or equilibrative (bidirectional) nucleoside transporters (ENTs) [9]. By analogy, similar release mechanisms have been entertained for nucleotides. Emerging work has also shown that adenosine is also created in large part by extracellular metabolism of ATP. Lessons can first be derived from the mitochondrion. Newly synthesized ATP is transported across the inner or cristine membrane of the mitochondrion by an adenine nucleotide transporter (ANT) that exchanges an ATP molecule for its metabolite, ADP. Mitochondrial porins (also known as voltage-dependent anion channels (VDACs)) conduct the ATP across the outer membrane into the cytosol. There is considerable biological debate about which ATP transport mechanism is more critical for mitochondrial export.

2.1. ATP-permeable release channels

Pictured in the context of our favorite cell model (Fig. 2), the polarized epithelial cell, ATP could be conducted passively down its favorable chemical concentration gradient by ATP-permeable release channels. These are likely anion channels (plasma membrane forms of VDAC or other chloride channels) that have significant permeability to larger anions like gluconate and ATP. These ATP release channels could reside in the apical or basolateral membrane. The existence of ion channels, that are permeated by ATP anions, was underscored by many laboratories investigating whether the cystic fibrosis transmembrane conductance regulator (CFTR) conducted ATP⁻ itself in addition to Cl⁻ or regulated a separate ion channel that was permeable to ATP⁻. One group suggested that CFTR and the multidrug resistance transporter (mdr or P-glycoprotein) conducted ATP⁻ [10,11]. Schwiebert et al. [12] showed that CFTR potentiated autocrine ATP release to upregulate a separate anion channel, the outwardly rectifying Cl⁻ channel (ORCC). The simplest interpretation was that CFTR conducted ATP⁻; however, this group was careful to point out that CFTR, as a conductance regulator, might also regulate an ATP release channel, transporter, or other release pathway [12]. Subsequently, several other laboratories failed to show conduction of ATP⁻ through CFTR [13–16]; each laboratory performed a limited number of experiments in their system of choice and stopped early in their study when the negative data mounted. Recent studies by Braunstein et al. [17] and by Sugita et al. [18] have shown that CFTR is likely not an ATP conductive channel itself; however, it is closely associated with a separate ATP-permeable channel that it regulates positively. Nevertheless, its membership in

the superfamily of ATP-binding cassette (ABC) transporters suggests that it could transport ATP and other larger anions non-conductively at larger rates, given the large range of substances transported promiscuously by ABC transporters.

A handful of laboratories have performed additional research to begin to identify ATP release pathways in cells, to understand why CFTR would potentiate ATP release from cells and in response to the best stimuli, and to identify more specifically any and all ATP-permeable release channels. An initial assumption is that ATP-permeable release channels are anion channels. ATP release assays in hepatocytes and cholangiocytes by Fitz et al., airway and renal epithelial cells by Schwiebert et al., and heterologous cells by both of these laboratories has identified the lanthanides, gadolinium and lanthanum, as blockers of ATP release under basal and stimulated conditions [17,19–21]. The lanthanides are known blockers of mechanosensitive ion channels that are permeable to cations as well as anions. Braunstein et al. [17] has also shown that the disulfonic stilbene, DIDS, is a blocker of ATP release that is even more potent than gadolinium. Taken together, blockade of ATP release in biological cells by these agents suggests that ATP release channels are important conduits for ATP release.

One assumption is that some specific anion channels may also be permeable to ATP⁻. Are there likely candidates for ATP-permeable anion channels? Thinnes et al. [22,23] among others have documented that plasma membrane forms of porins or voltage-dependent anion channels (PL-VDACs) exist in a variety of cell types. In one study, they show co-localization of CFTR with a PL-VDAC [22]. It is known that “maxi” Cl⁻ channels (or large conductance anion channels) with voltage-dependent inactivation characteristics similar to VDAC have been found by numerous investigators in numerous cell types. In fact, Fitz et al. and Schwiebert et al. have studied such “maxi” anion channels in the past in Chinese hamster ovary (CHO) cells [24,25] and renal cortical collecting duct (CCD) cells [26,27], respectively. Because VDAC is a major conduit for release of newly synthesized ATP in the outer membrane of the mitochondrion [28], an ATP-permeable VDAC in the plasma membrane may be a major conductive pathway for ATP exit into the extracellular milieu. Light, Schwiebert and Stanton [26,27] showed that the “maxi” anion channel in RCCT-28A cells, an A-type intercalated cell line from rabbit CCD, had significant permeability to gluconate (Cl:gluconate 8:1) and bicarbonate (Cl:HCO₃ 2:1). Sabirov et al. [29] have shown recently that an ATP-permeable “maxi” anion channel is expressed in mouse mammary carcinoma (C127) cells. Recent preliminary work from Liu et al. [30] have implicated a “maxi” anion channel in ATP release from the macula densa induced by changes in NaCl concentration in the cTAL. It is postulated that this ATP-permeable “maxi” anion channel is responsible for ATP release from the macula densa that diffuses to and binds to P2 receptors in the glomerulus as an important signal for tubuloglomerular feedback, a form of single nephron “autoregulation.” A

similar maxi anion channel (approximately 380–400 pS) has been found in cell-attached and excised patch-clamp recordings from non-CF and CF airway epithelial primary cultures and cell lines and is permeable to a multitude of different anions including ATP (E.M. Schwiebert, unpublished observations). Taken together, it is clear that the VDAC-like “maxi” anion channels are a leading candidate for ATP release channels in the plasma membrane of many cell types and tissues.

ATP-permeable anion channels may not be limited to “maxi” anion channels. At least two other candidates have been implicated indirectly in published studies. These include, but are not limited to, the ORCC and the volume-sensitive organic anion channel (VSOAC). In a study by Braunstein et al. [17], planar lipid bilayer experiments where bovine tracheal epithelial vesicle protein was fused with the bilayers containing or immunodepleted of CFTR protein. In each condition, an ATP conductance of approximately 20 pS was recorded that was potentiated by hydrostatic pressure applied to the bilayer and was inhibited by DIDS, gadolinium, and DPC. In the condition immunodepleted of CFTR protein, the ORCC was still present, as determined by removing ATP-containing solutions and replacing ATP with Cl^- containing solutions. The simplest interpretation was that the 40–80 pS ORCC Cl^- channel had a partial permeability to ATP. Because ORCCs may be conferred by CLC-3 and/or CLC-5 channels (or a heteromeric mixture of these two CLC channels along with additional CLC subtypes), CLC channels may also be candidates for ATP release channels. Another, equally valid, interpretation was that the 20 pS ATP channel was conferred by a separate protein. Another candidate for this ATP channel is the VSOAC channel first described and named as such by Strange et al. In an initial characterization, Jackson and Strange [31] showed that intracellular mM ATP concentrations supported VSOAC currents, while supraphysiologic external concentrations of mM ATP actually blocked macroscopic VSOAC currents carried by Cl^- or by organic osmolytes such as betaine or taurine. Because this external block was concentration- and voltage-dependent, ATP can be deduced to be a possible pore blocker of VSOAC and, thus, a partially permeable species along with large anions such as taurine and betaine. It has been shown that non-excitable cells, like hepatocytes, communicate via nucleotide release [32]. ATP efflux is not uniform across a field of cells but is restricted to abrupt point-source bursts [33]. Transient activation of connexin hemichannels is thought to mediate this ATP release [34].

It is important to note that these release channels may differ in their expression as well as their polarity of expression (if studied, in epithelial or endothelial cells or in neurons). The next few years of work by several laboratories should uncover much new information in the arena of ATP release channels. Arguably, this field was brought into the light via the controversy concerning CFTR, mdr, and ATP permeability through these ABC transporters.

Without that series of papers for and against this phenomenon, it is possible that this field may not have emerged this rapidly or at all.

2.2. Adenine nucleotide transporters

Like the nucleoside transporters, concentrative or equilibrative nucleotide transporters may also exist for ATP that are carriers or permeases. The ABC transporters such as the CFTR, the multidrug resistance proteins (mdr, MRP), and the multiple organic anion transporters (MOATs) may act as non-conductive transporters of ATP, along with a multitude of other substrates. Exchangers may exist for ATP in the plasma membrane, as they do in mitochondrial inner membrane, where ADP may be the exchanged substrate. Other substrates such as Na^+ or Cl^- , which have favorable entry gradients, may be exchanged for ATP. This could also occur apically or basolaterally. These possible transport mechanisms are also illustrated in Fig. 2.

Even though evidence is emerging that ABC transporters do not conduct ATP at rates consistent with an ionic channel, these transporters may transport ATP across membranes at rates that may lie in a range more consistent with a transporter. The fact that glibenclamide, tamoxifen, cyclosporin A, and verapamil inhibit ATP release in several systems underscores this possibility [35]. Indeed, Linsdell and Hanrahan [36] have shown that CFTR transports glutathione at rates that border channel conduction rates (10^7 ions/s and above) versus transporter rates (10^6 molecules/s or below). In fact, symport of glutathione and ATP or ATP with another substrate could occur. KCl symporters are critical in red blood cell and hematopoietic cell volume regulation [37]; a KATP symporter is also not out of the realm of possibility. Moreover, the promiscuity of ABC transporters (mdr, MRP) and the substrates that they move across membranes suggests that ATP could be carried along for the ride with other countless substrates [35]. MOATs are also possible candidates [35,38]. Investigators should keep an open mind to this possible mechanism of ATP release.

As with VDAC or porin channels in outer mitochondrial membrane, ANTs that transport newly synthesized ATP across inner mitochondrial membrane to the exchange of ADP, also play a critical role in intracellular ATP transport [39]. Once thought to be restricted to the mitochondrion, emerging evidence suggests that ANTs may also be expressed in endoplasmic reticulum, the nuclear envelope membrane, and in brain synaptic vesicles [40–42]. The latter result suggests that ANTs may reside, at least for a brief period of time, in the plasma membrane of neurons once synaptic vesicles fuse to release their contents. A reason for addressing possible expression in synaptic vesicles is the known fact that ATP is present in high (millimolar) concentrations along with neurotransmitters or neuroendocrine agonists such as histamine and epinephrine. Such exchange of ATP released into the extracellular milieu with a metabolite of ATP transported back into the cell for

re-synthesis to ATP is also a viable hypothesis. Atractyloside, a specific inhibitor of the ANTs, can be used as an extracellular inhibitor of ATP release to probe the role of ANTs in autocrine ATP release and signaling.

2.3. ATP-filled vesicle

ATP-filled vesicles, which may also contain additional agonists or co-agonists, may fuse with the plasma membrane releasing ATP. It is a known fact, dating back to the work of Gordon [1] and Burnstock [4] and their seminal reviews on the topic of extracellular ATP or “purinergic” signaling, that a high content of ATP is found in synaptic vesicles with other neurotransmitters, mast cell granules with histamine, and chromaffin granules with epinephrine. ATP and its metabolites are known co-transmitters that modulate the effect of excitatory or inhibitory neurotransmitters. ADP and ATP are also released by platelets on their own via exocytosis for a “self-aggregation” signal at the clotting zone. Release of ATP-filled vesicles is the principal transmitter signal for “purinergic” nerves in the gut, the nociceptive nodose neurons in the dorsal root ganglia of the spinal cord, and in specialized nerves in the brain. Thus, exocytosis of ATP-filled vesicles, preformed and poised to fuse beneath the plasma membrane, should be considered as a major release mechanism. One critical question regarding the presence of ATP in vesicles is: how does the ATP become loaded and concentrated in these vesicles to high millimolar concentrations? We hypothesize that ATP channels and transporters may function to transport or load ATP into these vesicles and concentrate the ATP within. As an anion, ATP transport into the vesicle could be facilitated by H^+ -ATPases, which would transport and concentrate H^+ in

the vesicle lumen. ATP would follow to preserve macroscopic electroneutrality across the vesicle membrane. It is important to note that, once a vesicle fuses and release its quanta of ATP, that ATP channels and/or transporters would then be inserted and present in the plasma membrane to drive ATP release further. These are the same channels and transporters that served to load the vesicle before its fusion. The potential issues surrounding the loading, fusion, and release of ATP from secretory vesicles is shown in Fig. 2.

3. Innovative methods to detect autocrine ATP release and signaling

3.1. Indirect pharmacological screening for extracellular nucleotide and nucleoside release and signaling: nucleotide and nucleoside scavengers

A potent and effective way of blocking autocrine and paracrine signaling by nucleotides and nucleosides is with inclusion of scavengers for purinergic agonists. Hexokinase (with inclusion of 5 mM glucose) will scavenge ATP in preparations, yielding ADP and donating the terminal or gamma phosphate of ATP to glucose forming glucose-6-phosphate. This maneuver eliminates ATP from solutions and prevents any endogenous ATP released in cell or tissue preparations from interacting with P2 receptors that prefer ATP. ADP is a better agonist at some P2Y receptors and a weak agonist for some P2X receptors. As such, in lieu of hexokinase, apyrase, an ATPase/ADPase, would eliminate ATP and ADP from solutions rapidly. However, apyrase generates 5'-AMP, a precursor of adenosine activating P1 adenosine receptors. Thus, a final maneuver is the inclusion

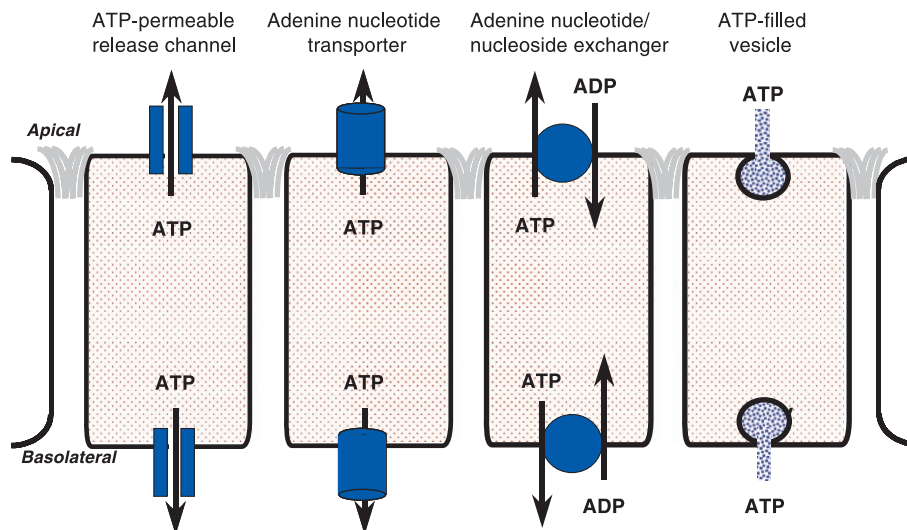


Fig. 2. Possible ATP release mechanisms in apical and basolateral membranes of polarized epithelia. From left to right: ATP-permeable release channels may be present in each membrane domain that are likely anion-permeable channels. Plasma membrane forms of the mitochondrial porins or VDACS may be candidates. Adenine nucleotide transporters may also exist that may be carriers or permeases not unlike the ABC transporters, CFTR, mdr, or MOAT. Adenine nucleotide/nucleoside exchangers are located in the mitochondrial membrane and may also be expressed in the plasma membrane. ATP-filled vesicles may also be present in epithelia as they are in neurons, neuroendocrine cells, mast cells, and platelets.

of adenosine deaminase, which converts active adenosine into inert inosine.

3.2. Indirect pharmacological screening for extracellular nucleotide and nucleoside release and signaling: global P2 and P1 receptor antagonists

An alternative maneuver to prevent autocrine or paracrine activation of purinergic receptors are non-selective or global antagonists that block most if not all P2 or P1 receptors. The best approach for broad blockade of P2 receptors is suramin. It is noteworthy, however, that suramin poorly inhibits certain P2X receptor subtypes, is also a weak antagonist for growth factors, and may also block other classes of calcium entry channels besides P2X receptor channels. In this case, pyridoxal phosphate-6-azophenyl 2',4'-disulfonic acid (PPADS) can be used together with suramin in a cocktail. Nonetheless, both PPADS and suramin are ecto-nucleotidase inhibitors complicating their use in indirect assays [43]. In addition, PPADS and trinitrophenyl-ATP (TNP-ATP), another P2X-selective agonist, change the color of the Ringer's solution and cannot be used in fluorescence experiments.

A similar approach can be taken for adenosine receptors. CPX (also known as DPCPX or 8-cyclopentyl-1,3-dipropyl-xanthine) is a broad specificity antagonist of P1 receptors.

4. Novel and direct assays to detect ATP release from cells

Ultimately, direct measurement of extracellular ATP in solution is the preferred course of action to study whether a cell or tissue is releasing ATP in a physiological or biological manner. There has been a recent revolution in the establishment of assays that can detect extracellular ATP signaling in cells and tissues. This has involved either adaptation of the luciferase/luciferin bioluminescence detection assay from the test tube to “sense” ATP release in biological preparations, the linkage of luciferase to cells via protein A and epitope antibodies to “sense” ATP release in the cell surface microenvironment, the development of the PC-12 pheochromocytoma cell as a “biosensor” that can measure ATP, and the invention of an atomic force microscopy (AFM) probe coated with myosin or luciferase to “sense” ATP.

4.1. Assays to detect ATP release: luciferase/luciferin bioluminescence detection

Firefly and *Renilla* luciferase and luciferin have been used for decades to measure ATP in preparations. Laboratories have taken aliquots of extracellular solution bathing cells and tissues, mixed these samples with luciferase and luciferin, and measured bioluminescence in a multi-step process. This has yielded much interesting and novel information. However, many laboratories have gone a step

further and included the luciferase/luciferin detection reagent directly into the medium or solution bathing the cells, cell monolayer, or tissue and measured ATP release.

Schwiebert et al. developed such an assay for detecting or “sensing” ATP release in real-time from non-polarized cells and more importantly, for polarized epithelial and endothelial cell monolayers grown on filter supports [17,19,21,44,45]. The same real-time assay has been used extensively by Fitz et al. to study ATP release from hepatocytes and cholangiocytes [20,35,46,47]. Both laboratories have demonstrated that cells release ATP constitutively under basal or unstimulated conditions and elevation of cyclic AMP (cAMP), increases in cytosolic calcium, and hypotonic challenge trigger further ATP release, while hypertonicity inhibits ATP release. Via this assay, it was shown that ATP release and signaling is lost in the apical microenvironment of CF monolayers versus controls [17,19], while ATP release and signaling in polycystic kidney disease (PKD) monolayers was as great or greater in the apical microenvironment and greater in the basolateral environment [21,44].

A groundbreaking study has applied luciferase/luciferin bioluminescence detection technology to a tissue preparation. Sorensen and Novak [48] used confocal imaging of the bioluminescence generated from ATP being catalyzed by luciferase. They studied individually dissected pancreatic acini to measure ATP release and signaling in this “in vivo-like” preparation. They showed elegantly that mechanical stimuli, hypotonic challenge, and carbachol, an agonist that increases cytosolic calcium in this tissue, all increased ATP release. They were also able to show intracellular ATP store depletion through caged ATP as well as quinacrine, which labeled a similar ATP pool. It was estimated that ATP release upon cholinergic stimulation generated an ATP concentration of 9 μ M in the acinus. It was postulated that this acinus-derived ATP not only could modulate acinar cell function in an autocrine manner but could also diffuse to the pancreatic ducts in acinar secretions to stimulate P2 receptors in a paracrine fashion. This laboratory, as well as our own, are trying to take this technology to more in vivo-like tissue preparations to relate the in vitro findings in cultured cell monolayers to freshly dissected tissues. One important issue is cell damage during the dissection. Novak et al. showed elegantly via multiple lines of evidence that this possibility was eliminated carefully in their work.

A limitation of the above methods of extracellular ATP “sensing” or detection is the fact that the luciferase/luciferin detection reagent is solubilized in the solution or medium; however, because of unstirred layers both in the cell cultures and cell monolayers in vitro and the freshly dissected tissues, the assay may miss ATP released into the microenvironment immediately above the cell surface. Beigi et al. [49] were aware of this issue and the fact that the ATP might be degraded by ecto-ATPases (ecto-apyrases) on the cell surface before it could be detected in bioluminescence assays. As such, they used molecular biology to develop a

conjugate that linked luciferase to protein A. This conjugate, through protein A chemistry, could be linked to any antibody that could be bound to an extracellular epitope of any cell surface antigen, usually a transmembrane protein. They took advantage of the fact that many extracellular epitope antibodies have been created for cell surface antigens on hematopoietic cells. They showed that they could detect micromolar amounts of ATP being released under basal conditions and that inhibition of ecto-ATPases could prolong the bioluminescence signal. Theoretically, this luciferase/protein A conjugate could be targeted to any cell surface antigen that had a well-characterized and high-affinity antibody that recognized an extracellular epitope. Targets may include CFTR or other ABC transporters implicated in the facilitation of ATP release, CD39 and other ecto-ATPases where the competition between degradation and detection could be studied, or P2 receptors themselves to sense what the local ATP concentration is at the receptor when it is engaged and activated.

4.2. Assays to detect ATP release: “biosensors”

Hazama et al. used much ingenuity in developing a technique where the PC-12 cell, a pheochromocytoma cell line was exploited to be used as a “biosensor” because it expressed the P2X₂ receptor and, possibly, other P2 receptors as well [50]. The initial paradigm developed involved establishing a whole cell patch-clamp recording designed to

record to P2X receptor channel currents. Then, the PC-12 cells was detached from the substrate (PC-12 cells do not attach well to tissue culture plastic as it is), and a single PC-12 cell, still in whole cell configuration, was moved into close proximity with a cultured cell of interest. If P2X receptor channels opened and current was recorded, then this would suggest that the cultured cell was releasing ATP. Hazama et al. [50] did this originally with pancreatic β cells to show that micromolar ATP was released along with insulin in response to glucose. Hazama et al. [51] have also applied this assay to non-CF versus CF cells as well as intestinal 407 cells. They have shown that ATP release is impaired in CF cells or in cells lacking CFTR when compared to controls.

Liu et al. [30] have extended this assay to study macula densa signaling in an *in vivo*-like preparation. Peti-Peterdi in Bell's group dissects nephron preparation in which the cTAL with the small patch of macula densa cells is attached to the glomerulus of the same nephron. Using the PC-12 “biosensor” cell either in whole cell patch-clamp mode or loaded with Fura-2 to measure calcium influx through P2X receptor channels, this group has shown that ATP is released from the serosal or basolateral aspect of the macula densa cells. Patch-clamp evidence suggests the presence of a maxi anion channel with significant permeability to ATP as the principal ATP release mechanism in macula densa. As with the AFM method below, the PC-12 cell “biosensor” method provides a probe that could be used in many other cultured or freshly dissected tissue culture preparations.

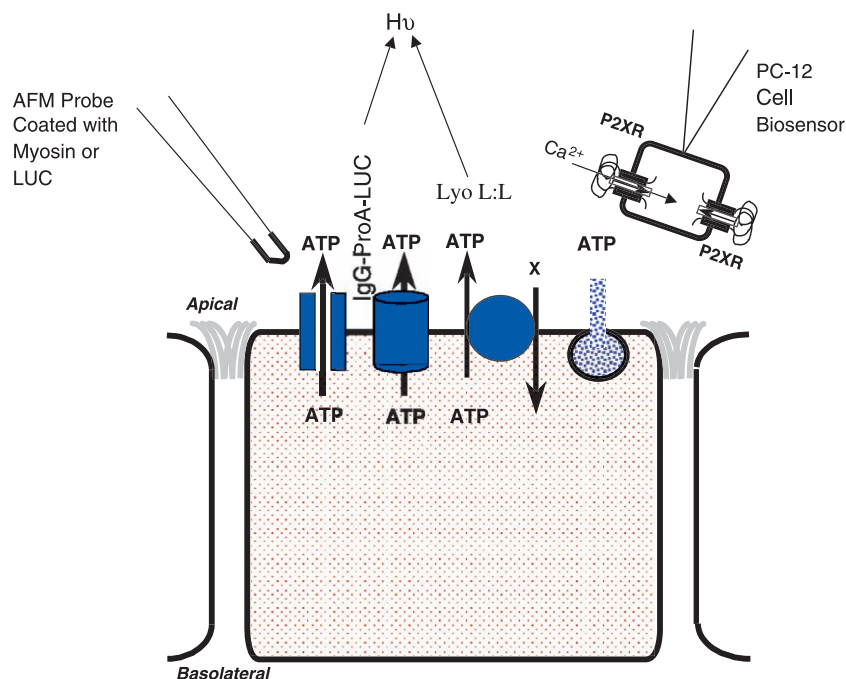


Fig. 3. Schematic summary of current real-time detection methods for released ATP. From left to right: AFM probe coated with a myosin fragment or luciferase where a conformational change and/or heat generated from the reaction (catalyzed by ATP) causes tip vibration. Luciferase linked to protein A and conjugated to an extracellular epitope IgG antibody at the cell surface or lyophilized luciferase/luciferin reagent resuspended in the medium bathing a monolayer are also used to detect released ATP in real-time within a luminometer or by microscopic imaging. A PC-12 cell loaded with Fura-2/AM or held in the whole cell patch-clamp configuration also can detect released ATP through activation of its endogenous, extracellular ATP-gated P2X₂ receptor.

Recently, a different functional biosensor was developed by Schneider et al. [52] for real-time ATP measurements, which allows for the direct detection of ATP on the surface of living cells. This sensor incorporates ultra high surface topography measurements using the principles of AFM and, at the same time, allows one to scan for changes in ATP concentrations only angstroms from the surface of cells. With the implementation of this new technology, one can obtain accurate and reproducible recordings from living cells of both the topography and surface ATP concentrations in real-time. By developing the concept of a biosensor attached to the surface of an AFM cantilever, it is now possible to generate specific biosensors that can probe the surface environment of living cells under resting and experimental conditions and record changes in both the topography and the microenvironment surrounding the cell membrane.

Using this assay, Schneider et al. [52] were able to demonstrate that CF airway cells stably complemented with wild-type CFTR released ATP, measured as localized changes in ATP concentration. These changes in ATP appeared as lines across the surface of the cells that were actively secreting ATP. This aspect was intriguing to this group, as one might have expected that the cell would have single “hot spots” where the ATP was being released. By calculating the small volume that the tip actually occupies, we could determine that we would need around four molecules of ATP to be present to activate the tip [52]. As it is now possible to attach biologically active molecules to the tip of the AFMP, it may now be possible to develop a series of “biosensors” that can detect other reactive effluents from cells. This group is currently developing a tip that would allow incorporation of luciferase on the surface of the tip. This would allow one to detect relative changes in fluorescence of the tip as well the deflection of the probe due to the heat generated by the luciferase reaction. One could then directly calculate the level of ATP being released per unit time (J.P. Geibel, personal communication).

Fig. 3 summarizes the known approaches to detection of released ATP in cell and tissue preparations. In our view, multiple approaches are prudent to validating that autocrine and paracrine nucleotide signaling is occurring in a preparation. Often, this includes pharmacological blockade of purinergic signaling along with luciferase-based detection of the released nucleotide.

5. Heptahelical nucleotide-activated G protein-coupled receptors (P2YRs)

Early work, primarily in the cardiovascular system, recognized first the potent extracellular actions of ATP and adenosine [2]. Burnstock [4,53] later identified and proposed the concept of “purinergic” nerves and “purinergic” receptors. The early classification proposed two major groups, P2 receptors (for ATP as the agonist) and P1 receptors (for adenosine as the agonist) [54]. Subsequently,

rank order potency profiles with different nucleotides and nucleotide analogs (as well as nucleoside and nucleoside analogs) revealed distinct pharmacological subtypes for the P2 and P1 subgroups. For example, P2U (later renamed P2Y₂) was characterized by UTP as its best agonist. Permeabilization of cells by ATP and other nucleotide agonists was classified as being mediated by the P2Z and/or P2X receptors. P2T was a receptor classified early on in thrombosis by platelets. It has still not been identified at the molecular biological level. P1 receptors were quickly split into two groups: A1 (for adenosine receptors that couple via G proteins to phospholipases) and A2 (for adenosine receptors that couple via G proteins to adenylyl cyclases).

The P2Y family of heptahelical or serpentine receptors is well characterized and has been reviewed extensively. The reader is referred to many seminal reviews on P2YRs for more detailed information [55–63]. Extracellular ATP-gated P2X receptor channels will be dealt with in detail below.

Rank order potency of agonists has always been the first method of differentiating P2YR subtypes. It was and still is an imperfect science. However, in the absence of a large array of selective agonists and a total absence of selective antagonists, it was all purinergic receptor laboratories had in their arsenal. Molecular biology verified this imperfect science, when the P2Y₁ and P2Y₂ receptors were cloned. In the old nomenclature, the P2YR (later renamed P2Y₁) was classified as being activated equally well by ATP and ATP analogs as well as ADP and ADP analogs. The analogs that were most effective were 2-methylthio ATP (2-MeS-ATP) and 2-MeS-ADP as well as ATPγS and ADPβS. Very recently, two new antagonists have been developed that are selective for P2Y₁, MRS 2179 and MRS 2269 [55]. P2Y₁ (together with P2Y₁₂) remains a candidate for being the actual P2T receptor on platelets, because ADP is the major co-agonist with thrombin that promotes platelet self-aggregation. The P2Y₂ receptor (P2UR in the old nomenclature) is identified by its equal or greater affinity for UTP and UTPγS versus ATP, while ADP, UDP and diphosphate analogs are ineffective. This became a less perfect diagnostic tool when the P2Y₄ receptor was cloned and characterized. P2Y₄ also binds UTP, UTPγS, and ATP. In contrast, P2Y₆ binds UDP with higher affinity than any other agonist. P2Y₃ is a species homolog of P2Y₆. More recently, P2Y₁₁, P2Y₁₂, and P2Y₁₃ were identified by homology cloning and were verified to be nucleotide receptors [64]. Interestingly, the UDP-glucose receptor that was originally cloned from human myeloid cells is structurally related to the P2Y receptors. Thus, this receptor has been tentatively included in the P2Y receptor family as P2Y₁₄ [65]. However, the pharmacology is quite broad again for these receptors and exhibits a similar profile to the P2Y₁ receptor. Verification of nucleotide receptors is an important point, because cDNA clones with significant homology to known G protein-coupled nucleotide receptors have subsequently been characterized and found not to be nucleotide receptors. These include P2Y₅, P2Y₇ (found to encode the leukotriene B4

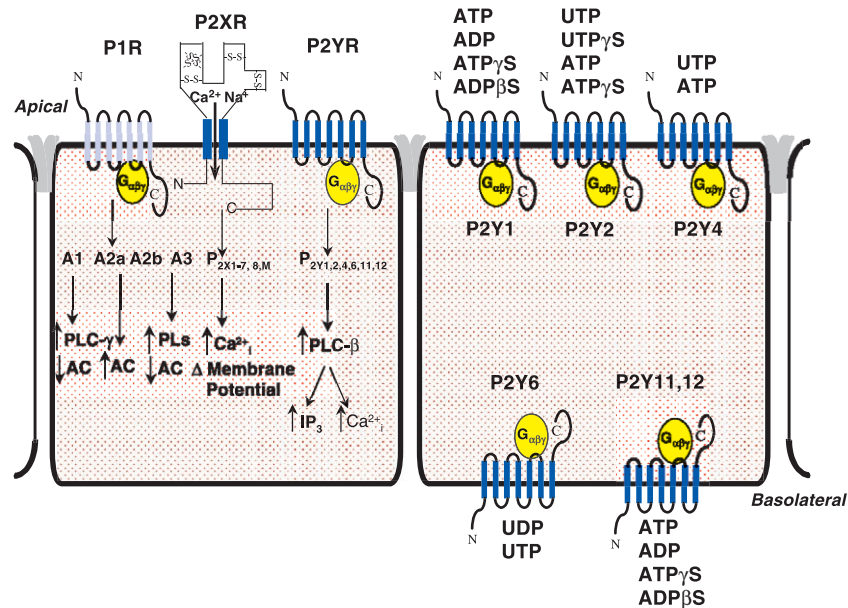


Fig. 4. Illustration of the P2Y receptor subtype classification. The imperfect science of using nucleotides or nucleotide analogs to decipher the presence of different P2Y subtypes is shown in this cartoon. Only UDP is really truly selective for P2Y₆. P2YRs can be dissected better from P2XRs and P1Rs by virtue of their signal transduction cascades (PLC=phospholipase C; AC=adenylyl cyclase) and the nature of the receptor-mediated increase in cytosolic calcium.

receptor), P2Y₈, P2Y₉, and P2Y₁₀. This may relate to the fact that there are hundreds of known heptahelical receptors in the G protein-coupled receptor superfamily, some of which are still “orphan” and searching for an agonist. Nevertheless, in our laboratory, we probe for P2YRs by using UTP (for P2Y₂ and P2Y₄), UDP (for P2Y₆), and ADP (for P2Y₁, P2Y₁₁, and P2Y₁₂).

Despite the wide-ranging and non-specific pharmacology, P2Y₁, P2Y₂, P2Y₄, P2Y₆ and P2Y₁₁ share a common signal transduction pathway involving heterotrimeric G_q protein, phospholipase C β , endoplasmic reticulum-dependent Ca²⁺ mobilization and activation of protein kinase C. In contrast, P2Y₁₂, P2Y₁₃ and P2Y₁₄ are G_i-coupled receptors and do not trigger increase in cytosolic Ca²⁺ concentration but do activate a host of G_i-initiated signaling cascades. It is interesting to note that P2Y₁₁ receptors can directly activate adenylyl cyclase and cAMP accumulation [66]. Fig. 4 illustrates the subclassification of P2Y G protein-coupled receptors. P1 adenosine receptors are also shown to be thorough. A brief summary of their classification and properties is included in this figure as well. For details concerning adenosine receptors, the reader is referred to recent reviews [60,67,68].

6. Extracellular ATP-activated ion channels (P2XRs)

6.1. Background

The fact has been known for decades that application of ATP as an extracellular agonist on a cell or tissue led to “permeabilization” of the cell plasma membrane. There

were many interpretations of this phenomenon, although a role in exacerbation of cell injury was a common conclusion. The receptors thought to underlie this effect were classified as the P2Z receptors in the early nomenclature and were thought to be a subtype of the P2Y family. P2X receptors were first distinguished from P2Y receptors based on pharmacological criteria by Burnstock and Kennedy in 1985 [69]. This early subdivision of P2 receptors was later validated based on molecular cloning and second messenger system of P2X and P2Y families [70].

In seminal papers and reviews about this original electrophysiological research on native cells, Bean et al. [71–74] showed that single channel conductances of as little as 1 picoSiemen (pS) to as large as 100 pS could be observed upon addition of ATP agonists. The different channels also had different biophysical current signatures, with differing kinetics, dependence on voltage, and rate of inactivation (later determined to be desensitization). The permeability of the channels to monovalent and divalent ions also varied. This was exceedingly frustrating, because the variability in the recordings often made this research difficult to decipher. Moreover, this issue of ATP permeabilization of cells always loomed in the background as a troubling issue. In hindsight, a subset of these channels were indeed P2XRs of varying types and, possibly, different multimeric mixtures. Other channels recorded immediately after ATP stimulation may have been separate ion channels that P2XRs and, possibly, P2Y G protein-coupled receptors, were stimulating via rapid signal transduction mechanisms.

There were also physiological reasons for believing that extracellular ATP-gated ion channels existed. Burnstock [4] proposed the existence of so-called “purinergic nerves” in

the gut and in the nervous system that were neither cholinergic nor adrenergic. By inference, the ATP that was released from the synapse had to bind to a receptor channel to propagate the action potential. Moreover, the ATP that was applied to whole cell patch-clamp and voltage-clamp preparations activated ion channels as rapidly as activation observed in the acetylcholine receptor channel in neurons and muscle. There was also a relative potency of different nucleotide agonists in the rapid activation of these ion channels, suggesting that this was a receptor-mediated effect that had physiological meaning.

6.2. Molecular identity

This physiological work has now been validated by molecular biology. At least nine P2X receptor channel subtypes (P2XRs, as we will refer to them) have now been cloned, identified, and characterized [75–83]. Other tissue-specific [84] and developmentally regulated P2XRs [85,86] are still emerging, as are P2XRs from lower model organisms such as zebrafish [87–89]. Transgenic knockout of P2XR genes has begun in an effort to understand their physiological roles more thoroughly. Mice lacking P2X₁ receptor channels expressed one major phenotype, reduced fertility due to lack of ejection of sperm from the testes into the vas deferens [90]. The interpretation was that P2X₁ receptors are the main purinergic receptor on testes and vas deferens vascular smooth muscle cells. The sympathetic-driven contractile response is mediated in large part by P2XRs; however, this study showed that P2X₁ was the principal postsynaptic receptor channel involved. Fertility was reduced by 90% in homozygous knockout mice, but not in wild-type or heterozygous mice, not because of defects in spermatogenesis, but in ejection of sperm through the vas deferens into the ejaculate [90]. Any other phenotypes in the mice were subtle and not detected as yet in this study.

Vlaskovska et al. [91] have generated a P2X₃-knockout mouse. With this mouse, this laboratory has shown that two different populations of sensory neurons are impaired in their function due to a lack of P2X₃ [91,92]. The suburothelial plexus of the mouse bladder showed abundant staining for P2X₃. Although ATP was released similarly in response to bladder distension in P2X₃ *+/+* versus P2X₃ *-/-* mice, the bladder afferent nerve activity was attenuated in response to distension [77]. The loss of this activity in the P2X₃ *-/-* mice could be rescued by exogenous ATP analogs or ATP itself, while normal activity in the P2X₃ *+/+* afferents was blocked by TNP-ATP, PPADS, and capsaicin [91]. These data suggest that P2X₃ is a major neural sensory receptor on a population of bladder nerve fibers that transduce bladder distension into an electrical signal. Specialized neurons of the dorsal root ganglia respond to ATP as a principal neurotransmitter by a mechanism that is transduced by different P2XR subtypes, P2X₂, P2X₂/P2X₃ heteromultimers, and P2X₃. Zhong et al. [92] also examined the activity of DRG and nodose neurons

(specialized neurons of the DRG involved in pain perception) in P2X₃ *-/-* mice. Because P2X₃ has a distinctive, rapidly desensitizing response to ATP, patch-clamp electrophysiology of the neurons was employed to look for differences between P2X₃ *+/+* and P2X₃ *-/-* cells. All P2X₃ *-/-* DRG neurons failed to desensitize after ATP stimulation, and both subsets of neurons failed to respond to $\alpha\beta$ -methylene ATP. The responses that were persistent in the P2X₃ *-/-* neurons were consistent with intact, endogenous expression of P2X₂. These studies showed that, although DRG and nodose neurons remained responsive to ATP, the nature of the neuronal sensory response to the ATP neurotransmitter in the spinal cord is significantly altered and more long-lived.

6.3. A member of the two transmembrane-spanning cation channel superfamily

P2XRs were assumed to be a subtype of the heptahelical P2Y family. Instead, P2XRs were predicted to form two transmembrane-spanning ion channels with intracellular N- and C-termini. Once more, two-thirds of the molecular mass of this protein was predicted to be extracellular. This overall structure made P2XRs closely related to the ENaC/degenerins family of cation channels found in mammalian cells and in the nematode, *C. elegans* [93–95]. Fig. 5 illustrates this similarity. In the extracellular domain of each cation channel family, 10 conserved cysteines are found in P2XRs, while 14 conserved cysteines are found in the ENaCs. Each extracellular domain is highly glycosylated, with at least three putative glycosylation sites [93–96]. This large extracellular domain, which accounts for two-thirds of the molecular mass of P2XRs, is shared by P2XRs and ENaCs; however, this domain is divergent from the large family of inwardly rectifying K⁺ (IRK) channels. P2X₂ and α ENaC appear to share the PPXXY motif that is mutated in Liddle's disease in α ENaC and is a recognition site for ubiquitination [93,95]. What is still unclear in both P2XR and ENaC families is the amino acids critical to the cation channel pore. Extracellular to the second transmembrane domain of ENaC is a putative H2 domain that has a GGQLG sequence that is somewhat similar to the GYG motif found in the P loop (equivalent to H2 domain) of two transmembrane-spanning IRK channels. P2XRs are not thought to have a P loop; however, recent alignment of the sequences of P2XRs did reveal a GVG motif in the second transmembrane α -helix of all P2XRs except P2X₇ [97]. It is important to note that there is little or no overall nucleotide sequence homology between any P2XR subtype and any ENaC subtype, despite the very similar structural characteristics.

The similarities in topology of P2XRs and ENaCs also extend to their cell physiology. As members of the two transmembrane-spanning ion channel superfamily (see above), P2XRs were long suspected to form homomultimers or, in some cell models, heteromultimers of mixed P2XR subtypes. ENaCs form fully functional amiloride-sensitive

- Display Eerily Similar Topology
- Form Homo- and Heteromultimers
- Have Two Cysteine-rich Regions in their Extracellular Domain
($\alpha\beta\gamma$ ENaCs Have 14 Conserved Cysteine Residues in this Domain)
(P2XRs Have 10 Conserved Cysteine Residues in this Domain)
- Are Heavily Glycosylated on Multiple N-linked Glycosylation Sites
- Two-Thirds of the Molecular Mass on ENaCs and P2XRs Is in the Extracellular Domain
- α ENaC and P2X2 Have a “PPPLY” Motif in Their C-Termini

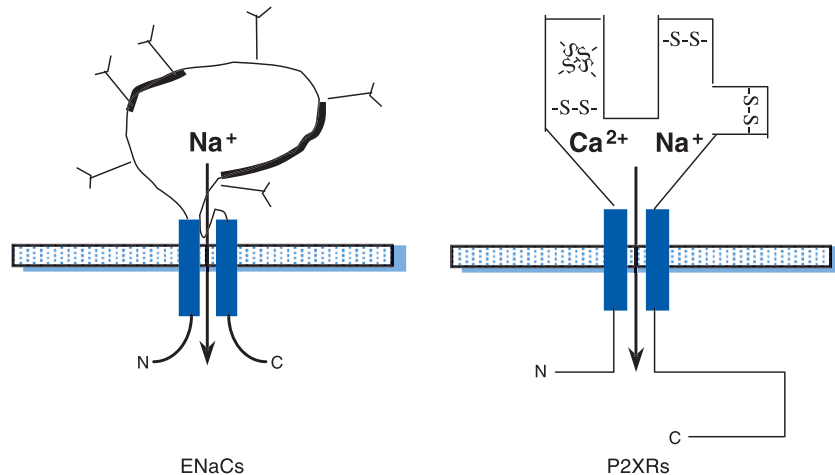


Fig. 5. Close and detailed comparison between P2XRs and ENaCs. These two transmembrane-spanning cation channel subfamilies exhibit similarity in their topology and, possibly, their overall structure. Other biochemical and cell biological similarities are listed, keeping in mind that there is little or no overall DNA or amino acid sequence homology. One major difference is the fact that the cation permeability/selectivity of each subfamily is very different.

and highly Na^+ -selective channels when configured as an $\alpha\beta\gamma$ -ENaC heteromultimer [93,95]. Torres et al. [98–101] explored multimerization elegantly with parallel biochemical and physiological methods in the HEK-293 cell heterologous cell system with multiple studies. The most elegant of these studies was the examination of the ability of all P2XR subtypes to oligomerize or multimerize [99]. Co-immunoprecipitation of epitope-tagged P2XRs was undertaken to probe the ability of P2XRs to form homomultimers and heteromultimers. HA and FLAG biochemical tags added to the C-terminus of each P2XR subtype did not affect cation channel function or other properties such as desensitization. The exception in this work was P2X₆, where even the wild-type construct failed to generate cation currents. Again with the exception of P2X₆, all other P2XRs tested (P2X₁ through P2X₅ and P2X₇) were capable of forming homomultimers. The authors maintain that the inability of P2X₆ to form oligomers may explain why it also fails to form functional channels. The stoichiometry of these multimers is unknown; however, dimers, trimers, and tetramers have been postulated [99]. With regard to heteromultimers, all P2XRs were capable of forming multimeric complexes with other subunits, with the notable exception of P2X₇. A helpful table in this paper [99] summarizes which P2XR subtypes oligomerize with specific other P2XR subtypes. P2X₁ and P2X₂ co-assemble with themselves as homomultimers and with P2X₃, P2X₅, and P2X₆,

but not P2X₄ or P2X₇. P2X₃ co-assembles with P2X₁, P2X₂, and P2X₅, but not with P2X₄, P2X₆, or P2X₇. P2X₄ expressed at very high levels in the HEK-293 cell system, making it difficult to assess in this analysis relative to the other subtypes. However, when the conditions were made favorable, P2X₄ was found to oligomerize only with itself and with P2X₅ and P2X₆. This result was very helpful to our laboratory, which found that P2X₄ and P2X₅ were most abundantly expressed in human vascular endothelial cells and in human and rodent airway, gastrointestinal, and kidney epithelial cell models. There is some preliminary evidence emerging from other laboratories that P2X₆ may also be a prominent epithelial subtype. Unfortunately, the lack of an antibody and the lack of an ability for our degenerate RT-PCR to detect P2X₆ has not allowed us to assess its expression. P2X₅ co-assembled with every other P2XR subtype, except P2X₇. P2X₆ co-assembles with P2X₁, P2X₂, and P2X₄, but fails to interact with P2X₃, itself, or P2X₇. These seminal results solidify a plethora of the functional studies [98,99,101–106] that show physiological evidence for heteromultimeric assembly of unique pairs of P2XR subunits.

6.4. P2XR biophysics

There is a profound difference between P2XRs and ENaCs with regard to selectivity of cation permeation.

The $\alpha\beta\gamma$ -ENaC heteromultimer is the most highly Na^+ -selective cation channel ever described. In sharp contrast, P2XRs are non-selective cation channels for monovalent and divalent cations. P2XRs are calcium-permeable non-selective cation channels that, like the glutamate, NMDA, and kainate receptor channels at excitatory synapses, are gated by an extracellular agonist, show divalent and monovalent permeation, and divalent cation block. P2XRs are thought to trigger signaling by mediating calcium influx from extracellular stores and by changing the plasma membrane potential; however, other signaling mechanisms may be governed by ATP-gated receptor channels. P2XRs, as well as the P2Y G protein-coupled receptors, also stimulate other ion channels in native cells, complicating their definition in specific cell models.

Ding and Sachs [107] studied elegantly the biophysics of the P2X₂ channel protein, expressed in HEK-293 cells devoid of endogenous P2XRs when maintained as isolated cells. Outside-out patches were performed so that the ATP agonist had free access to the extracellular domain of the receptor channel protein. While monovalent cations were permeant in a sequence that was $\text{K}^+ > \text{Rb}^+ > \text{Cs}^+ > \text{Na}^+ > \text{Li}^+$, divalent cations also entered the pore. However, divalent cations such as Mn^{2+} , Mg^{2+} , Ca^{2+} , and Ba^{2+} also blocked the channel in a manner characterized as “fast block,” reducing the amplitude of the single channel currents. Importantly, organic cations such as NMDG⁺, Tris⁺, TMA⁺, and TEA⁺ were virtually impermeant. The channels were “flickery,” in that they opened in brief bursts. The single channel conductance was 49 pS in the presence of K^+ and 35 pS in the presence of Na^+ . P2XR Na^+ currents were partially blocked by Mg^{2+} and Ca^{2+} . A subsequent paper showed that divalent cations also speeded inactivation of the P2X₂ channels [108].

6.5. Key amino acid residues within P2XRs

Site-directed mutagenesis has been used to probe many regions critical to the activity of P2XR channels. With regard to cation permeation through the pore, 5 amino acid residues in a 20-amino acid stretch corresponding to the first transmembrane α -helix (H33, R34, I50, K53, and S54) were implicated in cation binding and permeation within the P2X₂ receptor channel [109,110]. Another study of P2X₂ channels in HEK-293 cells probed a larger stretch of amino acids flanking and within the first transmembrane segment [111]. Their cysteine-scanning mutagenesis revealed that D15, P19, V23, V24, G30, Q37, and F44 were involved in cation binding and permeation. Migita et al. [112] also probed the second α -helical transmembrane domain for residues key in divalent cation binding and conduction through P2XRs. Ca^{2+} permeability through P2X₂ expressed in HEK-293 cells was thought to be mediated by amino acids with negatively charged side chains, D315 and D349. This had no effect on divalent cation permeation. Rather, the size of side chains that were exposed to the pore of the

channel was critical. Mutation of polar threonines at position 336 and 339 as well as a serine 340 affected cation permeation profoundly. The largest changes were induced by replacement of these residues with a tyrosine, whose bulky side chain prevented Ca^{2+} movement altogether. Taken together, these three studies by Egan and Voigt and one study by North et al. showed that the two transmembrane α -helices cooperate in conduction of monovalent and divalent cations through the pore.

In addition to the evidence generated by Haines et al. [109] regarding ATP gating of the channel by binding to the extracellular face of the first transmembrane segment, Jiang et al. [113] also addressed this issue in the P2X₂ receptor expressed in HEK-293 cells. Alanine-substitution mutagenesis on 30 polar residues in the presumptive extracellular domain revealed two positively charged lysine residues (L69 and L71) near the same region proximal to transmembrane domain 1 implicated by Egan and Voigt. Substitution with cysteines for these lysines and other flanking amino acid residues showed similar effects. These experiments also implicated S65 and I67 in ATP binding and gating of the P2X₂ channel. In particular, I67 was identified to be critical to the ATP-binding site [113]. Perhaps, anionic ATP is attracted to and bound by these lysines and the flanking serine and isoleucine help stabilize this interaction. Upon binding, ATP may also mask these closely coupled lysines with positively charged side chains, removing steric hindrance and allowing cations to move from the external channel vestibule into the pore. Ennion et al. [114] studied the extracellular domain of the P2X₁ receptor, searching for residues critical for ATP binding. This study and the one above came out concurrently. They too targeted conserved lysines and arginines, postulating that positively charged side chains might attract and/or bind anionic ATP. Many were irrelevant; however, like the P2X₂ receptor studies above, K68 and K70 external to transmembrane domain 1 and R292 and K309 external to transmembrane domain 2 were key to ATP recognition. Taken together, these two studies on different P2XR subtypes show that the ATP binding pocket is indeed at the extracellular face of the cation pore close to the channel vestibule.

P2X₁ and P2X₃ receptor channels desensitize rapidly upon binding ATP and opening, while the other major subtypes (P2X₂ and P2X₄ through P2X₇) inactivate slowly or not at all. Koshimizu et al. [115] swapped a stretch of six amino acids of P2X₃ and for P2X₄ with the corresponding stretch of arginine 371 through proline 376. P2X₄ sequence substitution slowed receptor desensitization, while P2X₁ and P2X₃ sequence substitution caused rapid desensitization. Co-expression of P2X₂ and P2X₃ caused a phenotype that had delayed desensitization, a phenotype intermediate to P2X₂ and P2X₃ expressed alone. Thus, this highly charged stretch of amino acids in the C-terminus plays a significant role in desensitization. Boue-Grabot et al. [116] identified a protein kinase C phosphorylation site, TX(K/R) at amino acids 18 through 20 in the N-terminus of the P2X₂

receptor, as critical for regulation of receptor desensitization. Normally, a slowly or poorly desensitizing P2X subtype, mutation of the N-terminus of P2X₂ (T18A, T18N, or K20T) showed rapid desensitization. Phosphorylation of this site within the N-terminus was verified biochemically. Examination of the N-terminal sequences of all P2X subtypes reveals that P2X₁ and P2X₃, rapidly desensitizing subtypes, lack this threonine at position 18, while the other more slowly desensitizing subtypes possess this conserved PKC site. Still another laboratory generated data suggesting that the hydrophobic transmembrane segments were critical in desensitization [117]. Chimeric swapping of the TM domains from P2X₁ and P2X₃ with P2X₂ affected desensitization markedly. Taken together, these results suggest that all regions of the P2X receptor accessible to the cytosol are involved in receptor desensitization following ATP binding and channel opening.

6.6. *Wide and robust expression of P2XRs*

P2XR subtypes are expressed abundantly in brain and spinal cord, and the most comprehensive analysis of their relative expression in these tissues was from Collo et al. [82]. The functional role of P2XRs in different excitable cell preparations will be addressed in more detail below. It was once thought that P2XR expression was restricted to excitable cells. Although the P2XR as an excitatory postsynaptic receptor channel is easy to envision and characterize, the physiological roles of P2XRs in non-excitable cells were more difficult to visualize. Even if *in situ* hybridization revealed staining for P2XRs on non-excitable cells, this was met with some skepticism.

Emerging studies have revealed abundant expression of P2XRs on non-excitable cells and tissues. Although sensory organs do contain neurons that convey sensory inputs to higher neural centers, evidence has emerged that P2XRs are expressed in other more specialized, non-excitable cell types in inner ear, retina, and taste bud. Multiple P2XRs have been localized to spiral and vestibular ganglia of the inner ear, the cochlear nucleus, and primary auditory neurons [118–120]. In addition, P2X₂ receptors or splice variants of P2X₂ [121] have been found biochemically, molecularly, and functionally in Dieters' cells of the cochlea [122], organ of Corti within the cochlea [123], outer hair cells [119], and epithelial cells lining the stria vascularis, Reissner's membrane, and the tectorial membrane [118]. P2X₂ staining was also intense in the hair cell stereocilia, indicating a key role in sound transduction [124]. In the retina, P2XRs are also abundant [125–130]. In addition to transduction of pain, light, and sound, P2XRs have also been identified in circumvallate fungiform papillae of the rat tongue [131].

The role of P2X₁ in the smooth muscle cells of the testes and vas deferens has already been well documented with regard to cloning of P2X₁ and the P2X₁ knockout mouse. The urinary bladder appears to be another important tissue regulated by local ATP release and P2XRs. In detrusor,

ureteral, and bladder blood vessel smooth muscle, P2X₁ immunoreactivity was observed routinely and markedly on the smooth muscle cell membrane [132]. While P2XR expression remains and is pronounced in smooth muscle, P2XR expression in skeletal muscle is notable during early stages of development, while expression fades during the postnatal period and in adult tissue [133,134]. Recently, P2X₄ was found in chick cardiac muscle myocytes. A positive ionotropic effect of ATP on heart muscle may be mediated by this P2XR subtype and allow ATP-induced calcium influx that was blocked by antisense oligonucleotides to P2X₄ [135]. In addition, glycosylated (58 kDa) and nonglycosylated (44 kDa) forms of the transfected cP2X₄ receptor were found in cardiac myocyte membranes, a similar phenotype to the epithelial P2X₄ receptor (see below). Only the 58 kDa glycosylated form of cP2X₄ could be biotinylated. These results provide a new tissue where P2XR expression and function may be critical.

Very recent work has shown the presence of P2XRs in human vascular endothelial cells [45,136–140]. In the context of expression profiling in excitable tissues, hints in these initial studies led to the characterization of P2XR expression and/or function in epithelial cells *in vitro* and *in vivo* [141]. An emerging role for purinergic receptors in the cells that constitute skeletal bone is being appreciated. Bone remodeling within microenvironments is regulated by autocrine and paracrine factors and by local mechanical forces that are poorly understood. A recent and comprehensive study on P2X and P2Y receptor expression in bone cells has been performed [142]. Three studies that followed added credence to these findings [143–145].

Burnstock et al. have led the field in documenting P2X receptor expression in endocrine tissues. Initial work documented abundant P2X₂ receptor expression in the nuclei and neurons of the hypothalamus [146,147]. Similar work has been performed in thyroid and adrenal gland [148–151]. Petit et al. showed roles for P2Y and P2X receptors in stimulating insulin secretion from pancreatic β cells in the absence or presence of the requisite extracellular glucose stimulus [152]. Burnstock's group has also studied expression of all P2XR subtypes in rat testis [153]. Taken together, expression of multiple P2XR subtypes in endocrine organs argues for tight, local control of endocrine tissue function by autocrine purinergic signaling.

6.7. *Biochemistry of P2XRs in native cells*

Recent studies have shed new light on P2XR biochemistry in native cells and tissue. Most of this biochemical work has been performed in heterologous cell systems with transfected and, often, epitope-tagged P2XR constructs. Recently, Hu et al. [135] made a step closer to studying native cells by studying the protein biochemistry of a transfected chick P2X₄ receptor in cultured embryonic ventricular myocytes. Not only did Hu et al. show compelling evidence for a role for P2X₄ in calcium influx from

extracellular stores and in contractile amplitude of the chick heart, they also showed the fact that P2X₄ receptors were resistant to various rather harsh detergents under various biochemical conditions. Initially, they verified that the P2X₄ receptor was found in two forms: a nonglycosylated 44 kDa form and a glycosylated 58 kDa form. Only the glycosylated form was biotinylated and reacted with streptavidin, suggesting that glycosylation was necessary for normal trafficking. Interestingly, the glycosylated form was soluble in all of the detergent combinations listed above.

Our laboratory has confirmed these results in human epithelial and endothelial cell models for the human and mouse P2X₄ receptor [44,45]. The novel aspect of these studies is the immunoblotting of native epithelial and endothelial P2X₄ receptor. Similar results have also been obtained in non-CF and CF human airway epithelial cells [154] and normal and PKD kidney epithelial cells (A.T. Boyce and E.M. Schwiebert, unpublished observations). Our laboratory has also seen higher molecular weight forms in immunoblotting that are competed away by the peptide immunogen, suggesting higher order glycosylation and/or a detergent-resistant multimer. The prominent carbohydrate addition on this large extracellular loop, elaborate disulfide bonding between conserved cysteines (see below), and the reaction with the extracellular domain of the ATP agonist as well as heavy metals such as zinc, protons, and cations (see below) suggests a complex and dynamic protein worth further investigation in native cells as well as crystallography of P2XRs.

As introduced above, the P2XR extracellular domain has two cysteine-rich regions, within which each P2XR has 10 conserved cysteine residues in identical locations. This argues for a complex, three-dimensional structure that begs to be crystallized. ENaCs have 14 conserved cysteine residues in their extracellular domains. Recent work suggests that ENaCs have Kunitz-like domains that are susceptible to protease cleavage, which is argued to be a major mode of activation for these channels [155]. Further proof for this is that protease inhibitors attenuate ENaC activity. The effect of proteases on P2XRs has not been tested.

The role of the cysteines in forming intra- and interchain disulfide bonds and creating trafficking-competent P2X₁ receptor channels was addressed very recently by Ennion and Evans [156]. A very important finding in this study was the inability to label wild-type receptors with MTSEA-biotin, suggesting that all 10 cysteine residues are engaged in disulfide bonds. When most single cysteines were mutated, only modest effects were observed on ATP potency at the receptor channel. However, exceptions were C261A and C270A, where the peak current amplitudes were reduced by almost 100%. This, however, was determined to be an effect on trafficking. The other single cysteine mutants did allow MTSEA-biotin labeling, suggesting that companion cysteines were not free to react with the methanethiosulfonate compound. Based on their work, they proposed the following pairs of cysteines that were disulfide-linked: C117–

C165, C126–C149, C132–C159 in the first cysteine-rich region and C217–C227 and C261–C270 in the second cysteine-rich region. Channel function is not affected significantly by these bonds; however, trafficking is severely disrupted by the elimination of the C261–C270 bond or by the C117–C165 bond together with another bond.

6.8. Pharmacology and chemistry of P2XR receptor channel activity

The extracellular domain of the P2X receptor channel is a rich background for complex chemistry. As it accounts for two-thirds of the molecular mass of the receptor channel protein like its relatives in the ENaC/degenerin family, this protein can be thought of more as a receptor than a channel. In fact, its extracellular domain is so large and complex that P2XRs can also be thought of as sensors rather than receptors. Along this line of reasoning, ENaCs and degenerins may have endogenous chemical ligands that are not yet appreciated.

This chemistry begins with the binding of its gating ligand, ATP. Agonists and antagonists have been presented in the context of work discussed above. However, recent work has identified additional antagonists for P2XR subtypes, including TNP-ATP [157,158], NF-279, a suramin analog [159,160], and pyridoxal-5'-phosphate-6-(2'-naphthylazo-6'-nitro-4',8'-disulfonate (PPNDS) [161]. Despite these recent efforts, these antagonists mainly affect P2X₁, P2X₂, and P2X₃ or mixtures thereof. The lack of agonists that are selective between P2Y and P2X receptor families, and the lack of agonists and antagonists that define particular P2XR subtypes (in particular, P2X₄, P2X₅, and P2X₆) is a major roadblock in the P2 receptor field and in the P2XR field that needs to be overcome.

Not only does the P2XR extracellular domain have sites for agonist and antagonist binding, N-linked glycosylation, cysteine bonding, and, possibly, protease cleavage, protons and heavy metals react within this extracellular domain as well. Stoop et al. [162] explored the sensitivity of four P2XR subtypes to changes in extracellular pH (pH_o). P2X₃ homomultimers are only mildly inhibited by acidic pH (pH_o of 6.3 versus 7.3) and are unaffected by an alkaline pH_o of 8.3. In contrast, P2X₂ homomultimers and P2X₂/P2X₃ heteromultimers show profound stimulation by acidic pH_o and almost complete inhibition at alkaline pH_o. The authors noted that the data pointed to a single site being modulated by protons. For P2X₁ and P2X₄, opposite effects were observed with acidic versus alkaline pH_o. Acidic pH_o profoundly inhibited P2X₄ currents in particular, while alkaline pH_o had little effect. Site-directed mutagenesis of the extracellular domain of the rat P2X₂ receptor revealed that acidic pH potentiated ATP stimulation more than 4-fold in wild-type channels and eight mutant channels in which extracellular histidines were mutated [163]. In P2X₂, only one histidine mutant, H319A, attenuated the effect of acidic pH down to 1.4-fold. Substitution of a lysine instead of an

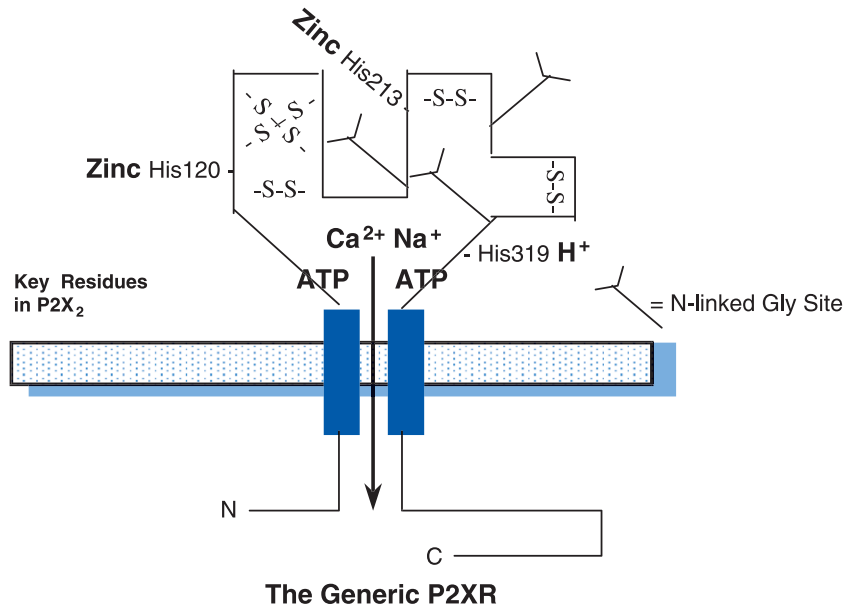


Fig. 6. Key residues within the generic P2XR. Most of the key residues highlighted in this cartoon have been defined in the P2X₁ and P2X₂ receptors. Not all characteristics may hold for the other P2XR subtypes, especially with regard to H⁺ and Zn²⁺ modulation. Cation binding residues were found by multiple laboratories throughout both α -helical regions.

alanine reduced the EC₅₀ for ATP 40-fold. Extracellular Zn²⁺ is known to potentiate and inhibit the responses of different P2XR subtypes to ATP. The maximal effective dose is only 20 μM , which falls within physiological limits for this trace element. Zn²⁺ potentiates ATP gating of P2X₂, P2X₃, P2X₄, P2X₂/P2X₃, P2X₂/P2X₆, and P2X₄/P2X₆, while it inhibits ATP's effect on P2X₁ and P2X₇. ZnCl₂ potentiated the response to ATP in wild-type P2X₂ and seven histidine mutants by 8-fold; however, in two mutants, H120A and H213A, Zn²⁺ had no effect [163]. Because these two Zn²⁺ reactive histidine residues are rather distant from one another within the external domain, two different sites may be required for the effect of Zn²⁺ or the two histidines may interact with each other in a three-dimensional model of the extracellular loop. Taken together, these results suggest that multiple but different histidine residues, whose pK_a falls within the range tested in these studies, bind protons and heavy metals to modulate the gating by the physiologic agonist, ATP. The opposite effects of pH and Zn²⁺ on P2X₂ versus P2X₄ is borne out by less total histidines in P2X₄ and locations of these cysteines that are completely different than in P2X₂. It is also possible that H⁺ and Zn²⁺ could act as agonists independent of ATP to open P2XRs. Fig. 6 highlights the histidine residues implicated in H⁺ and Zn²⁺ binding.

7. Physiological and pathophysiological paradigms for extracellular ATP-mediated effects in epithelia

Many of the figures included above were designed in the context of a polarized epithelium. This was no accident.

Autocrine and paracrine ATP signaling in extracellular microenvironments is robust on both the apical and basolateral sides of polarized epithelium. Epithelial cells are traditionally known as barrier cells that line the tissues of many organs of the body and separate the external environment from the interstitium. The apical membrane faces the lumen of a tissue. Often, this is the external environment, like the humidified air in the lung or a fluid-filled environment (e.g., the humor-filled eye, the ventricles of the brain filled with cerebrospinal fluid (CSF), or the endolymph-filled inner ear). The basolateral membrane faces the interstitium (e.g., basal cells, connective tissue, basement membrane, blood supply, and nerve innervation). The microenvironments on the surfaces of these two membrane domains are very different. These microenvironments often provide an ideal setting for autocrine and paracrine purinergic signaling in particular and autocrine and paracrine signaling in general. This is especially true if they are fluid-filled or fluid-covered microenvironments that have a medium to allow the autocrine or paracrine mediator to diffuse easily and rapidly.

Purinergic signaling has been implicated in the regulation of many epithelial cell functions. In addition to triggering cell signaling, mainly through cytosolic calcium and phospholipase-coupled signal transduction and, possibly, via other cellular mechanisms, extracellular nucleotide signaling also modulates the potency of other autacoids and hormones that regulate epithelial cell function. Extracellular nucleotides and nucleosides also regulate transepithelial ion transport. In general, extracellular nucleotides and nucleosides, through P2Y, P2X, and P1 receptors, stimulate secretory Cl⁻ and H₂O transport, activate K⁺ channels,

inhibit absorptive Na^+ transport, modulate acid–base transport, and potentiate regulatory volume decrease following hypotonic cell swelling. We are careful to say “in general,” because there are exceptions to this rule due, in large part, to where the epithelium resides and its function. For example, in highly secretory epithelium like choroid plexus or ciliary processes of the ciliary body of the eye, purinergic signaling may also stimulate secretory Na^+ transport. Purinergic receptor-driven functions include triggering of calcium sparks and waves, potentiating ciliary beat frequency, and promoting mucus, glandular, and acinar secretion. Constitutive ATP release and signaling has been implicated in the maintenance of cell signaling “setpoints” for cytosolic calcium, phosphoinositide turnover, and arachidonic acid metabolism. Purinergic signaling may even modulate gene expression in epithelial cells via specific transcription factors.

In epithelial cells, ATP is released from the cell in a polarized manner either at the apical or basolateral cell surfaces for the purpose of autocrine and paracrine regulation of the epithelial cell monolayer. In general, ATP release is directed apically. However, there may be physiological and pathophysiological exceptions to this rule as well (macula densa of the kidney as an example, see below). The mixture of P2Y, P2X, and P1 receptors in the apical and basolateral membrane domains may also differ. Nevertheless, a given epithelial cell commonly expresses all three purinergic receptor subfamilies and, often, multiple P2Y, P2X, and P1 receptor subtypes (see also below). That mixture of purinergic receptor subtypes governs what nature of signal is transduced from the released ATP and its metabolites, either in the luminal (apical) or interstitial (basolateral) microenvironments.

7.1. Lung and airway epithelium

There are two general sites of ATP release and signaling in the human lung and airways: the airway lumen and the submucosal gland secretions (Fig. 7). Although it has not been investigated to date, ATP secretion in the distal lung at the gas exchange zone may also occur with surfactant secretion. Airway surface epithelium in the smaller and larger conducting airways is capable of ATP and UTP release [164] in response to a myriad of stimuli (flow, touch, cyclic nucleotides, hypotonicity, and calcium agonists); moreover, secretions from submucosal glands that lie beneath the pseudostratified surface epithelium may also supply autocrine nucleotides and nucleosides. Neuroendocrine cells, mast cells, and goblet cells along the airway may also release ATP along with other agonists from their granules. The analogy of the submucosal gland secreting purinergic agonists with mucins and other substances can be extended to the hepatic and pancreatic acini and the secretory glands/coils of the sweat gland and the salivary gland.

With regard to microenvironments, however, the airway surface liquid (ASL) bathing the cilia on ciliated airways

epithelium in the large conducting airways is a microenvironment of interest in physiological paradigms and in pathophysiological contexts such as cystic fibrosis (CF) and primary ciliary dyskinesia (PCD) [165,166]. Because purinergic signaling governs ciliary beat, epithelial cell signaling, and epithelial solute and water transport, extracellular nucleotide and nucleoside signaling in this microenvironment may be essential to regulating the composition of the ASL and the function of this critical extracellular space. Several laboratories, including our own, have found a loss of purinergic signaling in CF epithelial and heterologous cell models lacking CFTR [17]; as such, loss of purinergic signaling may be critical to the loss of CFTR function, loss of ciliary beat, abnormal ASL composition, and overall loss of mucociliary clearance. These issues will be revisited below.

As agonists were being screened to restore chloride and fluid secretion in CF airways epithelium, nucleotide agonists emerged quickly as chloride and fluid secretagogues that stimulated chloride and fluid secretion independent of CFTR. Importantly, Knowles et al. [167] showed that extracellular nucleotides stimulated chloride secretion in human patients with CF, triggering interest in targeting any and all purinergic receptors for CF therapy. Importantly, purinergic agonists in addition to ATP such as UTP, UDP, and ADP (as well as poorly hydrolyzable analogs of those listed) were also efficacious in CF as well as non-CF airway epithelial model systems [168,169]. This led to the identification of P2Y1, P2Y2, P2Y4, and P2Y6 receptors in human airway epithelial model systems [170]. In addition, adenosine receptors (the P1 receptors) also stimulated chloride secretion in airway epithelial cells [171]; however, the major adenosine receptor, the A2 receptor, activates the cAMP/PKA signal transduction cascade and, eventually, CFTR. It is dysfunctional in CF. Several other laboratories have confirmed as well as extended these early findings in human epithelial cells or cells from other species [172–175].

Our laboratory has added work showing abundant expression and function of the P2X purinergic receptor channels in epithelia [141]. Biochemical characterization of P2X₄ and P2X₅ in human airway epithelial model systems with subtype-specific antibodies is currently in progress in our laboratory. We also cannot rule out the possible expression of P2X₆, which is not detected by our degenerate RT-PCR primers and for which antibodies are not available. A unifying theme in this chapter will be the fact that most, if not all, epithelial cell models express both P2Y G protein-coupled receptors and P2X receptor channels, sometimes in the same membrane domain of the polarized epithelium (Fig. 7). Because each class of receptor increases cytosolic calcium, albeit via different mechanisms, both receptor subtypes are viable targets for pharmacotherapy of CF in the lung and airways (see below).

Both P2Y G protein-coupled receptors, via phospholipase-induced release of Ca^{2+} from intracellular stores, and

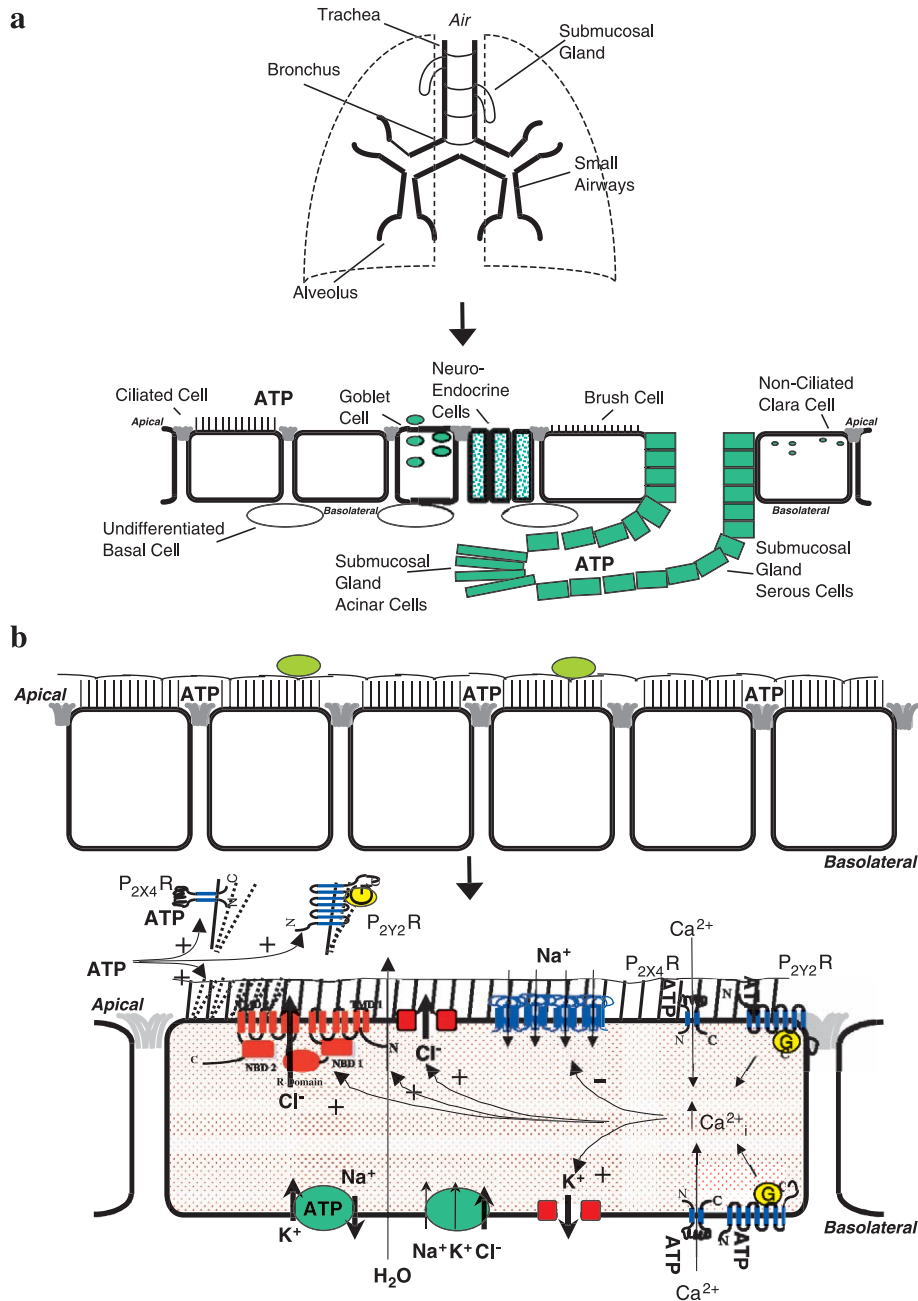


Fig. 7. Nucleotide signaling in the airways epithelium. Schematics of the whole lung and airways, a cross-section of a large airway with the many different subtypes on the surface and a submucosal gland beneath, a multi-ciliated airways epithelial segment of a large airway, and a single airway epithelial cell showing just some of the many functions that autocrine and paracrine purinergic signaling modulates. This regulation breaks down in CF (see text for details).

P2X receptor channels, via direct influx of Ca^{2+} through the channel from extracellular stores are capable of triggering calcium-dependent signal transduction cascades. P2Y-mediated effects on Ca^{2+}_i have been studied extensively in human airway epithelial cell models by Paradiso and others [176]. Zsembery et al. [154], using an IB3-1 CF human airway epithelial cell model for therapeutic implications in CF airway, have shown that both P2Y and P2X subtypes increase cytosolic calcium. Intriguingly, ATP stimulates both subtypes, although a fully transient increase in calcium is triggered by P2Y receptors, while P2X receptors cause a

sustained increase in Ca^{2+}_i (perhaps through the P2XR channels themselves and/or by opening store-operated or “Transient Receptor Polarization (TRP)” calcium channels). P2X receptor channel-mediated increases in cytosolic calcium are greatly potentiated by removal of extracellular Na^+ by replacement with NMDG [154]. We interpret this result to suggest that Na^+ competes with Ca^{2+} as each cation passes through the ATP-gated pore (each cation has a favorable gradient for entry). The P2X receptor-induced calcium influx is prevented by EGTA and augmented by raising extracellular Ca^{2+} [154].

Together, P2X and P2Y receptor activation leads to a pronounced, additive, and sustained increase in Ca^{2+}_i . This fact is critical for several reasons. First, either or both receptors could be targeted to trigger calcium-induced chloride secretion and potassium channel opening, which would be beneficial to the CF epithelium. Second, both receptors could be targeted to suppress absorptive Na^+ channels by calcium-dependent mechanisms. Such effects on all of the above would also correct abnormal cell volume regulation in the CF airways epithelium (see below). Local increases in calcium also augment ciliary beat frequency (see below), which would benefit attenuated mucociliary clearance in CF. Targeting either or both ATP receptor subfamilies for pharmacological therapy of the CF lung and airways is logical and feasible and takes full advantage of naturally expressed membrane proteins that are largely apical but are also basolateral.

Early work from Knowles et al. [167,171] showed that purinergic agonists stimulated chloride secretion in CF as well as non-CF airway epithelial model systems. The most important demonstration of this was in *in vivo* nasal potential difference (PD) measurements in CF patients [167]. Jiang et al. [177] subsequently showed that purinergic agonists stimulated fluid secretion in CF and non-CF airway epithelial cells. Purinergic agonists emerged from a “kitchen sink” approach of adding a large panel of agonists to CF epithelial model systems to identify which agonist, if any, could stimulate chloride secretion independent of CFTR. Many studies confirmed this work in other airway epithelial model systems from human and other species. Guggino et al. showed that purinergic receptors stimulated multiple types of chloride channels, including CFTR and the ORCCs from both the apical and basolateral membranes of primary rat tracheal epithelial cell monolayers [169]. It was concluded that the P2Y_2 receptor was critical to the apical-mediated stimulation of chloride secretion; however, rank order potency pharmacology most consistent with the P2Y_3 receptor (a species homolog to P2Y_1) stimulated chloride secretion from the basolateral side. As mentioned, UDP and ADP also stimulated chloride secretion in airway epithelia.

Epithelial cells release ATP in response to hypotonicity or dilution of the extracellular osmolality [17,19,21,47,51,178]. Hypotonicity-induced ATP release is potentiated by the expression of CFTR in the epithelial cell and is dampened when CFTR is absent from the plasma membrane [17,19]. Because CFTR is a regulator of other ion channels, transporters, and vesicle trafficking and fusion, CFTR may augment ATP release by positively regulating any and all of these ATP release mechanisms [17].

More recently, our laboratory has shown that CF human airway epithelial cells are sluggish in their recovery from a hypotonic insult, a process known as regulatory volume decrease or RVD [17]. Transient or stable transfection of the wild-type CFTR cDNA into CF human airway epithelial cells corrects defective cell volume recovery in response to hypotonicity. Wild-type CFTR modulation of human airway

epithelial cell volume regulation is blocked by the ATP scavengers, hexokinase or apyrase, and the global P2 receptor antagonist, suramin. Taken together, these data suggest that the presence of CFTR in the plasma membrane and CFTR-dependent ATP release govern epithelial cell RVD. This result begged the question: would addition of selective purinergic agonists to P2Y and P2X receptor subtypes rescue defective volume regulation in CF human airway epithelial cells. This is indeed the case. Both P2X receptors and P2Y receptors stimulate chloride and, likely, potassium efflux from epithelial cell during RVD. This is one critical answer to the question: why would a particular epithelial cell model express both P2Y and P2X receptors in the same cell? One answer is for protective redundancy against osmotic or other environmental insults (anoxia and ischemia, for example). Because epithelial cells are exposed to very different and dynamic microenvironments on their apical and basolateral sides, epithelial cells may express P2Y and P2X receptors in both membrane domains for this protective redundancy. A similar paradigm is evolving in hepatocytes and cholangiocytes in work by Feranchak et al. [47,178]. Another answer is simply that P2X receptors mediate fast and sustained increases in calcium signaling, while P2Y receptors mediate slower and only transient increases in cytosolic calcium.

In addition to stimulating Cl^- and K^+ efflux from the epithelial cell, ATP (and UTP) have also been observed to inhibit Na^+ influx pathways. Devor and Pilewski [179] have shown that UTP, by binding to purinergic receptors and increasing intracellular calcium concentrations, leads to a long-term inhibition of Na^+ entry to the cell from the apical media. This was studied in cells with normal and mutant forms of CFTR. They conclude that nucleotides (ATP and/or UTP) could have a dual therapeutic role in the airway, stimulating Cl^- efflux and inhibiting Na^+ entry. This conclusion has been borne out by a handful of studies in airway and other miscellaneous epithelial cell models, showing that stimulation of purinergic receptors stimulates Cl^- secretion while, at the same time, attenuating Na^+ absorption. Inglis et al. [180] studied these effects in distal bronchi and in rat fetal distal lung epithelial cells [181]. Iwase et al. [182] showed similar results in rabbit tracheal epithelium. While these were different preparation of distal airway epithelial cells, the conclusions were similar. ATP and UTP evoked a transient stimulation of Cl^- secretion and a sustained inhibition of Na^+ absorption in the polarized monolayers of distal airway epithelia. In the nasal PD measurements of porcine distal bronchi, transepithelial PD was measured in cannulated and perfused preparations. UTP hyperpolarized the PD transiently; this stimulation was inhibited by serosal bumetanide. PD then declined to a sustained level lower than basal; this sustained inhibition was prevented by luminal amiloride. Because thapsigargin failed to inhibit UTP-stimulated Cl^- secretion but did block the inhibition of Na^+ absorption, these results suggest that UTP stimulates Cl^- secretion by a calcium-independent mechanism, while

UTP inhibits Na^+ absorption via Ca^{2+}_i . Nevertheless, Inglis et al. argue that both effects of extracellular nucleotides should promote hydration of the airway.

The mucociliary system in the airway is necessary for optimal removal of mucus and inhaled pathogens and particles. Cilia on the surface of the airways epithelium beat at regular intervals and in a uniform direction toward the pharynx, and this facilitates the movement of materials along and up the “mucociliary escalator.” A key stimulus for enhancing ciliary beat is increased intracellular Ca^{2+} concentrations within the cilia themselves. If Ca^{2+} influx is impaired, this could lead to jeopardized mucociliary clearance and disease. Of the hormones and neurotransmitters that are known to stimulate ciliary beat, the most potent is ATP. ATP acts primarily in this system by stimulating Ca^{2+} influx from the external milieu, as well as stimulating internal stores to release Ca^{2+} . Ma et al. [183] have shown that extracellular sodium ions actually inhibit an ATP-gated calcium channel, perhaps through competition of both cations for the ATP-gated pore. Na^+ , therefore, attenuates ATP-dependent ciliary beat. Their findings suggest a physiologically significant relationship between Na^+ concentrations and ciliary beat. This has potentially significant therapeutic implications, suggesting that decreasing airway surface fluid Na^+ , while increasing Ca^{2+} in this fluid, may augment calcium influx into the cilium via P2X receptors and could increase mucociliary clearance in such diseases as cystic fibrosis, primary ciliary dyskinesia, or chronic bronchitis (Fig. 7).

7.2. Cystic fibrosis: a loss of extracellular purinergic signaling in the lung airways and in other tissues

Our laboratory as well as other laboratories have documented a role for CFTR and other ABC transporters in governing ATP release and autocrine and paracrine purinergic signaling. In the disease, cystic fibrosis (CF), purinergic signaling is attenuated. We believe that this defect, along with the primary defect in Cl^- channel function and Cl^- permeability [184], are major contributing factors to the abnormalities in the CF airway and, possibly, in other tissues affected in CF.

The CFTR protein is widely believed to form an anion channel in the apical membrane, but there is speculation as to exactly what it transports. There is a large amount of evidence that CFTR is a Cl^- channel activated by cAMP. Some believe that CFTR also has the capacity to conduct ATP [11], but this is very controversial [13]. Past and current research is focusing on a separate ATP conductance channel that is closely associated with the CFTR protein [17,18]. Because CFTR also regulates numerous other processes in the airway epithelial cell, CFTR may regulate ATP release, mediated by ATP channels and ATP-filled vesicles, to accomplish these other regulatory functions.

It has been shown that CFTR is necessary for extracellular nucleotide signaling. In CF epithelial cells that lack

functional CFTR at the apical membrane, nucleotide signaling is absent or insufficient. Therefore, the physiological consequences of this lost signal must be addressed. There is a loss of chloride conductance that may be necessary for the chloride secretion involved in RVD and transepithelial transport [12,167]. There could also be a loss of potassium and fluid secretion due to the loss of nucleotide signaling, two processes also critical in RVD. These consequences could lead to impaired intracellular cell volume regulation. An impairment in intracellular volume control, due to an inability of the epithelial cell to “sense” its external osmotic environment and/or to regulate its own volume, may also directly impact upon the abnormal ASL microenvironment observed in CF. Smith et al. [185] have observed a curious increase in ASL ionic strength in CF epithelia when compared to non-CF cells. This would also increase the tonicity of this microenvironment. Matsui et al. [186] observed a reduced ASL depth and volume in CF epithelia, but no difference in ionic strength. Zhang and Engelhardt [187], using their elegant xenograft model of well-differentiated non-CF and CF epithelia, showed defects in ionic strength and volume in the CF ASL versus the normal counterpart. These results and hypotheses relate back to an older and unappreciated study by Valverde et al. [188], who observed defective cell volume regulation in the intestinal crypts of CF knockout mice when compared to wild-type mice. The possibility that these defects in ASL composition and cell volume regulation may be caused by defects in autocrine ATP release and signaling remains to be determined.

8. Epithelial cells along the renal nephron

Once filtered at the glomerulus or secreted into the lumen of the nephron (proximal tubule cells release micromolar quantities of ATP) [21,44,189], the ATP is trapped in the tubular lumen as a signaling molecule. It is then propelled downstream by the tubular fluid rapidly and robustly where it can act on downstream tubules in a paracrine manner. Cells derived from multiple nephron segments express multiple P2Y, P2X, and P1 receptors, and Leipziger et al. and Satlin et al. [190–192] have shown the presence of luminal P2 receptors in isolated and perfused cortical collecting tubule or duct (CCT or CCD) preparations from mouse and rabbit. Even once that ATP is excreted in the final urine and exits the nephron, it can signal the uroepithelium (or urothelium) in the ureter and urinary bladder. Moreover, the urothelium releases ATP in response to increased distension of the ureter, the bladder, and associated structures [193]. Taken together, the lumen of the nephron and beyond provide an ideal microenvironment with a fluid medium that can transmit this autocrine and paracrine signaling molecule (Fig. 8).

The process of tubuloglomerular (TG) feedback, where changes in the luminal content of salt and water is sensed by

the small plaque of macula densa (MD) cells in the cTAL and where that sensation is transduced to the glomerulus of the same nephron, is widely accepted but poorly understood. A long-held hypothesis is that a local mediator or paracrine agonist may be released by MD cells and regulate vascular tone of the glomerulus by causing contraction of glomerular mesangial cells and constriction of the afferent arteriole of that glomerulus. Past work has suggested that adenosine may be that mediator. Through an elegant, freshly dissected cTAL/MD/glomerular preparation, Liu et al. [30] are examining TG feedback signaling mechanisms more directly. Briefly, they have found that changes in perfused NaCl concentrations are sensed in the lumen of the cTAL by the specialized MD cells, leading to ATP release from the basolateral surface of the MD plaque. ATP or its metabolites (adenosine, in particular) would then bind to glomerular mesangial cells in the interstitium and, ultimately, vascular smooth muscle cells in the afferent arteriole of the glomerulus. Via P2Y and/or P2X receptor channels, ATP would elevate cytosolic Ca^{2+} in both cell types, leading to constriction of the afferent arteriole and a decrease in renal blood flow and glomerular filtration rate to that single glomerulus. Adenosine could do the same via its A1 receptor. In short, it is classic paradigm for paracrine purinergic signaling involving specialized renal epithelial cells and their “cross-talk” with other renal glomerular cell types.

8.1. Collecting duct

McCoy et al. [194] studied a mouse IMCD cell line (mIMCD-K2) to determine if nucleotides regulated NaCl

transport and, if so, which purinergic receptor subtypes were involved. They observed that ATP, $\alpha\beta$ -methylene ATP and UTP stimulated Cl^- secretion and inhibited Na^+ absorption. These P2 agonists as well as specific and degenerate RT-PCR implicated four receptor subtypes: P2X3, P2X4, P2Y1, and P2Y2. Further analysis showed that apical nucleotide receptors were more effective in inhibiting Na^+ absorption and stimulating Cl^- secretion. Leipziger et al. have found similar results in M1-CCD cells and MDCK cells, and Deetjen and Leipziger and, later, Satlin et al. [190–192,195,196] found an apical P2Y2 receptor in isolated, perfused CCDs that increases cytosolic Ca^{2+} in these tubules. Similar modulation of ion transport in this segment is likely. Purinergic receptors also modulate water transport in the collecting duct. Kishore and Knepper found that P2Y2 receptors were expressed along the nephron in general and in renal medulla in particular. ATP and UTP, via this receptor, inhibited vasopressin-induced water permeability across the renal collecting duct. This paradigm is described in detail in a recent review [56]. Fig. 8 shows a collecting duct epithelial cell model illustrating this purinergic regulation in this nephron segment.

8.2. Autosomal dominant polycystic kidney disease: a change in nephron structure creates a detrimental autocrine signaling environment

Purinergic receptors and signaling are also critical along the nephron of the kidney. The richest source of ATP release in the nephron is the proximal tubule. There are many reasons why this is the case, including an accelerated

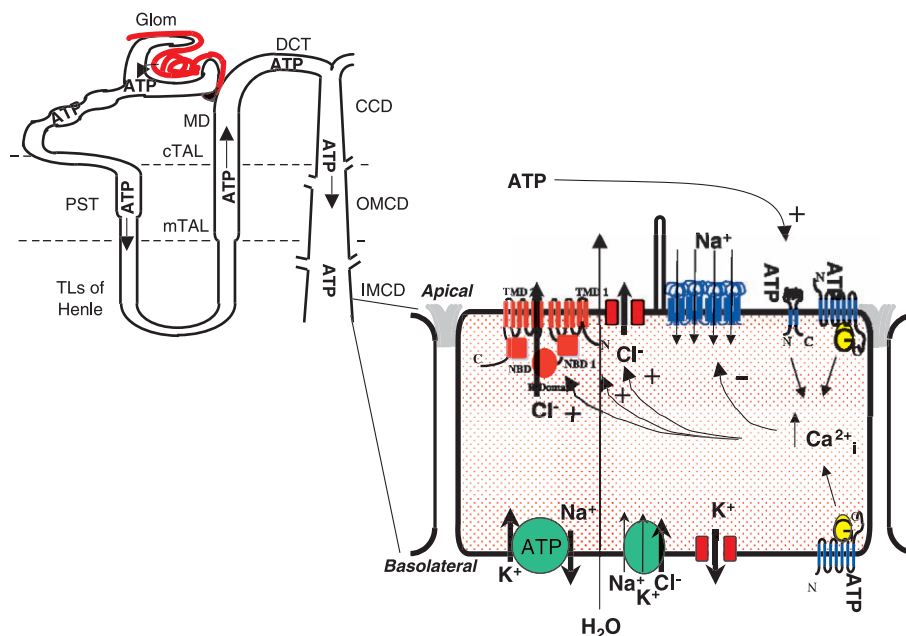


Fig. 8. Collecting duct epithelium in the context of the nephron. Schematic of the whole nephron and a cartoon of nucleotide regulation of a mono-ciliated collecting duct cell. Despite some similar modulation of NaCl and water transport, P2XRs have only been shown functionally to be present on the apical membrane on renal epithelia.

metabolic and transport rate in the proximal tubule and/or the expression of multiple ABC transporters like CFTR, mdx, and MOAT. Once released into the tubular lumen, ATP would be trapped as a charged anionic species and carried in the tubular fluid downstream to the other nephron segments, where it can bind to and interact with purinergic receptors. Autocrine and paracrine ATP signaling in the tubular fluid via purinergic receptors can affect any number of renal functions, due to the versatility of purinergic control over epithelial functions and signaling pathways (see recent reviews, Refs. [56,189]).

Because purinergic signaling plays an autocrine and paracrine role in the regulation of renal tubular function, defects in purinergic signaling could contribute significantly to kidney pathophysiology. Extracellular purinergic signaling is known to modulate water and salt balance along the nephron. Extracellular ATP in the apical environment or tubular lumen has been shown to inhibit water and salt reabsorption by the kidney. Therefore, the addition of purinergic agonists has been proposed to be of therapeutic benefit to decrease water and salt reabsorption, thus decreasing blood volume and pressure. A recent review examined this paradigm in some detail [56].

The relationship between autocrine and paracrine purinergic signaling and the renal disorder, PKD, is not intuitively obvious. However, PKD is a progressive disorder characterized mainly from the slow and gradual remodeling of the tubules of the kidney and the ducts of the pancreas and liver. In autosomal dominant PKD (ADPKD), this remodeling results in the formation of a fluid-filled cyst, created from the closure of two ends of a renal tubule. In autosomal recessive PKD (ARPKD), the tubules and ducts dilate; however, they only form cyst-like structures in end-stage disease that never fully close off. Either way, an abnormal microenvironment encapsulated by a single monolayer of epithelial cells develops. As alluded to above and in other reviews, such a microenvironment is ideal for autocrine and paracrine signaling [197].

Our laboratory has shown that ATP (and, likely, its metabolites) are present in micromolar quantities in a subset of ADPKD cyst fluid samples [21]. In this study and in another very recent one [44], ATP release was found to be as or more robust in PKD epithelia versus normal controls. This could be due to increased metabolism and/or proliferation of PKD epithelia during their reversion to an undifferentiated phenotype. More recent work has shown that both P2Y and P2X receptors are present on the luminal membrane of human ADPKD monolayers that stimulate Cl^- secretion by a cytosolic calcium-driven mechanism. As such, all of the elements are present for autocrine and paracrine ATP and ATP metabolite signaling to drive Cl^- secretion into the cyst. Obviously, this would be detrimental to the progression of ADPKD. An additional problematic feature of “trapped” purinergic signaling within the cyst is the fact that purinergic agonists are mitogens or co-mitogens along with growth factors for renal epithelial cells and

mesangial cells [198–200]. In PKD, growth factors are also released instead into the cyst. There, they interact with growth factor receptors mislocalized to the luminal membrane, leading to a devastating positive feedback loop for growth and proliferation of the cysts [201,202]. The autosomal dominant form of PKD (ADPKD) results in distinct cysts, or fluid-filled spheres lined by epithelial cells. Any normally apical ion or fluid transport is instead released into the encapsulated cyst. Therefore, any secretagogue could prove to be detrimental. Growth factors are normally released apically from the cell. Therefore, in some cell models, purinergic agonists were observed as mitogens or co-mitogens with growth factors. Therefore, ATP release into the cyst lumen could further prove to be detrimental.

9. Hair cell epithelium of the inner ear

The hair cells that line the cochlea of the inner ear respond to sound waves that enter the ear. ATP has been shown to be present in the endolymph, the fluid medium of the inner ear that bathes the hair cells [203]. Moreover, P2X purinergic receptor channels are present on the stereocilia that lie atop each hair cell [204]; the cilia bend in response to each sound wave and the mechanical changes in the cilia are transduced from a mechanical signal to an electrical one. Purinergic signaling is emerging as a critical process in sound transduction by the cilia on the hair cell [203]. Not only could ATP be released from the hair cells but that ATP could bind to the P2X receptors on the cilia to augment ciliary beat.

ATP is a critical autocrine and paracrine agonist in the endolymph and the scala media that fill the organs of the inner ear. P2 receptors have been found throughout the specialized epithelial cells and cell membranes that are present in the cochlear and vestibular system. This topic has been reviewed recently by Housley [203]. Basal levels of ATP in the perilymph and endolymph are nanomolar, and they increase in response to noise stress, sound waves, and hypoxia. Ecto-ATPases and ecto-apyrases may suppress the levels of extracellular ATP; however, the full range of stimuli for ATP release may not be appreciated and increases in ATP release (surrounding the stereocilia of the hair cells, for example) may not be readily detectable. Housley cites that the sources of released ATP are not appreciated and present an important future direction of this work. However, a recent study by Munoz et al. [205] showed that stores of ATP located in vesicles within marginal cells of the stria vascularis were released to increase ATP in the endolymph significantly following a sound stimulus. In contrast, hypoxia did not promote a statistically significant increase in endolymph ATP, although a slight increase was noted. It was also noted that substantial ATP was present under basal conditions, suggesting a role in the maintenance of inner ear and cochlear and vestibular function.

Despite continuing work on the sources of released ATP, it is known that extracellular ATP modulates transduction of sound waves by action of P2X receptors on the stereocilia and by P2Y receptors there and elsewhere. This is reviewed elegantly by Housley [203]. It is thought that P2X₂ receptors function together with stretch-activated non-selective cation channels in the stereocilia to depolarize the outer hair cell membrane, suggesting that ATP may play a significant role in the inner ear signaling transduction pathway [124,206,207]. However, it is possible that additional P2X receptor subtypes may contribute to the phenotype in particular inner ear cell types. P2X receptors also play critical roles in Reissner's membrane and in intermediate cells of the stria vascularis, where they mediate K⁺ shunt conductances [208]. It could be argued that the P2X receptor channels and other secretory K⁺ channels contribute to the high K⁺ concentrations in perilymph and endolymph. Indeed, mutation of the KvLQT channel in the stria vascularis marginal cell causes deafness in patients that also have long QT syndrome of the cardiac myocyte. The P2Y₄ and P2Y₂ receptors also play a critical role in regulating this KvLQT and other KCNE channels in strial marginal cells and vestibular dark cells [209,210]. Deeper in the inner ear, Marcus et al. have also found a role for P2X₂ receptors in parasensory cation absorption by cochlear outer sulcus cells and vestibular transitional cells [204]. In fact, guinea pigs with vestibular imbalance disorder were corrected by infusion of ATP and other purinergic agonists into the scala tympani.

Purinergic signaling also affects other inner ear epithelial cell functions. Hensen's cells of the cochlea, specialized epithelial cells in the inner ear, respond to extracellular ATP with changes in ionic currents and concomitant increases in Ca²⁺_i [211]. Ionic currents that were activated included a rapid inward current, a more slowly rising inward current, and a slowly developing reduction in input conductance. ATP also appeared to inhibit cell–cell communication via gap junctions. The fast current activated by ATP were the P2X receptor channels located on these and other specialized sensory epithelial cells in the cochlea, while P2Y receptors mediated the slow responses in ionic currents and Ca²⁺_i. The same group also performed similar work on Dieter's cells and showed that ATP promoted gap junctional communication between cells. Unfortunately, Fura-2 imaging of multiple cells within the tissue for Hensen's cells or Dieter's cells was not performed to monitor Ca²⁺ wave propagation. The inner ear and its specialized epithelial cells designed to sense and capture sound is a rich ground to study autocrine and paracrine nucleotide signaling. Taken together, there are profound physiological roles for extracellular ATP signaling and both P2X and P2Y receptors in the specialized ciliated and non-ciliated epithelial cells of the inner ear. Luciferase-based or other detection methods need to be applied to freshly dissected, endolymph-filled inner ear preparations to gauge the role of extracellular ATP in an *in vivo*-like preparation.

10. Future directions in the context of unanswered questions

10.1. Why does a specific cell need P2Y and P2X receptors?

There are answers to this question already; however, there will likely be many more. P2X receptors that allow calcium influx directly are thought to be the fast-acting purinergic receptor, while P2Y receptor mediate slower responses. Having said that, both increase cytosolic calcium within seconds; however, P2X receptors mediate sustained calcium increases in epithelial cells. Thus, a cell may indeed need both, and there is considerable evidence that neurons and epithelial cells express both subfamilies. Our laboratory has shown that both P2Y and P2X receptors are expressed functionally in the apical membrane of airway and kidney epithelia and vascular endothelia *in vitro* and *in vivo* [45,46,142,195]. Another reason may be for redundancy to protect against osmotic insult, anoxia or hypoxia, or other forms of cell injury. Or, related to the next question, a cell may need both for basal maintenance of essential functions and cell signaling. Nevertheless, study of the native P2X and P2Y receptors in these and other cells is becoming a necessity.

10.2. Does ATP release and signaling within microenvironments govern basal cell function and signaling?

Evidence is emerging that constitutive ATP release occurs under basal conditions to maintain physiological “setpoints” for signaling and function. Ostrom et al. [212] showed in Madin–Darby canine kidney (MDCK) cells that phosphatidylinositol turnover and arachidonic acid metabolism were altered when autocrine purinergic signaling was abolished. Our laboratory has published evidence that basal cytosolic calcium is modulated by endogenous ATP release and signaling in epithelial cells [46]. We also have preliminary evidence that endogenous ATP release and signaling modulates cell volume regulation under isotonic conditions and ciliary beat in airway and other preparations. Indeed, in past cardiovascular paradigms, ATP and adenosine have been characterized definitively as local metabolites that modulate vascular tone. Again, these studies can only be done in native cells and confirmed with heterologous cell systems that are carefully handled.

10.3. Is signaling emanating from P2R activation only dependent on calcium?

The answer to this question is likely to be complex. Sustained increases in cytosolic free calcium derived from P2XRs and extracellular stores may trigger calcium-dependent protein kinases (CaCMKs, Pyk2, ERKs, PKC, etc.) which may have many additional targets within the cell and affect cell function in limitless ways. Some or all of these calcium-dependent protein kinases affect the activity of

transcription factors and, thus, gene expression. Evidence is accumulating more slowly that P2YRs may couple to other signaling effector enzymes besides phospholipase C β , including PLA $_2$ and PLD. Native cells will likely aid this work and make it more physiologically relevant. Moreover, care must be taken to rule out or account for endogenous ATP release and signaling from the cell model or tissue preparation itself that may influence signaling cascades independent of exogenously applied agonists.

10.4. What is the stoichiometry of a P2XR multimer?

This is a ticklish question that is difficult to define or characterize. There is controversy over this question in the ENaC field as well as in every other ion channel field. Because IRK channels likely form tetramers, it is assumed that ENaCs and P2XRs may do the same. However, the large extracellular domain that these subfamilies share and is lacking in the IRK family may confound this multimeric assembly. There is no doubt that multimerization is critical for function; however, a consensus on stoichiometry would help understand P2XR expression and function better.

10.5. Are P2XRs targets for therapy of different diseases?

Exogenous ATP has been shown to correct hearing disorders. As such, it is possible that targeting of P2X $_2$ on stereocilia may be worth pursuing. P2XRs are a rich and important target for therapy of CF. In airway epithelia, multiple P2XR subtypes are expressed on both apical and basolateral membrane domains. In vivo nasal PD measurements showed a stimulation of chloride transport in CF knockout mice as well as normal mice when the agonists were added luminally. Current work has returned to this and other assays with different conditions designed to maximize P2XR activity and the sustained calcium increase that is mediated by P2XRs. More importantly, the P2XRs expressed in epithelia desensitize poorly (P2X $_2$, P2X $_4$, P2X $_5$, and, possibly, P2X $_6$); the same cannot be said for G protein-coupled receptors like P2Y $_2$ targeted by other groups for CF therapy. P2XRs, like P2Y $_2$, would restore chloride and fluid secretion and dampen sodium absorption but without desensitization and with a sustained increase in cytosolic calcium. This would correct abnormal cell volume regulation. Possibly, the most important effect would be to amplify ciliary beat frequency. Application of P2XR agonists would also require modified conditions of the saline in which it was nebulized and aerosolized to maximize its effect. Our laboratory is ardently pursuing this therapeutic approach.

On the other hand, inhibition of P2XRs and, possibly, other calcium entry channels may be beneficial for therapy of ADPKD. This could suppress chloride and fluid secretion and fluid accumulation as well as the enhanced proliferation rate of the monolayers of renal epithelial cells that encapsulates the cyst, two hallmarks that enhance the progression of the disease after cyst formation. At the same time,

inhibition of calcium entry might augment ENaC-mediated sodium and fluid absorption, causing the cysts to shrink. Our laboratory is pursuing this therapeutic hypothesis.

These questions are just a few of the many that drive those of us who are obsessed “purinergics.”

Acknowledgements

EMS is supported by an NIH NHLBI R01 grant HL63934 to study epithelial P2X purinergic receptor channels and an NIH NIDDK R01 grant DK54367 to study all aspects of purinergic signaling and the role that CFTR plays in amplifying ATP release and signaling. Past support from the American Heart Association (Southern Research Consortium), the Cystic Fibrosis Foundation, and the Polycystic Kidney Disease Foundation was also greatly appreciated.

References

- [1] J.L. Gordon, *Biochem. J.* 233 (1986) 309–319.
- [2] A.N. Drury, A. Szent-Gyorgyi, *J. Physiol.* 68 (1929) 213–237.
- [3] A. Sattin, T.W. Rall, *Mol. Pharmacol.* 6 (1970) 13–23.
- [4] G. Burnstock, *Pharmacol. Rev.* 24 (1972) 509–581.
- [5] V. Ralevic, G. Burnstock, *Pharmacol. Rev.* 50 (1998) 413–492.
- [6] R.A. North, *Physiol. Rev.* 82 (2002) 1013–1067.
- [7] G. Burnstock, *Neuropharmacology* 36 (1997) 1127–1139.
- [8] S.H. Donaldson, E.R. Lazarowski, et al., *Mol. Med.* 6 (2000) 969–982.
- [9] H.H. Dalziel, D.P. Westfall, *Pharmacol. Rev.* 46 (1994) 449–466.
- [10] E.H. Abraham, A.G. Prat, et al., *Proc. Natl. Acad. Sci. U. S. A.* 90 (1993) 312–316.
- [11] I.L. Reisin, A.G. Prat, et al., *J. Biol. Chem.* 269 (1994) 20584–20591.
- [12] E.M. Schwiebert, M.E. Egan, et al., *Cell* 81 (1995) 1063–1073.
- [13] M.M. Reddy, P.M. Quinton, et al., *Science* 271 (1996) 1876–1879.
- [14] R. Grygorczyk, J.W. Hanrahan, *Am. J. Physiol.* 272 (1997) C1058–C1066.
- [15] C. Li, M. Ramjeesingh, et al., *J. Biol. Chem.* 271 (1996) 11623–11626.
- [16] W.C. Watt, E.R. Lazarowski, et al., *J. Biol. Chem.* 273 (1998) 14053–14058.
- [17] G.M. Braunstein, R.M. Roman, et al., *J. Biol. Chem.* 276 (2001) 6621–6630.
- [18] M. Sugita, Y. Yue, et al., *EMBO J.* 17 (1998) 898–908.
- [19] A.L. Taylor, B.A. Kudlow, et al., *Am. J. Physiol., Cell Physiol.* 275 (1998) C1391–C1406.
- [20] R.M. Roman, A.P. Feranchak, et al., *Am. J. Physiol.: Gastrointest. Liver Physiol.* 277 (1999) G1222–G1230.
- [21] P.D. Wilson, J.S. Hovater, et al., *J. Am. Soc. Nephrol.* 10 (1999) 218–229.
- [22] S. Reyman, H. Florke, et al., *Biochem. Mol. Med.* 54 (1995) 75–87.
- [23] F.P. Thinnies, K.P. Hellman, et al., *Mol. Genet. Metab.* 69 (2000) 331–337.
- [24] A.W. Mangel, J.R. Raymond, et al., *Am. J. Physiol., Renal Physiol.* 264 (1993) F490–F495.
- [25] J.M. McGill, T.W. Gettys, et al., *J. Membr. Biol.* 133 (1993) 253–261.
- [26] D.B. Light, E.M. Schwiebert, et al., *Am. J. Physiol., Renal Physiol.* 258 (1990) F273–F280.
- [27] E.M. Schwiebert, J.W. Mills, et al., *J. Biol. Chem.* 269 (1994) 7081–7089.

- [28] R. Benz, L. Wojtczak, et al., *FEBS Lett.* 231 (1988) 75–80.
- [29] R.Z. Sabirov, A.K. Dutta, et al., *J. Gen. Physiol.* 118 (2001) 251–266.
- [30] R. Liu, P.D. Bell, et al., *J. Am. Soc. Nephrol.* 13 (2002) 1145–1151.
- [31] P.S. Jackson, K. Strange, *J. Gen. Physiol.* 105 (1995) 661–667.
- [32] S.F. Schlosser, A.D. Burgstahler, et al., *Proc. Natl. Acad. Sci. U. S. A.* 93 (1996) 9948–9953.
- [33] G. Arcuino, J.H. Lin, et al., *Proc. Natl. Acad. Sci. U. S. A.* 99 (2002) 9840–9845.
- [34] C.E. Stout, J.L. Costantin, et al., *J. Biol. Chem.* 277 (2002) 10482–10488.
- [35] R.M. Roman, N. Lomri, et al., *J. Membr. Biol.* 183 (2001) 165–173.
- [36] P. Linsdell, J.W. Hanrahan, *J. Gen. Physiol.* 111 (1998) 601–614.
- [37] H. Fujise, K. Higa, et al., *Am. J. Physiol., Cell Physiol.* 281 (2001) C2003–C2009.
- [38] H. Zeng, G. Liu, et al., *Cancer Res.* 60 (2000) 4779–4784.
- [39] N. Brustovetsky, A. Becker, et al., *Proc. Natl. Acad. Sci. U. S. A.* 93 (1996) 664–668.
- [40] J. Gualix, J. Pintor, et al., *J. Neurochem.* 73 (1999) 1098–1104.
- [41] E. Guillen, C.B. Hirschberg, *Biochemistry* 34 (1995) 5472–5476.
- [42] L.A. Bankston, G. Guidotti, *J. Biol. Chem.* 271 (1996) 17132–17138.
- [43] G.G. Yegutkin, G. Burnstock, *Biochim. Biophys. Acta* 1466 (2000) 234–244.
- [44] E.M. Schwiebert, D.P. Wallace, et al., *Am. J. Physiol., Renal Physiol.* 282 (2002) F763–F775.
- [45] L.M. Schwiebert, W.C. Rice, et al., *Am. J. Physiol., Cell Physiol.* 282 (2002) C282–C301.
- [46] A.P. Feranchak, J.G. Fitz, et al., *J. Hepatol.* 33 (2000) 174–182.
- [47] R.M. Roman, A.P. Feranchak, et al., *Am. J. Physiol.: Gastrointest. Liver Physiol.* 276 (1999) G1391–G1400.
- [48] C.E. Sorensen, I. Novak, *J. Biol. Chem.* 276 (2001) 32925–32935.
- [49] R. Beigi, E. Kobatake, et al., *Am. J. Physiol., Cell Physiol.* 276 (1999) C267–C278.
- [50] A. Hazama, S. Hayashi, et al., *Pflugers Arch.* 437 (1998) 31–35.
- [51] A. Hazama, H.T. Fan, et al., *J. Physiol.* 523 (2000) 1–11.
- [52] S.W. Schneider, M.E. Egan, et al., *Proc. Natl. Acad. Sci. U. S. A.* 96 (1999) 12180–12185.
- [53] G. Burnstock, *Prog. Biochem. Pharmacol.* 16 (1980) 141–154.
- [54] G. Burnstock, *Cell Membrane Receptors for Drugs and Hormones: A Multidisciplinary Approach*, Raven Press, New York, 1978, pp. 107–118.
- [55] G. Burnstock, *Extracellular Nucleotides and Nucleosides: Release, Receptors, and Physiological and Pathophysiological Effects*, Academic Press, San Diego, CA, 2003, Chapter 1.
- [56] E.M. Schwiebert, B.K. Kishore, *Am. J. Physiol., Renal Physiol.* 280 (2001) F945–F963.
- [57] E.R. Lazarowski, *Extracellular Nucleotides and Nucleosides: Release, Receptors, and Physiological and Pathophysiological Effects*, Academic Press, San Diego, CA, 2003, Chapter 3.
- [58] M.P. Abbracchio, G. Burnstock, *Pharmacol. Ther.* 78 (1998) 113–145.
- [59] V. Ralevic, G. Burnstock, *Pharmacol. Rev.* 50 (1998) 413–492.
- [60] J.P. Clancy, B.R. Cobb, *Extracellular Nucleotides and Nucleosides: Release, Receptors, and Physiological and Pathophysiological Effects*, Academic Press, San Diego, CA, 2003, Chapter 5.
- [61] M.R. Boarder, G.A. Weisman, et al., *Trends Pharmacol. Sci.* 16 (1995) 133–139.
- [62] E.A. Barnard, J. Simon, T.E. Webb, *Mol. Neurobiol.* 15 (1997) 103–129.
- [63] T.K. Harden, J.L. Boyer, R.A. Nicholas, *Annu. Rev. Pharmacol. Toxicol.* 35 (1995) 541–579.
- [64] F.L. Zhang, L. Luo, et al., *J. Pharmacol. Exp. Ther.* 301 (2002) 705–713.
- [65] M.P. Abbracchio, J.M. Boeynamems, et al., *Trends Pharmacol. Sci.* 24 (2003) 52–55.
- [66] T.D. Nguyen, S. Meichle, et al., *Am. J. Physiol.* 280 (2001) G795–G804.
- [67] M.E. Olah, G.L. Stiles, *Annu. Rev. Physiol.* 54 (1992) 211–225.
- [68] M.E. Olah, G.L. Stiles, *Annu. Rev. Pharmacol. Toxicol.* 35 (1995) 581–606.
- [69] G. Burnstock, C. Kennedy, *Gen. Pharmacol.* 16 (1985) 433–440.
- [70] M.P. Abbracchio, G. Burnstock, *Pharmacol. Ther.* 64 (1994) 445–475.
- [71] B.P. Bean, *Trends Pharmacol. Sci.* 13 (1992) 87–90.
- [72] B.P. Bean, *J. Neurosci.* 10 (1990) 1–10.
- [73] B.P. Bean, D.D. Friel, *Ion Channels* 2 (1990) 169–203.
- [74] B.P. Bean, C.A. Williams, et al., *J. Neurosci.* 10 (1990) 11–19.
- [75] A.J. Brake, M.J. Wagenbach, et al., *Nature* 371 (1994) 519–523.
- [76] S. Valera, N. Hussy, et al., *Nature* 371 (1994) 516–519.
- [77] P. Seguela, A. Haghighi, et al., *J. Neurosci.* 16 (1996) 448–455.
- [78] G. Buell, C. Lewis, et al., *EMBO J.* 15 (1996) 55–62.
- [79] F. Soto, M. Garcia-Guzman, et al., *Proc. Natl. Acad. Sci. U. S. A.* 93 (1996) 3684–3688.
- [80] C.Z. Wang, N. Namba, et al., *Biochem. Biophys. Res. Commun.* 220 (1996) 196–202.
- [81] M. Garcia-Guzman, F. Soto, et al., *FEBS Lett.* 388 (1996) 123–127.
- [82] G. Collo, R.A. North, et al., *J. Neurosci.* 16 (1996) 2495–2507.
- [83] A. Surprenant, F. Rassendren, et al., *Science* 272 (1996) 735–738.
- [84] T. Urano, H. Nishimori, et al., *Cancer Res.* 57 (1997) 3281–3287.
- [85] X. Bo, R. Schoepfer, et al., *J. Biol. Chem.* 275 (2000) 14401–14407.
- [86] P.J. Jensik, D. Holbird, et al., *Am. J. Physiol., Cell Physiol.* 281 (2001) C954–C962.
- [87] T.M. Egan, J.A. Cox, et al., *FEBS Lett.* 475 (2000) 287–290.
- [88] E. Boue-Grabot, M.A. Akimenko, et al., *J. Neurochem.* 75 (2000) 1600–1607.
- [89] W.H. Norton, K.B. Rohr, et al., *Mech. Dev.* 99 (2000) 149–152.
- [90] K. Mulryan, D.P. Gitterman, et al., *Nature* 403 (2000) 86–89.
- [91] M. Vlaskovska, L. Kasakov, et al., *J. Neurosci.* 21 (2001) 5670–5677.
- [92] Y. Zhong, P.M. Dunn, et al., *Eur. J. Neurosci.* 14 (2001) 1784–1792.
- [93] D.J. Benos, B.A. Stanton, *J. Physiol. (London)* 520 (1999) 631–644.
- [94] L. Bianchi, M. Driscoll, *Neuron* 34 (2002) 337–340.
- [95] S. Kellenberger, L. Schild, *Physiol. Rev.* 82 (2002) 735–767.
- [96] A. Newbolt, R. Stoop, et al., *J. Biol. Chem.* 273 (1998) 15177–15182.
- [97] A.T. Boyce, E.M. Schwiebert, *Extracellular Nucleotides and Nucleosides: Release, Receptors, and Physiological and Pathophysiological Effects*, Academic Press, San Diego, CA, 2003, Chapter 4.
- [98] W.R. Haines, G.E. Torres, et al., *Mol. Pharmacol.* 56 (1999) 720–727.
- [99] G.E. Torres, T.M. Egan, et al., *J. Biol. Chem.* 274 (1999) 6653–6659.
- [100] G.E. Torres, T.M. Egan, et al., *J. Biol. Chem.* 274 (1999) 22359–22365.
- [101] G.E. Torres, W.R. Haines, et al., *Mol. Pharmacol.* 54 (1998) 989–993.
- [102] C. Lewis, S. Neidhart, et al., *Nature* 377 (1995) 432–435.
- [103] V. Spelta, L.H. Jiang, et al., *Br. J. Pharmacol.* 135 (2002) 1524–1530.
- [104] A. Surprenant, D.A. Schneider, et al., *J. Auton. Nerv. Syst.* 81 (2000) 249–263.
- [105] K.T. Le, K. Babinski, et al., *J. Neurosci.* 18 (1998) 7152–7159.
- [106] B.F. King, A. Townsend-Nicholson, et al., *J. Neurosci.* 20 (2000) 4871–4877.
- [107] S. Ding, F. Sachs, *J. Membr. Biol.* 172 (1999) 215–223.
- [108] S. Ding, F. Sachs, *J. Physiol. (London)* 522 (2000) 199–214.
- [109] W.R. Haines, K. Migita, et al., *J. Biol. Chem.* 276 (2001) 32793–32798.
- [110] W.R. Haines, M.M. Voigt, et al., *J. Neurosci.* 21 (2001) 5885–5892.
- [111] L.H. Jiang, F. Rassendren, et al., *J. Biol. Chem.* 276 (2001) 14902–14908.
- [112] K. Migita, W.R. Haines, et al., *J. Biol. Chem.* 276 (2001) 30934–30941.
- [113] L.H. Jiang, F. Rassendren, et al., *J. Biol. Chem.* 275 (2000) 34190–34196.
- [114] S.S. Ennion, S. Hagan, et al., *J. Biol. Chem.* 275 (2000) 29361–29367.

- [115] T. Koshimizu, M. Koshimizu, et al., *J. Biol. Chem.* 274 (1999) 37651–37657.
- [116] E. Boue-Grabot, V. Archambault, et al., *J. Biol. Chem.* 275 (2000) 10190–10195.
- [117] P. Werner, E.P. Seward, et al., *Proc. Natl. Acad. Sci. U. S. A.* 93 (1996) 15485–15490.
- [118] Z. Xiang, X. Bo, et al., *Hear. Res.* 128 (1999) 190–196.
- [119] U. Brandle, H.P. Zenner, et al., *Neurosci. Lett.* 273 (1999) 105–108.
- [120] S.G. Salih, G.D. Housley, et al., *NeuroReport* 10 (1999) 2579–2586.
- [121] C. Chen, M.S. Parker, et al., *J. Neurophysiol.* 83 (2000) 1502–1509.
- [122] C. Chen, B.P. Bobbin, *Br. J. Pharmacol.* 124 (1998) 337–344.
- [123] M.S. Parker, M.L. Larroque, et al., *Hear. Res.* 121 (1998) 62–70.
- [124] G.D. Housley, R. Kanjhan, et al., *J. Neurosci.* 19 (1999) 8377–8388.
- [125] U. Brandle, E. Guenther, et al., *Brain Res.: Mol. Brain Res.* 59 (1998) 269–272.
- [126] U. Brandle, K. Kohler, et al., *Brain Res.: Mol. Brain Res.* 62 (1998) 106–109.
- [127] H. Taschenberger, R. Juttner, et al., *J. Neurosci.* 19 (1999) 3353–3366.
- [128] T.H. Wheeler-Schilling, K. Marquardt, et al., *Brain Res.: Mol. Brain Res.* 76 (2000) 415–418.
- [129] T.H. Wheeler-Schilling, K. Marquardt, et al., *Brain Res.: Mol. Brain Res.* 92 (2001) 177–180.
- [130] R. Jabs, E. Guenther, et al., *Brain Res.: Mol. Brain Res.* 76 (2000) 205–210.
- [131] X. Bo, A. Alavi, et al., *NeuroReport* 10 (1999) 1107–1111.
- [132] H.Y. Lee, M. Bardini, et al., *J. Urol.* 163 (2000) 2002–2007.
- [133] M.P. Meyer, U. Groschel-Stewart, et al., *Dev. Dyn.* 216 (1999) 442–449.
- [134] M. Rytén, A. Hoeberitz, et al., *Dev. Dyn.* 221 (2001) 331–341.
- [135] B. Hu, C. Senkler, et al., *J. Biol. Chem.* 277 (2002) 15752–15757.
- [136] K. Yamamoto, R. Korenaga, et al., *Circ. Res.* 87 (2000) 385–391.
- [137] K. Yamamoto, R. Korenaga, et al., *Am. J. Physiol., Heart Circ. Physiol.* 279 (2000) H285–H292.
- [138] K. Shinozuka, N. Tanaka, et al., *Clin. Exp. Pharmacol. Physiol.* 28 (2001) 799–803.
- [139] F.R. Ray, W. Huang, et al., *Atherosclerosis* 162 (2002) 55–61.
- [140] A.N. Ramirez, D.L. Kunze, *Am. J. Physiol., Heart Circ. Physiol.* 282 (2002) H2106–H2116.
- [141] A.L. Taylor, L.M. Schwiebert, et al., *J. Clin. Invest.* 104 (1999) 875–884.
- [142] A. Hoeberitz, A. Townsend-Nicholson, et al., *Bone* 27 (2000) 503–510.
- [143] A. Hoeberitz, S. Meghji, et al., *FASEB J.* 15 (2001) 1139–1148.
- [144] A. Gartland, R.A. Hipkind, et al., *J. Bone Miner. Res.* 16 (2001) 846–856.
- [145] L.N. Naemsch, S.J. Dixon, et al., *J. Biol. Chem.* 276 (2001) 39107–39114.
- [146] Z. Xiang, X. Bo, et al., *Brain Res.* 813 (1998) 390–397.
- [147] A. Loesch, S. Miah, et al., *J. Neurocytol.* 28 (1999) 495–504.
- [148] R. Glass, G. Burnstock, *J. Anat.* 198 (2001) 569–579.
- [149] M. Afework, G. Burnstock, *Cell Tissue Res.* 298 (1999) 449–456.
- [150] M. Afework, G. Burnstock, *Cells Tissues Organs* 167 (2000) 297–302.
- [151] M. Liu, P.M. Dunn, et al., *Br. J. Pharmacol.* 128 (1999) 61–68.
- [152] P. Petit, D. Hillaire-Buys, et al., *Br. J. Pharmacol.* 125 (1998) 1368–1374.
- [153] R. Glass, M. Bardini, et al., *Cells Tissues Organs* 169 (2001) 377–387.
- [154] A. Zsembery, A.T. Boyce, et al., *J. Biol. Chem.* (2003) (in press e-pub ahead of print).
- [155] R.J. Bridges, B.B. Newton, et al., *Am. J. Physiol., Lung Cell. Mol. Physiol.* 281 (2001) L16–L23.
- [156] S. Ennion, R.J. Evans, *Mol. Pharmacol.* 61 (2002) 303–311.
- [157] E.C. Burgard, W. Niforatos, et al., *Mol. Pharmacol.* 58 (2000) 1502–1510.
- [158] C.J. Lewis, A. Surprenant, et al., *Br. J. Pharmacol.* 124 (1998) 1463–1466.
- [159] J. Rettinger, G. Schmalzing, et al., *Neuropharmacology* 39 (2000) 2044–2053.
- [160] M. Klapperstock, C. Buttner, et al., *Eur. J. Pharmacol.* 387 (2000) 245–252.
- [161] G. Lambrecht, J. Rettinger, et al., *Eur. J. Pharmacol.* 387 (2000) R19–R21.
- [162] R. Stoop, A. Surprenant, et al., *J. Neurophysiol.* 78 (1997) 1837–1840.
- [163] J.D. Clyne, L.D. LaPointe, et al., *J. Physiol. (London)* 539 (2002) 347–359.
- [164] L. Homolya, T.H. Steinberg, et al., *J. Cell Biol.* 150 (2000) 1349–1360.
- [165] D.M. Morse, J.L. Smullen, et al., *Am. J. Physiol., Cell Physiol.* 280 (2001) C1485–C1497.
- [166] H.A. Brown, E.R. Lazarowski, et al., *Mol. Pharmacol.* 40 (1991) 648–655.
- [167] M.R. Knowles, L.L. Clarke, et al., *N. Engl. J. Med.* 325 (1991) 533–538.
- [168] E.R. Lazarowski, A.M. Paradiso, et al., *Proc. Natl. Acad. Sci. U. S. A.* 94 (1997) 2599–2603.
- [169] T.H. Hwang, E.M. Schwiebert, et al., *Am. J. Physiol., Cell Physiol.* 270 (1996) C1611–C1623.
- [170] D. Communi, P. Paindavoine, et al., *Br. J. Pharmacol.* 127 (1999) 562–568.
- [171] E.R. Lazarowski, S.J. Mason, et al., *Br. J. Pharmacol.* 106 (1992) 774–782.
- [172] B.R. Cobb, F. Ruiz, et al., *Am. J. Physiol., Lung Cell. Mol. Physiol.* 282 (2002) L12–L25.
- [173] P. Huang, E.R. Lazarowski, et al., *Proc. Natl. Acad. Sci. U. S. A.* 98 (2001) 14120–14125.
- [174] M.J. Stutts, E.R. Lazarowski, et al., *Am. J. Physiol., Cell Physiol.* 268 (1995) C425–C433.
- [175] S.V. Sitarman, L. Wang, et al., *J. Biol. Chem.* 277 (2002) 33188–33195.
- [176] M.R. Van Scott, T.C. Chinet, et al., *Am. J. Physiol., Lung Cell. Mol. Physiol.* 269 (1995) L30–L37.
- [177] C. Jiang, W.E. Finkbeiner, et al., *Science* 262 (1993) 424–427.
- [178] Y. Wang, R.M. Roman, et al., *Proc. Natl. Acad. Sci. U. S. A.* 93 (1996) 12020–12025.
- [179] D.C. Devor, J.M. Pilewski, *Am. J. Physiol., Cell Physiol.* 276 (1999) C827–C837.
- [180] S.K. Inglis, A. Collett, et al., *Pflugers Arch.* 438 (1999) 621–627.
- [181] S.J. Ramminger, A. Collett, et al., *Br. J. Pharmacol.* 128 (1999) 293–300.
- [182] N. Iwase, T. Sasaki, et al., *Respir. Physiol.* 107 (1997) 173–180.
- [183] W. Ma, A. Korngreen, et al., *Nature* 400 (1999) 894–897.
- [184] M.J. Welsh, L.C. Tsui, et al., *The Metabolic and Molecular Bases of Inherited Disease*, vol. III, 7th ed., McGraw-Hill, Health Professions Division, New York, 1995, Chapter 127.
- [185] J.J. Smith, S.M. Travis, et al., *Cell* 85 (1996) 229–236.
- [186] H. Matsui, B.R. Grubb, et al., *Cell* 95 (1998) 1005–1015.
- [187] Y. Zhang, J.F. Engelhardt, *Am. J. Physiol., Cell Physiol.* 276 (1999) C469–C476.
- [188] M.A. Valverde, J.A. O'Brien, et al., *Proc. Natl. Acad. Sci. U. S. A.* 92 (1995) 9038–9041.
- [189] E.M. Schwiebert, *Clin. Exp. Pharmacol. Physiol.* 28 (2001) 340–350.
- [190] P. Deetjen, J. Thomas, et al., *J. Am. Soc. Nephrol.* 11 (2000) 1798–1806.
- [191] L.M. Satlin, S. Sheng, et al., *Am. J. Physiol., Renal Physiol.* 280 (2001) F1010–F1018.
- [192] C.B. Woda, M. Leite, et al., *Am. J. Physiol., Renal Physiol.* 283 (2002) F437–F446.
- [193] G.E. Knight, P. Bodin, et al., *Am. J. Physiol., Renal Physiol.* 282 (2002) F281–F288.

- [194] D.E. McCoy, A.L. Taylor, et al., *Am. J. Physiol., Renal Physiol.* 277 (1999) F552–F559.
- [195] N. Gordjani, R. Nitschke, et al., *Cell Calcium* 22 (1997) 121–128.
- [196] J.E. Cuffe, A. Bielfeld-Ackermann, et al., *J. Physiol. (London)* 524 (2000) 77–90.
- [197] E.M. Schwiebert, A. Zsembery, et al., *Extracellular Nucleotides and Nucleosides: Release, Receptors, and Physiological and Pathophysiological Effects*, Academic Press, San Diego, CA, 2003, Chapter 2.
- [198] D. Erlinge, *Gen. Pharmacol.* 31 (1998) 1–8.
- [199] M.S. Paller, E.J. Schnaith, et al., *J. Lab. Clin. Med.* 131 (1998) 174–183.
- [200] D.J. Wang, N.N. Huang, et al., *J. Cell. Physiol.* 153 (1992) 221–233.
- [201] N.S. Murcia, R.P. Woychik, et al., *Pediatr. Nephrol.* 12 (1998) 721–726.
- [202] P.D. Wilson, *Am. J. Physiol., Renal Physiol.* 272 (1997) F434–F442.
- [203] G.D. Housley, *Clin. Exp. Pharmacol. Physiol.* 27 (2000) 575–580.
- [204] J.H. Lee, T. Chiba, et al., *J. Neurosci.* 21 (2001) 9168–9174.
- [205] D.J. Munoz, P.R. Thorne, et al., *Hear. Res.* 138 (1999) 56–64.
- [206] N.P. Raybound, G.D. Housley, *J. Physiol. (London)* 498 (1997) 717–727.
- [207] R. Kanjhan, G.D. Housley, et al., *J. Comp. Neurol.* 407 (1999) 11–32.
- [208] M. King, D. Housley, et al., *NeuroReport* 9 (1998) 2467–2474.
- [209] D.C. Marcus, H. Sunose, et al., *Am. J. Physiol., Cell Physiol.* 273 (1997) C2022–C2029.
- [210] C.L. Sage, D.C. Marcus, *J. Membr. Biol.* 185 (2002) 103–115.
- [211] L. Langostena, J.K. Ashmore, et al., *J. Physiol. (London)* 531 (2001) 693–706.
- [212] R.S. Ostrom, C. Gregorian, P.A. Insel, *J. Biol. Chem.* 275 (2000) 11735–11739.

Sustained Calcium Entry through P2X Nucleotide Receptor Channels in Human Airway Epithelial Cells*

Received for publication, December 3, 2002, and in revised form, January 21, 2003
Published, JBC Papers in Press, February 3, 2003, DOI 10.1074/jbc.M212277200

Ákos Zsemberý^{‡§¶}, Amanda T. Boyce^{§**}, Lihua Liang^{‡§}, János Peti-Peterdi^{‡‡}, P. Darwin Bell^{‡‡},
and Erik M. Schwiebert^{‡§***}

From the Departments of [‡]Physiology and Biophysics, ^{**}Cell Biology, and ^{‡‡}Medicine and the [§]Gregory Fleming James Cystic Fibrosis Research Center, University of Alabama, Birmingham, Alabama 35294-0005 and the [¶]Department of Pathophysiology, Semmelweis University, Budapest 1085, Hungary

Purinergic receptor stimulation has potential therapeutic effects for cystic fibrosis (CF). Thus, we explored roles for P2Y and P2X receptors in stably increasing $[Ca^{2+}]_i$ in human CF (IB3-1) and non-CF (16HBE14o⁻) airway epithelial cells. Cytosolic Ca^{2+} was measured by fluorospectrometry using the fluorescent dye Fura-2/AM. Expression of P2X receptor (P2XR) subtypes was assessed by immunoblotting and biotinylation. In IB3-1 cells, ATP and other P2Y agonists caused only a transient increase in $[Ca^{2+}]_i$ derived from intracellular stores in a Na^+ -rich environment. In contrast, ATP induced an increase in $[Ca^{2+}]_i$ that had transient and sustained components in a Na^+ -free medium; the sustained plateau was potentiated by zinc or increasing extracellular pH. Benzoyl-benzoyl-ATP, a P2XR-selective agonist, increased $[Ca^{2+}]_i$ only in Na^+ -free medium, suggesting competition between Na^+ and Ca^{2+} through P2XRs. Biochemical evidence showed that the P2X₄ receptor is the major subtype shared by these airway epithelial cells. A role for store-operated Ca^{2+} channels, voltage-dependent Ca^{2+} channels, or Na^+/Ca^{2+} exchanger in the ATP-induced sustained Ca^{2+} signal was ruled out. In conclusion, these data show that epithelial P2X₄ receptors serve as ATP-gated calcium entry channels that induce a sustained increase in $[Ca^{2+}]_i$. In airway epithelia, a P2XR-mediated Ca^{2+} signal may have therapeutic benefit for CF.

In cystic fibrosis (CF),¹ cyclic AMP- and protein kinase A-dependent transepithelial Cl^- transport is impaired because of

mutations in the CF gene that encodes for the protein, the “cystic fibrosis transmembrane conductance regulator” or CFTR (1). Originally, CFTR was thought to function exclusively as a low conductance Cl^- channel (2, 3). More recently, it has become clear that CFTR also regulates a series of other transporters and ion channels, such as the Cl^-/HCO_3^- exchanger, the $Na^+:HCO_3^-$ cotransporter, epithelial Na^+ channels, K^+ channels, and aquaporin water channels (4, 5). Although the exact mechanisms of the regulation of these proteins by CFTR are not yet fully understood, it is clear that impaired Cl^- transport is shared as a key disease phenotype by CF epithelia from all affected tissues and that this pathway is lost in CF. Therefore, activation of a cAMP-independent Cl^- secretory pathway through exploitation of a naturally expressed epithelial protein could be of interest for CF therapy. In certain cases, stimulation of Ca^{2+} -dependent Cl^- channels can correct the impaired HCO_3^- secretion in CF cells (6, 7).

It is widely accepted that CFTR plays a crucial role in ATP release from cells (8–10). The same is true for *mdr* ABC transporters in hepatocytes and heterologous cells (11, 12). Once ATP is released into the extracellular space, it can bind to purinoceptors regulating a variety of functions in different epithelia (13–15). ATP and other agonists of purinoceptors are known to increase intracellular Ca^{2+} concentration ($[Ca^{2+}]_i$) potentially in airway epithelial cells which, in turn, leads to stimulation of Cl^- secretion (14–17) and inhibition of Na^+ absorption (18–22). In fact, earlier studies have proposed the use of UTP and non-hydrolyzable UTP analogs as therapeutic agonists targeted to the P2Y₂ receptors in the treatment of CF lung disease (23, 24).

Purinoceptors are divided into two classes: P1 or adenosine receptors, and P2, which recognize primarily extracellular ATP, ADP, UTP, and UDP. The P2 receptors are further subdivided into two subclasses. P2X receptors are extracellular ATP-gated calcium-permeable non-selective cation channels that are modulated by extracellular Ca^{2+} , Mg^{2+} , H^+ , and metal ions such as Zn^{2+} and/or Cu^{2+} (25). P2Y receptors couple to heterotrimeric G proteins and phospholipases (primarily phospholipase C β) to raise intracellular free calcium concentration (26). In CF epithelial cells from multiple tissues, expression of P2X and P2Y receptors appears unaffected, offering the possibility to increase $[Ca^{2+}]_i$ through targeting a naturally expressed receptor in the apical or basolateral membrane domains (27, 28). Nonetheless, in different CF epithelial cell models, the desensitization of P2Y receptors and the transient nature of the Ca^{2+} response upon chronic and repeated delivery of a P2Y-specific agonist have made it difficult to generate stable stimuli for ion secretion (7, 29).

In this study, we used both CF (IB3-1) (30) and non-CF (16HBE14o⁻) (31) human airway epithelial cell models, to dissect out P2X-specific and P2Y-specific mechanisms of trigger-

* This work was supported by National Institutes of Health Grant R01 HL63934 (to E. M. S.), OTKA Grant T037524, and ETT Grant 226/2000 (to A. Z.). The costs of publication of this article were defrayed in part by the payment of page charges. This article must therefore be hereby marked “advertisement” in accordance with 18 U.S.C. Section 1734 solely to indicate this fact.

¶ To whom correspondence may be addressed: Dept. of Physiology and Biophysics and the Gregory Fleming James Cystic Fibrosis Research Center, University of Alabama, MCLM 740, 1918 University Blvd., Birmingham, AL 35294-0005. Tel.: 205-934-6235; Fax: 205-934-1445; E-mail: zsemberay@physiology.uab.edu.

§§ To whom correspondence may be addressed: Dept. of Physiology and Biophysics and Dept. of Cell Biology and the Gregory Fleming James CF Research Center, University of Alabama, MCLM 740, 1918 University Blvd., Birmingham, AL 35294-0005. Tel.: 205-934-6234; Fax: 205-934-1445; E-mail: eschwiebert@physiology.uab.edu.

¹ The abbreviations used are: CF, cystic fibrosis; ASL, airway surface liquid; CFTR, cystic fibrosis transmembrane conductance regulator; ER, endoplasmic reticulum; NMDG, N-methyl-D-glucamine; P2XR, P2X purinergic receptor channel; SOC, store-operated calcium channel; TRP, transient receptor potential channel; PBS, phosphate-buffered saline; ADP β S, adenosine 5'-[β -thioldiphosphate; 2MeSATP, 2-methylthio ATP; α,β -meATP, methylene ATP; BzBzATP, benzoyl-benzoyl-ATP; 2APB, 2-amino-ethoxyphenyl borate.

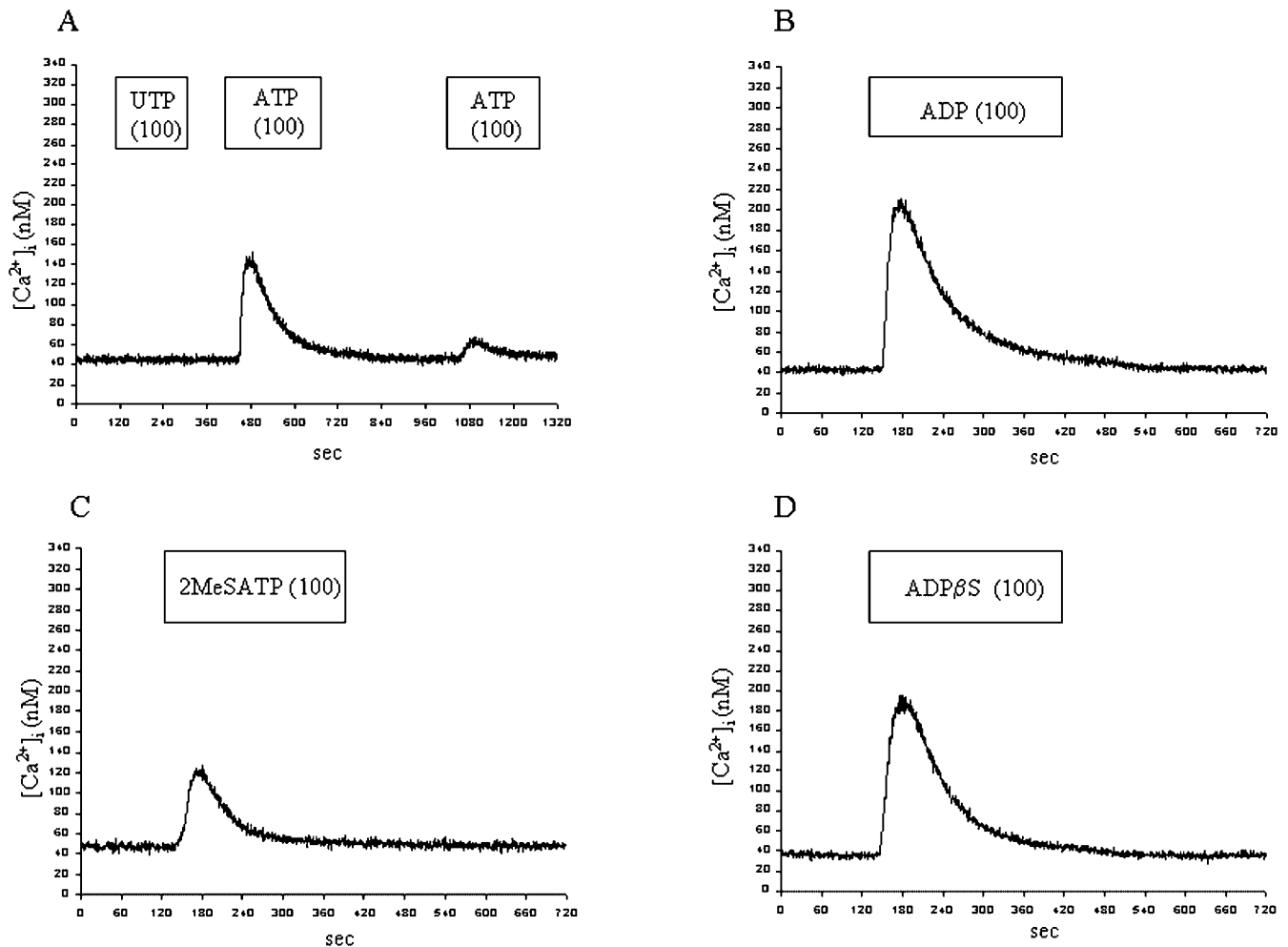


FIG. 1. Original traces showing the effects of ATP and UTP (100 μM each) (A), ADP (100 μM) (B), 2MeSATP (100 μM) (C), and ADP β S (100 μM) (D) on $[\text{Ca}^{2+}]_i$. IB3-1 cells were superfused with Na^+ -containing medium (solution A). A, please note that the second application of ATP was without effect. In these traces and in all others below, please note that there is a time lag of 10–15 s before agonist-containing perfusate enters the cuvette. As all of these experiments were performed on coverslips prepared on the same day, a calibration was used on the same cell preparation to allow conversion and plotting of the data as cytosolic calcium.

ing an increase in $[\text{Ca}^{2+}]_i$. We characterized a broad range of P2Y-selective, P2X-selective, and non-discriminant P2Y and P2X agonists under different chemical and ionic conditions to explore possible strategies to elicit an increase in $[\text{Ca}^{2+}]_i$ that is sustained and prolonged. Results described herein, using Fura-2/AM-based imaging, show that activation of P2Y and P2X receptors increases $[\text{Ca}^{2+}]_i$ by completely distinct mechanisms. P2Y receptors elicit a transient increase in $[\text{Ca}^{2+}]_i$ derived from intracellular endoplasmic reticulum (ER) stores, whereas P2X receptors trigger a sustained rise in $[\text{Ca}^{2+}]_i$, allowing Ca^{2+} influx from the extracellular space. In addition, biochemical evidence shows that the P2X₄ receptor is the major epithelial subtype present in both cell lines. Thus, we conclude that epithelial P2X receptors function as ATP-gated Ca^{2+} entry channels in the plasma membrane and have profound potential as a target for CF pharmacotherapy.

MATERIALS AND METHODS

Cell Cultures—IB3-1 cells derive from airway epithelia of a CF patient carrying two different mutations of the CFTR gene, the most common trafficking mutation ($\Delta\text{Phe-508}$) and a premature stop codon mutation (W1282X) (30). 16HBE14o[−] cells are non-CF or normal airway epithelial cells, which express CFTR at the plasma membrane. The cells were grown on Vitrogen 100-coated tissue-culture flasks in 5% CO_2 incubator at 37 °C. IB3-1 cells were cultured in LHC-8 (Biofluids, Rockville, MD) medium supplemented with 5% fetal bovine serum (Invitrogen), 100 units/ml penicillin/streptomycin (Invitrogen), 1 \times L-glutamine

(Invitrogen), and 1.25 $\mu\text{g}/\text{ml}$ Fungizone (Invitrogen). 16HBE14o[−] cells were cultured in minimum Eagle's medium (Invitrogen) supplemented with 10% fetal bovine serum and 100 units/ml penicillin/streptomycin. When cells reached confluency, they were washed twice with $\text{Ca}^{2+}/\text{Mg}^{2+}$ -free PBS. The cells were then suspended using trypsin/EDTA solution and plated on diluted Vitrogen-coated (collagen types I and IV diluted 1:15 in Dulbecco's phosphate-buffered saline) glass coverslips. For $[\text{Ca}^{2+}]_i$ measurements, cells were used 48–72 h after plating.

Fura-2 Imaging of Intracellular Ca^{2+} —Cytosolic Ca^{2+} concentration was measured with dual excitation wavelength fluorescence microscopy (Deltascan, Photon Technologies, Princeton, NJ) after cells were loaded with the permeant form of the fluorescence dye Fura-2/acetoxymethyl ester (Fura-2/AM; Teflabs, Austin, TX). Fura-2 fluorescence was measured at an emission wavelength of 510 nm in response to the excitation wavelength of 340 and 380 nm, alternated at a rate of 50 Hz by a computer-controlled chopper assembly. Ratios (340/380 nm) were calculated at a rate of 5 points/s using PTI software. Cells were incubated in Dulbecco's phosphate-buffered saline containing 2 mM CaCl_2 and 1 mM MgCl_2 in the presence of 5 μM Fura-2/AM and 1 mg/ml Pluronic F-127 dissolved in Me_2SO for 120 min to allow loading of the dye into the cells. After loading, coverslips were rinsed at least for 10 min in Dulbecco's phosphate-buffered saline to remove extracellular Fura-2/AM and the surfactant and were positioned in the cuvette at a 45° angle from the excitation light. Two glass capillary tubes were inserted into the top of the cuvette out of the patch of the excitation light. One tube was extended to the bottom of the cuvette and connected by way of polyethylene tubing to an infusion pump. The other capillary tube was positioned at the top of the cuvette and served to remove fluid from the cuvette. The volume of the cuvette was ~ 1.5 ml, and the flow rate was

~5 ml/min. It is important to note that switch in perfusion solutions is removed in time and space for the cuvette, such that a 10–15-s time lag exists before agonist is exposed to the cells. Experiments were performed at room temperature. Fluorescence intensities at both wavelengths were assessed, and only those preparations in which there were >200,000 counts/s for both wavelengths were used for experiments. At the beginning of each experiment, cells were perfused with solution A (see below), and the fluorescence ratio was monitored for at least for 100 s to establish a stable base-line value. Agonists and antagonists were then added to the appropriate solutions (see later). The 340/380 nm ratios (R) were converted into $[Ca^{2+}]_i$ values using the equations of Grynkiewicz *et al.* (32) as follows: $[Ca^{2+}]_i = K_d \times ((R - R_{min})/(R_{max} - R)) \times (S_{380}/S_{340})$ where K_d is the dissociation constant of Fura-2 for

Ca^{2+} , R_{max} and R_{min} are R values under saturating and Ca^{2+} -free conditions, respectively, and S_{380} and S_{340} are the fluorescent signals (S) emitted by Ca^{2+} -free (f) and Ca^{2+} -bound (b) forms of Fura-2 at a wavelength of 380 nm. *In situ* cell calibrations were accomplished after the cells were permeabilized with ionomycin (2 μ M) under Ca^{2+} -free (10 mM EGTA) and saturating Ca^{2+} (3 mM $CaCl_2$) conditions. The K_d was assumed to be 224 nM (32).

Fura-2 Quenching Experiments—Cells were loaded and washed as described for intracellular $[Ca^{2+}]$ measurement. Fluorescence signal was measured at 359 nm (isobestic wavelength) in the presence of $MnCl_2$ (500 μ M) to detect Ca^{2+} -independent changes in Fura-2 fluorescence (33).

Immunoblotting with P2X Receptor Channel Isoform-specific Antibodies—Cells were lysed in a buffer containing 10 mM Tris, 0.5 mM NaCl, 0.5% Triton X-100, 50 μ g/ml aprotinin (Sigma), 100 μ g/ml leupeptin (Sigma), and 100 μ g/ml pepstatin A (Sigma) adjusted to pH 7.2–7.4. Twenty micrograms of protein were run per lane and separated on an 8% SDS-polyacrylamide gel and then transferred to a polyvinylidene difluoride membrane (Osmonics, Westborough, MA). Immunoblotting was performed with a rabbit polyclonal antibody to P2X₄ (Alomone Laboratories, Jerusalem, Israel) at a dilution of 1:500. P2X₁, P2X₂, and P2X₇ antibodies were also obtained from Alomone Laboratories and were tested in a similar manner. Reactivity was detected by horseradish peroxidase-labeled goat anti-rabbit secondary antibody (1:3,000 dilution, New England Biolabs, Beverly, MA). Enhanced chemiluminescence was used to visualize the secondary antibody.

Biotinylation of Plasma Membrane P2X Receptor Channels—Cells were seeded on Vitrogen-coated (collagen types I and IV diluted 1:15 in Dulbecco's phosphate-buffered saline) 12-mm filters and grown as polarized monolayers with a transepithelial resistance that exceeded 400 ohms/cm². Cells were placed on ice and washed 3 times with cold PBS supplemented with 0.1 mM $CaCl_2$ and 1.0 mM $MgCl_2$. Cells were then incubated in 1.0 mg/ml poly(ethylene)oxid maleimide (Pierce) or sulfo-NHS-LC biotin (Pierce) in cold supplemented PBS for 25 min at 4 °C. Cells were washed 4 times with cold supplemented PBS, and the biotin was quenched with 0.1% bovine serum albumin (Sigma). Cells were then washed 3 times with cold supplemented PBS. Alternatively, cells could be biotinylated with biocytin hydrazide. Filters were first incubated in 300 μ l of a stock solution containing 30 mM $NaIO_4$ and 600 μ l of a stock solution containing 100 mM sodium acetate and 0.02% sodium azide, pH 5.5, for 30 min at room temperature in the dark. Filters were washed and subsequently incubated with 1.0 mg/ml biocytin hydrazide

TABLE I
Maximum changes in Fura-2 fluorescence in IB3-1 cells in Na^+ -containing medium

Δ ratios (340/380 nm) are maximum changes in Fura-2 fluorescence in response to purinergic agonists *versus* basal fluorescence. Values for % are percent changes in fluorescence *versus* ATP (100 μ M), except ADP (100 μ M) + Ca^{2+} free media whose value for % is *versus* ADP (100 μ M). Values are means \pm S.D.; n = number of experiments.

	Δ ratio	%	n
ATP (100 μ M)	0.30 \pm 0.11	100	15
ATP (10 μ M)	0.20 \pm 0.10	67	4
ATP (100 μ M) + suramin (100 μ M)	0.04 \pm 0.02 ^a	13	4
ATP (100 μ M) + Ca^{2+} -free media	0.18 \pm 0.03 ^a	60	5
ADP (100 μ M)	0.38 \pm 0.17	127	8
ADP (100 μ M) + Ca^{2+} -free media	0.16 \pm 0.05 ^b	42	4
ADP β S (100 μ M)	0.37 \pm 0.06	123	7
ADP β S (10 μ M)	0.28 \pm 0.07	93	3
2MeSATP (100 μ M)	0.24 \pm 0.06	80	3
ATP (100 μ M) + $ZnCl_2$ (20 μ M)	0.25 \pm 0.07	83	4
ATP (100 μ M) at $pH_e = 7.9$	0.38 \pm 0.18	127	2
ATP (100 μ M) at $pH_e = 6.4$	0.22 \pm 0.02	73	2
UTP (100 μ M)	No increase	0	6
UDP (100 μ M)	No increase	0	3
Adenosine (100 μ M)	No increase	0	4
BzBzATP (100 μ M)	No increase	0	3
α,β -MeATP (100 μ M)	No increase	0	3

^a $p < 0.05$ relative to ATP (100 μ M).
^b $p < 0.05$ relative to ADP (100 μ M).

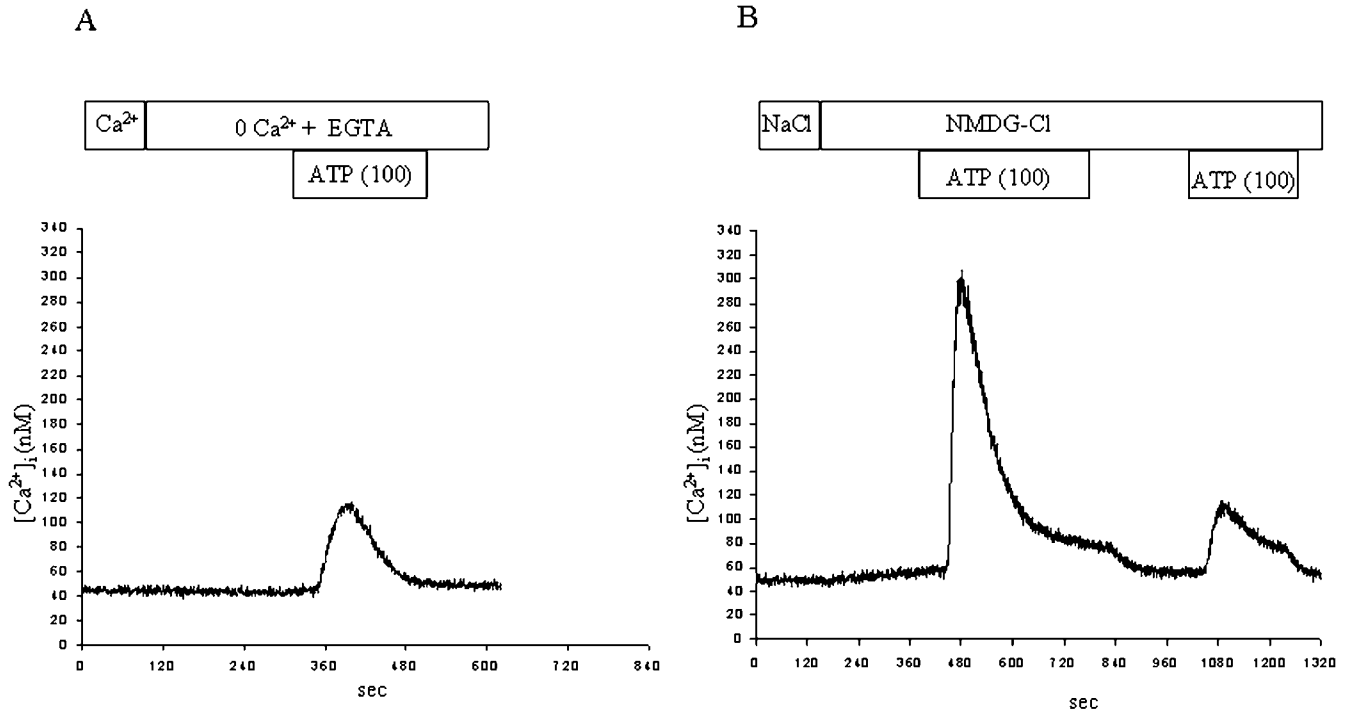


FIG. 2. Original traces showing the effects of ATP (100 μ M) on $[Ca^{2+}]_i$ in IB3-1 cells exposed to nominally Ca^{2+} -free, Na^+ -containing solution (A) and in cells exposed to Ca^{2+} -containing Na^+ -free solution (B) as indicated. B, please note the slight sustained increase in $[Ca^{2+}]_i$ upon substitution of Na^+ by NMDG. This sustained plateau was the first hint that in Na^+ -free medium Ca^{2+} entry channels could also be involved in the ATP-induced sustained Ca^{2+} response.

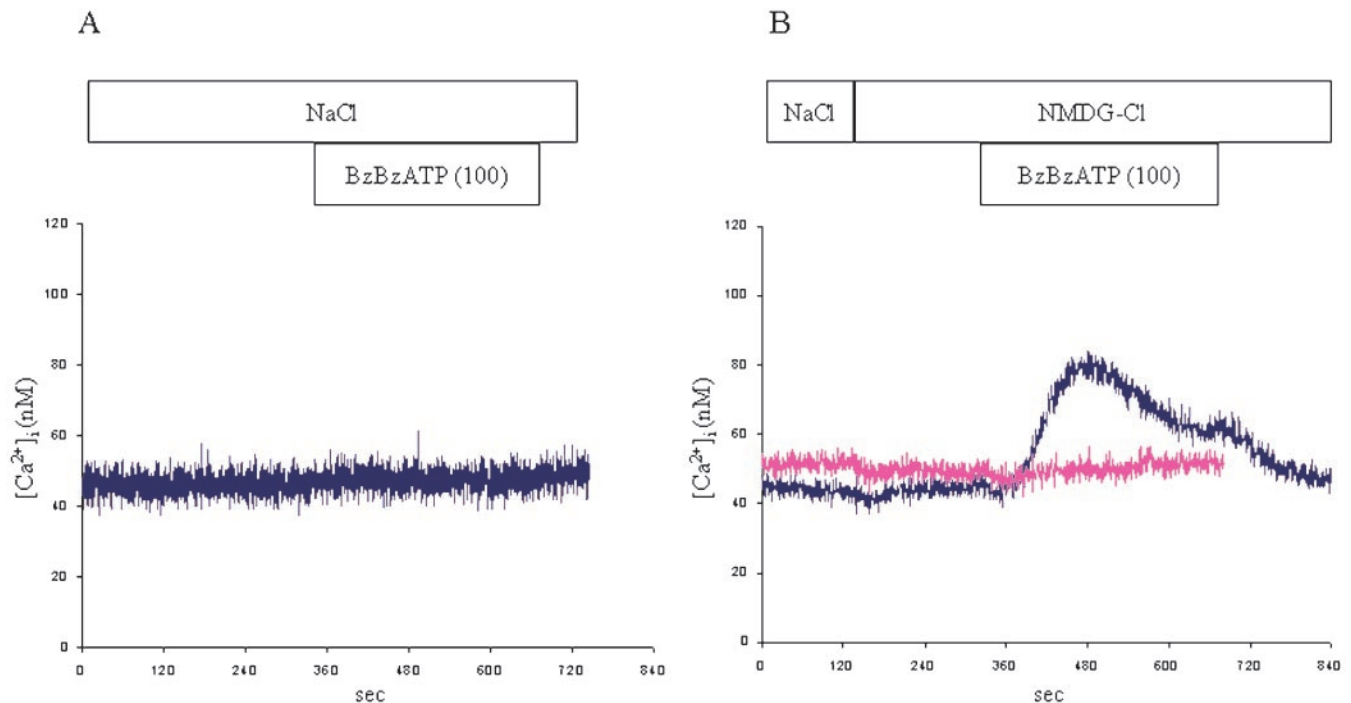


FIG. 3. *A* includes an original trace showing the lack of an effect of BzBzATP (100 μ M) on $[Ca^{2+}]_i$ in IB3-1 cells in Na^+ -containing medium. *B* shows an original trace where cells exposed to Na^+ -free medium are responsive to BzBzATP (100 μ M) with a rise in $[Ca^{2+}]_i$ in IB3-1 cells. Note that a second trace (in magenta) is shown to illustrate the lack of effect of BzBzATP (100 μ M) in a Ca^{2+} -free and Na^+ -free solution.

TABLE II
Maximum changes in Fura-2 fluorescence in IB3-1 cells in Na^+ -free medium

Δ ratios (340/380 nm) are maximum changes in Fura-2 fluorescence in response to purinergic agonists *versus* basal fluorescence. All values for % are percent changes in fluorescence *versus* ATP (100 μ M). Values are means \pm S.D.; n = number of experiments.

	Δ ratio	%	n
ATP (100 μ M)	0.82 ± 0.24^a	100	11
ATP (100 μ M) + Ca^{2+} -free media	0.25 ± 0.14^b	31	4
ATP (100 μ M) + $ZnCl_2$ (20 μ M)	0.77 ± 0.21	94	5
ATP (100 μ M) at $pH_e = 7.9$	0.78 ± 0.22	95	5
ATP (100 μ M) at $pH_e = 6.4$	0.22 ± 0.06^b	27	5
ATP (100 μ M) + KB-R7943 (30 μ M)	0.70 ± 0.13	85	3
ATP (100 μ M) + high $[KCl]_e$ (40 mM)	0.38 ± 0.08^b	46	4
ADP β S (100 μ M)	0.80 ± 0.23^c	98	3
BzBzATP (100 μ M)	0.15 ± 0.02^d	18	5
BzBzATP (100 μ M) + Ca^{2+} -free media	No increase	0	3
α,β -MeATP (100 μ M)	No increase	0	3

^a $p < 0.05$ relative to ATP (100 μ M) in sodium-containing medium (see Table I).

^b $p < 0.05$ relative to ATP (100 μ M) alone.

^c $p < 0.05$ relative to ADP β S (100 μ M) in sodium-containing medium (see Table I).

^d $p < 0.05$ relative to BzBzATP (100 μ M) in sodium-containing medium (see Table I).

(Pierce) for 1 h at 4 $^{\circ}C$. The reaction was quenched with 0.1 M Tris, pH 7.5. Cell lysates were collected as described above in immunoblotting procedures. Immobilized streptavidin beads (Pierce) were added to the lysates at a 1:10 dilution and rocked overnight at 4 $^{\circ}C$. Beads were washed 3 times with lysis buffer and incubated in sample buffer for 5 min at 95 $^{\circ}C$. The mixture was centrifuged, and the supernatant was loaded onto an SDS-PAGE gel. The immunoblotting procedure then continued as described above.

Solutions—Buffers for $[Ca^{2+}]_i$ measurement contained (mmol/liter) the following: for solution A: NaCl 140, KCl 3, KH_2PO_4 1.3, Na_2HPO_4 8, $MgCl_2$ 1, $CaCl_2$ 2; for solution B: NaCl 140, KCl 3, KH_2PO_4 1.3, Na_2HPO_4 8, $MgCl_2$ 1, Na-EGTA 1; for solution C: NMDG-Cl 140, KCl 4.5, Hepes 10, $MgCl_2$ 1, $CaCl_2$ 2; and for solution D: NMDG-Cl 100, KCl 40, Hepes 10, $MgCl_2$ 1, $CaCl_2$ 2. The solutions are at pH 7.3 unless indicated otherwise. In Fura-2 quenching experiments $MnCl_2$ (500 μ M) was added to Ca^{2+} - and EGTA-free solutions.

Data Analysis—Data are expressed as mean \pm S.D. An unpaired Student's t test was used to compare the data in different experimental groups. Results were considered significant if $p < 0.05$. For original Fura-2 traces shown in the figures, data are graphed with calibrated cytosolic free calcium on the y axis, because data from an individual preparation of cells was accumulated for all of the experiments in that figure where a calibration was also performed. Because not all data were generated from cells of the same passage or where a calibration was not performed for every preparation, the data in tables are shown as ratiometric data.

RESULTS

Purinergic Agonists Trigger a Transient Increase in $[Ca^{2+}]_i$ in the Presence of Extracellular Na^+ in IB3-1 Cells—To test for the presence of purinergic receptors in IB3-1 cells, we measured the cytosolic free Ca^{2+} concentration after stimulation with different agonists to both P2Y and P2X receptors in physiologic bath solution (solution A) containing Na^+ . Superfusion of cells with solution containing ATP (100 μ M) caused a rapid increase in the ratio (340/380 nm) of Fura-2 fluorescence ($r_{\text{basal}} = 0.89 \pm 0.09$ to $r_{\text{peak}} = 1.19 \pm 0.13$; $n = 15$). However, the response was transient, and the $[Ca^{2+}]_i$ returned close to basal value within 200 s after stimulation, even in the continuous presence of agonist ($r = 0.92 \pm 0.09$; $n = 15$) (Fig. 1A). Furthermore, when cells were exposed to ATP for the second time, only a small and even more transient change was detected in Fura-2 fluorescence (Fig. 1A). Administration of 10 μ M ATP caused a comparable but smaller change in $[Ca^{2+}]_i$ (Table I). The effect of ATP was completely inhibited by the application of suramin (100 μ M) (Table I). ADP, 2MeSATP (100 μ M each), and ADP β S (10 and 100 μ M) also caused an increase in cytosolic Ca^{2+} concentration, showing similar characteristics described for ATP (Fig. 1, B–D, and Table I). Because 2MeSATP and ADP β S increased $[Ca^{2+}]_i$ in a similar manner to ATP and ADP, these data argue strongly for activation of P2Y₁ receptors over other P2Y subtypes. In contrast, neither UTP (100 μ M) (Fig. 1A) nor UDP (100 μ M) had any effect on Ca^{2+} concentration (Table I). To explore whether degradation of ATP or ADP plays role in elevation of $[Ca^{2+}]_i$, we tested the effects of adenosine (100 μ M).

TABLE III
Changes in Fura-2 fluorescence in IB3-1 cells 5 min after the peak stimulation

Δ ratios (340/380 nm) are changes in Fura-2 fluorescence 5 min after the peak stimulation *versus* unstimulated conditions. All values for % are percent changes in fluorescence *versus* ATP (100 μ M) in Na⁺-containing medium. Values are means \pm S.D.; n = number of experiments.

	Na ⁺ -containing medium			Na ⁺ -free medium		
	Δ ratio	%	n	Δ ratio	%	n
ATP (100 μ M)	0.03 \pm 0.02	100	15	0.10 \pm 0.03 ^a	333	11
ATP (100 μ M) + Ca ²⁺ -free media	No increase	0	5	No increase	0	3
ATP (100 μ M) + ZnCl ₂ (20 μ M)	0.02 \pm 0.01	66	4	0.26 \pm 0.04 ^{a,b}	866	5
ATP (100 μ M) at pH _e = 7.9	0.04 \pm 0.01	133	2	0.18 \pm 0.02 ^{a,b}	600	5
ATP (100 μ M) at pH _e = 6.4	0.02 \pm 0.01	66	2	0.02 \pm 0.01	66	5
ATP (100 μ M) + KB-R7943 (30 μ M)	Not tested			0.14 \pm 0.05 ^a	466	3
ATP (100 μ M) + high [KCl] _e (40 mM)	No increase	0	3	0.01 \pm 0.01	33	4
ADP β S (100 μ M)	0.01 \pm 0.02	33	3	0.03 \pm 0.01	100	3
BzBzATP (100 μ M)	No increase	0	3	0.05 \pm 0.01 ^a	167	5
ATP (100 μ M) + 2APB (75 μ M)	0.02 \pm 0.02	66	2	0.12 \pm 0.04 ^a	400	3
ATP (100 μ M) + SKF-56365 (50 μ M)	Not tested			0.25 \pm 0.08 ^{a,b}	833	4

^a $p < 0.05$ relative to ATP (100 μ M) in Na⁺-containing medium.

^b $p < 0.05$ relative to ATP (100 μ M) in Na⁺-free medium.

Because adenosine did not increase [Ca²⁺]_i, we did not pursue the participation of P1 receptors in increasing [Ca²⁺]_i (Table I).

Purinergic Agonists Trigger a Transient Increase in [Ca²⁺]_i in the Absence of Extracellular Ca²⁺—Activation of P2Y₁ receptors leads to G protein-coupled phospholipase C- and inositol 1,4,5-trisphosphate-dependent release of Ca²⁺ from intracellular stores. As such, P2Y agonists should increase cytosolic Ca²⁺ even in the absence of extracellular Ca²⁺. Therefore, we repeated the experiments with ATP (100 μ M) (Fig. 2A) and ADP (100 μ M) superfusing IB3-1 cells with solutions containing EGTA (1 mM) instead of CaCl₂ (solution B). Similar to control conditions, both agonists increased [Ca²⁺]_i transiently, indicating that their effects, at least partially, were independent from extracellular Ca²⁺ (Table I). Nonetheless, the absence of extracellular Ca²⁺ reduced the agonist-induced peak increase in [Ca²⁺]_i (Table I). Again, under these conditions, the Ca²⁺ transients decayed fully back to base line within 200 s. Interestingly, these data did suggest that, besides P2Y₁ receptor activation, purinergic agonists may also trigger Ca²⁺ influx from extracellular stores, which contributes to the peak increase in [Ca²⁺]_i. Nevertheless, under these ionic conditions, Ca²⁺ influx was not sufficient to support a sustained elevation of [Ca²⁺]_i, the goal of this study. Experiments described below lend clarification to these early data.

P2X Receptor-selective Agonists Fail to Trigger an Increase in [Ca²⁺]_i in the Presence of Extracellular Na⁺ and Ca²⁺—Multiple subtypes of P2X receptors have already been described in human, rabbit, and rodent airway epithelial cells (27, 34, 35). Thus, we speculated that the higher peak in [Ca²⁺]_i in the presence of extracellular Ca²⁺ and the loss of the full response in Ca²⁺-free extracellular solution could be explained by the concomitant activation of P2X receptors activated by ATP. To test this hypothesis, we superfused IB3-1 cells with “solution A” containing either α,β -methylene ATP (α,β -MeATP, 100 μ M) or benzoyl-benzoyl-ATP (BzBzATP, 100 μ M) (Fig. 3A), selective agonists for different P2X receptor subtypes. Under these conditions, P2X-selective purinergic agonists failed to change [Ca²⁺]_i (Table I). However, we were aware of the fact that α,β -MeATP and BzBzATP, although potent agonists at P2X₁, P2X₃, and P2X₇ receptors, have little or no effect at other P2XR subtypes. Thus, we hypothesized that changing the ionic composition of the superfusion medium might reveal activation of a Ca²⁺ entry mechanism by these agonists (see below).

ATP and BzBzATP Trigger an Increase in [Ca²⁺]_i with Transient and Sustained Components in the Absence of Extracellular Na⁺—Despite the negative data above with regard to P2X-selective agonists, we maintained the hypothesis that P2X receptors were involved in the full Ca²⁺ response induced by

ATP in the presence of extracellular Ca²⁺. Rationale for this hypothesis is given by the fact that, in human and mouse lymphocytes, Na⁺ might compete with Ca²⁺ for entry through P2X receptors from extracellular stores (36–38) as well as other families of Ca²⁺ entry channels like the transient receptor potential channels (TRPs) or the store-operated Ca²⁺ channels (SOCs) (39, 40). Thus, we speculated that extracellular Na⁺ might suppress the Ca²⁺ permeability of P2X receptor channels in IB3-1 cells. To verify this hypothesis, we substituted extracellular Na⁺ by N-methyl-D-glucamine (NMDG) (solution C) and tested the effects of a non-discriminant P2Y and P2X agonist (ATP), P2X-specific agonists (BzBzATP and α,β -MeATP), and a P2Y₁-specific agonist (ADP β S). As shown in Fig. 2B (and in Fig. 5B and Fig. 7, A and B), substitution of extracellular Na⁺ by NMDG itself caused a small but sustained increase in [Ca²⁺]_i ($r_{\text{basal}} = 0.89 \pm 0.04$ to $r_{\text{NMDG}} = 0.94 \pm 0.04$; $n = 31$; $p < 0.05$) which was completely absent when extracellular Ca²⁺ was also omitted from the superfusion medium. These observations suggest the presence of a mechanism that allows sustained Ca²⁺ entry, even in non-stimulated cells.

Following removal of extracellular Na⁺ and changes in [Ca²⁺]_i, we applied ATP (100 μ M). Under these conditions, ATP induced a further increase in [Ca²⁺]_i displaying a biphasic Ca²⁺ response consisting of an initial transient peak and a sustained component (Fig. 2B and Tables II and III). In addition, as shown in Fig. 2B, a second application of ATP elicited a smaller increase in the [Ca²⁺]_i peak; however, the sustained Ca²⁺ plateau was comparable with that observed after the first stimulation by ATP. When [Ca²⁺]_i reached a stable value after withdrawal of extracellular Na⁺, we also added either BzBzATP (100 μ M) (Fig. 3B) or α,β -MeATP (100 μ M). BzBzATP, but not α,β -MeATP, induced a small increase in [Ca²⁺]_i (Fig. 3B and Tables II and III). This increase was completely dependent on the presence of extracellular Ca²⁺, indicating a role for P2X receptors in Ca²⁺ influx (Fig. 3B and Table II). In Na⁺-free media, P2Y₁-specific agonist, ADP β S (100 μ M), augmented the peak increase in [Ca²⁺]_i (Table II) but failed to elicit a sustained Ca²⁺ plateau (Table III). Taken together, these data argue for a role for P2X receptors as Ca²⁺ entry channels in IB3-1 cells.

P2X₄ Receptor Channel Protein Biochemistry—Due to the lack of other specific agonists or inhibitors, our functional studies did not distinguish further agonists among the P2XR subtypes. However, biochemical evidence suggests that IB3-1 cells express the P2X₄ receptor channel robustly. Membrane protein lysates from IB3-1 cells were prepared and were subjected to immunoblotting with a P2X₄-specific polyclonal antibody. Fig. 4A shows the positive results for P2X₄ receptor channel protein

in total membrane protein lysates from IB3-1 cells grown on collagen-coated plastic as confluent monolayers. Inconsistent signals or a lack of signal was observed for P2X₁, P2X₂, and P2X₇ using specific antibodies to those subtypes (data not shown). The P2X₄ signal displayed a similar biochemical phenotype compared with human vascular endothelial cells and human polycystic kidney disease renal epithelial cells performed in our laboratory (13, 41) as well as a recent study of P2X₄ receptor biochemistry in cardiac tissue and myocytes (42). An unglycosylated band was detected at ~46 kDa (the predicted molecular mass for P2X₄) and a larger and broader glycosylated band at 60–65 kDa. These immunoblotting data show that P2X₄ is the most abundant P2X subtype expressed in IB3-1 cells. However, these data do not rule out less abundant expression of other P2X subtypes that is below the limit of detection with these antibodies. Further chemical modification of the extracellular solution also supports the abundant expression of P2X₄ receptor channels as the major P2X receptor subtype mediating Ca²⁺ entry (see below).

Fig. 4, B–D, shows additional data in 16HBE140[−] non-CF airway epithelial cells. Immunoblotting of non-polarized cells grown in flasks (Fig. 4, B and C) as well as biotinylation (Fig. 4D) of polarized monolayers grown on permeable supports revealed robust and apical membrane-localized expression of P2X₄. In these lysates, a third band of ~100 kDa was also found. Biotinylation was performed on the apical and basolateral surface of these monolayers. Only the apical signal is shown in Fig. 4D, although a detectable signal was also observed in basolateral biotinylated material (data not shown). Secondary antibody controls and blocking of antibody binding with the peptide immunogen, provided with the primary antibody in all biochemical assays, verified the specificity of P2X₄ receptor expression (data not shown). These data suggest that P2X₄ receptors are expressed abundantly by human airway epithelial cells grown under non-polarized and polarized conditions.

The Extracellular ATP-gated P2X₄ Receptor Channel Is the Major Ca²⁺ Entry Channel Stimulated by ATP in IB3-1 and 16HBE140[−] Cells—Like other subtypes of the P2X receptor channel family, the P2X₄ receptors are also regulated by different cations, such as H⁺ or Zn²⁺ (25). Thus, if it is true that in IB3-1 cells the prolonged Ca²⁺ response in Na⁺-free medium was due to activation of P2X₄ receptors, then extracellular pH and Zn²⁺ should modify the ATP-induced Ca²⁺ signal. To test this hypothesis, we measured [Ca²⁺]_i after changing extracellular pH or in the presence of Zn²⁺ in both IB3-1 and 16HBE140[−] cells. We exposed IB3-1 cells to ATP after changing the pH of the superfusion solution. As shown in Table III, increasing extracellular pH potentiated the ATP-induced sustained increase in [Ca²⁺]_i only in Na⁺-free medium. Furthermore, in a Na⁺-free environment, acidic pH significantly reduced the ATP-induced peak increase in [Ca²⁺]_i (Table II). To demonstrate directly the effect of ATP on Ca²⁺ influx from extracellular sources via another approach, we measured quenching of Fura-2 at 359 nm in the presence of MnCl₂ (500 μM). Mn²⁺ is known to permeate the same entry channels as Ca²⁺ and quenches Fura-2 fluorescence when it enters the cells. As shown in Fig. 5A, in Na⁺-free medium, acidic extracellular pH (6.4) inhibited Mn²⁺ entry, whereas alkaline extracellular pH (7.9) potentiated markedly Mn²⁺ entry and quenching of the dye. To further support the involvement of P2X₄ receptor channels, we tested the effect of the P2X receptor co-agonist, Zn²⁺, on ATP-induced Ca²⁺ entry mechanisms. Inclusion of ZnCl₂ (20 μM) further augmented the sustained increase in [Ca²⁺]_i induced by ATP in Na⁺-free medium (Fig. 5B and Table III) but had no effect in Na⁺-containing medium

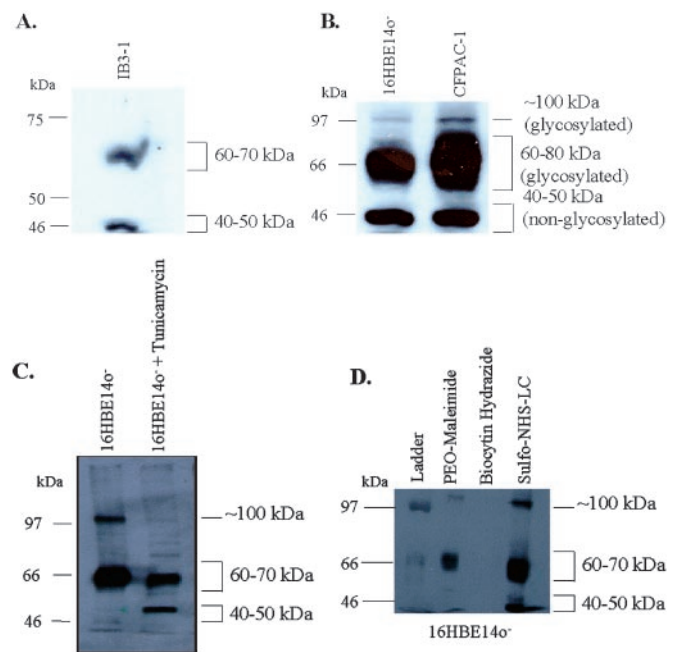


FIG. 4. A, immunoblot analysis of IB3-1 cells grown as non-polarized monolayers in flasks using rabbit polyclonal antibodies against P2X₄ receptors. A smaller band of the predicted molecular mass for P2X₄ (46 kDa) was detected, as was a larger, broader, glycosylated band at 60–70 kDa. The positions of molecular mass markers are shown on the left (in kDa). This is representative of 3 such experiments. B, immunoblot analysis of 16HBE140[−] cells and CFPAC-1 cells grown as polarized cell monolayers (CFPAC-1 cells were screened as another CF-relevant cell line and were grown in a similar manner than 16HBE140[−] cells except that Iscove's modified essential medium was used for the basal medium with all other additives kept similar). Note the stronger expression in polarized cell monolayers and the presence of a 40–50-kDa band (unglycosylated predicted molecular mass), a 60–80-kDa band (glycosylated form), and an even larger form at ~100 kDa (glycosylated form). This is representative of 6 such experiments. C, tunicamycin (10 μM), an inhibitor of glycosylation, added to the culture medium in an overnight 24-h incubation of confluent cell monolayers grown in flasks abolished the 100-kDa form and inhibited the expression of the 60–80-kDa band, yielding more of the 40–50-kDa unglycosylated form. This is representative of 2 such experiments. D, three water-soluble forms of biotin reagents were used to biotinylate apical membrane P2X₄. The data reveal that poly(ethylene)oxid-maleimide biotin, a reagent that reacts with primary amines primarily on lysine residues, detected only the glycosylated forms in the apical plasma membrane of 16HBE140[−] epithelial cell monolayers. Biocytin hydrazide failed to work in this experiment, likely because our conditions for oxidizing the carbohydrate residues were not optimal. Sulfo-NHS-LC-biotin detected all of the forms, indicating that it may have detected apical P2X₄; however, it may have gained access to the cell interior to find the unglycosylated form as well. This is representative of 2 such experiments. Note pertaining to all panels: no secondary antibody controls were performed for all of the above experiments, as were peptide immunogen blocking experiments that effectively blocked the signal. Peptide immunogens for P2X₁, P2X₂, and P2X₇ did not block the P2X₄ signaling, revealing additional specificity. In addition to data from our laboratory in human ADPKD kidney epithelial cells (41) and human vascular endothelial cells (13), this is the first documentation of biochemical detection of native airway epithelial P2X₄ receptor protein.

(Table III). Since our biochemical data (see above) indicated that P2X₄ receptors are also present in 16HBE140[−] non-CF airway epithelial cells, we tested whether increasing extracellular pH or addition of Zn²⁺ augmented the ATP-induced sustained Ca²⁺ entry in Na⁺-free medium in 16HBE140[−] cells. As shown in Fig. 6A, ATP elicited extracellular pH-dependent quenching of Fura-2, suggesting that ATP-stimulated Ca²⁺ influx is facilitated by alkaline pH. In addition, similar to results obtained with IB3-1 cells, both inclusion of Zn²⁺ and increasing pH potentiated the effects of ATP on sustained Ca²⁺ signal (Fig. 6B). Taken together, these data argue for a prom-

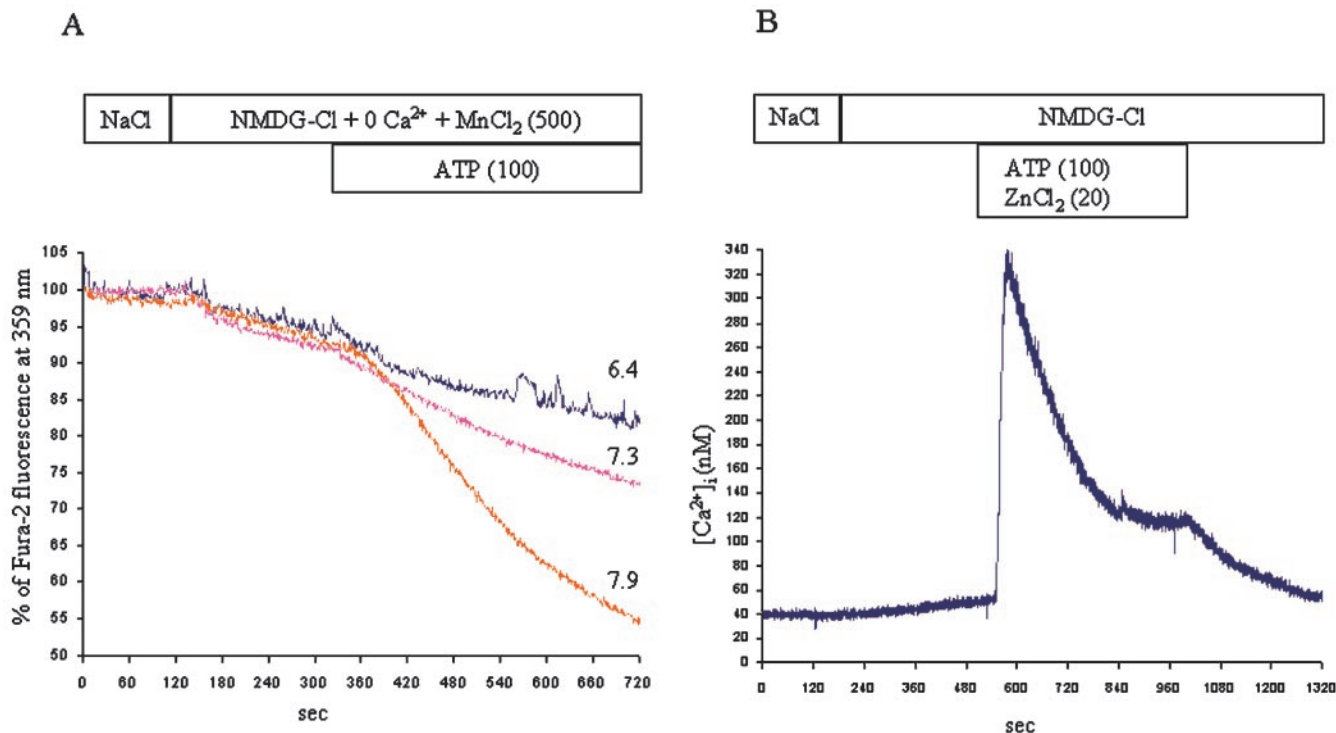


FIG. 5. Representative traces showing the pH dependence of ATP-induced Mn^{2+} entry in IB3-1 cells. A, quenching of Fura-2 was measured at the isosbestic wavelength of Fura-2 (359 nm). Cells were exposed to $MnCl_2$ (500 μM) in Na^+ - and Ca^{2+} -free medium at pH 7.3. After 200 s, ATP (100 μM) was added to the superfusion medium having three different pH values, as indicated. At least 3 experiments have been done in each group with similar results. A representative trace shows the effects of ATP (100 μM) in presence of $ZnCl_2$ (20 μM) in cells exposed to Na^+ -free medium (B) as indicated. Please note the augmentation of the sustained plateau of increased $[Ca^{2+}]_i$ in IB3-1 cells by inclusion of $ZnCl_2$ (compare with original trace in Fig. 2B).

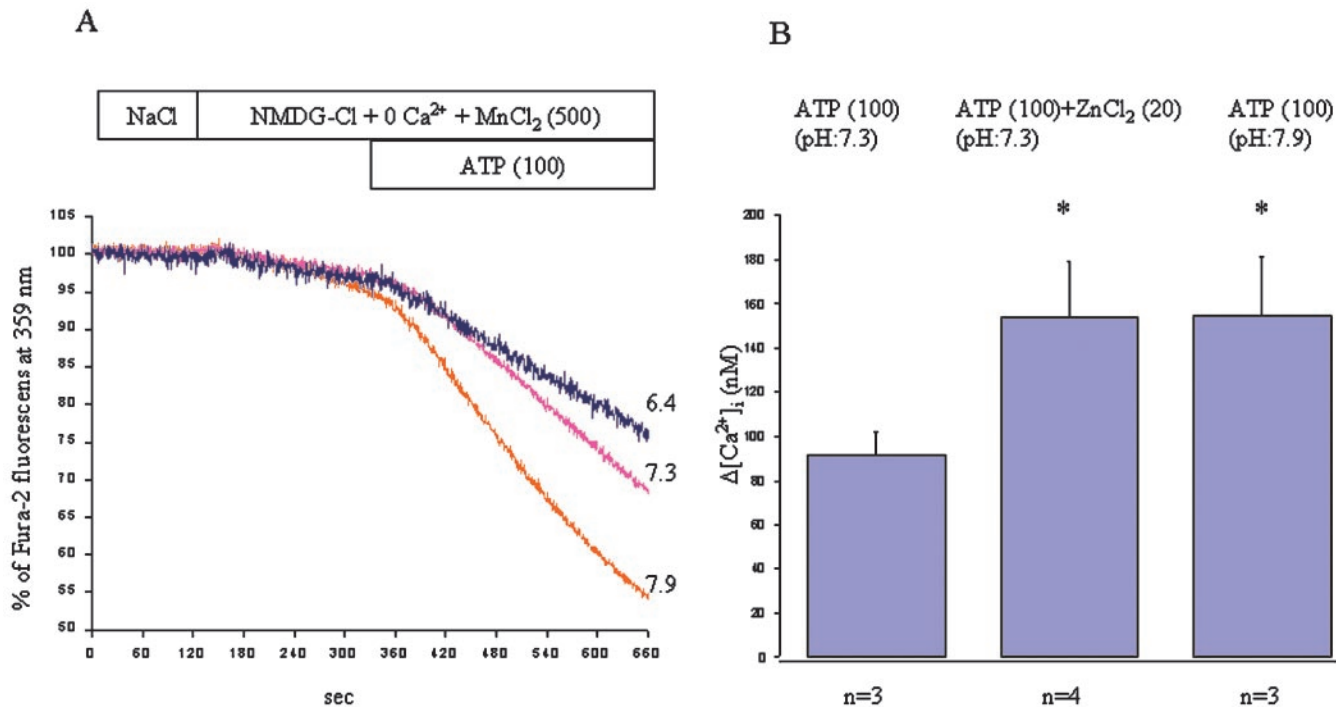


FIG. 6. Representative traces on the left showing the pH dependence of ATP-induced Mn^{2+} entry in 16HBE14o⁻ cells. A, experiments were performed in a similar manner to those in Fig. 5A. Changes in cytosolic Ca^{2+} concentration 5 min after the peak stimulation versus the basal $[Ca^{2+}]_i$ in 16HBE14o⁻ cells are shown in B. Effects on the sustained plateau of increased $[Ca^{2+}]_i$ in 16HBE14o⁻ cells are shown illustrating the potentiating effect of $ZnCl_2$ and of alkaline pH. All experiments have been done in Na^+ -free medium. *, $p < 0.05$

inent role for the $P2X_4$ receptor as a Ca^{2+} entry channel in human airway epithelial cells and argue against a functional role for other $P2X$ receptor subtypes.
The $P2X_4$ -mediated Ca^{2+} Entry Is Sustained, Long Lived,

Reversible, and Re-acquired upon Re-addition of Agonist—For any therapeutic approach to be effective, especially one that targets an endogenous receptor, stimulation should be sustained and long lived. Even more desirable, the effect should be

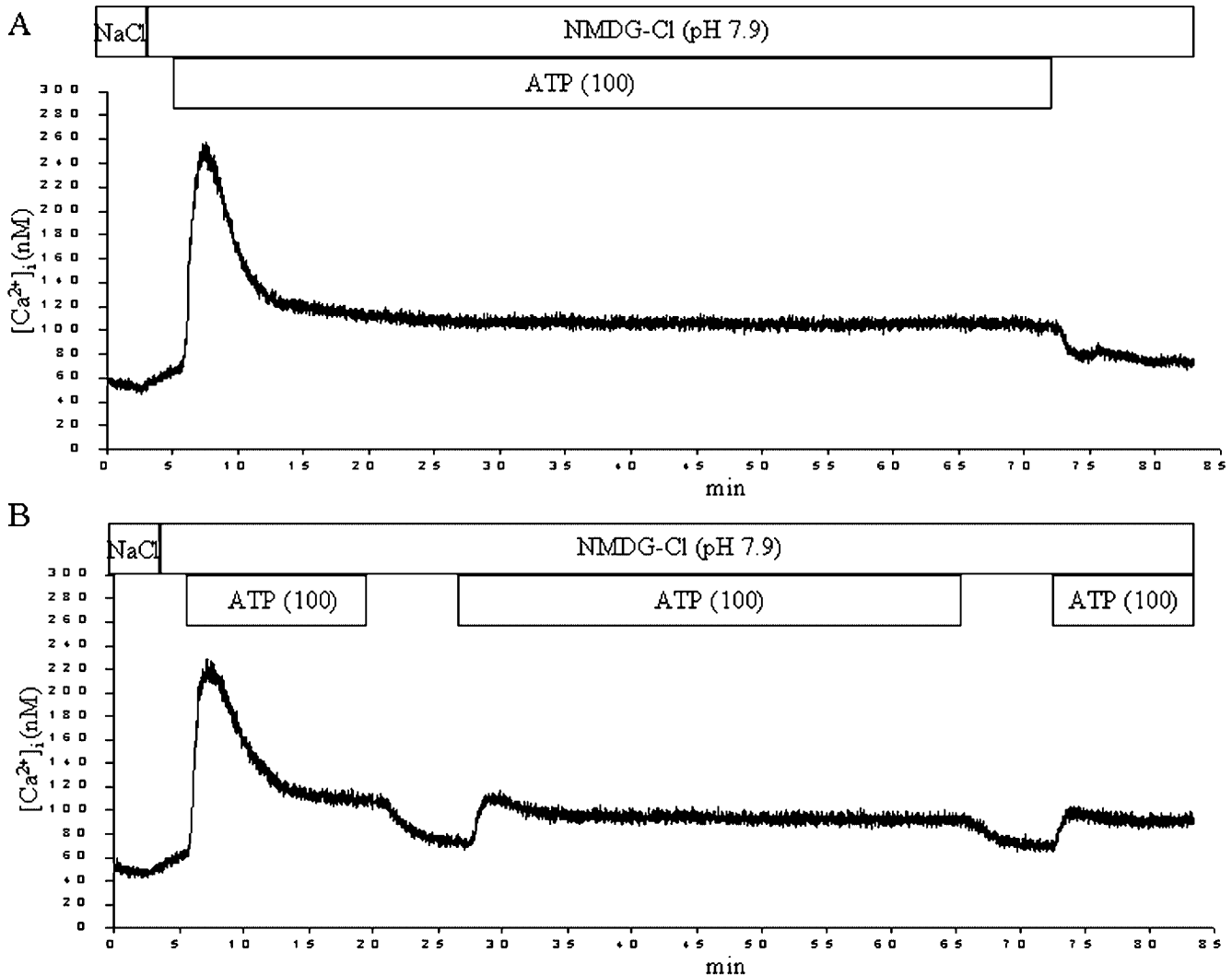


FIG. 7. Representative traces showing the duration of the sustained plateau in $[Ca^{2+}]_i$ in IB3-1 CF cells induced by ATP under Na^+ -free conditions (pH 7.9) (A) and the reversibility, long lived, and reproducible nature of the sustained plateau induced by ATP and mediated by P2X₄ (B). Each trace for each protocol is typical of 3 such experiments.

reversible to control the response. Ultimately, it is ideal if this endogenous receptor target did not desensitize or inactivate, as is apparent in this study for P2Y-mediated transient Ca^{2+} signal. Fig. 7 shows experiments designed to determine whether P2X₄-mediated Ca^{2+} entry was sustained and long lived in IB3-1 cells. In the first protocol, ATP (100 μ M) was added in Na^+ -free solution that has pH 7.9. A transient increase in $[Ca^{2+}]_i$ mediated by P2Y receptors was followed by a sustained plateau that persisted for over 60 min, until ATP was removed (Fig. 7A). In a second approach, a 15-min stimulation was performed with ATP and then was reversed with washout. Following re-addition of ATP, a similar sustained calcium plateau was acquired that persisted for 40 min. A third washout and stimulation was performed at the end of the protocol (Fig. 7B), showing lack of desensitization of the P2X₄ receptors or inactivation of their channel function. In contrast, the transient spike observed in the first application of ATP was lost. These data show, these data show that the P2X₄-mediated Ca^{2+} entry is sustained, long lived, reversible, and re-acquirable upon washout and re-addition of agonist.

Neither the Reverse Operation Mode of the Na^+/Ca^{2+} Exchanger Nor Voltage-dependent Ca^{2+} Channels or Store-operated Ca^{2+} Channels Are Involved in ATP-induced Ca^{2+} Entry in IB3-1 Cells—Theoretically, both the initial increase in

$[Ca^{2+}]_i$ after removal of extracellular Na^+ and the sustained Ca^{2+} plateau induced by administration of ATP could be due to the activation of the Na^+/Ca^{2+} exchanger in its reverse operation mode and/or other classes of Ca^{2+} entry channels. Thus, we removed extracellular Na^+ and added ATP in the presence of KB-R7943 (30 μ M), a specific inhibitor of reverse operation mode of the Na^+/Ca^{2+} exchanger (43). Since KB-R7943 had no effect under these experimental conditions, we excluded the presence of this exchanger at the plasma membrane (Fig. 8A and Tables II and III). Although airway epithelial cells are non-excitable cells and should not express voltage-dependent Ca^{2+} channels, we asked the question whether cell membrane depolarization stimulated or inhibited the Ca^{2+} response induced by ATP. Therefore, we exposed the cells to high extracellular KCl concentration (40 mM) in Na^+ -free medium (solution D), and then we added ATP. As shown in Fig. 8B and Tables II and III, membrane depolarization inhibited the peak increase of $[Ca^{2+}]_i$, and the sustained Ca^{2+} plateau was completely abolished, indicating that IB3-1 cells do not express voltage-dependent Ca^{2+} channels.

SOCs or TRPs represent other pathways by which Ca^{2+} can enter non-excitable cells besides the ATP-gated P2X receptor channels. Theoretically, both SOC and TRPs could be responsible for the sustained Ca^{2+} influx induced by ATP in Na^+ -free

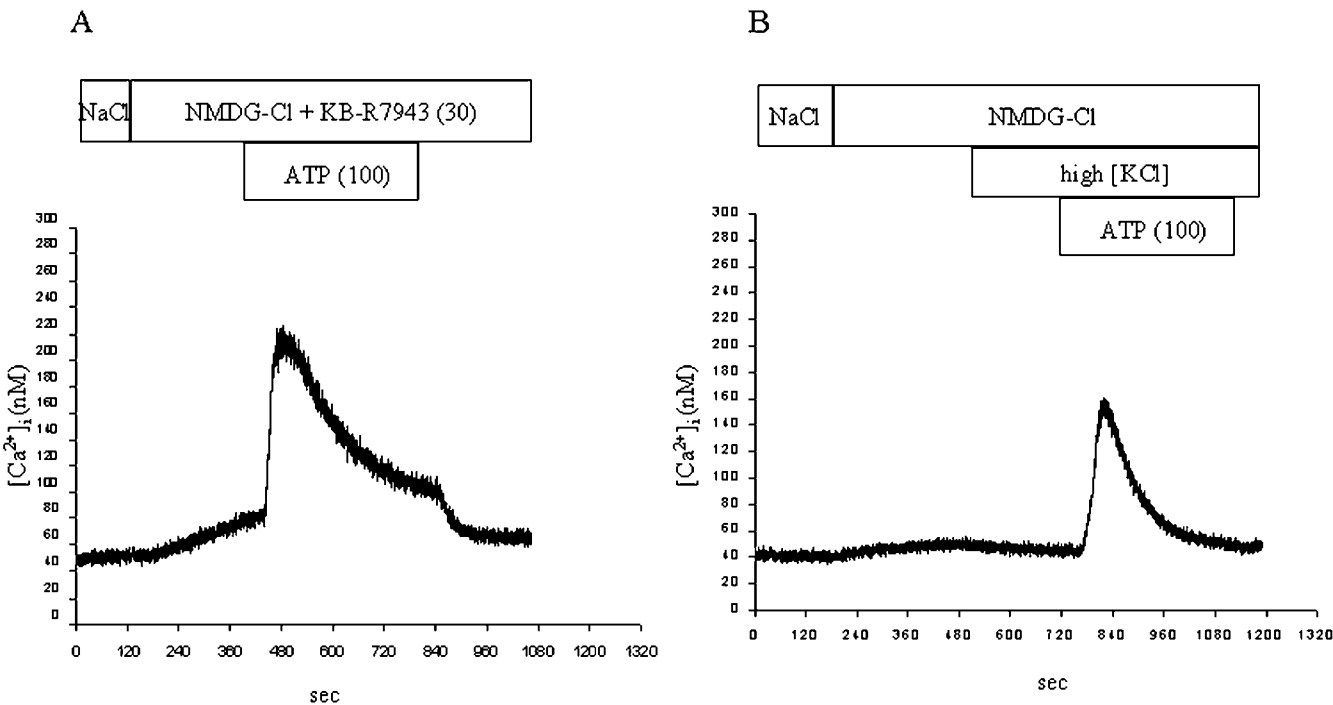


FIG. 8. Representative traces showing the effects of KB-R7943 (30 μ M) (A) and high $[KCl]_e$ (40 mM) (B) on ATP-induced Ca^{2+} signal. Experiments were done in a Na^+ -free environment. B, note that substitution of Na^+ by NMDG causes a slight increase in $[Ca^{2+}]_i$, an effect that was inhibited in high KCl-containing solution.

medium. Therefore, we tested whether SOC are present in IB3-1 cells. We treated the cells with thapsigargin (100 nM), an inhibitor of Ca^{2+} pump in the ER membrane, in the presence of extracellular Ca^{2+} . This maneuver induced a large initial increase in Fura-2 fluorescence ratio ($r_{\text{basal}} = 1.00 \pm 0.05$ to $r_{\text{peak}} = 2.92 \pm 0.17$; $n = 3$) followed by a sustained Ca^{2+} plateau ($r_{\text{sustained}} = 1.58 \pm 0.29$; $n = 3$). In the absence of extracellular Ca^{2+} , stimulation with thapsigargin resulted in a small transient increase in $[Ca^{2+}]_i$ due to the depletion of intracellular Ca^{2+} stores, and the re-addition of extracellular Ca^{2+} elicited a large $[Ca^{2+}]_i$ increase (Fig. 9). These data indicate that IB3-1 cells possess SOC, which are activated by a decrease in $[Ca^{2+}]_{ER}$. Next, we have asked whether SOC or store-independent TRP-like channels contribute to the sustained Ca^{2+} increase after $P2Y_1$ receptor stimulation in Na^+ -free medium. To address this question, we used 2APB, which has recently been reported to inhibit SOC (44, 45), and SKF-96365, which is a blocker of the store-independent TRPs (46). Neither 2APB (75 μ M) nor SKF-56365 (50 μ M) abolished the ATP-induced sustained increase in $[Ca^{2+}]_i$ in the absence of extracellular Na^+ (Table III). Interestingly, the sustained Ca^{2+} plateau was further augmented by the SKF-96365 compound (Table III). These data indicate that, in IB3-1 cells, SOC and/or TRPs do not play a role in regulating $[Ca^{2+}]_i$ following purinergic receptor stimulation.

DISCUSSION

Stimulation of purinergic receptors exerts biological effects, which are mediated in part through elevation of intracellular Ca^{2+} concentration (47–52). In the present study, we show evidence that IB3-1 cells express $P2Y_1$ and $P2X_4$ receptors abundantly. $P2Y_1$ receptors have been found recently in airway epithelia of $P2Y_2$ receptor-knockout mice (54), in rat lung (55), and in Calu-3 human airway epithelial cells (56). ADP β S, a specific agonist of $P2Y_1$ receptors, increased $[Ca^{2+}]_i$ to a similar extent as ATP, ADP, and 2MeSATP, suggesting the presence of $P2Y_1$ receptors. Although recent data (57) indicate that 2MeSATP and, possibly, ADP β S at a concentration of 100 μ M may

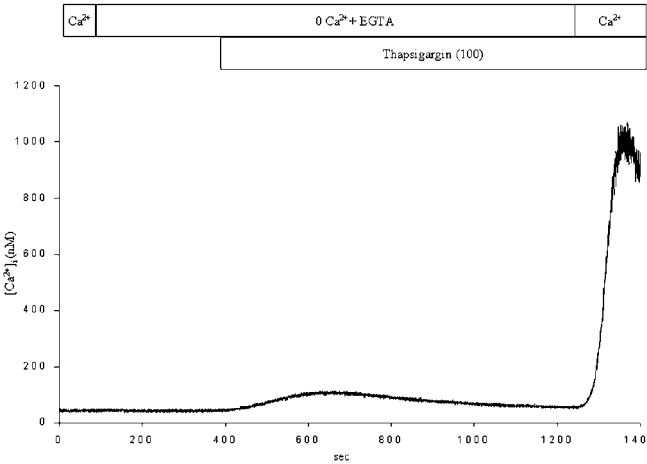


FIG. 9. Representative trace shows the effect of thapsigargin (100 nM) on $[Ca^{2+}]_i$ in the absence and in the presence of extracellular Ca^{2+} as indicated. This maneuver reveals the presence of SOC involved in Ca^{2+} entry, albeit induced by emptying ER stores completely.

activate $P2Y_{11}$ receptors, we believe it is very unlikely that the increase in $[Ca^{2+}]_i$ observed in this study was due to the activation of $P2Y_{11}$ receptors. This conclusion derives from the fact that $P2Y_{11}$ receptors are poorly stimulated by ADP (26), whereas our data show that ADP is at least as potent an agonist as ATP. In addition, ADP β S also elicited a significant increase in $[Ca^{2+}]_i$ at a concentration of 10 μ M. In other airway epithelial cell models, the presence of $P2Y_2$ has already been demonstrated (16, 58, 59). Furthermore, *in vivo* studies demonstrate that aerosolized UTP has beneficial effects in treatment of CF lung disease, confirming the presence of $P2Y_2$ and/or $P2Y_4$ on the apical membrane of airway epithelium (23, 48). Interestingly, neither UTP nor UDP increased $[Ca^{2+}]_i$ in IB3-1 cells; however, both agonists do rescue impaired cell

volume regulation in IB3-1 cells.² These differences may reveal additional signal transduction pathways triggered by P2Y receptors that are independent of cytosolic calcium.

Nevertheless, in addition to the beneficial targeting of P2Y receptors for CF therapy, we argue here for the beneficial targeting of P2X receptors as well. Activation of these receptors would also have the added benefit of eliciting a sustained increase in $[Ca^{2+}]_i$, an effect not observed with P2Y-specific agonists. The transient nature of the Ca^{2+} signal induced by purinergic agonists accounts presumably for transient Cl^- and fluid secretion observed in different CF epithelial cell models (7, 29). Activation of P2X receptor channels under appropriate conditions would lead to Ca^{2+} influx from the extracellular space. Furthermore, this Ca^{2+} response is sustained for at least 1 h, is reversible, and is re-acquired to the same sustained level upon re-addition of agonists under conditions designed to stimulate P2X₄.

However, our data could conceivably be explained in the following ways: 1) opening of extracellular ATP-gated P2X receptor channels; 2) activation of Na^+/Ca^{2+} exchanger in reverse operation mode due to Na^+ removal; 3) opening of voltage-dependent Ca^{2+} channels following membrane depolarization; and 4) activation of SOCs or TRPs after depletion of intracellular Ca^{2+} stores. All lines of evidence indicate that activation of ATP-gated P2X₄ receptor channels led to augmentation of Ca^{2+} signal and the sustained Ca^{2+} plateau. First, in IB3-1 cells, BzBzATP, a P2X receptor-specific agonist, increases $[Ca^{2+}]_i$ only in Na^+ -free medium. Second, the ATP-induced Ca^{2+} plateau was enhanced by alkaline extracellular pH and inhibited by acidic extracellular pH. Third, ATP-induced Mn^{2+} entry caused quenching of Fura-2 in a pH-dependent manner exhibiting significant increase in Mn^{2+} permeability at alkaline pH. Fourth, application of Zn^{2+} further enhanced the effects of ATP. Fifth, a P2Y₁ receptor-specific agonist, ADP β S, did not cause a sustained increase in $[Ca^{2+}]_i$. Sixth, neither 2APB, an inhibitor of SOCs, nor SKF-56365, a blocker of store-independent TRP-like channels, abolished the sustained increase in $[Ca^{2+}]_i$ induced by ATP. Seventh, recent data (60, 61) indicate that Zn^{2+} inhibits SOCs. Eighth, biochemical evidence showed abundant expression of P2X₄. Roles for the reverse mode of the Na^+/Ca^{2+} exchanger and/or voltage-dependent Ca^{2+} channels were ruled out with a variety of different cell biological maneuvers and/or pharmacological inhibitors. It is noteworthy that Vennekens *et al.* (62) have recently reported that epithelial Ca^{2+} channels are regulated by extracellular pH. However, these channels are mainly expressed in kidney and intestinal epithelia and inhibited by metal ions at low micromolar concentration (63).

Although BzBzATP is primarily known to be an agonist of P2X₇ and antibodies used in this study were raised against rat P2X receptors, stimulation by Zn^{2+} and inhibition by H^+ are most consistent with activation of the P2X₄ receptors and inconsistent with other P2X receptor subtypes (25). For instance, stimulatory effects by Zn^{2+} rule out a role for P2X₇, because Zn^{2+} is a P2X₇ antagonist (25). Inhibition of Ca^{2+} entry by acidic pH rules out P2X₂ receptors, which are stimulated by acidic pH (25). The only phenotype that is not completely explained by P2X₄ alone is the alkaline pH stimulation. Heterologously expressed P2X₄ is only mildly stimulated by alkaline pH (64). As such, we cannot rule out that additional P2X receptor subtypes (perhaps P2X₅ (65), P2X₆ (66), or splice variants of P2X₄, P2X₅, and P2X₆ (67)) may be conferring these pH effects in a P2XR heteromultimer. Interestingly, in 16HBE140⁻ cells, ATP-driven Mn^{2+} entry was also enhanced by alkaline pH, and Zn^{2+} potentiated the ATP-induced sus-

tained increase in $[Ca^{2+}]_i$. Taken together, these data indicate that P2X₄ receptors function as ATP-gated Ca^{2+} entry channels in both CF and non-CF airway epithelial cells.

In a past study (27), our laboratory showed that a P2X-selective agonist, BzBzATP, stimulated transepithelial chloride secretion in Ussing chamber experiments on airway epithelia that had both transient and sustained components and in nasal potential difference assays on mouse nasal mucosa that were transient stimulations that averaged 1–2 mV. These stimulations occurred in Na^+ -rich solutions (27). Despite this knowledge, we did not perform experiments designed to examine P2XR-mediated signaling in this study (27). Because Na^+ is in great excess to Ca^{2+} in physiological saline, the contribution of Ca^{2+} -permeable non-selective cation channels to a Ca^{2+} entry phenotype is often masked. This was true for our CF cell model. In IB3-1 cells, removal of extracellular Na^+ was required to observe any increase in $[Ca^{2+}]_i$ with BzBzATP and a sustained Ca^{2+} signal with ATP. Nonetheless, in 16HBE140⁻ non-CF cells, extracellular Na^+ (140 mM) prevented neither the BzBzATP-dependent Ca^{2+} response nor the ATP-induced Ca^{2+} plateau³; however, responses to both BzBzATP and ATP were much more profound under Na^+ -free conditions. Thus, we speculate that P2XR agonists might be useful in CF therapy regardless of extracellular Na^+ concentration, although modification of the extracellular environment (Na^+ removal, among other maneuvers) may strengthen their efficacy and was required to optimally study Ca^{2+} entry mechanisms in Fura-2 spectrofluorometry. Nevertheless, further studies are required to determine whether the presence of extracellular Na^+ inhibits P2XR-mediated rescue of Cl^- secretion in CF therapy.

Interestingly, although controversial, recent data indicate that airway surface liquid (ASL) in non-CF subjects is hypotonic and low in Na^+ with respect to the plasma (68). In contrast, other studies (69) have concluded that non-CF and CF ASL are isotonic. Nevertheless, it is noteworthy that, in Na^+ -replete medium, extracellular ATP stimulation of ciliary beat is attenuated, whereas in Na^+ -free medium, ATP induction of ciliary beat was profound, suggesting a role for P2X receptors on cilia (35). Because cilia reside and need to function optimally in the ASL environment, we postulate that normal ASL may be hypotonic and, in particular, low in Na^+ , allowing P2X receptor agonists to stimulate sustained signaling that may impact ion transport and ciliary beat. These specialized chemical and ionic conditions may also be critical in the delivery of agonists for CF therapy. This is tenable, because the vehicle for delivery during nebulization, aerosolization, or instillation would merely need to be modified to suit these optimal conditions.

Taken together, these findings are profound with regard to therapy in CF, because they suggest that endogenously expressed P2X receptors do not desensitize or inactivate, and under appropriate conditions, their activation leads to a prolonged Ca^{2+} signal that could translate into a sustained Cl^- secretion in CF and non-CF epithelia.

REFERENCES

1. Riordan, J. R., Rommens, J. M., Kerem, B., Alon, N., Rozmahel, R., Grzelczak, Z., Zielenski, J., Lok, S., Plavsky, N., Chou, J. L., Drummond, M. L., Iannuzzi, M. C., Collins, F. S., and Tsui L. C. (1989) *Science* **245**, 1066–1073
2. Gregory, R. J., Cheng, S. H., Rich, D. P., Marshall, J., Paul, S., Hehir, K., Ostedgaard, L., Klinger, K. W., Welsh, M. J., and Smith, A. E. (1990) *Nature* **27**, 382–386
3. Berger, H. A., Anderson, M. P., Gregory, R. J., Thompson, S., Howard, P. W., Maurer, R. A., Mulligan, R., Smith, A. E., and Welsh, M. J. (1991) *J. Clin. Invest.* **88**, 1422–1431
4. Schreiber, R., Greger, R., Nitschke, R., and Kunzelmann, K. (1997) *Pfluegers Arch.* **434**, 841–847
5. Schwiebert, E. M., Benos, D. J., Egan, M. E., Stutts, M. J., and Guggino, W. B. (1999) *Physiol. Rev.* **79**, S145–S166

² G. M. Braunstein and E. M. Schwiebert, unpublished observations.

³ A. Zsembery and E. M. Schwiebert, unpublished observations.

6. Zsembery, A., Strazzabosco, M., and Graf, J. (2000) *FASEB J.* **14**, 2345–2356
7. Zsembery, A., Jessner, W., Sitter, G., Spirli, C., Strazzabosco, M., and Graf, J. (2002) *Hepatology* **35**, 95–104
8. Braunstein, G. M., Roman, R. M., Clancy, J. P., Kudlow, B. A., Taylor, A. L., Shylonsky, V. G., Jovov, B., Peter, K., Jilling, T., Ismailov, I. I., Benos, D. J., Schwiebert, L. M., Fitz, J. G., and Schwiebert, E. M. (2001) *J. Biol. Chem.* **276**, 6621–6630
9. Schwiebert, E. M., Egan, M. E., Hwang, T. H., Fulmer, S. B., Allen, S. S., Cutting, G. R., and Guggino, W. B. (1995) *Cell* **81**, 1063–1073
10. Schwiebert, E. M. (1999) *Am. J. Physiol.* **276**, C1–C8
11. Lomri, N., Fitz, J. G., and Scharschmidt, B. F. (1996) *Semin. Liver Dis.* **16**, 201–210
12. Roman, R. M., Wang, Y., Lidofsky, S. D., Feranchak, A. P., Lomri, N., Scharschmidt, B. F., and Fitz, J. G. (1997) *J. Biol. Chem.* **272**, 21970–21976
13. Schwiebert, L. M., Rice, W. C., Kudlow, B. A., Taylor, A. L., and Schwiebert, E. M. (2002) *Am. J. Physiol.* **282**, C289–C301
14. Stutts, M. J., Lazarowski, E. R., Paradiso, A. M., and Boucher, R. C. (1995) *Am. J. Physiol.* **268**, C425–C433
15. Hwang, T. H., Schwiebert, E. M., and Guggino, W. B. (1996) *Am. J. Physiol.* **270**, C1611–C1623
16. Watt, W. C., Lazarowski, E. R., and Boucher, R. C. (1998) *J. Biol. Chem.* **273**, 14053–14058
17. Huang, P., Lazarowski, E. R., Tarran, R., Milgram, S. L., Boucher, R. C., and Stutts, M. J. (2001) *Proc. Natl. Acad. Sci. U. S. A.* **98**, 14120–14125
18. Devor, D. C., and Pilewski, J. M. (1999) *Am. J. Physiol.* **276**, C827–C837
19. Kunzelmann, K., Schreiber, R., Nitschke, R., and Mall, M. (2000) *Pfluegers Arch.* **440**, 193–201
20. Mall, M., Wissner, A., Gonska, T., Calenborn, D., Kuehr, J., Brandis, M., and Kunzelmann, K. (2000) *Am. J. Respir. Cell Mol. Biol.* **23**, 755–761
21. Inglis, S. K., Collett, A., McAlroy, H. L., Wilson, S. M., and Olver, R. E. (1999) *Pfluegers Arch.* **438**, 621–627
22. Iwase, N., Sasaki, T., Shimura, S., Yamamoto, M., Suzuki, S., and Shirato, K. (1997) *Respir. Physiol.* **107**, 173–180
23. Knowles, M. R., Olivier, K., Noone, P., and Boucher, R. C. (1995) *Am. J. Respir. Crit. Care Med.* **151**, S65–S69
24. Bennett, W. D., Olivier, K. N., Zeman, K. L., Hohneker, K. W., Boucher, R. C., and Knowles, M. R. (1996) *Am. J. Respir. Crit. Care Med.* **153**, 1796–1801
25. North, R. A., and Surprenant, A. (2000) *Annu. Rev. Pharmacol. Toxicol.* **40**, 563–580
26. Ralevic, V., and Burnstock, G. (1998) *Pharmacol. Rev.* **50**, 413–492
27. Taylor, A. L., Schwiebert, L. M., Smith, J. J., King, C., Jones, J. R., Sorscher, E. J., and Schwiebert, E. M. (1999) *J. Clin. Invest.* **104**, 875–884
28. Kunzelmann, K., and Mall, M. (2001) *Clin. Exp. Pharmacol. Physiol.* **28**, 857–867
29. Warth, R., and Greger, R. (1993) *Cell. Physiol. Biochem.* **3**, 2–16
30. Zeitlin, P. L., Lu, L., Rhim, J., Cutting, G., Stetten, G., Kieffer, K. A., Craig, R., and Guggino, W. B. (1991) *Am. J. Physiol.* **4**, L313–L319
31. Gruenert, D. C., Basbaum, C. B., and Widdicombe, J. H. (1990) *In Vitro Cell. Dev. Biol.* **26**, 411–418
32. Grynkiewicz, G., Poenie, M., and Tsien, R. Y. (1985) *J. Biol. Chem.* **260**, 3440–3450
33. Merritt, J. E., Jacob, R., and Hallam, T. J. (1989) *J. Biol. Chem.* **264**, 1522–1527
34. Korngreen, A., Ma, W., Priel, Z., and Silberberg, S. D. (1998) *J. Physiol. (Lond.)* **508**, 703–720
35. Ma, W., Korngreen, A., Uzlaner, N., Priel, Z., and Silberberg, S. D. (1999) *Nature* **400**, 894–897
36. Wiley, J. S., and Dubyak, G. R. (1989) *Blood* **73**, 1316–1323
37. Pizzo, P., Zanovello, P., Bronte, V., and Di Virgilio, F. (1991) *Biochem. J.* **274**, 139–144
38. Baricordi, O. R., Ferrari, D., Melchiorri, L., Chiozzi, P., Hanau, S., Chiari, E., Rubini, M., and Di Virgilio, F. (1996) *Blood* **87**, 682–690
39. Balzer, M., Lintschinger, B., and Groschner, K. (1999) *Cardiovasc. Res.* **42**, 543–549
40. Arnon, A., Hamlyn, J. M., and Blaustein, M. P. (2000) *Am. J. Physiol.* **278**, C163–C173
41. Schwiebert, E. M., Wallace, D. P., Braunstein, G. M., King, S. R., Peti-Peterdi, J., Hanaoka, K., Guggino, W. B., Guay-Woodford, L. M., Bell, P. D., Sullivan, L. P., Grantham, J. J., and Taylor, A. L. (2002) *Am. J. Physiol.* **282**, F763–F775
42. Hu, B., Mei, Q. B., Yao, X. J., Smith, E., Barry, W. H., and Liang, B. T. (2001) *FASEB J.* **15**, 2739–2741
43. Wang, X., Kim, S. U., van Breemen, C., and McLarnon, J. G. (2000) *Cell Calcium* **27**, 205–212
44. Dobrydyneva, Y., and Blackmore, P. (2001) *Mol. Pharmacol.* **60**, 541–552
45. Gregory, R. B., Rychkov, G., and Barritt, G. J. (2001) *Biochem. J.* **354**, 285–290
46. Bennett, B. D., Alvarez, U., and Hruska, K. A. (2001) *Endocrinology* **142**, 1968–1974
47. Rugolo, M., Mastrocola, T., Whorle, C., Rasola, A., Gruenert, D. C., Romeo, G., and Galletta, L. J. (1993) *J. Biol. Chem.* **268**, 24779–24784
48. Lazarowski, E. R., Boucher, R. C., and Harden, T. K. (1994) *Am. J. Physiol.* **266**, C406–C415
49. Van Scott, M. R., Chinnet, T. C., Burnette, A. D., and Paradiso, A. M. (1995) *Am. J. Physiol.* **269**, L30–L37
50. Furukawa, M., Ikeda, K., Yamaya, M., Oshima, T., Sasaki, H., and Takasaka, T. (1997) *Am. J. Physiol.* **272**, C827–C836
51. Zsembery, A., Spirli, C., Granato, A., LaRusso, N. F., Okolicsanyi, L., Crepaldi, G., and Strazzabosco, M. (1998) *Hepatology* **28**, 914–920
52. Okada, Y., Maeno, E., Shimizu, T., Dezaki, K., Wang, J., and Morishima, S. (2001) *J. Physiol. (Lond.)* **532**, 3–16
53. Lazarowski, E. R., Watt, W. C., Stutts, M. J., Boucher, R. C., and Harden, T. K. (1995) *Br. J. Pharmacol.* **116**, 1619–1627
54. Homolya, L., Watt, W. C., Lazarowski, E. R., Koller, B. H., and Boucher, R. C. (1999) *J. Biol. Chem.* **274**, 26454–26460
55. Laubinger, W., and Reiser, G. (1998) *Biochem. Pharmacol.* **55**, 687–695
56. Communi, D., Paindavoine, P., Place, G. A., Parmentier, M., and Boeynaems, J. M. (1999) *Br. J. Pharmacol.* **127**, 562–568
57. Sak, K., and Webb, T. E. (2002) *Arch. Biochem. Biophys.* **397**, 131–136
58. Donaldson, S. H., Lazarowski, E. R., Picher, M., Knowles, M. R., Stutts, M. J., and Boucher, R. C. (2000) *Mol. Med.* **6**, 969–982
59. Homolya, L., Steinberg, T. H., and Boucher, R. C. (2000) *J. Cell Biol.* **150**, 1349–1360
60. Uehara, A., Yasukochi, M., Imanaga, I., Nishi, M., and Takeshima, H. (2002) *Cell Calcium* **31**, 89–96
61. Jung, S., Pfeiffer, F., and Deitmer, J. W. (2000) *J. Physiol. (Lond.)* **527**, 549–561
62. Vennekens, R., Prenen, J., Hoenderop, J. G., Bindels, R. J., Droogmans, G., and Nilius, B. (2001) *Pfluegers Arch.* **442**, 237–242
63. Nilius, B., Prenen, J., Vennekens, R., Hoenderop, J. G., Bindels, R. J., and Droogmans, G. (2001) *Br. J. Pharmacol.* **134**, 453–462
64. Wildman, S. S., King, B. F., and Burnstock, G. (1999) *Br. J. Pharmacol.* **126**, 762–768
65. Collo, G., North, R. A., Kawashima, E., Merlo-Rich, E., Neidhart, S., Surprenant, A., and Buell, G. (1996) *J. Neurosci.* **16**, 2495–2507
66. Le, K. T., Babinski, K., and Seguela, P. (1998) *J. Neurosci.* **18**, 7152–7159
67. Dhulipala, P. D., Wang, Y. X., and Kotlikoff, M. I. (1998) *Gene (Amst.)* **207**, 259–266
68. Smith, J. J., Travis, S. M., Greenberg, E. P., and Welsh, M. J. (1996) *Cell* **85**, 229–236
69. Matsui, H., Grubb, B. R., Tarran, R., Randell, S. H., Gatzky, J. T., Davis, C. W., and Boucher, R. C. (1998) *Cell* **95**, 1005–1015

Extracellular Zinc and ATP Restore Chloride Secretion across Cystic Fibrosis Airway Epithelia by Triggering Calcium Entry*

Received for publication, December 8, 2003, and in revised form, December 22, 2003
Published, JBC Papers in Press, December 29, 2003, DOI 10.1074/jbc.M313391200

Ákos Zsembery^{¶§¶}, James A. Fortenberry[§], Lihua Liang[‡], Zsuzsa Bebok^{§**}, Torry A. Tucker[‡],
Amanda T. Boyce^{**}, Gavin M. Braunstein[‡], Elisabeth Welty[‡], P. Darwin Bell^{‡‡},
Eric J. Sorscher^{‡‡‡}, J. P. Clancy^{§‡‡}, and Erik M. Schwiebert^{‡§***§§}

From the Departments of [‡]Physiology and Biophysics, ^{**}Cell Biology, and ^{‡‡}Medicine and the [§]Gregory Fleming James Cystic Fibrosis Research Center, University of Alabama, Birmingham, Alabama, 35294-0005 and the [¶]Hungarian Academy of Science and Semmelweis University Nephrology Research Group, 1089 Nagyváradi tér 4, Budapest H-1089, Hungary

Cystic fibrosis (CF) is caused by defective cyclic AMP-dependent cystic fibrosis transmembrane conductance regulator Cl[−] channels. Thus, CF epithelia fail to transport Cl[−] and water. A postulated therapeutic avenue in CF is activation of alternative Ca²⁺-dependent Cl[−] channels. We hypothesized that stimulation of Ca²⁺ entry from the extracellular space could trigger a sustained Ca²⁺ signal to activate Ca²⁺-dependent Cl[−] channels. Cytosolic [Ca²⁺]_i was measured in non-polarized human CF (IB3-1) and non-CF (16HBE14o[−]) airway epithelial cells. Primary human CF and non-CF airway epithelial monolayers as well as Calu-3 monolayers were used to assess anion secretion. *In vivo* nasal potential difference measurements were performed in non-CF and two different CF mouse ($\Delta F508$ homozygous and bistransgenic gut-corrected but lung-null) models. Zinc and ATP induced a sustained, reversible, and reproducible increase in cytosolic Ca²⁺ in CF and non-CF cells with chemistry and pharmacology most consistent with activation of P2X purinergic receptor channels. P2X purinergic receptor channel-mediated Ca²⁺ entry stimulated sustained Cl[−] and HCO₃[−] secretion in CF and non-CF epithelial monolayers. In non-CF mice, zinc and ATP induced a significant Cl[−] secretory response similar to the effects of agonists that increase intracellular

cAMP levels. More importantly, in both CF mouse models, Cl[−] permeability of nasal epithelia was restored in a sustained manner by zinc and ATP. These effects were reversible and reacquirable upon removal and readdition of agonists. Our data suggest that activation of P2X calcium entry channels may have profound therapeutic benefit for CF that is independent of cystic fibrosis transmembrane conductance regulator genotype.

Because morbidity in cystic fibrosis (CF)¹ often results from lung disease (1), several approaches have been contemplated to control and cure CF in the lung and airways. They include introduction of the wild-type cystic fibrosis transmembrane conductance regulator (CFTR) gene, repair of mutated CFTR proteins, attenuation of airway inflammation, stimulation of Cl[−] channels alternative to CFTR, and/or inhibition of epithelial sodium channel-mediated Na⁺ hyperabsorption (2). While methods of gene and protein therapy are defined, pharmacological intervention remains feasible in CF for dysregulated NaCl transport and airway inflammation (3). Ca²⁺-activated Cl[−] channels (4) have been proposed to substitute for cyclic AMP-dependent CFTR Cl[−] channels, offering a target for CF pharmacotherapy to rescue anion transport.

An ideal therapeutic compound would ameliorate multiple defects in ion transport as well as quell airway inflammation. Increases in cytosolic calcium concentration ([Ca²⁺]_i) activate epithelial Cl[−] channels (2, 5) but inhibit epithelial Na⁺ channels (2). Many laboratories have shown that stimulation of G protein-coupled P2Y nucleotide receptors increases [Ca²⁺]_i derived from intracellular stores and may affect both ion transport mechanisms (2, 5). Although P2Y nucleotide receptors are currently a target for CF pharmacotherapy (6, 7), they trigger transient increases in [Ca²⁺]_i and are desensitized or down-regulated via multiple mechanisms (8–10).

Our laboratory has shown that airway epithelia express another subclass of nucleotide receptors, the P2X receptor channels (P2XRs) (8, 11). P2XRs function as extracellular ATP-gated, Ca²⁺-permeable, non-selective cation channels (8, 12). Recently we have reported that stimulation of airway epithelial P2XRs leads to sustained Ca²⁺ entry from extracellular stores (8). The magnitude and sustained nature of the [Ca²⁺]_i increase was dependent on extracellular pH and the presence or

* This work was supported by National Institutes of Health R01 Grants HL 63934 and DK 54367 (to E. M. S.) and by the Hungarian Scientific Research Fund (OTKA) Grant T037524 (to A. Z.). Two provisional patents have been filed and established (Serial Nos. 60/441,045 and 60/475,423) with the United States Patent and Trademark Office to claim our findings. A full utility patent application will be filed in January 2004. No licensing agreements have been established to date. A dialogue has begun with the Cystic Fibrosis Foundation Therapeutics, Inc. and the Cystic Fibrosis Foundation Therapeutic Development Network with regard to beginning "proof of concept" clinical trials for cystic fibrosis with zinc-based formulations. The costs of publication of this article were defrayed in part by the payment of page charges. This article must therefore be hereby marked "advertisement" in accordance with 18 U.S.C. Section 1734 solely to indicate this fact.

¶ Co-director of the Cystic Fibrosis Center's Electrophysiology Assay CORE within a Specialized Center of Research (SCOR) grant (with logistical support from National Institutes of Health Grant DK 62397). To whom correspondence may be addressed: Dept. of Physiology and Biophysics, University of Alabama, MCLM 740, 1918 University Blvd., Birmingham, AL 35294-0005. Tel.: 205-934-6235; Fax: 205-934-1445; E-mail: zsembery@physiology.uab.edu.

§§ Director of the Cystic Fibrosis Center's Electrophysiology Assay CORE within a Specialized Center of Research (SCOR) grant (with logistical support from National Institutes of Health Grant DK 62397). To whom correspondence may be addressed: Dept. of Physiology and Biophysics, University of Alabama, MCLM 740, 1918 University Blvd., Birmingham, AL 35294-0005. Tel.: 205-934-6234; Fax: 205-934-1445; E-mail: eschwiebert@physiology.uab.edu.

¹ The abbreviations used are: CF, cystic fibrosis; CFTR, cystic fibrosis transmembrane conductance regulator; P2XR, P2X purinergic receptor channel; NMDG, N-methyl-D-glucamine; NPD, nasal potential difference.

absence of extracellular calcium, sodium, and zinc. Moreover the degree of alkaline pH potentiation of zinc and ATP stimulation and the lack of desensitization or inactivation of the receptor or channel properties was novel. In this study, we hypothesized that a combination of zinc and ATP could induce a prolonged Ca^{2+} signal that may rescue impaired Cl^- secretion in CF airway epithelium in a sustained and reversible manner.

MATERIALS AND METHODS

Cell Cultures—IB3-1 cells² are CF human bronchial epithelial cells carrying two different mutations of the CFTR gene ($\Delta\text{F508}/\text{W1282X}$) (13). 16HBE14o⁻ cells are non-CF or normal bronchial epithelial cells expressing wild-type CFTR (14). Culture of these two cell lines has been described previously (15). Human airway epithelial cell monolayers (primary CF isolated from patients homozygous for ΔF508 mutations, primary non-CF, and immortalized Calu-3 cells) were grown in air/fluid interface culture on Costar 6.5-mm-diameter permeable filter supports in Dulbecco's modified Eagle's medium/Ham's F-12 medium supplemented in a manner similar to the medium used for IB3-1 cells.

Fura-2 Imaging and Quenching—Cytosolic Ca^{2+} concentration was measured with dual excitation wavelength fluorescence microscopy after cells were loaded with the Fura-2-acetoxymethyl ester as described previously in detail (8). At the beginning of each experiment, cells were perfused with Ringer's solution containing 140 mM NaCl, 5 mM KCl, 1 mM MgCl_2 , 2 mM CaCl_2 , and 10 mM Hepes at pH 7.3 adjusted with NaOH. The effects of hexokinase and apyrase solutions were tested in solutions containing 5 mM glucose. In all Na^+ -substituted solutions, *N*-methyl-D-glucamine (NMDG) was used as a replacement cation. In NMDG-containing solutions, CaCl_2 was raised to 3 mM, while MgCl_2 was reduced to 0 mM, and external pH was adjusted with HCl. Fura-2 quenching experiments with MnCl_2 were performed as described previously (8).

Measurement of Cl^- Permeability—Cells were loaded with 6-methoxy-*N*-(3-sulfolopropyl)quinolinium (2 mg/ml) fluorescent dye overnight. At the beginning of each experiment, cells were perfused with Ringer's solution containing 140 mM NaCl, 5 mM KCl, 1 mM MgCl_2 , 2 mM CaCl_2 , and 10 mM Hepes at pH 7.3 adjusted with NaOH to establish a base-line fluorescence over 3 min. Then NMDG-containing solution (0 mM NaCl, 3 mM CaCl_2 , and 0 mM MgCl_2) at pH 7.9 was added for 3 min followed by addition of zinc alone or with ATP. Effects of the agonists were tested in both Ca^{2+} -free and Na^+ -containing medium. Specifics concerning the 6-methoxy-*N*-(3-sulfolopropyl)quinolinium assay and system have been published previously (16).

Measurement of Transepithelial Anion Current—Primary cultures of human CF and non-CF as well as immortalized Calu-3 cells grown as monolayers on 6.5-mm collagen-coated permeable supports were studied as described previously (11). Monolayers had electrical resistance at least 1,000 ohms/cm². When $\text{HCO}_3^-/\text{CO}_2$ -free solutions were used, the apical side of the monolayers were bathed in a 140 mM NMDG- and 20 μM amiloride-containing solution with 3 mM CaCl_2 and 0 mM MgCl_2 at pH 7.9 (adjusted with gluconic acid). Basolaterally we added a 140 mM NaCl-containing solution with 1.5 mM CaCl_2 and 1 mM MgCl_2 at pH 7.3 (adjusted with NaOH). Both solutions contained 10 mM Hepes. In $\text{HCO}_3^-/\text{CO}_2$ -containing solutions, apical and basolateral solutions contained 125 mM NMDG, 25 mM choline- Cl^- and 100 mM NaCl, 50 mM NaHCO_3 , respectively. Both solutions were gassed with 5% CO_2 . The pH of the apical solution was adjusted to 7.9 with gluconic acid. Concentrations of CaCl_2 and MgCl_2 were the same as described for $\text{HCO}_3^-/\text{CO}_2$ -free experiments.

Measurement of Nasal Potential Difference (NPD)—A three-step protocol was used as described previously (11); however, the solutions were modified as below. First, the nasal cavity of anesthetized mice was perfused with Ringer's solution containing 140 mM NaCl, 5 mM KCl, 1 mM MgCl_2 , 2 mM CaCl_2 , 10 mM Hepes, and 50 μM amiloride (pH 7.3 adjusted with NaOH). Second, we switched to low Cl^- -containing solution (6 mM) either in Na^+ - or NMDG-containing solution (pH was adjusted to 7.3 with NaOH and to 7.9 with gluconic acid, respectively). Third, zinc (40 μM) and ATP (100 μM) were added in Na^+ -free, NMDG-containing solution at pH 7.9. Because of the continuous presence of

amiloride (50 μM) and the complete replacement of Na^+ with a membrane-impermeant cation, NMDG (140 mM), in the perfusion solution, hyperpolarization reflects only Cl^- secretion rather than cation absorption.

Data Analysis—Data are expressed as mean \pm S.E. and tested for significance using paired or unpaired Student's *t* test with analysis of variance as appropriate. Results with $p < 0.05$ were considered significant. Values given in the text that refer to $\Delta[\text{Ca}^{2+}]_i$ or absolute $[\text{Ca}^{2+}]_i$ refer to the sustained plateau of cytosolic Ca^{2+} concentration measured 5 min after peak stimulation except where noted.

RESULTS

Extracellular Zinc and ATP Trigger a Sustained Increase in $[\text{Ca}^{2+}]_i$ in CF and Non-CF Airway Epithelial Cells—Based on our previous observations (8, 11), we hypothesized that combined stimulation of P2XRs by ATP and zinc in sodium-free medium at pH 7.9 could induce a more robust and sustained increase in cytosolic calcium than achieved previously (8). In IB3-1 cells, administration of ATP (100 μM) and ZnCl_2 (20 μM) stimulated a rapid increase in $[\text{Ca}^{2+}]_i$ followed by a sustained plateau (Fig. 1A). The plateau was markedly higher than basal $[\text{Ca}^{2+}]_i$ ($\Delta[\text{Ca}^{2+}]_i = 317 \pm 23$ nM, $n = 8$). Similar results were also obtained in 16HBE14o⁻ non-CF cells ($\Delta[\text{Ca}^{2+}]_i = 444 \pm 28$ nM, $n = 6$). The sustained Ca^{2+} plateau was abolished in the presence of 140 mM extracellular sodium ($\Delta[\text{Ca}^{2+}]_i = 32 \pm 9$ nM, $n = 4$) (Fig. 1A) or by reducing external pH to 7.3 ($\Delta[\text{Ca}^{2+}]_i = 45 \pm 7$ nM, $n = 4$) or 6.4 ($\Delta[\text{Ca}^{2+}]_i = 12 \pm 5$ nM, $n = 4$) (Fig. 1B). Titration of external pH in a range of 7.9 to 7.4 revealed a gradual decrease in Ca^{2+} plateau levels, exhibiting the largest decline between pH 7.9 ($[\text{Ca}^{2+}]_i = 383 \pm 11$ nM, $n = 4$) and pH 7.7 ($[\text{Ca}^{2+}]_i = 135 \pm 8$ nM, $n = 4$) (Fig. 1C). Because external Mg^{2+} inhibits P2X₄Rs (17), we hypothesized that removal of Mg^{2+} from the superfusion medium might further support Ca^{2+} entry mechanisms. In addition, we predicted that increasing external Ca^{2+} from 1.5 mM to 3 mM would enhance Ca^{2+} entry. Because our data show that ATP- and zinc-induced Ca^{2+} entry was potentiated in Mg^{2+} -free and Ca^{2+} -enriched medium (Fig. 1D), we studied Ca^{2+} entry under these ionic conditions (see below).

Zinc Alone Is an Agonist for Ca^{2+} Entry in IB3-1 Cells—Zinc has been reported to trigger an increase in $[\text{Ca}^{2+}]_i$ in many cell models (18–20). Thus, we tested the effects of zinc alone on cytosolic $[\text{Ca}^{2+}]_i$. Addition of ZnCl_2 (20 μM) to Na^+ -free medium that was pH 7.9 increased $[\text{Ca}^{2+}]_i$ ($\Delta[\text{Ca}^{2+}]_i = 312 \pm 22$ nM, $n = 10$) in a sustained manner (Fig. 2A) similar to that observed in combination with ATP (compare with Fig. 1A above). The Ca^{2+} plateau was abolished by removal of external Ca^{2+} ($\Delta[\text{Ca}^{2+}]_i = 11 \pm 5$ nM, $n = 4$) (Fig. 2B), reducing external pH to 7.3 ($[\text{Ca}^{2+}]_i$ was not significantly different from the basal value), or replenishment of 140 mM external Na^+ ($\Delta[\text{Ca}^{2+}]_i = 10 \pm 6$ nM, $n = 4$) (Fig. 2C). To define the concentration range in which zinc stimulates sustained Ca^{2+} entry, we exposed IB3-1 cells to ZnCl_2 in increasing concentrations from 2 to 200 μM . Significant stimulation was achieved at 10 μM ($\Delta[\text{Ca}^{2+}]_i = 187 \pm 12$ nM, $n = 4$) with maximal effects at 50 μM ($\Delta[\text{Ca}^{2+}]_i = 551 \pm 42$ nM, $n = 4$) (Fig. 2D). Although zinc alone caused robust Ca^{2+} entry from extracellular solution, we postulated that superfusion of cells might cause mechanically induced release of endogenous ATP that could act synergistically with exogenous zinc. Indeed elimination of ATP from the superfusion medium by ATP scavengers hexokinase (5 units/ml) and apyrase (1 unit/ml) caused a partial but not complete inhibition of zinc-induced Ca^{2+} entry ($\Delta[\text{Ca}^{2+}]_i = 312 \pm 22$ nM, $n = 10$ versus $\Delta[\text{Ca}^{2+}]_i^{\text{hexok. + apyr.}} = 145 \pm 15$ nM, $n = 4$; $p < 0.05$). Interestingly, in Ca^{2+} -free medium, zinc-induced increases in $[\text{Ca}^{2+}]_i$ were transient ($\Delta[\text{Ca}^{2+}]_i^{\text{peak}} = 123 \pm 16$ nM, $n = 5$) (Fig. 2E), an effect that was completely abolished by thapsigargin pretreatment (no significant changes in $[\text{Ca}^{2+}]_i$) (Fig. 2F). These

² Because all human cells and mice were handled by the University of Alabama at Birmingham Cystic Fibrosis Center, University of Alabama at Birmingham Cystic Fibrosis Center human subjects (assurance of compliance number M1149) and vertebrate animals (animal welfare assurance number A3255-01) protocols were followed.

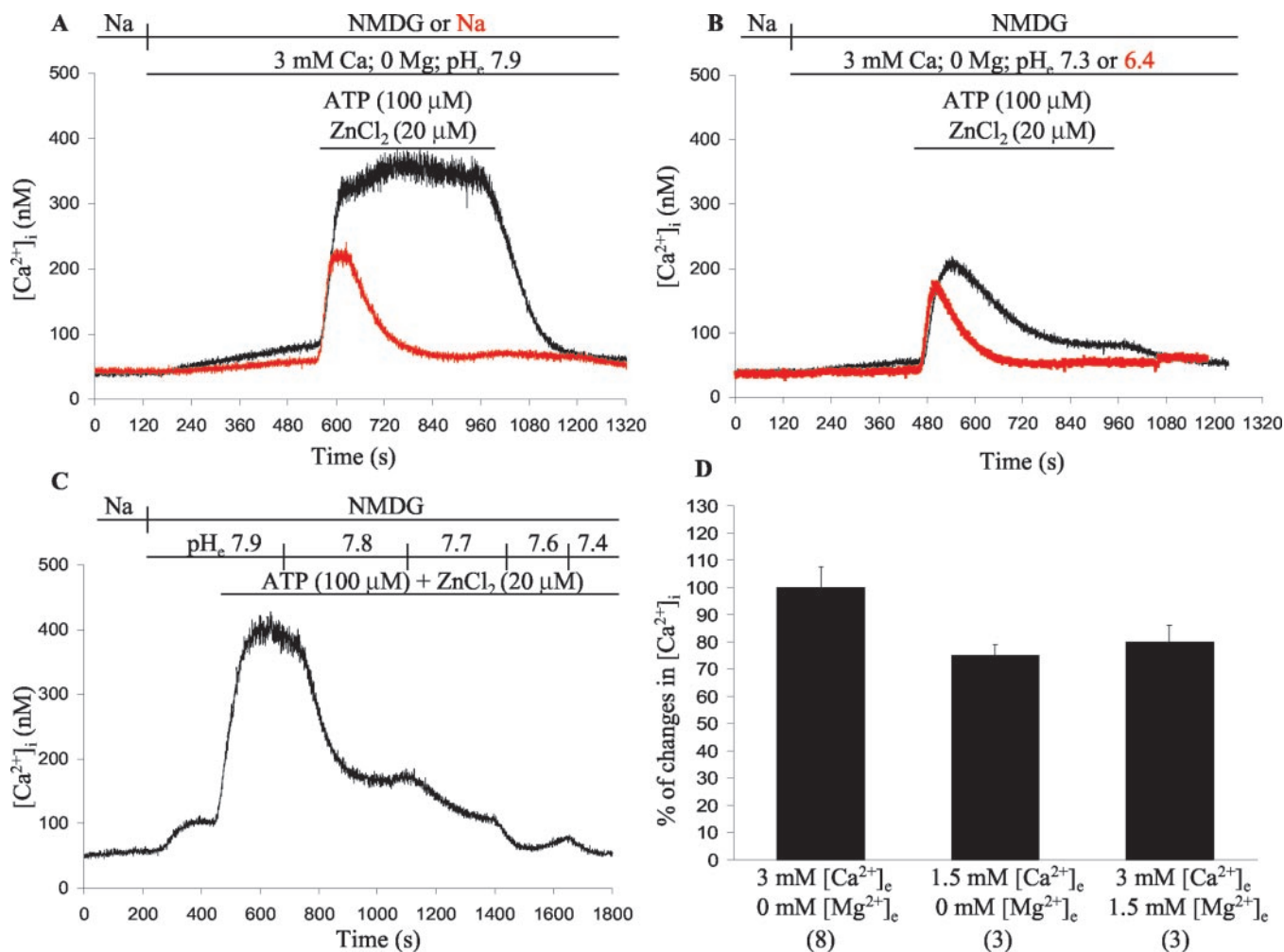


FIG. 1. Effects of ATP and zinc on $[Ca^{2+}]_i$ in IB3-1 cells. A, original traces showing the effect of combined administration of ATP (100 μ M) and ZnCl₂ (20 μ M) in the absence (black trace) and presence (red trace) of 140 mM extracellular Na⁺. Cells were perfused with Na⁺-containing Ringer's solution (pH_e 7.3), and then extracellular pH was raised to 7.9, and extracellular [Ca²⁺]_e was increased from 1.5 to 3 mM in Mg²⁺-free medium. At the same time, extracellular Na⁺ was substituted by NMDG in Na⁺-free experiments. B, combined administration of ATP and ZnCl₂ in the absence of external Na⁺ at pH_e 7.3 (black trace) and 6.4 (red trace). Cells were perfused with the same medium as in A. Extracellular [Ca²⁺]_e was increased to 3 mM in a Na⁺- and Mg²⁺-free medium. At the same time, pH_e was dropped to 6.4 (red). C, effects of ATP and ZnCl₂ on the sustained Ca²⁺ plateau in a pH_e range between 7.9 and 7.4. External pH was raised to 7.9, and Na⁺ was removed as indicated. Changes in [Ca²⁺]_e and [Mg²⁺]_e were similar to those indicated for A and B. After addition of agonists, pH_e was decreased in a stepwise manner. D, ATP- and ZnCl₂-induced sustained increase in [Ca²⁺]_i relative to basal [Ca²⁺]_i. In optimized solution (3 mM Ca²⁺_e and 0 Mg²⁺_e), a sustained increase in [Ca²⁺]_i ($\Delta[Ca^{2+}]_i = 317 \pm 23$ nM) was considered 100%. A reduction in [Ca²⁺]_e or an increase in [Mg²⁺]_e attenuated the Ca²⁺ plateau. Numbers of experiments are indicated in parentheses. Each experiment shown in A–C was performed four to six times with similar results.

data show that zinc increases $[Ca^{2+}]_i$ from cytosolic calcium stores and extracellular solution. However, a sustained Ca²⁺ plateau was only observed when external calcium was present, suggesting that activation of Ca²⁺ entry mechanisms plays a key role in this prolonged Ca²⁺ signal.

P2XR-independent Ca²⁺ Entry Pathways Are Not Involved in Zinc-induced Ca²⁺ Entry—Because Ca²⁺ entry was stimulated by zinc even in the absence of ATP, we were required to investigate whether P2XR-independent mechanisms were involved in this process. First, we assessed the effects of the zinc-activated cation channel inhibitor tubocurarine (21) on zinc-induced Ca²⁺ entry. Tubocurarine (100 μ M) had no effect on Ca²⁺ entry in IB3-1 cells ($\Delta[Ca^{2+}]_i = 282 \pm 23$ nM, $n = 4$) (Fig. 3A). We have shown previously that activation of the reverse operation mode of Na⁺/Ca²⁺ exchange did not contribute to ATP-induced Ca²⁺ entry in Na⁺-free solution (8). Zinc also inhibits Na⁺/Ca²⁺ exchange in rat brain (22). However, we could not exclude the possibility that zinc might influence activity of the Na⁺/Ca²⁺ exchanger under Na⁺-free experimental conditions. Thus, we tested the effects of KB-R7943, a selective inhibitor of the reverse operation mode of this exchanger. Surprisingly,

instead of inhibition of zinc-induced Ca²⁺ entry, KB-R7943 (10 μ M) potentiated zinc stimulation ($\Delta[Ca^{2+}]_i = 727 \pm 51$ nM, $n = 4$) (Fig. 3B). Store-operated Ca²⁺ channels play an important role in Ca²⁺ entry in non-excitable cells (23, 24) and in epithelial cells (25–27). Although zinc has been described as an inhibitor of store-operated Ca²⁺ channels (23–27), we tested its effects on thapsigargin-induced Ca²⁺ entry. At concentrations shown to activate sustained Ca²⁺ entry in human airway epithelial cells, zinc inhibited store-operated Ca²⁺ entry channels ($[Ca^{2+}]_i = 685 \pm 34$ nM before and after zinc exposure *versus* $[Ca^{2+}]_i = 94 \pm 21$ nM during zinc exposure, $n = 5$; $p < 0.01$) stimulated by thapsigargin depletion of intracellular endoplasmic reticulum Ca²⁺ stores (Fig. 3C). Because zinc has been reported to modify the properties of Fura-2 (28), we tested whether zinc enters the cells and affects Fura-2 when added at the concentration that induces sustained Ca²⁺ entry. Zinc did not change Fura-2 fluorescence until manganese was subsequently added, showing that zinc triggered Mn²⁺ entry and Mn²⁺-dependent Fura-2 quenching (Fig. 3D). Taken together, these data show that P2XR-independent Ca²⁺ entry mechanisms are likely not involved in zinc-induced Ca²⁺ entry. Our

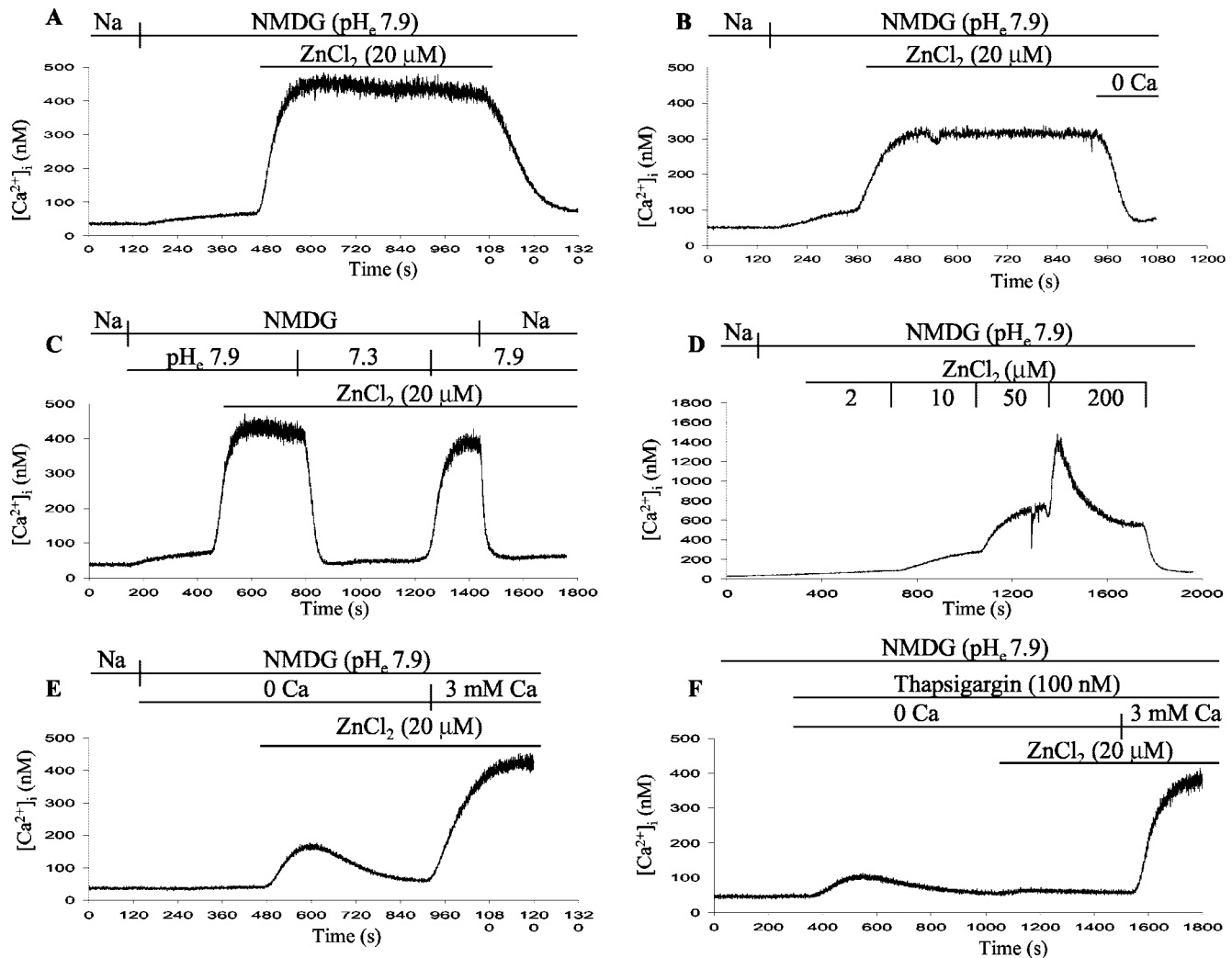


FIG. 2. **Effects of zinc alone on $[Ca^{2+}]_i$ in IB3-1 cells.** Original traces show the effects of zinc alone. In experiments shown in A–D, early changes of external ionic composition were performed as described in Fig. 1A. A, addition and removal of zinc as indicated. B, external Ca^{2+} was removed in the continuous presence of zinc. C, external pH was dropped from 7.9 to 7.3 and restored again to 7.9 followed by replenishment of sodium in the continuous presence of zinc. D, $ZnCl_2$ was added in increasing concentrations. E, $ZnCl_2$ was added in Ca^{2+} -free medium followed by readdition of external Ca^{2+} . F, cells were pretreated with thapsigargin in the absence of external Na^+ and Ca^{2+} , and then zinc was added. At the end of the experiment, external calcium was replenished. Each experiment shown in A–F was performed four to six times with similar results.

previous results (8) and the properties of zinc- or zinc and ATP-induced Ca^{2+} entry argue for a prominent role for P2X receptor Ca^{2+} entry channels.

Zinc Alone or in Combination with ATP Restores Cl^- Transport in IB3-1 Cells—To test the hypothesis whether a sustained increase in cytosolic Ca^{2+} of greater than 300 nM could restore Cl^- transport in IB3-1 CF cells grown on collagen-coated glass coverslips, we assessed Cl^- efflux using 6-methoxy-N-(3-sulfo-propyl)quinolinium halide fluorescence assay. $ZnCl_2$ (20 μM) alone or in combination with ATP (100 μM) stimulated Cl^- efflux when administered in Na^+ -free alkaline (pH 7.9) medium (Fig. 4, A and B). These effects were dependent upon the presence of extracellular Ca^{2+} (Fig. 4A), suggesting a key role of Ca^{2+} entry mechanisms in stimulating Cl^- transport. It is important to note that stimulation of Cl^- efflux was achieved under the same conditions that resulted in a prolonged cytosolic Ca^{2+} increase. It is also probable that flow-induced release of endogenous ATP contributed to zinc-induced rescue of Cl^- efflux in a manner similar to the Fura-2 imaging assays (see above).

Zinc and ATP Stimulate Cl^- Secretion in Polarized CF and Non-CF Human Airway Epithelial Cell Monolayers—We next tested the efficacy of zinc and ATP in rescuing transepithelial

Cl^- transport in primary human CF and non-CF airway epithelial cell monolayers as well as in Calu-3 immortalized human non-CF submucosal gland serous cell monolayers in Ussing chambers. In the presence of amiloride (20 μM) and a “basolateral toward apical” Cl^- gradient, apical ATP (100 μM) and $ZnCl_2$ (40 μM) in Na^+ -free solution (pH 7.9) stimulated transepithelial chloride current in both CF and non-CF airway epithelial cells (Fig. 5A). This Cl^- current was biphasic, showing transient and sustained components (Fig. 5, A–D). Removal of the agonists abolished the sustained Cl^- current, which was stimulated again upon readdition of agonists (Fig. 5B). Calu-3 cell monolayers are a preferred respiratory cell model system to study anion and water transport. It has been shown that forskolin-stimulated anion current is carried mainly by bicarbonate in these monolayers (29). Furthermore Cuthbert *et al.* (30) have recently reported that HCO_3^-/CO_2 removal inhibits Cl^- secretion in Calu-3 monolayers. Thus, we hypothesized that, in the presence of HCO_3^-/CO_2 , ATP and zinc could stimulate a more robust and sustained anion secretion than we observed in HEPES-buffered solution. Indeed, under these conditions, ATP (100 μM) and $ZnCl_2$ (40 μM) elicited significantly higher peak ($100.4 \pm 10.0 \mu A/cm^2$, $n = 5$ versus $16.4 \pm 1.2 \mu A/cm^2$, $n = 18$; $p < 0.01$) and sustained currents ($76.6 \pm 6.8 \mu A/cm^2$, $n = 5$

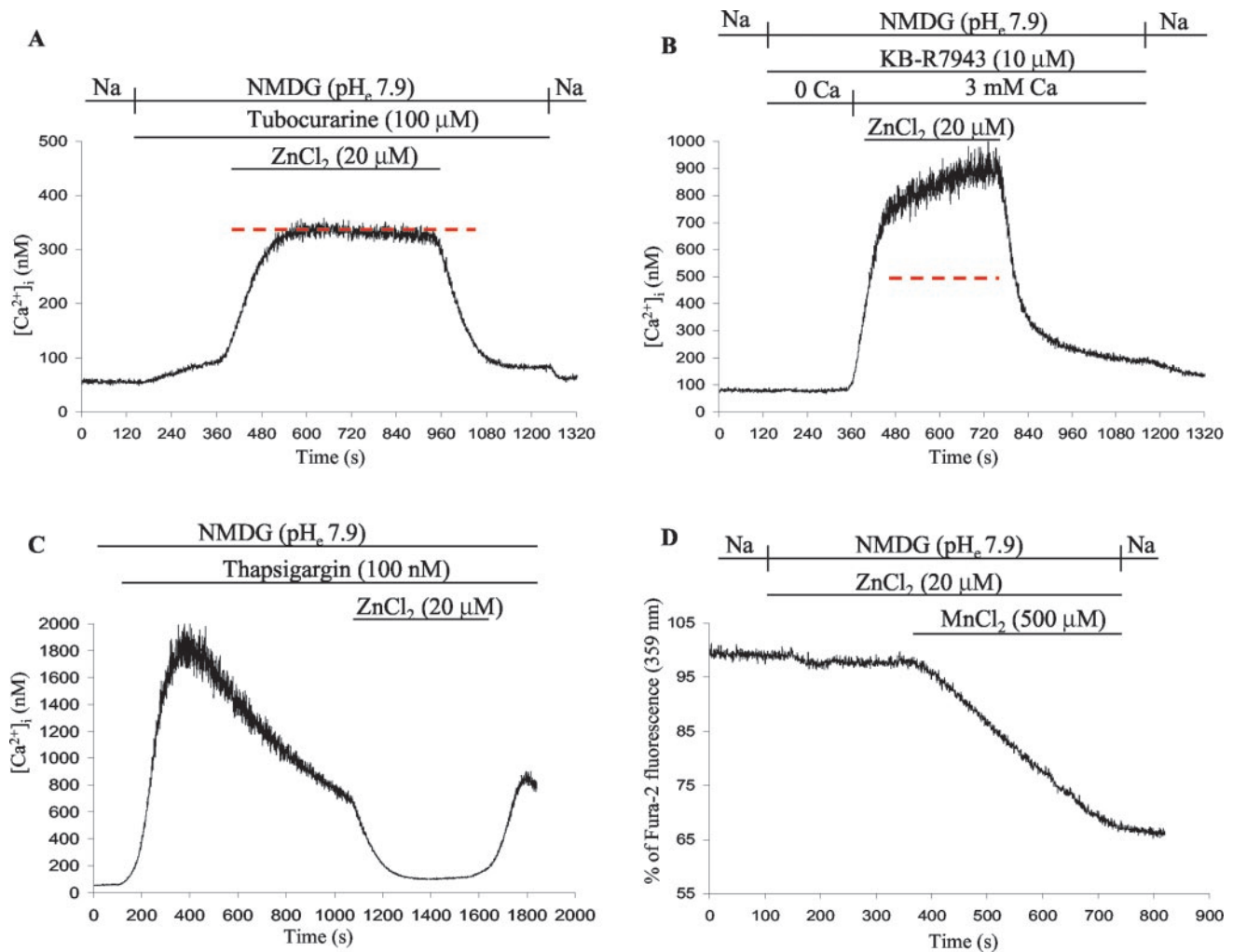


FIG. 3. **P2XR-independent Ca^{2+} entry is not involved in zinc-induced sustained $[\text{Ca}^{2+}]_i$ increases.** Original traces show the effects of tubocurarine (A) and KB-R7943 (B) on zinc-induced $[\text{Ca}^{2+}]_i$ increases. The dashed red lines indicate the levels of the zinc-induced sustained Ca^{2+} plateau in parallel experiments performed on the same day in the absence of tubocurarine and KB-R7943, respectively. C, thapsigargin-induced increase in $[\text{Ca}^{2+}]_i$ in Na^+ -free, Ca^{2+} -containing (3 mM) medium that was pH 7.9. Addition of ZnCl_2 inhibited Ca^{2+} influx as indicated, while withdrawal of zinc revealed residual store-operated Ca^{2+} entry channel activity. D, quenching of Fura-2 was assessed in the presence of ZnCl_2 (20 μM) followed by addition of MnCl_2 . At the beginning of each experiment Fura-2 fluorescence was considered 100%, which was not changed significantly by ZnCl_2 ($98 \pm 2\%$). Each experiment shown in A–D was performed four times with similar results.

versus $12.0 \pm 1.0 \mu\text{A}/\text{cm}^2$, $n = 18$; $p < 0.01$) (Fig. 5, B and D). The sustained current was inhibited by chelation of extracellular Ca^{2+} , a maneuver that did not prevent the forskolin-stimulated anion secretion (Fig. 5D). These data show that zinc and ATP under optimal Ca^{2+} entry conditions stimulated sustained Cl^- and/or HCO_3^- secretion in polarized CF and non-CF human airway and submucosal gland serous cell epithelia by a mechanism that, at least in part, requires extracellular Ca^{2+} .

Zinc and ATP Correct Defective Cl^- Transport in NPD Assays of Mice—A critical test for these agonists and vehicle was the NPD assay in anesthetized mice (31). We applied zinc and ATP onto the nasal mucosa of different strains of control and CF mice in the identical saline vehicle optimized for marked Ca^{2+} entry. In mice with at least one wild-type CFTR allele, the NPD depolarized with gradual decay in the presence of amiloride (50 μM). Under these conditions, reduction of mucosal $[\text{Cl}^-]$ caused significant hyperpolarization, indicating Cl^- secretion by nasal epithelial cells (Table I and Fig. 6A). Addition of ZnCl_2 (40 μM) and ATP (100 μM) induced further hyperpolarization that was sustained and indicative of Cl^- secretion (Fig. 6A). This magnitude of hyperpolarization was as large as that elicited by isoproterenol stimulation of CFTR-mediated Cl^- secretion in our studies (data not shown). The hyperpolarization was

transient and markedly attenuated by removal of extracellular Ca^{2+} (Table I). We also tested this protocol in a ΔF508 -CFTR homozygous CF mouse (32) and a bitransgenic mouse in which the lungs are null for CFTR but intestinal dysfunction was corrected with a fatty acid-binding protein promoter-driven CFTR construct. In the presence of amiloride (50 μM), reduction of mucosal Cl^- was without effect (Fig. 6, B–F), illustrating the loss of Cl^- permeability in CF. However, administration of ZnCl_2 and ATP caused marked and sustained hyperpolarization in both CF models (Table I and Fig. 6, B–E). This degree of rescue of Cl^- permeability and the sustained nature of this rescue are novel to the CF NPD field.

The duration, reversibility, and reproducibility of a potential therapeutic compound are key issues, especially one that targets an endogenous receptor. Therefore, we tested the duration of effect as well as removal and readministration of agonists. To our knowledge, these are the first CF NPD assays in which such protocols have been performed. In CF mice, administration of ATP and zinc hyperpolarized the NPD in a sustained manner for 15 min (Fig. 6D). This long lasting stimulation was reversible upon removal of agonists (Fig. 6D). In addition, multiple exposures to agonists elicited similar Cl^- secretory responses, suggesting that P2XRs do not become desensitized

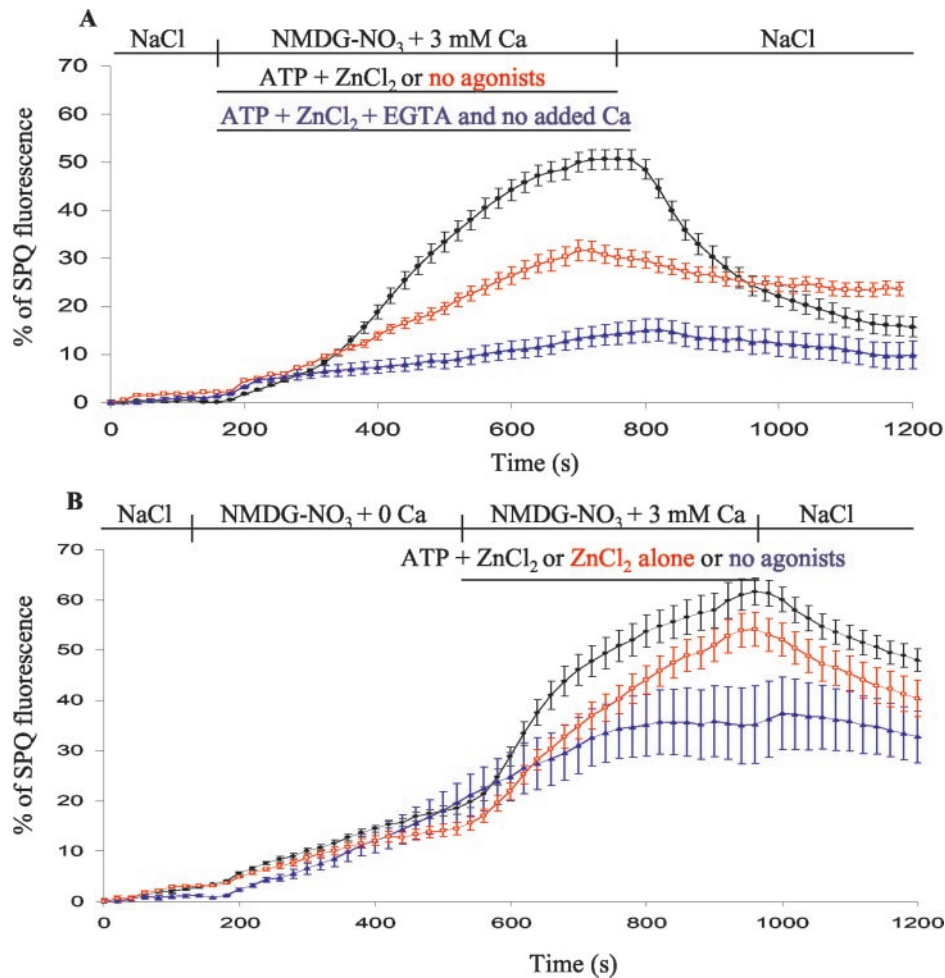


FIG. 4. **Effects of zinc and ATP on Cl⁻ efflux in IB3-1 cells.** A, effects of combined administration of ATP and ZnCl₂ on Cl⁻ efflux. Extracellular Na⁺ and Cl⁻ were replaced by NMDG and NO₃⁻, respectively. At the same time, the concentration of CaCl₂ was increased to 3 mM, and pH_e was elevated to 7.9 in the presence of ATP and ZnCl₂ (black trace) or in the absence of the agonists (red trace). In the blue trace, Na⁺, Cl⁻, and pH_e were changed as described above, but CaCl₂ was removed, and EGTA was added in the presence of ATP and ZnCl₂. Na⁺-containing solution without agonists was given back as indicated, although the point at which it was given in the three separate traces was slightly different (the deflections in the traces show when agonist-free solutions affected the cells in the different experiments). Values are means \pm S.E. ($n = 17$ cells in each group). B, effects of combined administration of the agonists versus ZnCl₂ alone on Cl⁻ efflux. Cells were superfused with Ca²⁺-free, Na⁺-containing solution that had a pH of 7.3. Ionic composition of the solutions was changed as described for A with the exception that no added CaCl₂ was present in NMDG-containing solutions. ATP and ZnCl₂ (black trace), ZnCl₂ alone (red trace), or no agonists (blue trace) were added with CaCl₂. Values are means \pm S.E. ($n = 17$ cells in each group). SPQ, 6-methoxy-N-(3-sulfoethyl)quinolinium.

or inactivated (Fig. 6E). Notably Cl⁻ secretion induced by ATP and zinc was more rapid when the low Cl⁻ solution added prior to the agonist-containing solution was also pH 7.9, independent of the absence or presence of extracellular Na⁺ (Table I and Fig. 6, D and E). Interestingly ATP, when administered alone in Na⁺-free, alkaline solution, caused significantly smaller and transient hyperpolarization responses in bitransgenic CF mouse NPD (Table I and Fig. 6F). Comparison of Fig. 6E with Fig. 6F illustrates the pivotal role for zinc in triggering sustained Cl⁻ secretion *in vivo*. Finally, as in transepithelial anion current recordings, administration of ZnCl₂ alone was not sufficient to produce significant Cl⁻ secretion in either CF mouse model (data not shown).

DISCUSSION

Having ruled out P2XR-independent Ca²⁺ entry mechanisms (22–27) and zinc-activated channels (21), P2XRs are the most likely candidates to conduct Ca²⁺ into airway epithelial cells when stimulated with zinc and ATP. Because of alkaline pH potentiation of ATP and zinc-induced Ca²⁺ entry, we speculate that the P2X₄ subtype is involved in this process. However, it is possible that P2X₅ and/or P2X₆ may also contribute to Ca²⁺ entry because they co-assemble with P2X₄ (12, 33) and

are also expressed in human airway epithelial cells.³ Zinc is an antagonist for P2X₁ and P2X₇, while P2X₂ receptors are stimulated by acidic pH (12). Furthermore P2X₁ and P2X₃ can also be excluded because of their rapid inactivation (12). Thus, functional, biochemical, and immunohistochemical definition of the relative roles of P2X₄, P2X₅, and/or P2X₆ in alkaline pH-dependent, zinc-induced Ca²⁺ entry is in progress.

The sustained nature of the Ca²⁺ signal induced by zinc and/or ATP was surprising and intriguing. In addition to the fact that Ca²⁺ entry was essential, two additional factors may explain this phenotype. First, both zinc and ATP also cause endoplasmic reticulum Ca²⁺ release. Second, since zinc inhibits the human erythrocyte plasma membrane Ca²⁺ ATPase pump (34), it is conceivable that submicromolar concentrations of zinc could accumulate in the cells that might inhibit Ca²⁺ extrusion without altering Fura-2 properties. Nonetheless we emphasize that removal of zinc or of extracellular Ca²⁺ quickly lowered and reversed the signal back to base-line [Ca²⁺]_i, suggesting that the overall Ca²⁺ buffering capacity is not affected by zinc. Interestingly zinc alone stimulated sustained cell Ca²⁺

³ L. Liang and E. M. Schwiebert, unpublished observations.

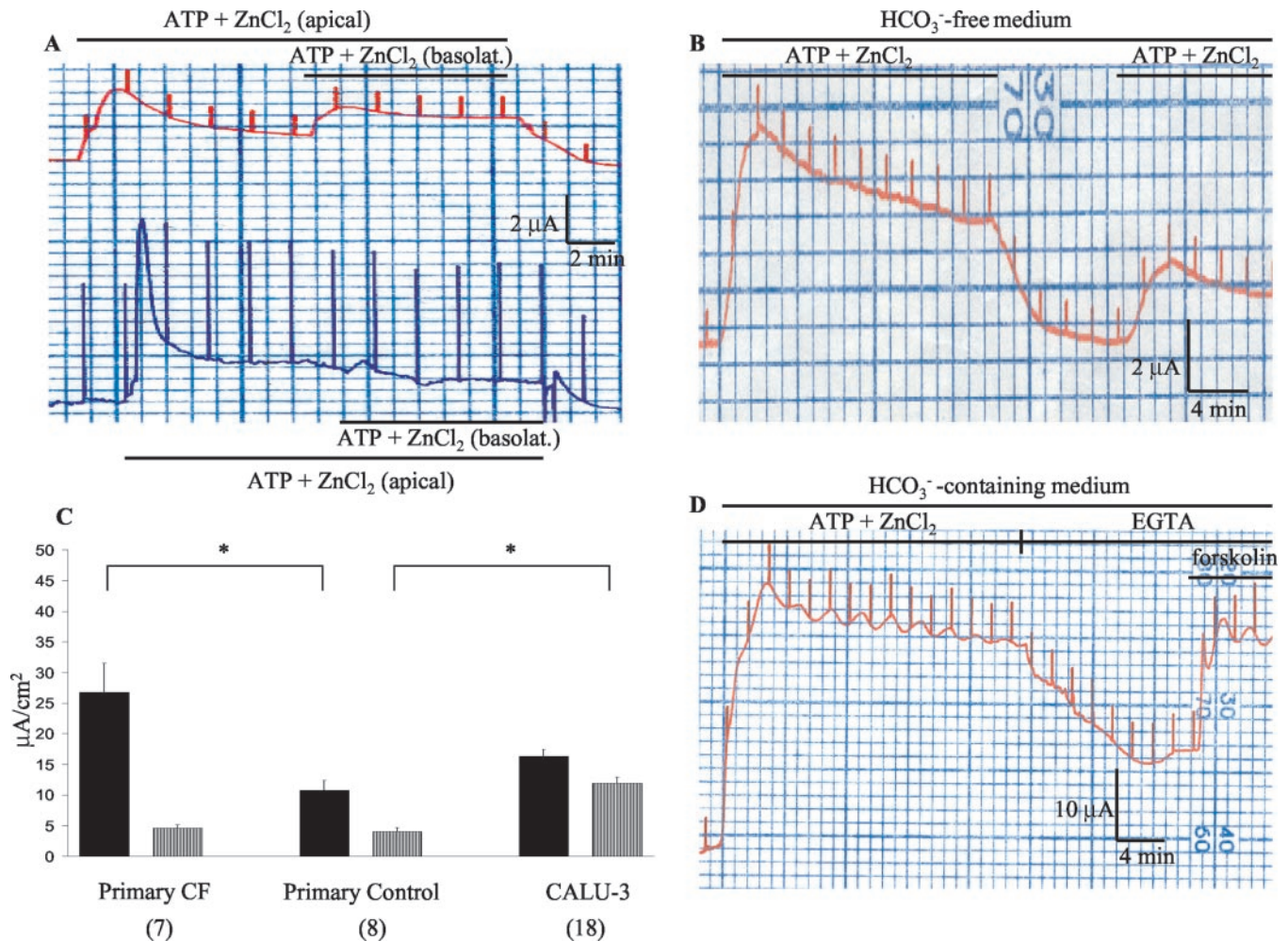


FIG. 5. Effects of zinc and ATP on secretory Cl^- and HCO_3^- currents in polarized airway epithelia. A, representative tracings of transepithelial chloride current measurement are shown using non-CF (red trace) and CF (blue trace) human primary airway epithelial cell monolayers. ATP and ZnCl_2 were added apically and basolaterally as indicated. B, representative tracing of transepithelial chloride current in the absence of $\text{HCO}_3^-/\text{CO}_2$ using Calu-3 monolayers. ATP and ZnCl_2 were added apically followed by washout and by readdition of the agonists. C, summarized data for transepithelial chloride current experiments. Black columns represent the peak stimulation by ATP and ZnCl_2 , while gray columns represent currents measured 5 min after the peak. Please note that primary CF cells exhibited the highest peak current component, while Calu-3 cells had the highest sustained current component. Numbers of experiments are shown in parentheses (*, $p < 0.05$). D, representative tracing of transepithelial anion current in the presence of $\text{HCO}_3^-/\text{CO}_2$ using Calu-3 monolayers. ATP and ZnCl_2 were added apically followed by addition of EGTA (2 mM). Forskolin (5 μM) was given to the apical side of the monolayers as indicated. basolat., basolateral.

TABLE I
Transepithelial nasal potential difference values of control, $\Delta 508$ CF, and bitransgenic CF mice

Starting points represent values (mV) obtained in Ringer's solution containing amiloride immediately after the beginning of experiments. Low $[\text{Cl}^-]_e$ responses represent the changes in values (mV) reducing $[\text{Cl}^-]_e$ to 6 mM in Na^+ - or NMDG-containing medium at different pH_e . Negative and positive values reflect changes toward hyperpolarization and depolarization, respectively. Effects of ATP and ZnCl_2 were tested in NMDG-containing medium at pH 7.9 following reduction of $[\text{Cl}^-]_e$. n = number of experiments.

	Control		CF		Bitransgenic CF	
	Cftr (+/-)	n	Cftr($\Delta F508/\Delta F508$)	n	Cftr(-/-)	n
Starting point	-18.7 ± 1.5	19	-26.3 ± 2.2^a	11	-26.1 ± 1.0^a	14
Low $[\text{Cl}^-]_e$ (Na^+ pH 7.3)	-5.5 ± 0.5	8	$+3.7 \pm 0.9^a$	3	$+4.8 \pm 0.9^a$	7
ATP + ZnCl_2 (NMDG, pH 7.9)	-4.7 ± 0.7	6	-4.0 ± 1.2	3	-3.8 ± 0.6	12
Low $[\text{Cl}^-]_e$ (Na^+ pH 7.9)	-4.8 ± 0.8	6	$+5.4 \pm 1.1^a$	7	$+6.7 \pm 2.3^a$	3
ATP + ZnCl_2 (NMDG, pH 7.9)	-6.0 ± 1.0	2	$-9.4 \pm 0.6^{a,b}$	8	$-9.7 \pm 1.8^{a,c}$	3
Low $[\text{Cl}^-]_e$ (NMDG, pH 7.9)	-4.8 ± 1.5	5			$+5.8 \pm 1.0^a$	4
ATP + ZnCl_2 (NMDG, pH 7.9)	-5.7 ± 0.7	3			$-10.2 \pm 0.5^{a,c}$	6
ATP alone (NMDG, pH 7.9)					-2.3 ± 0.5^d	4
Low $[\text{Cl}^-]_e$ (NMDG, no added Ca^{2+} , pH 7.9)	-7.3 ± 0.3	3			$+6.0 \pm 0.4^a$	4
ATP + ZnCl_2 (NMDG, no added Ca^{2+} , pH 7.9)	-1.3 ± 0.3^e	3			-2.0 ± 0.6^e	4

^a $p < 0.05$ vs. control animals.

^b $p < 0.05$ vs. CF animals; ATP + ZnCl_2 after low $[\text{Cl}^-]_e$ response with Na^+ (pH 7.3).

^c $p < 0.05$ vs. bitransgenic CF animals (a generous gift from Dr. Jeffrey A. Whitsett); ATP + ZnCl_2 after low $[\text{Cl}^-]_e$ response with Na^+ (pH 7.3).

^d The effect of ATP alone was assessed by the peak of the hyperpolarization response because of the transient nature of the response.

^e $p < 0.05$ vs. ATP + ZnCl_2 with NMDG in the presence of extracellular Ca^{2+} .

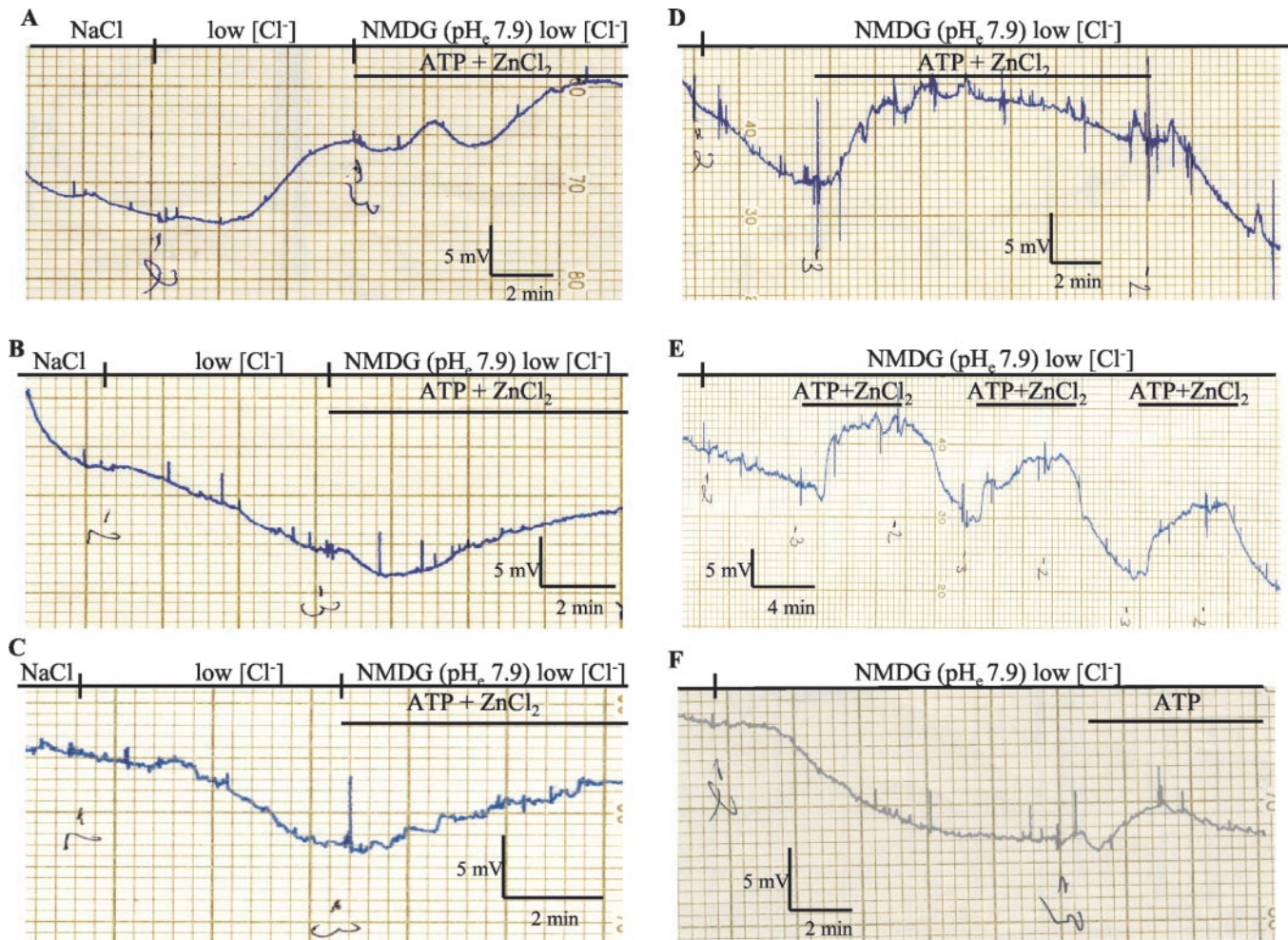


FIG. 6. Effects of zinc and ATP on Cl^- secretion in mouse NPD measurements. *A*, typical experiment in control animals. The nasal cavity of the mouse was perfused with Na^+ -containing Ringer's solution (pH 7.3) in the presence of amiloride ($50 \mu\text{M}$) showing a gradual decay in NPD (depolarization). Then we switched to a low Cl^- -containing (6 mM) solution. Please note the hyperpolarization upon lowering external $[\text{Cl}^-]$. Due to a delay in the perfusion system, hyperpolarization occurred approximately 2 min after changing solutions. ATP ($100 \mu\text{M}$) and ZnCl_2 ($40 \mu\text{M}$) were added in Na^+ -free medium that was pH 7.9. Please note an additional hyperpolarization in the presence of agonists. Shown are typical experiments in a ΔF508 homozygous CF mouse (in *B*) and in a bitransgenic CF mouse (in *C*) using the same protocol as in *A*. Please note that in both CF mouse models hyperpolarization occurred only upon addition of agonists. *D*, long exposure to agonists in a ΔF508 homozygous mouse. Extracellular Na^+ was substituted by NMDG, and pH was raised to 7.9 in low Cl^- -containing medium before addition of agonists, and then ATP and ZnCl_2 were added. Please note that the time lag between switching to agonist-containing solution and hyperpolarization is shorter (approximately 1 min), and the amplitude of the response is greater than that achieved in *B*. Also note that washout of agonists reversed the response completely. *E*, multiple exposures to ATP and ZnCl_2 in a ΔF508 homozygous mouse. Please note that the amplitude of the responses did not decline with the time even upon removal and readdition of agonists two additional times. *F*, a bitransgenic CF mouse was exposed to ATP alone in Na^+ -free low $[\text{Cl}^-]_e$ solution at pH 7.9. Before adding the agonists, nasal epithelia were perfused with Na^+ -free low $[\text{Cl}^-]_e$ solution at pH 7.9. Note the transient nature of the response.

increases and Cl^- efflux in non-polarized cells. In polarized monolayers, however, both zinc and ATP were required to stimulate sustained Cl^- secretion. It is probable that Ca^{2+} -activated Cl^- channel expression is regulated by epithelial polarity (35), which might underlie the different Cl^- secretory responses in polarized and non-polarized airway epithelial cells. Furthermore administration of ATP scavengers inhibited partially the zinc-induced sustained Ca^{2+} plateau, suggesting that rapid perfusion triggers endogenous ATP release in fluorescence-based assays (36, 37) and that addition of both co-agonists provides full stimulation of epithelial P2XRs.

Modifications of the saline vehicle appear essential to activate P2XR Ca^{2+} entry channels. These include a low extracellular Na^+ concentration (which benefits all other Ca^{2+} entry channels (38–43)) and an alkaline extracellular pH (which potentiates P2X_4 (8, 12)). Removal of extracellular Mg^{2+} and increased external Ca^{2+} concentrations also potentiated the effects of zinc and ATP. Applying these modifications, P2X agonists induced a sustained increase in $[\text{Ca}^{2+}]_i$ of 300–450 nM

above basal levels in CF and non-CF airway epithelial cells. This signal would be sufficient for marked stimulation of Ca^{2+} -activated Cl^- channels (44) and ciliary beat (45, 46). Silberberg and coworkers (46) hypothesized that the latter effects were conferred by “P2X cilia.” Of note, a low Na^+ environment and extracellular ATP potentiated P2XR-modulated ciliary beat in their studies (46). Together our studies argue for possible improvement in CF mucociliary clearance.

A sustained Ca^{2+} signal also stimulates Ca^{2+} -dependent K^+ channels and may inhibit epithelial Na^+ channels (2). K^+ efflux would lead to a hyperpolarization of cell membrane potential, establishing a favorable electrical gradient for Cl^- secretion. Reduction of Na^+ hyperabsorption would promote rehydration of airway surfaces. Furthermore zinc inhibition of a recently described proton conductance could also alkalize the airway surface, which may be acidic during airway inflammation (47). Thus, inclusion of zinc might correct multiple airway epithelial ion transport dysfunctions. Interestingly, in Calu-3 submucosal gland serous cells, ATP and zinc

stimulated marked anion secretion (especially in $\text{HCO}_3^-/\text{CO}_2$ -containing medium), suggesting that P2XRs may also be useful for more general rescue of anion secretion in submucosal glands.

Stimulation of sustained Ca^{2+} entry in CF therapy must also occur in a controlled manner because of possible induction of apoptosis (48). Cytosolic Ca^{2+} imaging, Ussing chamber, and NPD experiments show that zinc- and ATP-stimulated Ca^{2+} entry and Cl^- secretion are reversible upon removal of agonists and reacquirable after readdition of agonists. These features indicate that P2XRs and Ca^{2+} -activated Cl^- channels are not desensitized or inactivated under these experimental conditions. However, it is noteworthy that administration of ATP alone caused only transient Cl^- secretion in CF mouse nasal epithelia, underscoring the importance of zinc co-application along with ATP.

The most novel and compelling aspect of this proposed P2XR-targeted CF therapy is the inclusion of zinc. Zinc is a trace element and transition metal. It is derived from human diets and is required for healthy function of the body, and no chronic disorders are known to be associated with its accumulation (49, 50). Zinc oxide creams alleviate dermatitis, including acrodermatitis enteropathica in at least 30% of CF patients caused by zinc malabsorption and deficiency (51). Defective activity of a zinc transporter, hZip4, in the intestinal mucosa is also linked to this form of dermatitis (52). Of note, homeopathic remedies such as ZicamTM and ColdEezeTM, based on zincum gluconicum (53, 54), are available for treatment of the common cold. Oral zinc sulfate is also Food and Drug Administration-approved in milligram quantities as an adjunct therapy for Wilson's disease (55). Despite current therapeutic use, the anti-inflammatory mechanisms of and receptors for zinc are poorly defined. It is possible that luminal epithelial P2XRs function, at least in part, as zinc-sensing receptors and participate in these mechanisms.

One could argue that zinc and a nucleotide would require a low sodium, alkaline environment to activate P2XRs, conditions that would make its application difficult in therapeutic trials. Nevertheless efficacy was achieved in the mouse nasal cavity. We speculate that inhalation of Na^+ -free alkaline solution of a volume markedly greater than the estimated volume of the airway surface liquid in the large ciliated airways (56) might reduce Na^+ concentration and increase pH of the airway surface liquid, allowing zinc to exert its beneficial effects. CF aerosol administration of drugs, such as tobramycin, is often administered in markedly diluted saline (75% diluted saline in water in the case of TobitTM; information is provided in *Physician's Desk Reference*). There is also precedence for an inhaled isotonic alkaline solution (pH 8.0–9.0) containing bicarbonate that improved radioaerosol clearance significantly in patients with chronic cough (57). Importantly, in contrast to acidic aerosols, alkaline aerosols do not trigger bronchoconstriction (58). These previous observations suggest that properly compiled aerosols may have significant influence on the efficacy of zinc in future human studies. Thus, we propose that zinc and ATP (or an equivalent nucleotide) added to the nasal passages and airways may be of significant benefit to CF pharmacotherapy that is independent of CFTR genotype. Zinc-based therapy for CF, other airway diseases, and the common cold could also be improved by delivery in an optimized saline vehicle inhaled as a solution.

Acknowledgments—We thank the Gregory Fleming James Cystic Fibrosis Research Center at the University of Alabama at Birmingham (especially Timea Kovács and Marina Mazur) and its CORE facilities for assistance in nasal potential difference assays, Ussing chamber recordings, and polarized epithelial monolayer culture. The bitransgenic CF mouse was a generous gift to the University of Alabama at

Birmingham Cystic Fibrosis Center Transgenic Mouse CORE from Dr. Jeffrey A. Whitsett (University of Cincinnati, Cincinnati, OH). We thank Lucy Hicks, Esquire; Gregory Peterson, Esquire; and Sam Pointer with the University of Alabama at Birmingham Research Foundation, and we appreciate the direct efforts of Tina McKeon, Esquire and Janell Cleveland with Needle and Rosenberg in Atlanta, GA in preparing the provisional patent applications. We thank Preston Campbell, M.D. and Bonnie Ramsey, M.D. for helpful advice.

REFERENCES

- Davis, P. B., Drumm, M., and Konstan, M. W. (1996) *Am. J. Respir. Crit. Care Med.* **154**, 1229–1256
- Kunzelmann, K., and Mall, M. (2001) *Clin. Exp. Pharmacol. Physiol.* **28**, 857–867
- Zeitlin, P. L. (1999) *J. Clin. Invest.* **103**, 447–452
- Fuller, C. M., and Benos, D. J. (2000) *News Physiol. Sci.* **15**, 165–171
- Clarke, L. L., and Boucher, R. C. (1992) *Am. J. Physiol.* **263**, C348–C356
- Kellerman, D., Evans, R., Mathews, D., and Shaffer, C. (2002) *Adv. Drug Delivery Rev.* **54**, 1463–1474
- Knowles, M. R., Clarke, L. L., and Boucher, R. C. (1991) *N. Engl. J. Med.* **325**, 533–538
- Zsembery, A., Boyce, A. T., Liang, L., Peti-Peterdi, J., Bell, P. D., and Schwiebert, E. M. (2003) *J. Biol. Chem.* **278**, 13398–13408
- Clarke, L. L., Harline, M. C., Otero, M. A., Glover, G. G., Garrad, R. C., Krugh, B., Walker, N. M., Gonzalez, F. A., Turner, J. T., and Weisman, G. A. (1999) *Am. J. Physiol.* **276**, C777–C787
- Otero, M., Garrad, R. C., Velazquez, B., Hernandez-Perez, M. G., Camden, J. M., Erb, L., Clarke, L. L., Turner, J. T., Weisman, G. A., and Gonzalez, F. A. (2000) *Mol. Cell. Biochem.* **205**, 115–123
- Taylor, A. L., Schwiebert, L. M., Smith, J. J., King, C., Jones, J. R., Sorscher, E. J., and Schwiebert, E. M. (1999) *J. Clin. Invest.* **104**, 875–884
- North, R. A. (2002) *Physiol. Rev.* **82**, 1013–1067
- Zeitlin, P. L., Lu, L., Rhim, J., Cutting, G. R., Stetten, G., Kieffer, K. A., Craig, R., and Guggino, W. B. (1991) *Am. J. Respir. Cell Mol. Biol.* **4**, 313–319
- Gruenert, D. C., Basbaum, C. B., Welsh, M. J., Li, M., Finkbeiner, W. E., and Nadel, J. (1988) *Proc. Natl. Acad. Sci. U. S. A.* **85**, 5951–5955
- Tucker, T. A., Varga, K., Bebek, Z., Zsembery, A., McCarty, N. A., Collawn, J. F., Schwiebert, E. M., and Schwiebert, L. M. (2003) *Am. J. Physiol.* **284**, C791–C804
- Braunstein, G. M., Roman, R. M., Clancy, J. P., Kudlow, B. A., Taylor, A. L., Shylonsky, V. G., Jovov, B., Peter, K., Jilling, T., Ismailov, I. I., Benos, D. J., Schwiebert, L. M., Fitz, J. G., and Schwiebert, E. M. (2001) *J. Biol. Chem.* **276**, 6621–6630
- Negulyaev, Y. A., and Markwardt, F. (2000) *Neurosci. Lett.* **279**, 165–168
- Hershinkel, M., Moran, A., Grossman, N., and Sekler, I. (2001) *Proc. Natl. Acad. Sci. U. S. A.* **98**, 11749–11754
- Jan, C. R., Wu, S. N., and Tseng, C. J. (1999) *Naunyn-Schmiedeberg's Arch. Pharmacol.* **360**, 249–255
- McNulty, T. J., and Taylor, C. W. (1999) *Biochem. J.* **339**, 555–561
- Davies, P. A., Wang, W., Hales, T. G., and Kirkness, E. F. (2003) *J. Biol. Chem.* **278**, 712–717
- Colvin, R. A. (1998) *Neuroreport* **9**, 3091–3096
- Zitt, C., Halaszovich, C. R., and Luckhoff, A. (2002) *Prog. Neurobiol.* **66**, 243–264
- Uehara, A., Yasukochi, M., Imanaga, I., Nishi, M., and Takeshima, H. (2002) *Cell Calcium* **31**, 89–96
- Rychkov, G., Brereton, H. M., Harland, M. L., and Barritt, G. J. (2001) *Hepatology* **33**, 938–947
- Vennekens, R., Prenen, J., Hoenderop, J. G., Bindels, R. J., Droogmans, G., and Nilius, B. (2001) *Pflug. Arch. Eur. J. Physiol.* **442**, 237–242
- Nilius, B., Prenen, J., Vennekens, R., Hoenderop, J. G., Bindels, R. J., and Droogmans, G. (2001) *Br. J. Pharmacol.* **134**, 453–462
- Gryniewicz, G., Poenie, M., and Tsien, R. Y. (1985) *J. Biol. Chem.* **260**, 3440–3450
- Devor, D. C., Singh, A. K., Lambert, L. C., DeLuca, A., Frizzell, R. A., and Bridges, R. J. (1999) *J. Gen. Physiol.* **113**, 743–760
- Cuthbert, A. W., Supuran, C. T., and MacVinish, L. J. (2003) *J. Physiol.* **551**, 79–92
- Brady, K. G., Kelley, T. J., and Drumm, M. L. (2001) *Am. J. Physiol.* **281**, L1173–L1179
- Zeiber, B. G., Eichwald, E., Zabner, J., Smith, J. J., Puga, A. P., McCray, P. B. Jr., Capechi, M. R., Welsh, M. J., and Thomas, K. R. (1995) *J. Clin. Invest.* **96**, 2051–2064
- Torres, G. E., Egan, T. M., and Voigt, M. M. (1999) *J. Biol. Chem.* **274**, 6653–6659
- Hogstrand, C., Verboost, P. M., and Wendelaar Bonga, S. E. (1999) *Toxicology* **133**, 139–145
- Tarran, R., Loewen, M. E., Paradiso, A. M., Olsen, J. C., Gray, M. A., Argent, B. E., Boucher, R. C., and Gabriel, S. E. (2002) *J. Gen. Physiol.* **120**, 407–418
- Ostrom, R. S., Gregorian, C., and Insel, P. A. (2000) *J. Biol. Chem.* **275**, 11735–11739
- Guyot, A., and Hanrahan, J. W. (2002) *J. Physiol.* **545**, 199–206
- Ferrari, D., Munerati, M., Melchiorri, L., Hanau, S., Di Virgilio, F., and Baricordi, O. R. (1994) *Am. J. Physiol.* **267**, C886–C892
- Baricordi, O. R., Ferrari, D., Melchiorri, L., Chiozzi, P., Hanau, S., Chiari, E., Rubini, M., and Di Virgilio, F. (1996) *Blood* **87**, 682–690
- Camello, C., Pariente, J. A., Salido, G. M., and Camello, P. J. (1999) *J. Physiol.* **516**, 399–408
- Arnon, A., Hamlyn, J. M., and Blaustein, M. P. (2000) *Am. J. Physiol.* **278**, C163–C173
- Balzer, M., Lintschinger, B., and Groschner, K. (1999) *Cardiovasc. Res.* **42**,

- 543–549
43. Wiley, J. S., and Dubyak, G. R. (1989) *Blood* **73**, 1316–1323
44. Giovannucci, D. R., Bruce, J. I., Straub, S. V., Arreola, J., Sneyd, J., Shuttleworth, T. J., and Yule, D. I. (2002) *J. Physiol.* **540**, 469–484
45. Lansley, A. B., and Sanderson, M. J. (1999) *Biophys. J.* **77**, 629–638
46. Ma, W., Korngreen, A., Uzlaner, N., Priel, Z., and Silberberg, S. D. (1999) *Nature* **400**, 894–897
47. Fischer, H., Widdicombe, J. H., and Illek, B. (2002) *Am. J. Physiol.* **282**, C736–C743
48. Gabriel, S. E., Makhlina, M., Martsen, E., Thomas, E. J., Lethem, M. I., and Boucher, R. C. (2000) *J. Biol. Chem.* **275**, 35028–35033
49. Truong-Tran, A. Q., Carter, J., Ruffin, R., and Zalewski, P. D. (2001) *Immunol. Cell Biol.* **79**, 170–177
50. Novick, S. G., Godfrey, J. C., Pollack, R. L., and Wilder, H. R. (1997) *Med. Hypotheses* **49**, 347–357
51. Krebs, N. F., Westcott, J. E., Arnold, T. D., Kluger, B. M., Accurso, F. J., Miller, L. V., and Hambidge, K. M. (2000) *Pediatr. Res.* **48**, 256–261
52. Wang, K., Zhou, B., Kup, Y.-M., Zemansky, J., and Gitschier, J. (2002) *Am. J. Hum. Genet.* **7**, 66–73
53. Mossad, S. B. (2003) *QJM* **96**, 35–43
54. Mossad, S. B., Macknin, M. L., Medendorp, S. V., and Mason, P. (1996) *Ann. Intern. Med.* **125**, 81–88
55. Brewer, G. J. (1999) *J. Lab. Clin. Med.* **134**, 322–324
56. Widdicombe, J. H. (2002) *Am. J. Respir. Crit. Care Med.* **165**, 1566
57. Haidl, P., Schönhofe, B., Siemon, K., and Köhler, D. (2000) *Eur. Respir. J.* **16**, 1102–1108
58. Eschenbacher, W. L., Gross, K. B., Muench, S. P., and Chan, T. L. (1991) *Am. Rev. Respir. Dis.* **143**, 341–345

Original Paper

Investigation of the Inhibitory Effects of the Benzodiazepine Derivative, 5-BDBD on P2X₄ Purinergic Receptors by two Complementary Methods

Bernadett Balázs^a Tamás Dankó^a Gergely Kovács^{b,c} László Köles^d Matthias A. Hediger^{b,c} Ákos Zsembery^a

^aInstitute of Human Physiology and Clinical Experimental Research, Semmelweis University, Budapest;

^bInstitute of Biochemistry and Molecular Medicine, University of Bern; ^cSwiss National Centre of Competence in Research, NCCR TransCure, University of Bern; ^dDepartment of Pharmacology and Pharmacotherapy, Semmelweis University, Budapest

Key Words

Calcium influx • Electrophysiology • ATP • 5-BDBD • P2X receptors

Abstract

Background/Aims: ATP-gated P2X₄ purinergic receptors (P2X₄Rs) are cation channels with important roles in diverse cell types. To date, lack of specific inhibitors has hampered investigations on P2X₄Rs. Recently, the benzodiazepine derivative, 5-BDBD has been proposed to selectively inhibit P2X₄Rs. However, limited evidences are currently available on its inhibitory properties. Thus, we aimed to characterize the inhibitory effects of 5-BDBD on recombinant human P2X₄Rs. **Methods:** We investigated ATP-induced intracellular Ca²⁺ signals and whole cell ion currents in HEK 293 cells that were either transiently or stably transfected with hP2X₄Rs. **Results:** Our data show that ATP (< 1 μM) stimulates P2X₄R-mediated Ca²⁺ influx while endogenously expressed P2Y receptors are not activated to any significant extent. Both 5-BDBD and TNP-ATP inhibit ATP-induced Ca²⁺ signals and inward ion currents in a concentration-dependent manner. Application of two different concentrations of 5-BDBD causes a rightward shift in ATP dose-response curve. Since the magnitude of maximal stimulation does not change, these data suggest that 5-BDBD may competitively inhibit the P2X₄Rs. **Conclusions:** Our results demonstrate that application of submicromolar ATP concentrations allows reliable assessment of recombinant P2XR functions in HEK 293 cells. Furthermore, 5-BDBD and TNP-ATP have similar inhibitory potencies on the P2X₄Rs although their mechanisms of actions are different.

Copyright © 2013 S. Karger AG, Basel

Introduction

Extracellular ATP and its breakdown products regulate a number of cellular functions by stimulating purinergic receptors [1]. In the last two decades 19 different purinergic receptors have been identified including four adenosine-activated P1 receptors, seven ATP-gated P2X receptor (P2XR) channels and eight metabotropic P2Y receptors which can be stimulated by adenosine and uridine tri- and diphosphates [2].

The seven P2X receptor subunits (P2X₁₋₇) are widely distributed in both excitable and non-excitable cells providing cation permeable pathways (mainly for Ca²⁺ and Na⁺) through the plasma membrane. Previous studies revealed that these subunits might assemble as either homo- or heterotrimeric receptors [2]. Importantly, heteromerization can change functional and pharmacological properties of the P2XRs [2]. P2XRs are involved in presynaptic and postsynaptic actions of ATP [3-5] including taste sensation [6], hearing [7] and chemoreception [8]. P2XRs are also necessary for proper function of immune system [9]. In cardiovascular, respiratory, genitourinary and gastrointestinal systems several P2X receptor subunits seem to play pivotal role in both endothelial and epithelial cell functions [10]. Using pharmacological approaches and knockout animals, it has also become evident that P2XRs are involved in a broad range of pathophysiological processes such as chronic and inflammatory pain [11-15] arthritis [16] male infertility [17] and hypertension [18, 19].

A role for P2X₄ receptors has been proposed in neuropathic pain [15], endothelial NO production [18], regulation of airway ciliary epithelia [20] and chloride secretion of respiratory [21, 22] and biliary epithelia [23]. However, validation of P2X₄R involvement has been often hampered by the lack of specific inhibitors. In fact, P2X₄ receptors are insensitive to the nonselective inhibitors, such as suramin and PPADS [24]. TNP-ATP has been found as a putative antagonist of P2X₄ receptors. However, it blocks other P2X subtypes as well, such as P2X₁, P2X₂ and P2X₃ [25]. Furthermore, TNP-ATP has been shown to be a weak blocker of P2X₄ receptors (IC₅₀ = 15 μM for 10 μM ATP stimulation) compared to its inhibitory potency at P2X₁ and P2X₃ receptors [26].

The benzodiazepine derivative, 5-(3-bromophenyl)-1,3-dihydro-2H-benzofuro[3,2-e]-1,4-diazepin-2-one (5-BDBD), has been recently shown to selectively inhibit P2X₄ receptors (IC₅₀ ~ 0.5 μM) [27]. Nonetheless, these results are described in a patent and details of the experimental procedure are not available. So far, limited experience has been available with 5-BDBD and there is no consensus about its pharmacologically relevant concentration range. In some studies low micromolar (5-10 μM) concentrations were used [28, 29] whereas others applied significantly higher doses of 5-BDBD (30-100 μM) [30, 31].

In the present study, we investigated ATP-induced cytosolic Ca²⁺ signals and inward ion currents in HEK 293 cells transfected either transiently or stably with hP2X₄ receptors. We characterized P2X₄ receptor-mediated whole cell ion currents and identified P2YR- and P2XR-dependent calcium signals using electrophysiological and fluorescence ion measurement techniques, respectively. Despite endogenous expression of P2YRs we were able to discern P2XR-dependent Ca²⁺ signals stimulating the cells with submicromolar concentrations of ATP. We also assessed the inhibitory effects of 5-BDBD and TNP-ATP on both intracellular Ca²⁺ signals and inward ion currents. Our data suggest that 5-BDBD and TNP-ATP have similar inhibitory potencies on P2X₄Rs. Furthermore, we show that 5-BDBD functions as a competitive antagonist of hP2X₄Rs.

Materials and Methods

Materials

Cell culture medium, fetal bovine serum, cell culture supplements and antibiotics were purchased from Cseretex Inc. (Budapest, Hungary). TurboFect™ *in vitro* Transfection Reagent was purchased from Biocenter (Szeged, Hungary). Lipofectamine 2000 was obtained from Invitrogen (Life Technologies Europe B.V, Zug, Switzerland). Fluo-3/AM was purchased from Invitrogen Inc. (Carlsbad, CA). 5-BDBD was obtained

from Tocris Inc. (Minneapolis, USA). Calcium-5 was purchased from Molecular Devices (Molecular Devices LLC, Sunnyvale, CA, USA). Ivermectin (IVM) was obtained from Merck AG (Merck, Zug, Switzerland). All other chemicals were purchased from Sigma-Chemical (St. Louis, MO).

DNA Construct

The human P2X₄R (imaGenes GmbH, Berlin, Germany) was amplified from human cDNA with the following primer pair: 5'-TAT AAG ATC TCG CGG CCA TGG CGG GC-3',

5'-TAT AGA ATT CCC TGG TCC AGC TCA CTA GCA AGA CCC TGC-3'

The amplified product was subcloned into the pmCherry-N1 (Clontech Laboratories Inc.) vector by using BglII and EcoRI restrictions sites. Amino acid sequence of the human P2X₄ receptors fully corresponds to the isoform 3 described in gene database of the National Institute of Health.

Cell culture and establishment pmCherry-N1-hP2X₄ expressing HEK 293 cell clones

Human embryonic kidney (HEK) 293 cells were grown in plastic tissue culture flasks in DMEM/Ham's F-12 (1:1) medium supplemented with 5% fetal bovine serum, 100 U/ml penicillin and 100 µg/ml streptomycin at 37°C in a cell culture incubator supplied with 5% CO₂. Cells were subcultivated when confluency reached 90-95%. To establish pmCherry-N1-hP2X₄ expressing HEK 293 cell clones, cells plated the day before on poly-D-lysine coated 35 mm dish were transfected with 2 µg pmCherry-N1-hP2X₄ using 5 µl Lipofectamine 2000 per well as described in the manufacturer's protocol. Transfection medium was changed to antibiotic-free medium after 4 hours. On the following day the medium was then changed with selection antibiotic (G418) containing medium. From then on, the cells were kept in this selection medium. After a massive cell death of the non-transfected cells, surviving cells were trypsinized and replated in a 96-well plate at such a dilution that 1 cell/well density was obtained. After several days, colonies of cells displaying red fluorescence were selected as hP2X₄-expressing positive clones using fluorescence microscopy.

Transient transfection

Before the day of transfection, cells were plated on poly-D-lysine coated round glass coverslips (25 mm in diameter) at a density of 500,000 cells in 40 mm plastic Petri dishes. After 16-24 h, cells were transfected with 3 µg pmCherry-N1-hP2X₄ DNA and 5 µl of TurboFect™ transfection reagent in 200 µl of serum-free medium. Cells were subjected to experiments 16-48 h after transfection. The efficiency of transfection was 60-70%.

Cell surface biotinylation and western blotting

P2X₄ expressing HEK 293 cell clones were plated at 1.000.000 cell density into poly-D-lysine coated 60 mm dishes. 24 hours after plating, cells were rinsed with ice-cold PBS-Ca-Mg (PBS containing 0.1 mM CaCl₂ and 1 mM MgCl₂) followed by biotinylation of proteins at the plasma membrane with 1.5 mg/ml sulfo-NHS-LC-biotin in 10 mM triethanolamine (pH 7.4), 1 mM MgCl₂, 2 mM CaCl₂, and 150 mM NaCl for 90 minutes with horizontal shaking at 4°C. Next, excess biotin was quenched with PBS containing 1 mM MgCl₂, 0.1 mM CaCl₂, and 100 mM glycine for 20 minutes at 4°C, and then rinsed three times with PBS. Cells were finally lysed in lysis buffer for 30 minutes and lysates were cleared by centrifugation. Protein concentrations were determined by DC Protein Assay. Portion of cell lysates of equivalent amounts of protein (1.33 mg/ml) were equilibrated overnight with streptavidin agarose beads at 4°C. Beads were washed sequentially with solutions A [50 mM Tris-HCl (pH 7.4), 100 mM NaCl, and 5 mM EDTA] three times, B [50 mM Tris-HCl (pH 7.4) and 500 mM NaCl] twice, and C (50 mM Tris-HCl, pH 7.4) once. Biotinylated surface proteins were then released by heating to 95°C with 4x Laemmli buffer. Proteins from the intracellular fraction were also heated to 95°C for 5 minutes with 4x Laemmli buffer.

Samples were run on a 10% SDS gel with 40 µl protein loaded from the cytosolic protein (1 mg/ml) and the plasma membrane samples. Samples were transferred onto a PVDF membrane in Towbin's buffer using the semi-dry transfer method. Membranes were blocked with PBS containing 5% milk, 0.5% BSA and 0.02% NaN₃ at room temperature for 1 hour. Afterwards, samples were incubated in blocking solution containing the appropriate primary antibody (1:1000 for mouse anti-mCherry (Clontech, 632543)) at 4°C for overnight followed by three washes with PBST. HRP-conjugated goat anti-mouse antibody (1:4000, BioRad) was used as secondary antibody. After three consecutive washes with PBST and a final wash

with PBS, the enhanced chemiluminescence (ECL) method was used for detection. For loading control the membrane probed with anti-mCherry was stripped and blotted with avidin-HRP (1:1000, BioRad).

Histochemistry

After 24 hours of plating 400.000 P2X₄-expressing HEK 293 clonal cells into a 35 mm dish, cells were washed thoroughly with PBS. Next, cells were incubated with 0.1 mg/ml LC-sulfo-NHS(+)-biotin (Molbio) at room temperature for 1 hour followed by three washes with PBS. Thereafter, cells were fixed with 4% PFA at 37°C for 15 minutes. Cells were washed three times with PBS before staining with Streptavidin conjugated to Alexa 488 (1:4000 dilution, Invitrogen) at room temperature for one hour. After washing the cells four times with PBS, samples were mounted with CitiFluor AF2 (EMS). Images were captured with a Nikon C1 confocal laser scanning microscopy system equipped with Multiline Argon and HeNe lasers using 40x magnification.

Measurement of intracellular calcium levels

Transiently transfected HEK 293 cells were loaded with Fluo-3/AM (4μl) in standard extracellular solution for 45 min at room temperature. Fluorescence dye was dissolved in DMSO containing 20% Pluronic-F127. Additionally, the loading solution contained 1 mM probenecid to prevent dye leakage. After dye loading, cells were washed with standard extracellular solution. Standard extracellular solution contained (in mM): 145 NaCl, 5 KCl, 2 CaCl₂, 1 MgCl₂, 10 D-glucose and 10 HEPES, pH 7.4 (with NaOH). Nominally Ca²⁺-free solutions were prepared by simply omitting CaCl₂.

Measurements were performed with a Axiovert 200 M Zeiss LSM 510 Meta (Carl Zeiss, Jena, Germany) confocal laser scanning microscope equipped with a 20x Plan Apochromat (NA=0.80) DIC objective. For the excitation, 488-nm argon-ion laser was used. The emitted light was collected with BP 505-570 band pass filter. Data were obtained at a rate of 0.5 Hz. Changes in [Ca²⁺]_i are displayed as the percentage of fluorescence relative to the intensity at the beginning of each experiment. The baseline fluorescence (100 %) was calculated from the average fluorescence of ROIs while bathing the cells with standard extracellular solution. Background fluorescence was subtracted from fluorescence intensity by measuring a cell-free area on every coverslip. Agonists and antagonists were administered directly to the solution at the desired concentrations. All experiments were done at room temperature (22-24 °C).

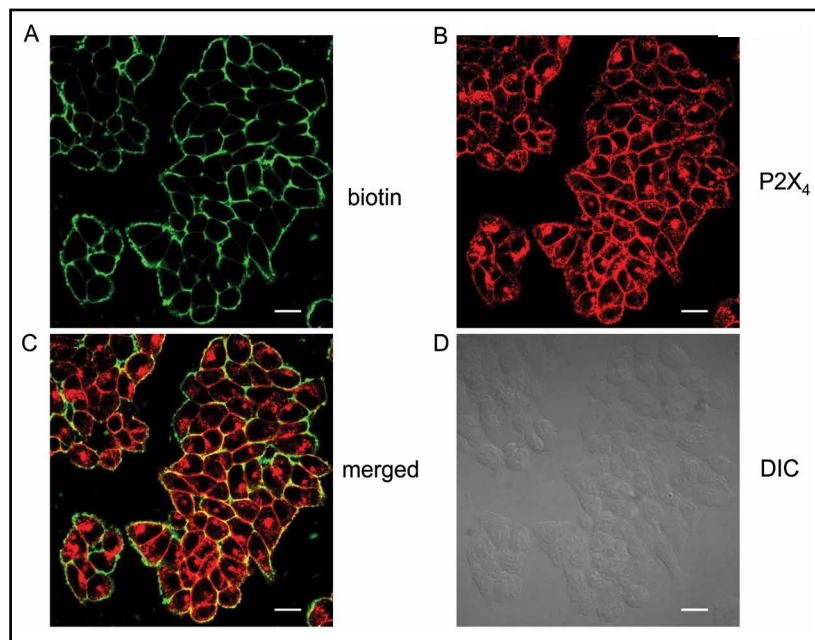
Fluorescence ion measurement experiments using FLIPRTetra

Cells were trypsinized and plated at 40,000 cells/well density in 100 μl volume onto 96-well black plates coated with 100μg/ml poly-D-lysine 36 hours before the experiments. HEK 293 cells were used for testing the effects of compounds on endogenous P2Y receptors; whereas P2X₄ activity was measured using P2X₄-expressing HEK 293 cell clones. 36 hours later the medium was replaced with 100 μl of loading buffer (modified Krebs buffer containing 117 mM NaCl, 4.8 mM KCl, 1 mM CaCl₂, 1 mM MgCl₂, 5 mM D-glucose, 10 mM HEPES, and Calcium-5 fluorescence dye). Cells were then incubated in the loading buffer at 37°C for one hour. Fluorescence calcium measurements were carried out using FLIPRTetra high-throughput, fluorescence microplate reader. Cells were excited using a 470-495 nm LED module, and the emitted fluorescence signal was filtered with a 515-575 nm emission filter. After establishment of a stable baseline, cells were incubated with the compounds for five minutes followed by the administration of ATP with or without the tested compounds.

Electrophysiology

Voltage-clamp recordings were carried out in the standard whole-cell configuration using an Axopatch 200B amplifier (Axon Instruments) [32]. Human P2X₄-expressing cells were selected using a Diaphot 300 inverted patch clamp microscope (Nikon) equipped with an epifluorescent attachment (Elektro-Optika, Érd, Hungary). Micropipettes were pulled by a P-97 Flaming-Brown type micropipette puller (Sutter Instrument) from borosilicate glass capillary tubes (Harvard Apparatus) and had a tip resistance of 3–6 MΩ when filled with pipette solution. Patch pipette filling solution contained (in mM): 135 KCl, 5 NaCl, 1 MgCl₂, 1 EGTA, 10 HEPES and an appropriate concentration of CaCl₂, to give free [Ca²⁺]_i = 0.1 μM. Free [Ca²⁺]_i was estimated using MaxChelator software (Stanford University, Palo Alto, USA). The pH was adjusted to 7.2 with KOH. Standard extracellular solution contained (in mM): 145 NaCl, 5 KCl, 2 CaCl₂, 1 MgCl₂, 10 D-glucose, 10 HEPES, pH 7.4 (with NaOH). Solutions were delivered by continuous perfusion with a gravity-fed delivery system. Antagonists were added to the bath solutions 3-5 min. prior to agonist application.

Fig. 1. Cellular localization of P2X₄Rs by immunohistochemistry. Panel A: Cell surface proteins stained with LC-sulfo-NHS(+)-biotin and streptavidin-Alexa488. Panel B: Fluorescence image of mCherry tagged P2X₄Rs in HEK 293 cells. Panel C: Merged image showing co-localization of P2X₄Rs and biotinylated cell surface proteins. Panel D: Differential interference contrast (DIC) image of the P2X₄Rs expressing cells. Scale bar represents 20 μ m.



Experiments were performed at a holding potential of -60 mV. Command protocols and data acquisition were controlled by pClamp 6.03 software (Axon Instruments). Capacitive currents were compensated with analog compensation. Series resistance was accepted if lower than five times the pipette tip resistance. Analog data were filtered at 1 kHz with a low-pass Bessel filter and digitized at 5 kHz using a Digidata 1200 interface board. Data were analyzed using Clampfit 6.03 and Microsoft Excel softwares. All experiments were performed at room temperature.

Data presentation

Areas under the curve (AUC) values were calculated using the trapezoidal rule, in the first 4 minutes following agonist application (SigmaPlot 12.0 software). To estimate P2X receptor function, non-expressing cell responses were subtracted from the AUC values obtained in P2X₄R expressing cells on the same coverslip.

Antagonist concentration-inhibition curves were obtained by using progressively increasing antagonist concentrations and a fixed agonist concentration close to the EC₅₀ unless otherwise stated. IC₅₀ values were calculated by least squares fitting to $I = I_0 / [1 + (IC_{50}/[Ant])^{-nH}]$, where I and I₀ represent peak responses in the presence and absence of antagonist at concentration [Ant].

Results were presented as means \pm SEM of n observations if not otherwise indicated. Statistical significance was determined using paired Student's t-test for parametric, whereas one-way ANOVA followed by Mann-Whitney U test for non-parametric variables. Differences were considered statistically significant when $p < 0.05$. Non-linear curve fitting was performed using the SigmaPlot 12.0 program.

Results

Localization and functional characterization of transfected hP2X₄ receptors in HEK 293 cells

In order to study the localization of transfected hP2X₄ receptors in HEK 293 cells we used immunohistochemical techniques. Co-localization of biotinylated cell surface proteins and mCherry fluorescent protein suggested the expression of P2X₄Rs in the plasma membrane (Fig. 1). Furthermore, cell surface biotinylation and western blotting were used to separate the cytosolic and membrane fractions of proteins in HEK 293 cells. The P2X₄-bound mCherry protein was detected at the plasma membrane and its expression was not altered by the presence of ivermectin (Fig. 2A). In control experiment we used avidin-HRP-conjugated antibody to confirm the localization of proteins in the membrane fraction (Fig. 2B).

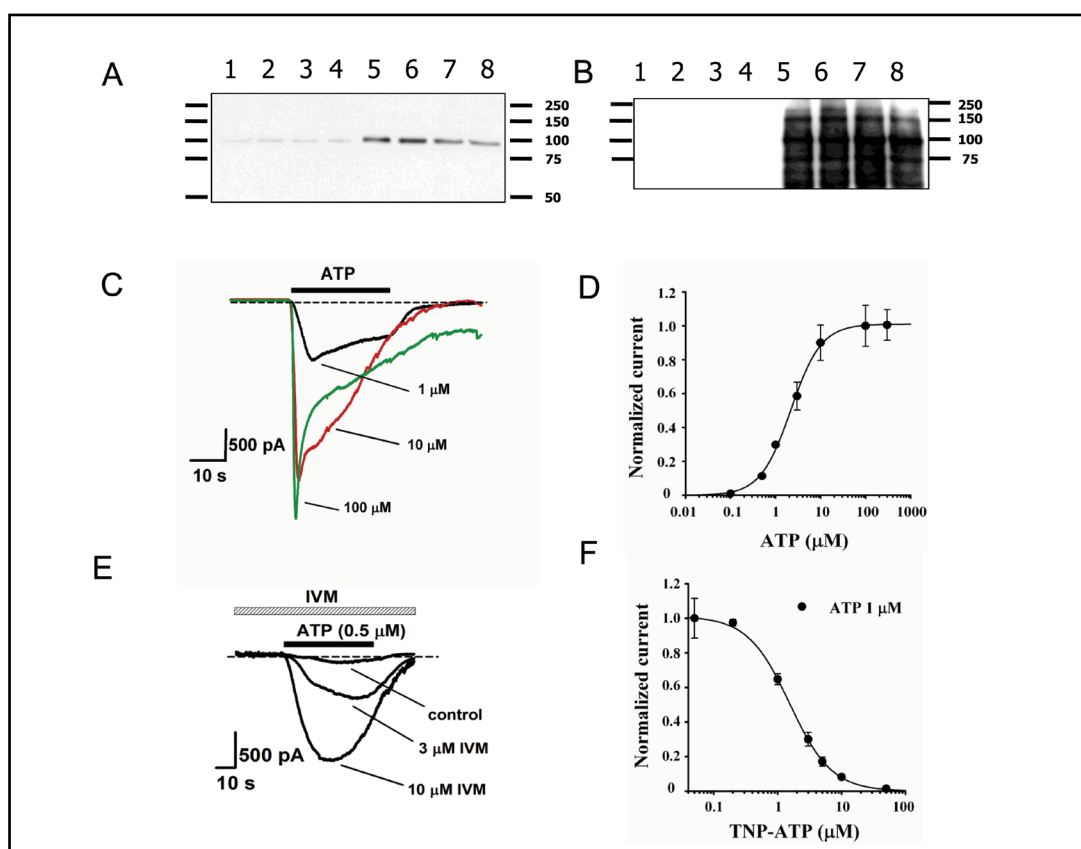


Fig. 2. Localization and functional characterization of transfected hP2X₄ receptors in HEK 293 cells. Panel A: Cytosolic and cell surface proteins were separated. Human P2X₄Rs are expressed both in cytosolic (lanes 1-4) and plasma membrane (lanes 5-8) fractions of proteins. Lane 1 and 5 indicate unstimulated cells, lanes 2 and 6 DMSO-pretreated (1:1000) cells, lanes 3 and 7 IVM-pretreated (10 μM) cells and lanes 4 and 8 IVM-pretreated (20 μM) cells. Panel B: In control experiments we obtained protein expression only in cell surface fraction (lanes 5-8) using avidin-HRP. Panel C: Representative traces showing ATP-induced inward currents in the absence; and panel E: presence of ivermectin (IVM). Panel D: Concentration-responses to ATP (0.1-300 μM) are shown. Panel F: Concentration-inhibitions to TNP-ATP (0.05-50 μM) in ATP-stimulated (1 μM) cells are shown. Values are means ± SEM. The error bars are not always visible due to the small SEM values. Experiments at each concentration were performed at least 3 times.

To functionally characterize the plasma membrane localized hP2X₄ receptors we measured whole cell currents in transfected HEK 293 cells. ATP (0.1-300 μM) elicited increasing maximal current amplitudes in cells expressing P2X₄Rs (Fig. 2C and D). The agonist concentration-response curve for ATP were fit with the Hill-equation; $E = E_{\max} [1 + (EC_{50}/[A])^{nH}]^{-1}$ where E stands for the peak current evoked by agonist concentration $[A]$, E_{\max} is the peak current evoked by a maximal agonist concentration, EC_{50} is the concentration giving half the maximal current, and nH represents the Hill coefficient. Our results showed that the EC_{50} value of ATP was 2.1 μM (Fig. 2D). Cells lacking P2X₄ expression failed to respond to ATP (100 μM) (data not shown). To confirm the role of P2X₄Rs in ATP-induced inward currents we pretreated the cells with ivermectin (IVM) (3 and 10 μM). As expected, IVM potentiated currents induced by ATP (0.5 μM) in a concentration-dependent manner (Fig. 2E). In addition, we tested the effects of TNP-ATP on ATP-induced (1 μM) currents. Under these conditions, we found that the half-maximal inhibitory concentration (IC_{50}) of TNP-ATP was 1.5 μM (Fig. 2F). These data show the plasma membrane localized hP2X₄ receptors are fully functional in transfected HEK 293 cells.

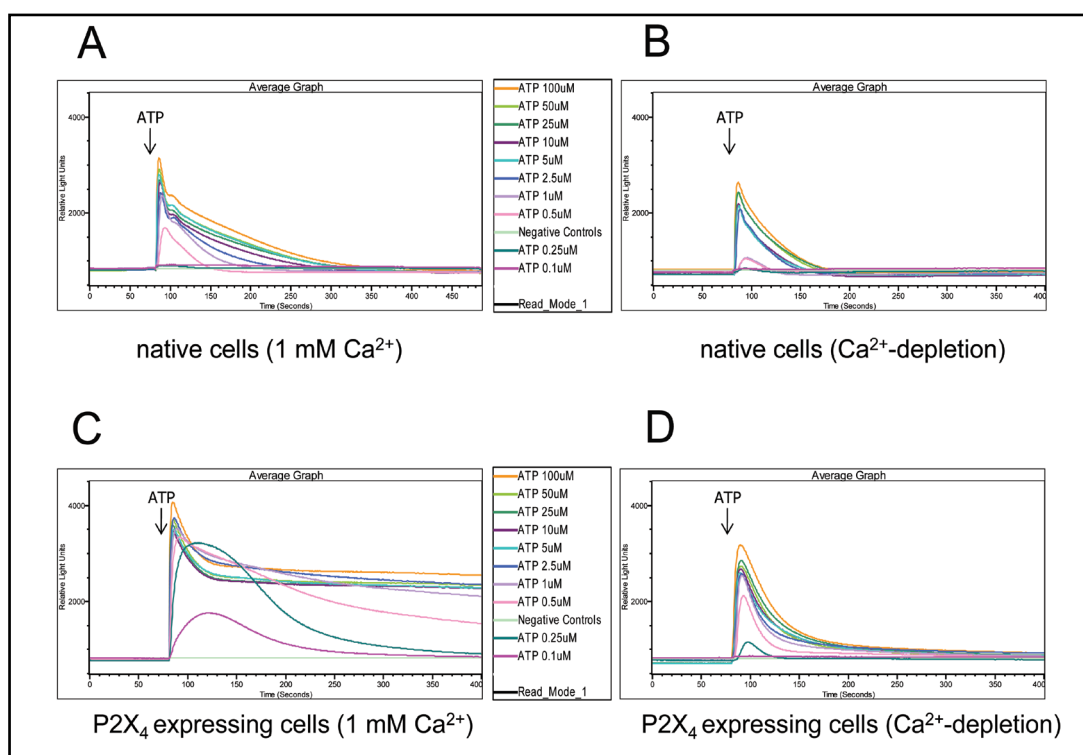


Fig. 3. ATP-induced changes of cytosolic calcium concentration measured using FLIPRTetra. Panels A and B: Administration of extracellular ATP induced dose-dependent, similar transient changes of cytosolic calcium in HEK 293 cells in the presence or absence of extracellular calcium. Panel C: In contrast, in HEK 293 cells stably expressing hP2X₄ ATP-induced sustained calcium response in the presence of extracellular calcium. Panel D: whereas in calcium-free buffer the responses were similar to the ones obtained in non-transfected cells. Average tracings of 6 individual experiments are shown.

ATP-induced Ca²⁺ influx is inhibited by 5-BDBD in cells stably expressing P2X₄Rs

In native HEK 293 cells ATP (0.1–100 μM) caused transient increases in cytosolic calcium concentrations whereas lower doses of the agonist (0.1–0.25 μM) elicited no change in calcium levels (Fig. 3A). In nominally calcium-free buffer ATP (0.1–100 μM) caused similar effects suggesting that the calcium signal was due to P2Y receptor-dependent Ca²⁺ release from the intracellular stores (Fig. 3B). Although the presence of external Ca²⁺ prolonged ATP-induced calcium signals, sustained responses could not be observed (Fig. 3A). Next, we studied ATP-induced Ca²⁺ signals in HEK 293 cell clones stably expressing P2X₄Rs (see methods). In these cells ATP (0.1–0.25 μM) elicited changes in Ca²⁺ concentrations that were abolished in Ca²⁺-depleted medium indicating that Ca²⁺ entered the cells from the extracellular space (Fig. 3C and D). In addition, higher concentrations of ATP (≥ 1 μM) caused sustained Ca²⁺ signals (Fig. 3C). Importantly, the P2X₄ receptor-specific positive allosteric modulator IVM (20 μM) potentiated the ATP-induced (0.25 μM) Ca²⁺ entry ($AUC_{ATP} = 852 \pm 47$; $n=5$ vs. $AUC_{ATP+IVM} = 1026 \pm 46$; $n=5$; $p<0.05$). These data indicate that using low concentrations of ATP (≤ 0.25 μM) allows assessment of P2X₄R-mediated Ca²⁺ signals independent of P2Y receptor activation. Thus, we next studied the effects of the benzodiazepine derivative 5-BDBD in the presence of 0.25 μM ATP. Under these conditions 5-BDBD (2–20 μM) significantly inhibited P2X₄R-mediated Ca²⁺ entry (Fig. 4A). We obtained similar inhibitory effects of 5-BDBD when cells were stimulated by 0.5 μM ATP (Fig. 4B). Regardless of ATP concentrations used, 5-BDBD (1–20 μM) had no effects in native HEK 293 cells suggesting that endogenously expressed P2Y receptors were not inhibited (data not shown).

Fig. 4. 5-BDBD inhibited the ATP-induced Ca²⁺ signals in HEK 293 cells stably expressing hP2X₄ receptors. Panels A and B: Concentration-dependent inhibition of Ca²⁺ signals by 5-BDBD when cells were stimulated with 0.25 μM and 0.5 μM ATP. Values are means ± SD. Each experiment was performed at least 4 times. A.U. means arbitrary units. *p<0.05 and **p<0.005 vs. ATP positive controls (ANOVA).

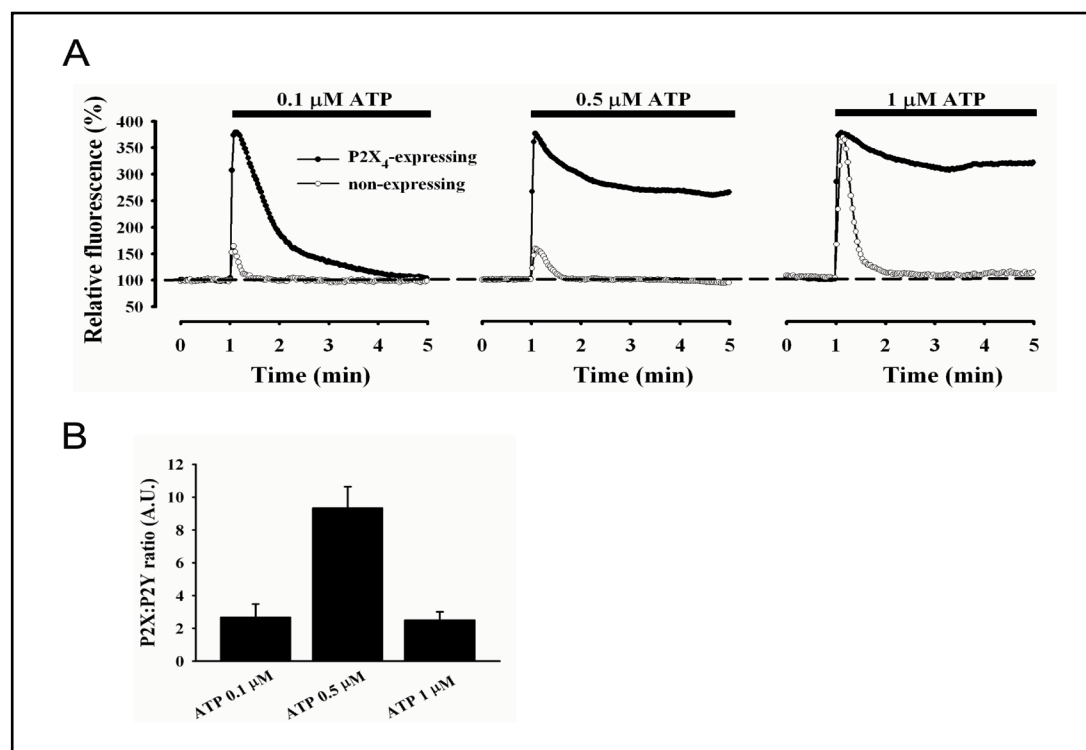
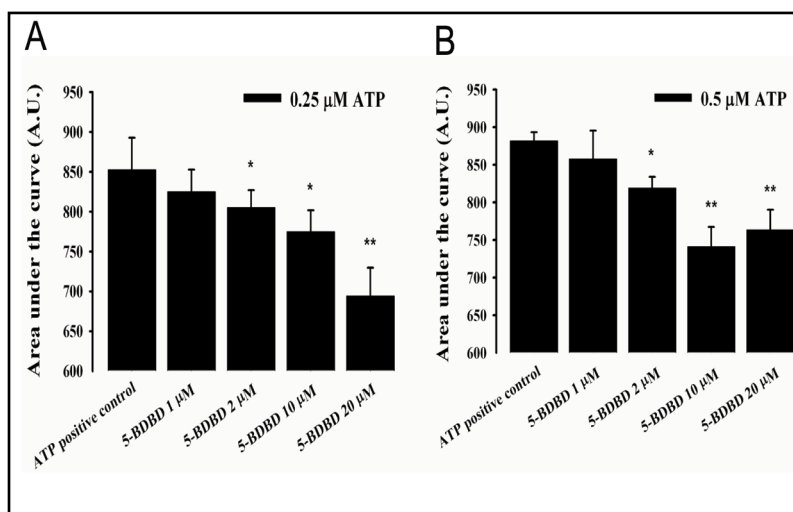
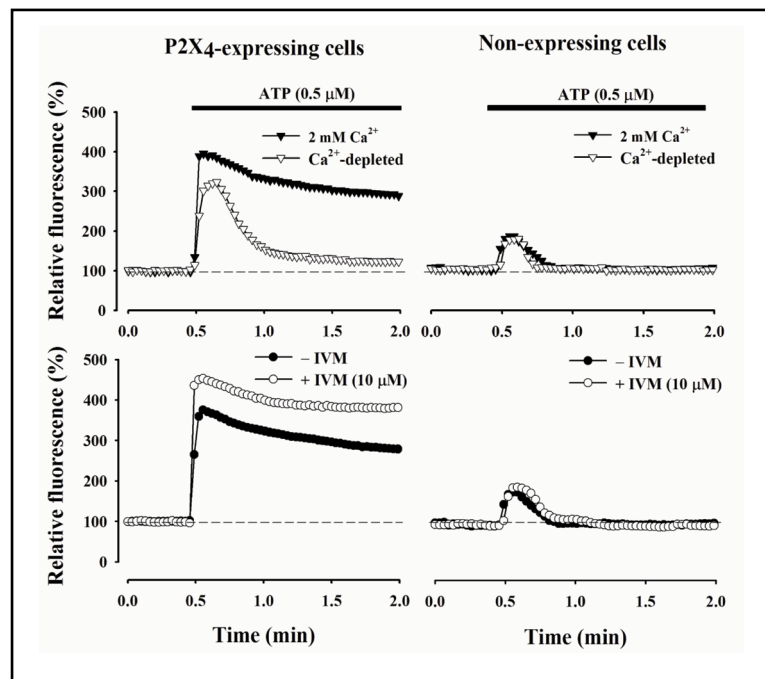


Fig. 5. ATP induced concentration-dependent changes in [Ca²⁺]_i in hP2X₄-expressing and non-expressing HEK 293 cells. Panel A: Representative traces showing the effects of different ATP concentrations (0.1–1 μM) on [Ca²⁺]_i. Each experiment was performed at least 5 times; Panel B: P2XR: P2Y-mediated Ca²⁺ response ratios are shown at different ATP concentrations. P2YR-mediated responses were estimated by the amplitude of cytosolic Ca²⁺ peaks while P2XR-mediated responses were assessed by “area under the curve” (AUC) values referring to the sustained nature of the Ca²⁺ signal. S.E.M. values are not shown for the representative traces because they were within 10% of the mean. A.U. means arbitrary units.

Single cell calcium imaging in cells transiently expressing P2X₄Rs

Single cell calcium imaging has been shown to provide an alternative method for the assessment of P2X receptor channel activity [33]. Therefore, we also studied the ATP-induced intracellular Ca²⁺ signals at the single cell level. In order to conduct simultaneous measurements of cytosolic Ca²⁺ levels in P2X₄R-expressing and non-expressing cells, we used

Fig. 6. Top panels: ATP induced changes in $[Ca^{2+}]_i$ in Ca^{2+} -containing or Ca^{2+} -depleted medium. Bottom panels: Ivermectin (IVM) potentiated the ATP-induced Ca^{2+} signal only in hP2X₄-expressing cells.



the transient transfection method. First, we identified the extracellular ATP concentration at which P2XR:P2YR-mediated Ca^{2+} response ratio was the highest. The P2YR-mediated responses were estimated by the amplitude of cytosolic Ca^{2+} peaks while P2XR-mediated responses were assessed by “area under the curve” (AUC) values referring to the sustained nature of the Ca^{2+} signal. In cells lacking P2X₄R expression, administration of 0.1 μ M and 0.5 μ M ATP evoked small peak increases without sustained Ca^{2+} signals (Fig. 5A). In cells expressing P2X₄Rs, the magnitude of Ca^{2+} peaks induced by 0.1 μ M and 0.5 μ M ATP were significantly higher than in non-expressing cells. However, robust Ca^{2+} plateau was induced only by 0.5 μ M ATP (Fig. 5A). Further increasing ATP concentrations (1 μ M), a considerable rise in cytosolic Ca^{2+} peak was observed in cells lacking P2X₄R expression. In contrast, the sustained component of the Ca^{2+} signal induced by 1 μ M ATP did not significantly differ from that elicited by 0.5 μ M ATP in P2X₄R expressing cells (Fig. 5A). Consequently, as P2XR:P2YR-mediated Ca^{2+} response ratio was the highest at 0.5 μ M ATP (Fig. 5B), in subsequent experiments this concentration was chosen to investigate single cell Ca^{2+} signals. To demonstrate that extracellular Ca^{2+} was necessary for ATP-induced sustained Ca^{2+} signal in cells expressing P2X₄Rs, we repeated the experiments in Ca^{2+} -depleted medium. Under these circumstances, the Ca^{2+} signal was only transient suggesting that Ca^{2+} entry was due to functional expression of P2X₄Rs (Fig. 6). In cells lacking P2X₄R expression, external Ca^{2+} did not influence the ATP-induced transient nature of cytosolic Ca^{2+} signal (Fig. 6). These data excluded the possibility that store-operated calcium channels played significant role in Ca^{2+} entry when cells were stimulated with 0.5 μ M ATP. To further characterize the sustained Ca^{2+} signal, we pretreated the cells with IVM (10 μ M) 5 min prior the application of ATP. Our results showed that ATP-induced Ca^{2+} plateau was significantly elevated in P2X₄R expressing but not in non-expressing cells (Fig. 6).

Next, we tested the effects of 5-BDBD on ATP-induced (0.5 μ M), P2X₄R-mediated Ca^{2+} entry. Sustained Ca^{2+} signals were diminished in cells pretreated with different concentrations of 5-BDBD (0.5–20 μ M). We observed 50% reduction of the AUC values in the presence of approx. 2 μ M 5-BDBD (Fig. 7A). We also studied inhibitory effects of TNP-ATP which was reported as a putative antagonist of P2X₄Rs [25]. As shown in Figure 7B, TNP-ATP (0.5–50 μ M) reduced ATP-induced (0.5 μ M) sustained Ca^{2+} signal in a concentration-dependent manner. Taken together, these data indicate that ATP-induced sustained Ca^{2+} signals were inhibited by both 5-BDBD and TNP-ATP in HEK 293 cells transfected with P2X₄Rs.

Fig. 7. Both 5-BDBD and TNP-ATP inhibited the ATP-induced Ca²⁺ signals in HEK 293 cells transiently transfected with hP2X₄ receptors. Panels A and B: Concentration-dependent inhibition of the ATP-induced Ca²⁺ response by 5-BDBD (0.5–20 μM); and TNP-ATP (0.5–50 μM). The number of independent experiments is indicated in parenthesis beneath the columns.

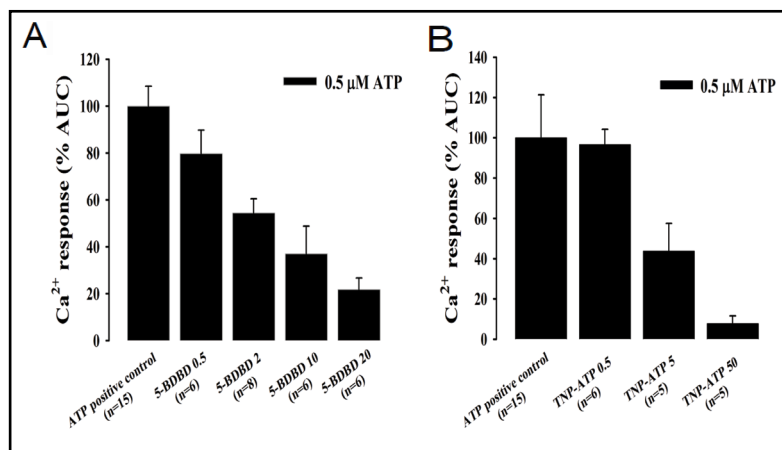
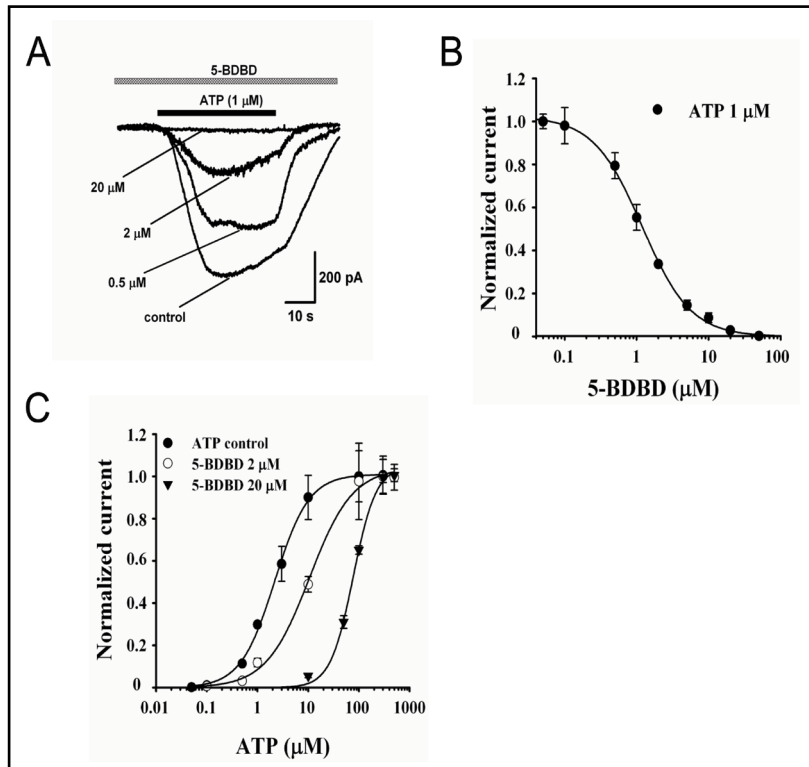


Fig. 8. 5-BDBD competitively inhibited the ATP-induced whole cell inward ion currents in HEK 293 cells transiently expressing hP2X₄ receptors. Panel A: Representative original traces showing the inhibitory effects of 5-BDBD at various concentrations. Panel B: Concentration-dependent inhibition of 5-BDBD (0.1–50 μM) in ATP-stimulated (1 μM) cells are shown. Panel C: Concentration-dependent responses to ATP (0.1–300 μM) in cells that were pretreated with 2 or 20 μM 5-BDBD. The rightward shift of the ATP control curve and the unchanged maximal



stimulation suggest that 5-BDBD competitively inhibited the P2X₄ receptor channels. In the absence of 5-BDBD the Hill coefficient was 1.26. In the presence of 2 μM and 20 μM 5-BDBD nH values were 1.11 and 2.17, respectively. Values are means ± SEM. The error bars are not always visible due to the small SEM values. Experiments at each concentration were performed at least 3 times.

P2X₄ receptor channels are competitively inhibited by 5-BDBD

Data presented in this paper show that 5-BDBD inhibited the P2X₄R-mediated Ca²⁺ entry in both stably and transiently transfected HEK 293 cells (see above). Nonetheless, during measurements of intracellular Ca²⁺ concentrations activation of endogenous P2YRs and/or ion transporters that eliminate Ca²⁺ from the cytosol (i.e. plasma membrane Ca²⁺-ATPase, sarcoplasmic reticulum Ca²⁺-ATPase) might possibly interfere with the effectiveness of 5-BDBD. Therefore, we also tested the inhibitory effects of 5-BDBD in HEK 293 cells using the whole cell configuration of the patch clamp technique. We stimulated the cells with 1 μM

ATP (close to EC₃₀ of ATP) because higher concentrations of the agonist induced premature cell damage in a number of experiments. Under these circumstances, 5-BDBD (0.1–50 μM) dose-dependently inhibited P2X₄R-mediated inward currents (I_{control} : 1239 ± 105 pA, n=8 vs. $I_{0.5\mu\text{M}}$: 983 ± 148 pA, n=4 vs. $I_{2\mu\text{M}}$: 417 ± 33, n=4 vs. $I_{20\mu\text{M}}$: 13 ± 1 pA, n=4) with an IC₅₀ of 1.2 μM (Fig. 8A and B). To investigate whether the inhibitory effect of 5-BDBD was due to competitive or allosteric interaction with P2X₄Rs, we performed additional electrophysiological experiments. Application of two different concentrations of 5-BDBD (2 μM and 20 μM) caused a rightward shift in ATP dose-response curve (from EC₅₀ = 2.1 μM to 11.2 μM and 79.2 μM, respectively, using non-linear regression analysis). Since the magnitude of maximal stimulation did not change, these data suggest that 5-BDBD competitively inhibited the P2X₄Rs (Fig. 8C).

Discussion

P2X₄ receptors are involved in important physiological and pathophysiological functions such as afferent signalling, chronic pain and autocrine/paracrine communications of endothelial and epithelial cells. In these processes, investigations on the role of P2X₄Rs are often hindered by lack of selective inhibitors. In recent years, considerable efforts have been made to discover novel effective antagonists of P2X₄Rs. Although the benzodiazepine derivative 5-BDBD has been recently proposed to selectively block P2X₄Rs [27], only limited experiences have been available concerning its inhibitory properties [28–31]. Moreover, to the best of our knowledge, there are no previous studies attempting to compare the inhibitory effects of 5-BDBD using both electrophysiological and intracellular calcium measurements. Therefore, we aimed to investigate the inhibitory potency of 5-BDBD on P2X₄R-dependent Ca²⁺ entry. Our data provide evidence for competitive though moderate inhibitory effects of 5-BDBD. Depending on experimental conditions the degree of inhibition varied significantly. In patch clamp experiments, assessing the effects of 5-BDBD directly on its target protein, we obtained the strongest inhibition. In intracellular calcium measurements, 5-BDBD exhibited more robust effects in transiently transfected cells. This was probably due to both the higher level of P2X₄R expression and the single cell calcium measurements. However, it is important to emphasize that AUC values are not in a linear fashion with [Ca²⁺]_i and quantitative analyses of fluorometric Ca²⁺ assay may provide only a rough orientation.

Despite the endogenous expression of at least three different P2Y receptor subtypes [34, 35] HEK 293 cells are frequently used to study properties of P2X receptors [34, 36]. To assess the role of P2XRs in inducing changes of intracellular Ca²⁺ concentrations, some investigators often choose cell lines (i.e. excitable mouse immortalized gonadotropin-releasing hormone-secreting cells (GT1) and human astrocytoma cells (1321N1)) that are lacking P2Y receptors [33, 37]. Stojilkovic and his colleagues transfected both GT1 and HEK 293 cells with different P2X subtypes and compared ATP-induced Ca²⁺ signals. They concluded that intracellular Ca²⁺ measurements could be used for the characterization of P2X receptors only in GT1 but not in HEK 293 cells because activation of endogenously expressed P2Y receptors interferes with P2X receptor-mediated Ca²⁺ signals [33]. This is indeed the case when HEK 293 cells are stimulated with high concentrations of ATP (>10 μM). Nonetheless, here we propose an alternative approach to investigate P2XR functions in HEK 293 cells applying low doses of agonist. In the present study, we show that submicromolar concentrations of ATP (≤ 0.25 μM) cause changes in intracellular Ca²⁺ concentrations solely in P2X₄R expressing cells. The ATP-induced increase in Ca²⁺ concentrations was further enhanced by pretreatment with ivermectin and was completely abolished in Ca²⁺-depleted medium suggesting that P2X₄Rs were involved in Ca²⁺ influx. Furthermore, we found that higher doses of ATP (≥1 μM) prolonged the duration of Ca²⁺ signals in native HEK 293 cells. These effects were abolished in Ca²⁺-depleted medium suggesting the activation of P2X₄R-independent Ca²⁺ influx mechanisms. The significantly higher initial phase of Ca²⁺ response in P2X₄R expressing cells compared to native cells was probably due to the fact that we used

nominally Ca²⁺ free solutions. Nonetheless, according to our previous experience, we could not add calcium chelators because HEK 293 cells require extracellular Ca²⁺ to remain attached to the coverslip. We assume that, as a result of P2Y receptor-dependent Ca²⁺ release, store-operated Ca²⁺ entry could contribute to the overall Ca²⁺ signal when cells are stimulated with higher concentrations of ATP (>1 μM). Therefore, our results suggest that when sufficiently low ATP concentrations are applied, measurement of intracellular Ca²⁺ concentrations is a useful approach to assess properties of P2XR in HEK 293 cells.

Considering the fact that Ca²⁺ measurement in stably transfected cells did not allow concurrent investigations of the P2X₄R-expressing and non-expressing cells, we also performed single cell calcium measurements in transiently transfected HEK 293 cells. Thus, we could simultaneously measure ATP-induced Ca²⁺ signals in P2X₄R-expressing and non-expressing cells on the same coverslip. Our data suggest that up to the concentration of 0.5 μM, ATP causes only small transient changes in Ca²⁺ concentration whereas 1 μM ATP significantly enhances the signal amplitude in non-expressing cells. This phenomenon was probably due to the gradual activation of different endogenous P2Y receptor subtypes [35].

To our surprise, we found that amplitudes of ATP-induced Ca²⁺ signals were significantly higher in P2X₄R-expressing than in non-expressing cells when experiments were performed in Ca²⁺-depleted medium (Fig. 6). Since we obtained similar results in stably transfected cells as well, we speculate that the difference was due to P2X₄R-mediated Ca²⁺ entry rather than additional release of Ca²⁺ from the internal stores. High levels of P2X₄R-expression and lack of Ca²⁺-chelation could both contribute to the Ca²⁺ entry. Furthermore, our data show that IVM enhances the ATP-induced Ca²⁺ entry only in P2X₄R-expressing cells. In accordance with previous observations, IVM potentiated ATP-induced Ca²⁺ entry but did not increase surface expression of P2X₄Rs [38, 39].

Our electrophysiological data confirmed the presence of functional P2X₄Rs in transiently transfected HEK 293 cells. ATP caused IVM-sensitive activation of inward currents in P2X₄R-expressing but not in non-expressing cells. We found EC₅₀ value of ATP close to what was previously reported [26]. However, it is noteworthy that, in some experiments ATP-stimulated currents exhibited incomplete recovery following withdrawal of the agonist when its concentration was higher than 1 μM. This was probably due to the high level of P2X₄R expression and massive Ca²⁺ influx which could consequently cause cellular damage. Therefore, inhibitory properties of both TNP-ATP and 5-BDBD were tested at 1 μM ATP stimulation.

Activation of P2X₄Rs plays a key role in the pathogenesis of neuropathic pain [15]. In an attempt to mitigate the neuropathic pain Inoue and his colleagues investigated the possible role of antidepressants as inhibitors of P2X₄Rs [37]. They found that paroxetine inhibited P2X₄Rs dose-dependently. Paroxetine behaved as a noncompetitive antagonist with IC₅₀ values of 2.5 μM and 1.9 μM for rat and human P2X₄Rs, respectively. Interestingly, inhibitory effects of paroxetine were significantly stronger on rat P2X₄Rs than that of TNP-ATP [37]. It is known that TNP-ATP is more than 1,000-fold more potent in blocking P2X₁ and P2X₃ than P2X₄ receptors [24]. Nonetheless, TNP-ATP has been used as P2X₄ antagonist in a number of studies [40, 41]. Our data also demonstrate that TNP-ATP inhibits both intracellular Ca²⁺ signals and inward ion currents induced by ATP. We found that TNP-ATP had an IC₅₀ value of 1.5 μM for 1 μM ATP stimulation which was comparable with previous observations [25]. Noncompetitive antagonism of TNP-ATP at the P2X₃Rs suggests similar mechanisms of action at P2X₄Rs as well [25].

Recently, 5-BDBD has been proposed to selectively inhibit P2X₄Rs [27]. Since then 5-BDBD has been used in a number of studies with contradictory results [28-31]. It has weak potency to inhibit recombinant human P2X₄Rs [28] or native P2X₄Rs in vascular endothelial cells (IC₅₀ ~ 30 μM) [30]. In contrast, P2X₄Rs were potently blocked by 10 μM 5-BDBD in prechondrogenic cell line [29]. Here we report that 5-BDBD and TNP-ATP have similar inhibitory potencies at recombinant human P2X₄Rs expressed in HEK 293 cells. Our data suggest that 5-BDBD may competitively inhibit the P2X₄Rs. However, we cannot exclude the possibility that 5-BDBD decreases the ligand-binding affinity of the channels. Such allosteric

alterations of ATP-binding affinity have been previously reported for P2X receptors [42, 43].

In conclusion, the present study demonstrates that intracellular measurement of Ca²⁺ concentration in HEK 293 cells could be a useful method to investigate pharmacological properties of P2X receptor antagonists provided that submicromolar concentrations of ATP are used. 5-BDBD and TNP-ATP have similar inhibitory potencies at human recombinant P2X₄Rs. Our data show that 5-BDBD shifts the ATP concentration-response curve to the right. This feature differs from the previously described noncompetitive behavior of other P2X₄R antagonists such as TNP-ATP and paroxetine.

Acknowledgements

This work was supported by the OTKA K79189 grant and Swiss National Science Foundation (SNSF) through the National Centre of Competence in Research (NCCR) TransCure (website: <http://www.transcure.org>). The authors thank Péter Várnai and Dániel Tóth for their help to create the pmCherry-N1-hP2X₄ construct.

References

- 1 Schwiebert EM, Zsembery A: Extracellular ATP as a signaling molecule for epithelial cells, *Biochim Biophys Acta* 2003;1615:7-32.
- 2 Burnstock G, Fredholm BB, North RA, Verkhratsky A: The birth and postnatal development of purinergic signalling. *Acta Physiol* 2010;199:93-147.
- 3 Jo YH, Role LW: Coordinate release of ATP and GABA at in vitro synapses of lateral hypothalamic neurons. *J Neurosci* 2002;22:4794-4804.
- 4 Sim JA, Chaumont S, Jo J, Ulmann L, Young MT, Cho K, Buell G, North RA, Rassendren F: Altered hippocampal synaptic potentiation in P2X₄ knock-out mice. *J Neurosci* 2006;26:9006-9009.
- 5 Khakh BS, Kennedy C: Adenosine and ATP: Progress in their receptors' structures and functions. *Trends Pharmacol Sci* 1998;19:39-41.
- 6 Roper SD: Signal transduction and information processing in mammalian taste buds. *Pflugers Arch* 2007;454:759-776.
- 7 Housley GD, Marcotti W, Navaratnam D, Yamoah EN: Hair cells--beyond the transducer. *J Membr Biol* 2006;209:89-118.
- 8 Rong W, Gourine AV, Cockayne DA, Xiang Z, Ford AP, Spyer KM, Burnstock G: Pivotal role of nucleotide P2X₂ receptor subunit of the ATP-gated ion channel mediating ventilatory responses to hypoxia. *J Neurosci* 2003;23:11315-11321.
- 9 Di Virgilio F: Purinergic signalling in the immune system. A brief update. *Purinergic Signal* 2007;3:1-3.
- 10 Surprenant A, North RA: Signaling at purinergic P2X receptors. *Annu Rev Physiol* 2009;71:333-359.
- 11 Barclay J, Patel S, Dorn G, Wotherspoon G, Moffatt S, Eunson L, Abdel'al S, Natt F, Hall J, Winter J, Bevan S, Wishart W, Fox A, Ganju P: Functional downregulation of P2X₃ receptor subunit in rat sensory neurons reveals a significant role in chronic neuropathic and inflammatory pain. *J Neurosci* 2002;22:8139-8147.
- 12 Cockayne DA, Dunn PM, Zhong Y, Rong W, Hamilton SG, Knight GE, Ruan HZ, Ma B, Yip P, Nunn P, McMahon SB, Burnstock G, Ford AP: P2X₂ knockout mice and P2X₂/P2X₃ double knockout mice reveal a role for the P2X₂ receptor subunit in mediating multiple sensory effects of ATP. *J Physiol* 2005;567:621-639.
- 13 Coull JA, Beggs S, Boudreau D, Boivin D, Tsuda M, Inoue K, Gravel C, Salter MW, De Koninck Y: BDNF from microglia causes the shift in neuronal anion gradient underlying neuropathic pain. *Nature* 2005;438:1017-1021.
- 14 Chizh BA, Illes P: P2X receptors and nociception. *Pharmacol Rev* 2001;53:553-568.
- 15 Tsuda M, Shigemoto-Mogami Y, Koizumi S, Mizokoshi A, Kohsaka S, Salter MW, Inoue K: P2X₄ receptors induced in spinal microglia gate tactile allodynia after nerve injury. *Nature* 2003;424:778-783.
- 16 Labasi JM, Petrushova N, Donovan C, McCurdy S, Lira P, Payette MM, Brissette W, Wicks JR, Audoly L, Gabel CA: Absence of the P2X₇ receptor alters leukocyte function and attenuates an inflammatory response. *J Immunol* 2002;168:6436-6445.
- 17 Mulryan K, Gitterman DP, Lewis CJ, Vial C, Leckie BJ, Cobb AL, Brown JE, Conley EC, Buell G, Pritchard CA, Evans RJ: Reduced vas deferens contraction and male infertility in mice lacking P2X₁ receptors. *Nature* 2000;403:86-89.

- 18 Yamamoto K, Korenaga R, Kamiya A, Qi Z, Sokabe M, Ando J: P2X₄ receptors mediate ATP-induced calcium influx in human vascular endothelial cells. *Am J Physiol Heart Circ Physiol* 2000;279:H285-292.
- 19 Yamamoto M, Jin JJ, Wu Z, Abe M, Tabara Y, Nagai T, Yamasaki E, Igase M, Kohara K, Miki T, Nakura J: Interaction between serotonin 2A receptor and endothelin-1 variants in association with hypertension in Japanese. *Hypertens Res* 2006;29:227-232.
- 20 Ma W, Korngreen A, Weil S, Cohen EB, Priel A, Kuzin L, Silberberg SD: Pore properties and pharmacological features of the P2X receptor channel in airway ciliated cells. *J Physiol* 2006;571:503-517.
- 21 Zsembery A, Fortenberry JA, Liang L, Bebock Z, Tucker TA, Boyce AT, Braunstein GM, Welty E, Bell PD, Sorscher EJ, Clancy JP, Schwiebert EM: Extracellular zinc and ATP restore chloride secretion across cystic fibrosis airway epithelia by triggering calcium entry. *J Biol Chem* 2004;279:10720-10729.
- 22 Liang L, Zsembery A, Schwiebert EM: RNA interference targeted to multiple P2X receptor subtypes attenuates zinc-induced calcium entry. *Am J Physiol Cell Physiol* 2005;289:C388-396.
- 23 Doctor RB, Matzakos T, McWilliams R, Johnson S, Feranchak AP, Fitz JG: Purinergic regulation of cholangiocyte secretion: Identification of a novel role for P2X receptors. *Am J Physiol Gastrointest Liver Physiol* 2005;288:G779-786.
- 24 Gum RJ, Wakefield B, Jarvis MF: P2X receptor antagonists for pain management: Examination of binding and physicochemical properties. *Purinergic Signal* 2012;8:41-56.
- 25 Virginio C, Robertson G, Surprenant A, North RA: Trinitrophenyl-substituted nucleotides are potent antagonists selective for P2X₁, P2X₃, and heteromeric P2X_{2/3} receptors. *Mol Pharmacol* 1998;53:969-973.
- 26 Jarvis MF, Khakh BS: ATP-gated P2X cation-channels. *Neuropharmacology* 2009;56:208-215.
- 27 Fisher R, Grützmann R, Blasco HPJ, Kalthof B, Gadea PC, Stelte-Ludwig B, Woltering E, Wutke M: Benzofuro-1,4-diazepin-2-one derivatives. 2005; Patent Number: EP1608659A1
- 28 Norenberg W, Sobottka H, Hempel C, Plotz T, Fischer W, Schmalzing G, Schaefer M: Positive allosteric modulation by ivermectin of human but not murine P2X₇ receptors. *Br J Pharmacol* 2012;167:48-66.
- 29 Kwon HJ: Extracellular ATP signaling via P2X₄ receptor and cAMP/PKA signaling mediate ATP oscillations essential for prechondrogenic condensation. *J Endocrinol* 2012;214:337-348.
- 30 Wu T, Dai M, Shi XR, Jiang ZG, Nuttall AL: Functional expression of P2X₄ receptor in capillary endothelial cells of the cochlear spiral ligament and its role in regulating the capillary diameter. *Am J Physiol Heart Circ Physiol* 2011;301:H69-78.
- 31 Casati A, Frascoli M, Traggiai E, Proietti M, Schenk U, Grassi F: Cell-autonomous regulation of hematopoietic stem cell cycling activity by ATP. *Cell Death Differ* 2011;18:396-404.
- 32 Hamill OP, Marty A, Neher E, Sakmann B, Sigworth FJ: Improved patch-clamp techniques for high-resolution current recording from cells and cell-free membrane patches. *Pflugers Arch* 1981;391:85-100.
- 33 He ML, Zemkova H, Koshimizu TA, Tomic M, Stojilkovic SS: Intracellular calcium measurements as a method in studies on activity of purinergic P2X receptor channels. *Am J Physiol Cell Physiol* 2003;285:C467-479.
- 34 Fischer W, Wirkner K, Weber M, Eberts C, Koles L, Reinhardt R, Franke H, Allgaier C, Gillen C, Illes P: Characterization of P2X₃, P2Y₁ and P2Y₄ receptors in cultured HEK293-hP2X₃ cells and their inhibition by ethanol and trichloroethanol. *J Neurochem* 2003;85:779-790.
- 35 Fischer W, Franke H, Groger-Arndt H, Illes P: Evidence for the existence of P2Y_{1,2,4} receptor subtypes in HEK-293 cells: Reactivation of P2Y₁ receptors after repetitive agonist application. *Naunyn Schmiedeberg Arch Pharmacol* 2005;371:466-472.
- 36 Serrano A, Mo G, Grant R, Pare M, O'Donnell D, Yu XH, Tomaszewski MJ, Perkins MN, Seguela P, Cao CQ: Differential expression and pharmacology of native P2X receptors in rat and primate sensory neurons. *J Neurosci* 2012;32:11890-11896.
- 37 Nagata K, Imai T, Yamashita T, Tsuda M, Tozaki-Saitoh H, Inoue K: Antidepressants inhibit P2X₄ receptor function: A possible involvement in neuropathic pain relief. *Mol Pain* 2009;5:20.
- 38 Khakh BS, Proctor WR, Dunwiddie TV, Labarca C, Lester HA: Allosteric control of gating and kinetics at P2X₄ receptor channels. *J Neurosci* 1999;19:7289-7299.
- 39 Asatryan L, Popova M, Perkins D, Trudell JR, Alkana RL, Davies DL: Ivermectin antagonizes ethanol inhibition in purinergic P2₄ receptors. *J Pharmacol Exp Ther* 2010;334:720-728.
- 40 Manohar M, Hirsh MI, Chen Y, Woehrle T, Karande AA, Junger WG: ATP release and autocrine signaling through P2X₄ receptors regulate $\gamma\delta$ T cell activation. *J Leukoc Biol* 2012;92:787-794.
- 41 Gong QJ, Li YY, Xin WJ, Zang Y, Ren WJ, Wei XH, Li YY, Zhang T, Liu XG: ATP induces long-term potentiation of c-fiber-evoked field potentials in spinal dorsal horn: The roles of P2X₄ receptors and p38 MAPK in microglia. *Glia* 2009;57:583-591.
- 42 Li C, Peoples RW, Weight FF: Ethanol-induced inhibition of a neuronal P2X purinoceptor by an allosteric mechanism. *Br J Pharmacol* 1998;123:1-3.
- 43 Michel AD, Chambers LJ, Walter DS: Negative and positive allosteric modulators of the P2X₇ receptor. *Br J Pharmacol* 2008;153:737-750.



Bicarbonate Inhibits Bacterial Growth and Biofilm Formation of Prevalent Cystic Fibrosis Pathogens

Orsolya Dobay¹, Krisztina Laub^{1†}, Balázs Stercz¹, Adrienn Kéri², Bernadett Balázs³, Adrienn Tóthpál¹, Szilvia Kardos¹, Pongsiri Jaikumpun², Kasidid Ruksakiet², Paul M. Quinton⁴ and Ákos Zsemlery^{2*}

¹ Institute of Medical Microbiology, Semmelweis University, Budapest, Hungary, ² Department of Oral Biology, Semmelweis University, Budapest, Hungary, ³ Department of Physiology, Semmelweis University, Budapest, Hungary, ⁴ Department of Pediatrics, UC San Diego School of Medicine, University of California, San Diego, San Diego, CA, United States

OPEN ACCESS

Edited by:

Manuel Simões,
Universidade do Porto, Portugal

Reviewed by:

Florence Dubois-Brissonnet,
AgroParisTech – Institut des Sciences
et Industries du Vivant et
de l'Environnement, France

Brett Mellbye,
Oregon State University,
United States

*Correspondence:

Ákos Zsemlery
zsemlery.akos@
dent.semmelweis-univ.hu

†Present address:

Krisztina Laub,
Hetényi Géza Hospital,
Szolnok, Hungary

Specialty section:

This article was submitted to
Microbial Physiology and Metabolism,
a section of the journal
Frontiers in Microbiology

Received: 29 March 2018

Accepted: 03 September 2018

Published: 19 September 2018

Citation:

Dobay O, Laub K, Stercz B, Kéri A,
Balázs B, Tóthpál A, Kardos S,
Jaikumpun P, Ruksakiet K,
Quinton PM and Zsemlery Á (2018)
Bicarbonate Inhibits Bacterial Growth
and Biofilm Formation of Prevalent
Cystic Fibrosis Pathogens.
Front. Microbiol. 9:2245.
doi: 10.3389/fmicb.2018.02245

We investigated the effects of bicarbonate on the growth of several different bacteria as well as its effects on biofilm formation and intracellular cAMP concentration in *Pseudomonas aeruginosa*. Biofilm formation was examined in 96-well plates, with or without bicarbonate. The cAMP production of bacteria was measured by a commercial assay kit. We found that NaHCO₃ (100 mmol l⁻¹) significantly inhibited, whereas NaCl (100 mmol l⁻¹) did not influence the growth of planktonic bacteria. MIC and MBC measurements indicated that the effect of HCO₃⁻ is bacteriostatic rather than bactericidal. Moreover, NaHCO₃ prevented biofilm formation as a function of concentration. Bicarbonate and alkalinization of external pH induced a significant increase in intracellular cAMP levels. In conclusion, HCO₃⁻ impedes the planktonic growth of different bacteria and impedes biofilm formation by *P. aeruginosa* that is associated with increased intracellular cAMP production. These findings suggest that aerosol inhalation therapy with HCO₃⁻ solutions may help improve respiratory hygiene in patients with cystic fibrosis and possibly other chronically infected lung diseases.

Keywords: cystic fibrosis, bicarbonate, pH, biofilm, *Pseudomonas aeruginosa*, *Staphylococcus aureus*, cAMP, HCO₃⁻

INTRODUCTION

Cystic fibrosis (CF) is caused by mutations in the gene encoding the cystic fibrosis transmembrane conductance regulator (CFTR) protein (Riordan et al., 1989). CFTR is a cAMP/protein kinase A (PKA)-dependent epithelial anion channel that conducts both chloride and bicarbonate (Linsdell et al., 1997; Reddy and Quinton, 2003). Defective transepithelial anion transport impairs mucociliary clearance (MCC) leading to the retention of thick, viscid mucus in the airways (Quinton, 2007a, 2010). The poor clearance of viscous CF mucus contributes to a vicious cycle of airway obstruction, infection, and inflammation (Hoffman and Ramsey, 2013). However, the links between the primary defect in anion transport and CF lung disease appear to be multifactorial. It was recently shown that impaired HCO₃⁻ secretion is likely responsible for aggregated mucus in CF mice (Garcia et al., 2009; Gustafsson et al., 2012) and pigs (Birket et al., 2014).

In addition, the abnormally lower pH of the airway surface liquid (ASL) was associated with decreased bacterial killing in the CF porcine lung. Aerosolizing a HCO₃⁻ solution onto the CF porcine airways increased innate bacterial killing *in vivo* (Pezzulo et al., 2012). Recruitment of

lymphocytes may promote epithelial HCO_3^- secretion during infection and, intriguingly, epithelial HCO_3^- secretion may require CFTR expression in lymphocytes as yet another deficiency impacting on CF lung disease (Tang et al., 2012).

For decades, HCO_3^- has been used and indicated for use as a microbial disinfectant in food and agriculture industries, but usually as an adjuvant (Rutala et al., 2000). Earlier, HCO_3^- , in combination with lidocaine was reported to exert antibacterial activity (Thompson et al., 1993). Immunologically, it is crucial for the optimal activity of antimicrobial peptides (Dorschner et al., 2006) but, apparently, it can have an independent bactericidal effect on *Escherichia coli* (Xie et al., 2010). In medicine, it is an accepted treatment for chlorine gas intoxication (Bosse, 1994) and has been suggested for use as a mucolytic as well as an adjuvant for nebulized drug delivery (Kaushik et al., 2016). It has also been long recommended for dental hygiene (Newbrun et al., 1984; Drake et al., 1995). Most of the antibacterial reports on HCO_3^- have been limited to planktonic growth and do not include effects on biofilm formation.

Bicarbonate directly and indirectly affects lung function (Quinton, 2007a,b). It is required for sequestering calcium and protons from secreted mucin granules to allow for normal expansion upon release (Garcia et al., 2009; Quinton, 2010). It may also affect neutrophil killing capacity as well as bacterial colonization in the lungs (Quinton, 2007a, 2008; Abou Alaiwa et al., 2014). Importantly, HCO_3^- influences the H^+ concentration (pH) of the ASL via the $\text{HCO}_3^-/\text{CO}_2$ buffer system (Shah et al., 2016a). These effects directly affect the properties of the ASL and its critical ability to trap inhaled and endogenous debris for export by the ciliated surfaces of the airways. They indirectly affect the lungs by maintaining an airway environment that also enables the immune system to clear viral and bacterial pathogens. Any maneuver such as adding exogenous HCO_3^- , as suggested here, that improves or helps maintain airway patency is expected to enhance lung function.

Successful antimicrobial therapy for bacterial lung infections is crucial for increasing life expectancy and improving CF patients' quality of life. In CF lungs, however, bacteria colonize in biofilms (Rogers et al., 2011), making eradication of pathogens difficult. It is also known that bacteria in biofilms are more resistant compared to planktonic cells (Stewart and Costerton, 2001; Venkatesan et al., 2015). Biofilm formation is thought to be regulated largely by the second messenger molecules cAMP and c-di-GMP in bacterial cells. An increase in intracellular cAMP concentrations along with a decrease in c-di-GMP levels is associated with the production of acute virulence factors and reduced biofilm formation (Almblad et al., 2015). Accordingly, HCO_3^- stimulates soluble adenylate cyclase (sAC) and increases the activity of phosphodiesterase that breaks down c-di-GMP (Chen et al., 2000; Koestler and Waters, 2014a). Of note is that HCO_3^- , CO_2 , and external pH affect soluble adenylate cyclase activity and consequently intracellular cAMP levels (Hammer et al., 2006), which is a hallmark for *Pseudomonas aeruginosa* virulence factors that decrease when bacteria form biofilms in chronic infection (Valentini and Filloux, 2016). Thus, bacterial life style (planktonic vs. biofilm) is, at least partially, dictated by intracellular cAMP levels.

Herein, we focus on the effects of HCO_3^- on planktonic growth on several pathogens common to cystic fibrosis and consider biofilm forming capacity for two of the more prevalent bacteria in CF, *P. aeruginosa* and *S. aureus*. This work presents a novel proposal that HCO_3^- may therapeutically help prevent colonization and biofilm formation of CF-associated bacteria by increasing intracellular cAMP levels. Not only do the data confirm earlier notions, but they also add further reasons to consider inhaled HCO_3^- as a potential therapy, especially in the context of CF where defective HCO_3^- secretion is a well-established basic defect.

MATERIALS AND METHODS

Growth Experiments

The growth of ATCC control strains and clinical isolates of different Gram-positive and Gram-negative bacteria in Brain-Heart Infusion (BHI) broth (Mast Group Ltd., Merseyside, United Kingdom) were compared with and without 100 mmol l^{-1} NaHCO_3 in the medium and equilibrated with CO_2 to control pH. Growth experiments were carried out with the following reference strains: *S. aureus* ATCC 25923 (MSSA), *S. aureus* ATCC 29213 (MSSA), *S. aureus* ATCC 33591 (MRSA), *Streptococcus agalactiae* ATCC 80200, *Enterococcus faecalis* ATCC 29212, *E. faecalis*, vanB+, ATCC 51299, *P. aeruginosa* ATCC 27853, *E. coli* ATCC 25922, *Haemophilus influenzae* ATCC 49766, *H. influenzae* ATCC 49247. Some of the experiments were repeated with clinical isolates of the same species, obtained from the Central Bacteriological Diagnostic Laboratory of Semmelweis University, Budapest, obtained from daily routine specimens.

The density of bacterial suspensions was set at 0.5 McFarland (approximately 10^8 CFU ml^{-1}) with a VITEK Densichek apparatus (Biomérieux, Marcy l'Etoile, France). The pH of the 100 mmol l^{-1} NaHCO_3 -containing BHI broth was set at pH approximately 7.4 by bubbling the autoclaved solution to equilibration with 20% CO_2 -balance air for at least 16 h at 37°C before inoculation. The pH of these unstirred solutions in hermetically capped bottles remained stable for at least 24 h. To achieve other pH values, the CO_2 concentration required was calculated from the Henderson-Hasselbalch equation for the $\text{HCO}_3^-/\text{CO}_2$ buffer system (Story, 2004). When BHI broth containing 100 mmol l^{-1} NaHCO_3 was equilibrated with 5% CO_2 , the measured pH (~ 8.5) was somewhat higher than that calculated from the Henderson-Hasselbalch equation (pH ~ 8.0).

Aliquots of each suspension (200 μl) were dispensed into 96-well microtiter plates in duplicate. Bacterial suspensions were then incubated in ambient air ($\sim 0.04\%$ CO_2), in 5% or in 20% CO_2 by design. Bacterial growth was followed by measuring the optical density (OD) at 595 nm using a PR2100 microplate reader (Bio-Rad Laboratories, Hercules, Canada) 60 min after inoculating and subsequently every 15 min for 5.5 h. Optical density of a negative control (without bacterial growth) was subtracted from all OD values. The results of the parallel measurements of duplicate samples were averaged and normalized to the control media. The growth rates were determined by calculating the area under the curve (AUC)

(Horváth et al., 2012) using Microsoft Excel, based on the summation of small trapezoids.

The osmolality of BHI broth was approximately 360 mosm kg^{-1} in accordance with the data published earlier (Montgomerie et al., 1972). Since supplementation of BHI broth with 100 mmol l^{-1} NaHCO_3 increased the osmolality of the solution to approximately 470 mosm kg^{-1} , bacterial growth was also determined in BHI broth containing 100 mmol l^{-1} NaCl (pH 7.4 adjusted with NaOH) as a control. As a pH control, the growth of bacteria was measured in unsupplemented BHI broths adjusted with HCl or NaOH to pH values ranging from 6.8 to 9.0 as required.

Determination of Minimum Inhibitory Concentration (MIC) and Minimum Bactericidal Concentration (MBC) by Broth Microdilution

To determine MIC and MBC, two strains of *P. aeruginosa* (ATCC 27853 and a clinical isolate) and two strains of *S. aureus* (ATCC 29213 and a clinical isolate) were selected. Bacteria were cultured for 18–20 hours on blood agar plates. The following day, a 0.5 McFarland suspension was prepared in physiological salt solution. This suspension was diluted 1:20 in Mueller–Hinton (MH) Broth (cation adjusted). For further measurements this standardized inoculum was used. NaHCO_3 was diluted serially twofold in MH Broth (cation adjusted) in a plastic microdilution plate with round bottom wells to a final volume of 0.1 ml. The concentration of NaHCO_3 varied from 1000 to 1.95 mmol l^{-1} in 10 steps of twofold dilutions. The wells were inoculated with 0.01 ml of standardized inoculum, positive and negative growth controls were also used. After 24 h incubation, the growth of bacteria was evaluated based on the visible change of turbidity. MIC was identified as the lowest concentration of HCO_3^- at which no visible growth was observed. To determine MBC, specimens from the wells without visible bacterial growth were inoculated onto antibiotic-free agar plates and incubated for 24 h. MBC was defined as the lowest concentration of HCO_3^- where no colonies were observed.

Biofilm Experiments

Although almost all bacteria involved in CF lung disease can form biofilms, *P. aeruginosa* presents the largest clinical challenge. Therefore, we investigated *P. aeruginosa* for biofilm formation. Isolates were grown overnight to stationary phase in bouillon containing meat extract 0.3%, yeast extract 0.2%, pepton 1%, NaCl 0.5%; pH adjusted to 7.5 with NaOH. The overnight cultures were diluted 1:100 in the desired medium. All solutions were prepared by filtration using 0.22 μm filter membranes. Aliquots of 100 μl of diluted cultures were pipetted into eight parallel wells of a 96-well microtiter plate. The covered plates were incubated at 37°C in ambient air, 5%, or 20% CO_2 for 48 h. Planktonic bacteria were then removed by rigorous washing with PBS three times. Bacteria attached to the wells were air-dried and subsequently stained with 125 μl of 0.1% crystal violet solution for 10 min. Excess crystal violet was removed by water-washing; that is, submerging the plates in tap water several times.

After air-drying, crystal violet was solubilized in 30% acetic acid (200 μl per well) for 10 min. From each well, 125 μl of this solution was then transferred to separate wells of an optically clear, flat-bottom 96-well plate. Optical density was measured at 595 nm in a PR2100 microplate reader (see above) (Merritt et al., 2011).

To measure the influence of glucose-content on biofilm formation, the bouillon was supplemented with 0.2, 1.0, 2.0, and 4.0 g l^{-1} glucose. Biofilm formation was absent at low glucose content and was the strongest at 4.0 g l^{-1} glucose, consequently all experiments were performed using bouillon containing 4.0 g l^{-1} glucose.

Measurement of Intracellular cAMP Levels

The bacterial production of cAMP was determined with the Cyclic AMP XP® Assay Kit (Cell Signaling Technology, Leiden, Netherlands, originally designed for eukaryotic cells, but applicable for bacteria as well). Bacterial cultures were first grown in the desired medium for 15–16 h to stationary phase for conditioning, then diluted 1:500 in 10 ml of the same fresh medium and allowed to grow for a few hours until reaching log phase, that is, $\text{OD}_{595} = 0.4$ – 0.5 . Cultures were then centrifuged (4000 \times g, 5 min), bacteria were re-suspended in 200 μl of the kit lysis buffer for 30 min on ice and centrifuged again (8000 \times g, 5 min); 50 μl of the supernatant was transferred to the assay plate. According to kit protocol, absorbance was measured at 450 nm in a PR2100 microplate reader.

Statistical Analysis

For statistical analysis Statistica for Windows 7.0 (Statsoft) was used. Data presented are means \pm SD, if not indicated otherwise. The values were compared using ANOVA followed by LSD *post hoc* comparison test. Changes were considered statistically significant at $P < 0.05$.

RESULTS

Reduction of Bacterial Growth by Bicarbonate

Since high external HCO_3^- concentrations and/or alkaline pH are reported to inhibit the growth of *E. coli* (Xie et al., 2010), we tested the effect of HCO_3^- on the growth of *E. coli*. The growth rate of bacteria was significantly inhibited in BHI broth supplemented with 100 mmol l^{-1} NaHCO_3 (pH 7.4, equilibrated with 20% CO_2) as compared to control media (pH 7.4) without added HCO_3^- (Figure 1A). We tested the growth of bacteria in BHI broth supplemented with 100 mmol l^{-1} NaCl (pH 7.4; $\sim \Delta 110$ mosm kg^{-1}), which did not suppress the growth of bacteria, indicating that the inhibitory effect of NaHCO_3 was not due to increased osmolality or ionic strength.

Next, we tested whether alkaline pH affects bacterial growth. In BHI broth at pH 8.5, the growth capacity was not significantly influenced (Figure 1A); however, when bacteria were incubated

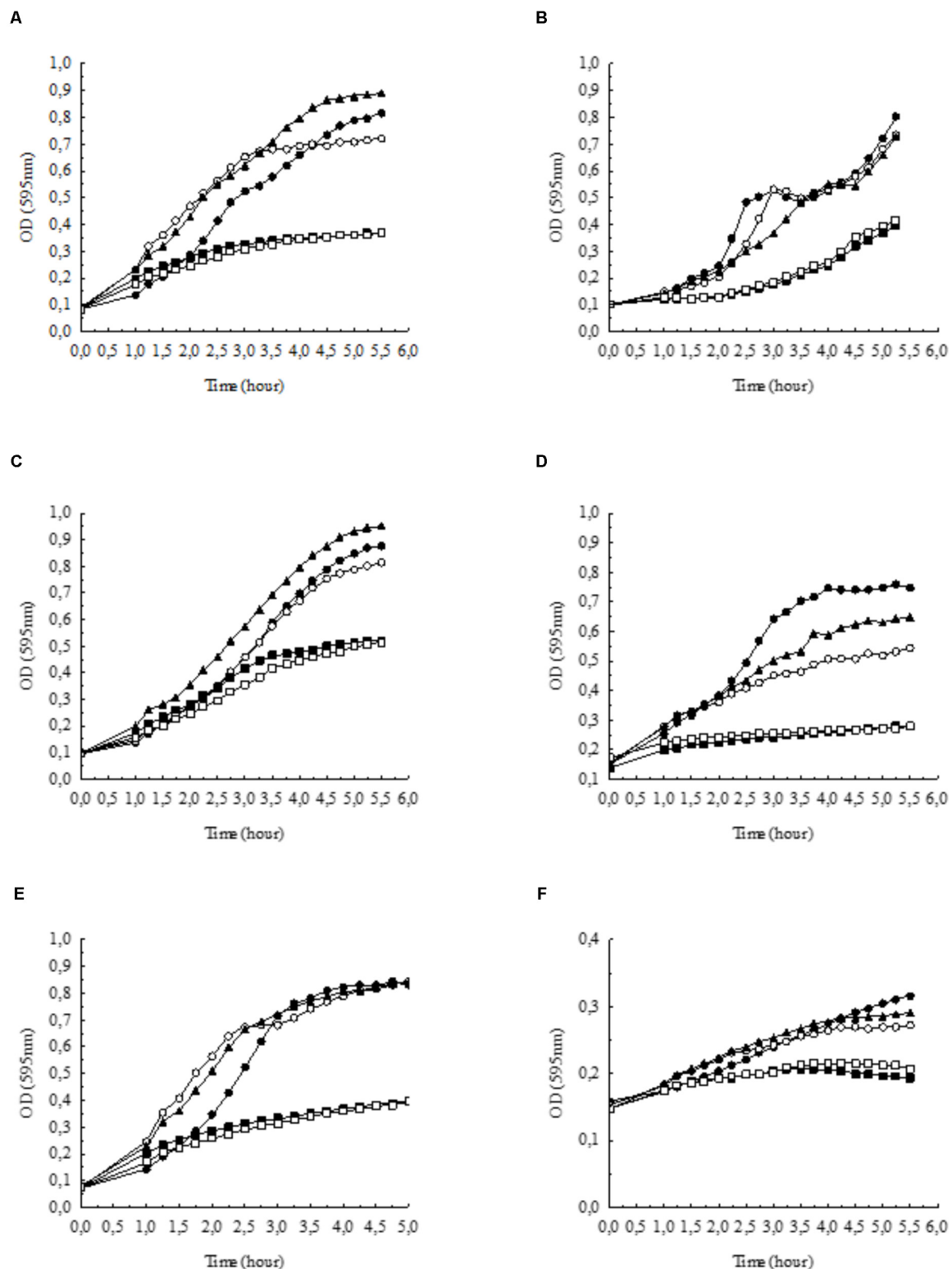


FIGURE 1 | Growth of (A) *Escherichia coli*, (B) *Pseudomonas aeruginosa*, (C) *Staphylococcus aureus*, (D) *Streptococcus agalactiae*, (E) *Enterococcus faecalis*, and (F) *Haemophilus influenzae* in BHI broth supplemented with NaHCO₃ compared to control conditions (●: control pH = 7.4, ▲: 100 mmol l⁻¹ NaCl, pH = 7.4). Bicarbonate-containing solutions were equilibrated with either 5% (□: 100 mmol l⁻¹ NaHCO₃, pH = 8.5) or 20% CO₂ (■: 100 mmol l⁻¹ NaHCO₃, pH = 7.4). In the absence of bicarbonate, pH was adjusted to 8.5 with NaOH (○: growth at pH = 8.5). Each curve shows the average of two parallel experiments. Standard Deviations were generally less than 1% of the mean and are not shown. Note that in panel (F) the scale on the y axis differs from the other panels.

TABLE 1 | Calculated AUC values of different bacteria, based on growth curves in **Figures 1A–F**.

Bacterium	Growth control pH = 7.4	Growth at pH = 8.5	100 mM NaCl pH = 7.4	100 mM NaHCO ₃ pH = 7.4	100 mM NaHCO ₃ pH = 8.5
<i>E. coli</i>	2.45	2.82	3.04	1.57	1.49
<i>P. aeruginosa</i>	2.05	1.92	1.82	1.01	1.06
<i>S. aureus</i>	2.48	2.41	2.93	1.92	1.76
<i>S. agalactiae</i>	2.84	2.20	2.48	1.27	1.35
<i>E. faecalis</i>	2.90	3.21	3.18	1.64	1.54
<i>H. influenzae</i>	1.28	1.26	1.31	1.05	1.07

in BHI broth supplemented with 100 mmol l⁻¹ NaHCO₃ at pH 8.5 (5% CO₂), the inhibitory effects were similar to those observed at pH 7.4 (20% CO₂) (**Figure 1A**). Thus, the data show that NaHCO₃ *per se* inhibited bacterial growth, which was not simply due to higher osmolality or alkaline media.

In order to test whether the inhibitory effect of HCO₃⁻ is specific to *E. coli* cells, we investigated other species such as *P. aeruginosa*, *S. aureus*, *S. agalactiae*, *E. faecalis*, and *H. influenzae*. Similarly to the effects on *E. coli*, NaHCO₃ (100 mmol l⁻¹) significantly inhibited the growth of all these species as well, suggesting that HCO₃⁻ can suppress bacterial growth in general (**Figures 1B–F**). In order to compare the growth rates of bacteria under different conditions more quantitatively, AUC values were determined as a measure of the reduced growth rates in HCO₃⁻-enriched medium for each bacterial specie (**Table 1**).

In the previous experiments, to maintain the initial pH of the media near 7.4, all bicarbonate-containing solutions were equilibrated with calculated levels of CO₂. Therefore, we asked the question whether HCO₃⁻-containing media without CO₂ equilibration influences growth of *P. aeruginosa*. Despite the fact that media pH continued to increase during the exponential growth phase (i.e., the first six hours), bacterial density remained similar to those observed with CO₂ equilibration (**Figures 2A,B**). When bacteria were grown until reaching the stationary phase (i.e., 24 h), significant increases in OD values were observed in the presence of both 25 and 100 mmol l⁻¹ HCO₃⁻ suggesting that HCO₃⁻ is bacteriostatic rather than bactericidal. Of note is that a lower bacterial density was observed at 24 h when 100 mmol l⁻¹ HCO₃⁻ was present, but it should be kept in mind that excessive alkalization at atmospheric CO₂ levels, may exert inhibitory effects on growth rate (**Figure 2A**). Nonetheless, HCO₃⁻-containing media of concentrations up to 100 mmol l⁻¹ equilibrated with appropriate levels of CO₂ did not inhibit maximal bacterial growth at 24 h, suggesting that the bacteriostatic effects of HCO₃⁻ occur within the initial period of the exponential growth phase (**Figure 2B**). We obtained similar results when the above experiments were repeated with *S. aureus*, at least with respect to bacterial growth profile (**Figures 3A,B**).

Results of the MIC and MBC Determination

In the case of all four tested isolates, an MIC of 125 mmol l⁻¹ was obtained. The MBCs for the two *P. aeruginosa* strains

were 500 mmol l⁻¹, meanwhile the two *S. aureus* isolates remained alive even in the highest HCO₃⁻ concentration tested (MBC > 1000 mmol l⁻¹).

Bicarbonate Inhibits Biofilm Formation of *P. aeruginosa*

One of the most severe complications of CF lung disease involves biofilm formation of pathogenic bacteria, which may be due to depleted levels of HCO₃⁻ in CF airways. Thus, we asked the question whether HCO₃⁻ could not only inhibit planktonic bacterial growth, but biofilm formation as well. Glucose starvation leads to impaired biofilm formation associated with elevated cAMP levels (Huynh et al., 2012), hence glucose is required for optimal biofilm formation. Similarly, our data show that although bacteria achieved high density (OD₅₉₅ = 0.94 ± 0.12, *n* = 7), no biofilm was detected in the medium without added glucose (**Figure 4**). On the other hand, in the presence of glucose, bacterial growth was similar (OD₅₉₅ = 0.81 ± 0.06, *n* = 7) and robust biofilm formation was observed. However, the supplementation of glucose-containing medium with 100 mmol l⁻¹ HCO₃⁻ prevented biofilm formation and significantly inhibited planktonic growth as well (OD₅₉₅ = 0.45 ± 0.04, *n* = 8). To demonstrate the reduced number of viable cells in HCO₃⁻-containing media, a bacteria count was performed after 48 h' incubation. In the absence of HCO₃⁻, the calculated CFU in bouillon with and without glucose was 2.8 × 10¹² and 4.5 × 10¹¹, respectively. In contrast, the average CFU ml⁻¹ was 6.6 × 10⁶ in media supplemented with 100 mmol l⁻¹ HCO₃⁻. In addition, 50 mmol l⁻¹ HCO₃⁻ partially blocked biofilm formation suggesting a concentration-dependent inhibitory mechanism (**Figure 4**). When NaCl (100 mmol l⁻¹) replaced NaHCO₃, biofilm formation capacity was fully maintained.

Bicarbonate Increases Intracellular cAMP Levels in Bacteria

Inhibition of biofilm formation may be induced by HCO₃⁻ effects on the levels of cAMP and c-di-GMP. Thus, we investigated the effects of HCO₃⁻ on intracellular cAMP production in *P. aeruginosa*. Supplementation of BHI medium with 25 and 100 mmol l⁻¹ HCO₃⁻ resulted in significant concentration-dependent increases in cAMP levels (**Figure 5A**). Importantly, administration of 100 mmol l⁻¹ NaCl did not influence cAMP concentrations (**Figure 5A**). Since it is well known that sAC

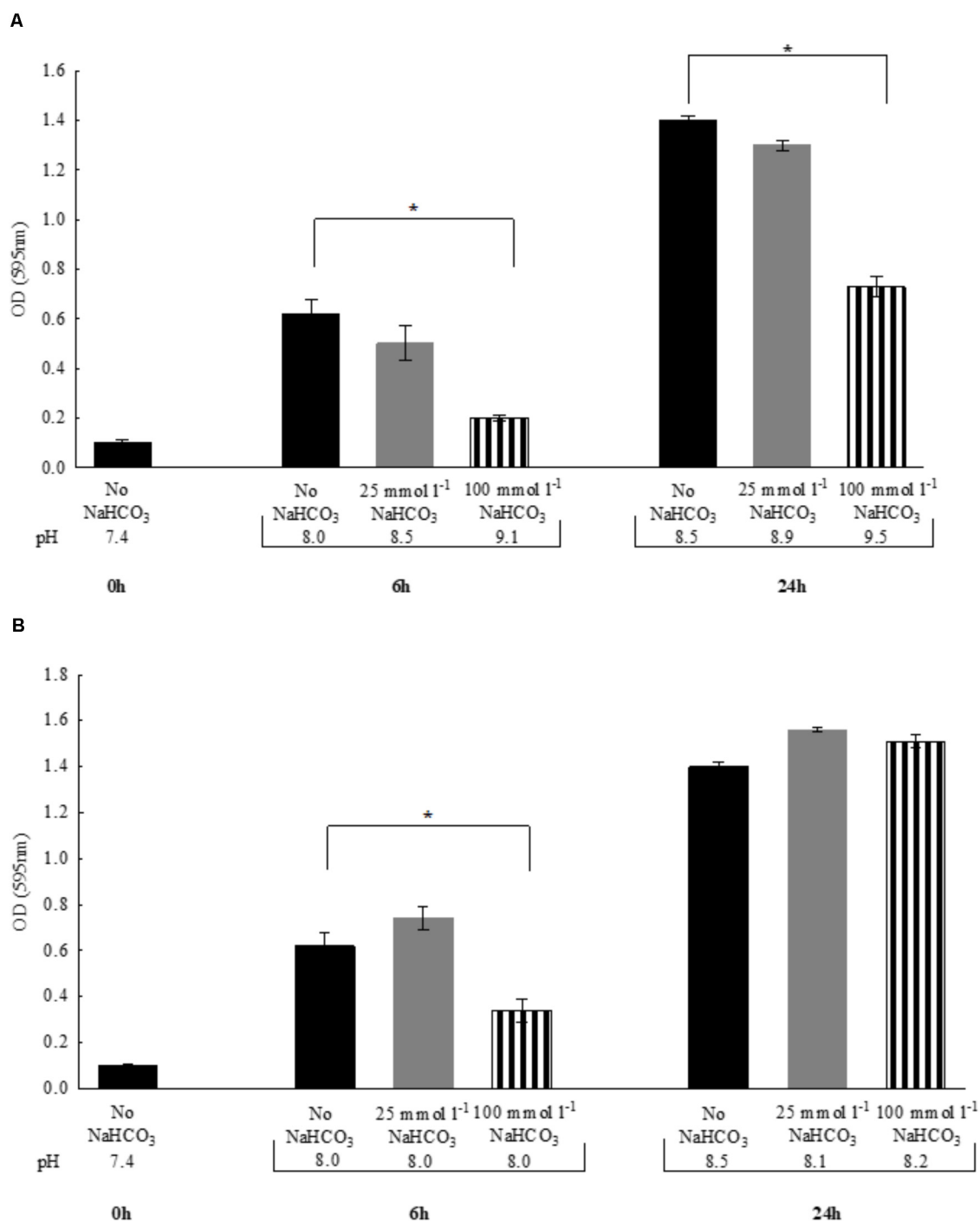


FIGURE 2 | Changes in bacterial density of *Pseudomonas aeruginosa* and media pH following 6 vs. 24 h incubations either **(A)** in air atmosphere, or **(B)** in the presence of appropriate levels of CO₂. Black bars: NaHCO₃-free controls, gray bars: 25 mmol l⁻¹ NaHCO₃; striped bars: 100 mmol l⁻¹ NaHCO₃. Statistically significant, **P* < 0.05.

activity depends on intracellular pH (Rahman et al., 2013), we tested the effects of media pH changes between 6.0 and 9.0 on cAMP production. In this pH range, a slight increase in cAMP levels, parallel to alkalinization was observed (**Figure 5B**). Of note, even the highest pH-induced increase in cAMP level was

significantly lower than the increase induced by 100 mmol l⁻¹ HCO₃⁻. Similar results were obtained when the experiments were repeated with *S. aureus* (**Figure 5A**). Taken together, the data suggest that biofilm suppression by HCO₃⁻ is mediated through an increased production of intracellular cAMP.

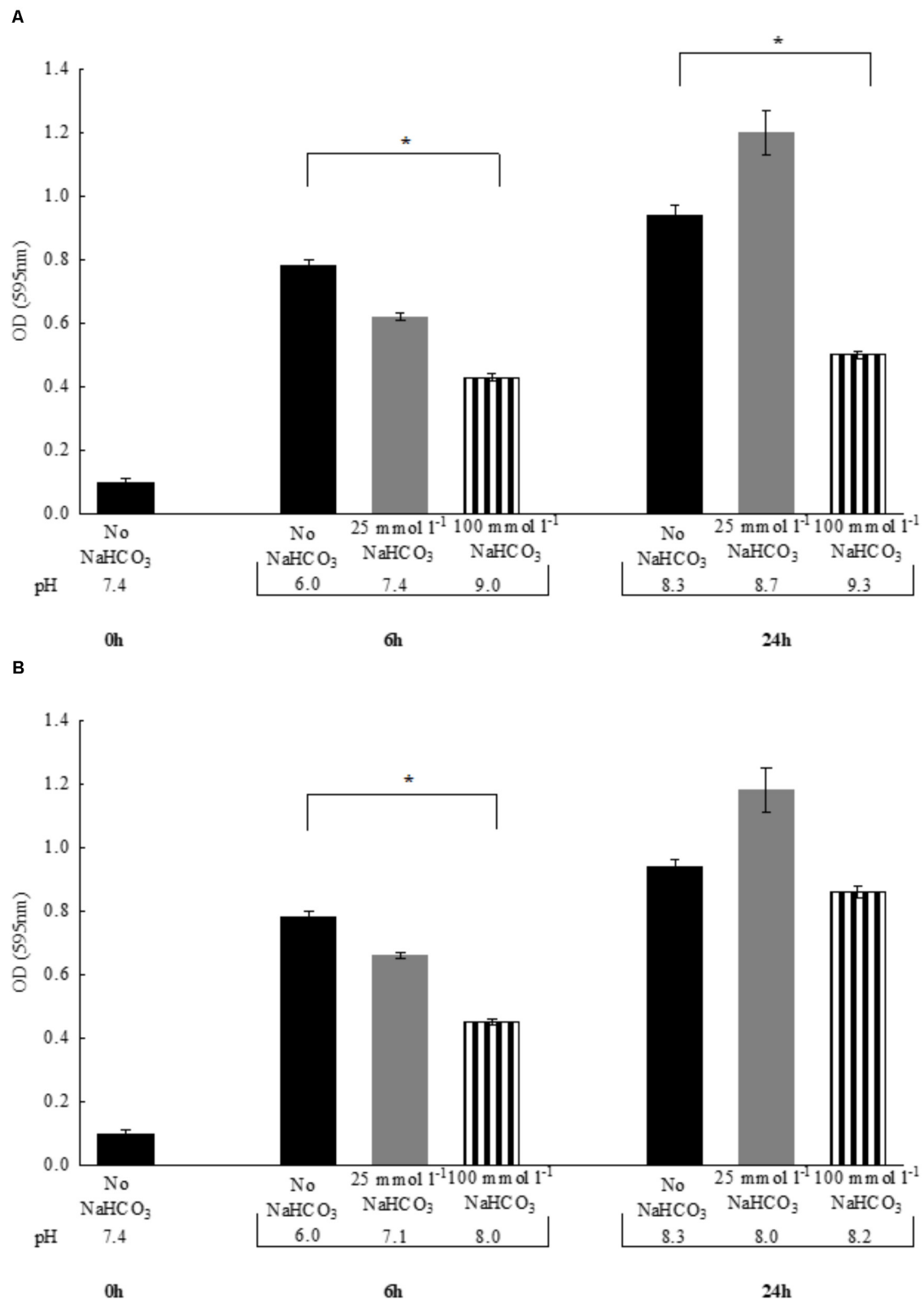


FIGURE 3 | Changes in bacterial density of *Staphylococcus aureus* and media pH following 6 vs. 24 h incubations either **(A)** in air atmosphere or **(B)** in the presence of appropriate CO₂ levels. Black bars: NaHCO₃-free controls, gray bars: 25 mmol l⁻¹ NaHCO₃, striped bars: 100 mmol l⁻¹ NaHCO₃. **P* < 0.05.

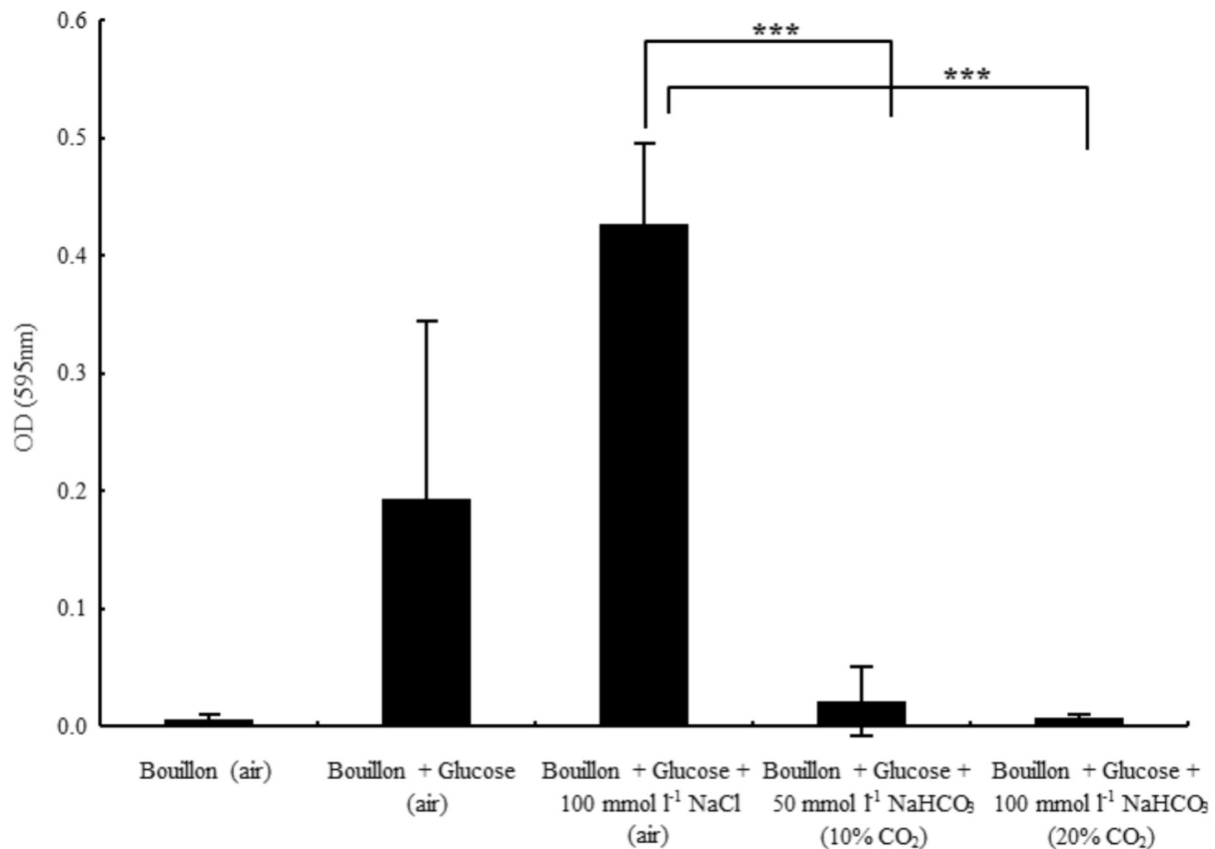


FIGURE 4 | Biofilm formation capacity of *Pseudomonas aeruginosa* in glucose-containing bouillon (4 g l⁻¹) in the presence of sodium chloride and two different concentrations of sodium bicarbonate. Please note that in the absence of glucose no biofilm formation was observed. ****P* < 0.001.

DISCUSSION

Early studies using the human serous cell line (Calu-3) showed that airway-derived epithelial cells can secrete HCO₃⁻ (Lee et al., 1998). Recently, active HCO₃⁻ secretion was demonstrated in native intact small airway epithelium as well (Shamsuddin and Quinton, 2014). Loss of HCO₃⁻ secretion seems to be associated with different pathological consequences in CF airways, such as formation of thickened mucus (Quinton, 2010), reduced microbial susceptibility to antimicrobial peptides (Dorschner et al., 2006) and impaired bacterial killing capacity (Pezzulo et al., 2012; Abou Alaiwa et al., 2014). Therefore, the delivery of HCO₃⁻ into the airways may be potentially therapeutic in CF (Pezzulo et al., 2012; Li et al., 2016). Moreover, beyond CF, decreased pH (likely due to decreased HCO₃⁻) of airway surface liquid and chronic bacterial infections have also been described in other chronic airway diseases such as COPD (Mall and Hartl, 2014; Li et al., 2016; Shah et al., 2016a,b).

A shift to either acidic or alkaline external pH presents a stress for bacteria, which may influence survival and growth (Padan et al., 2005). In alkaline environments the growth rate of neutrophilic bacteria is reduced (Maurer et al., 2005). When grown in media at pH 7.0, *E. coli* cells exhibit shorter generation time compared to that when it is cultured at pH

8.7 (Maurer et al., 2005). Our data show that 100 mmol l⁻¹ NaHCO₃ significantly inhibit the growth of *E. coli* equally, at both pH 7.4 and 8.5, but in the absence of HCO₃⁻, neither alkaline pH (up to 8.5) nor equivalent increases in osmolality (NaCl) inhibit bacterial growth, indicating that HCO₃⁻ *per se* plays a pivotal role in growth suppression. Alkaline conditions may alter cytosolic pH of bacteria when protons must be taken up from the extracellular medium. Under alkaline conditions proton scavengers markedly decrease *E. coli* viability (Vanhautegehem et al., 2013). This phenomenon can be explained by partitioning of unprotonated scavengers into the cytosol where they become protonated and increase cytosolic pH. To maintain pH homeostasis, bacteria require high ATP consumption and membrane hyperpolarization. We surmise that higher HCO₃⁻ concentrations in the media increase the gradient for increased HCO₃⁻ entry into the cytosol of bacteria elevating intracellular pH. The higher energy consumption occurs at the expense of bacterial growth rate. Importantly, similar results were observed with *S. aureus*, *P. aeruginosa*, *S. agalactiae*, *E. faecalis*, and *H. influenzae* as well, again suggesting that HCO₃⁻ might be used to inhibit the growth of bacteria more generally.

S. aureus and *P. aeruginosa* are of particular interest because of their high incidence in CF patients with chronic pulmonary infections. We observed that during the first few hours of

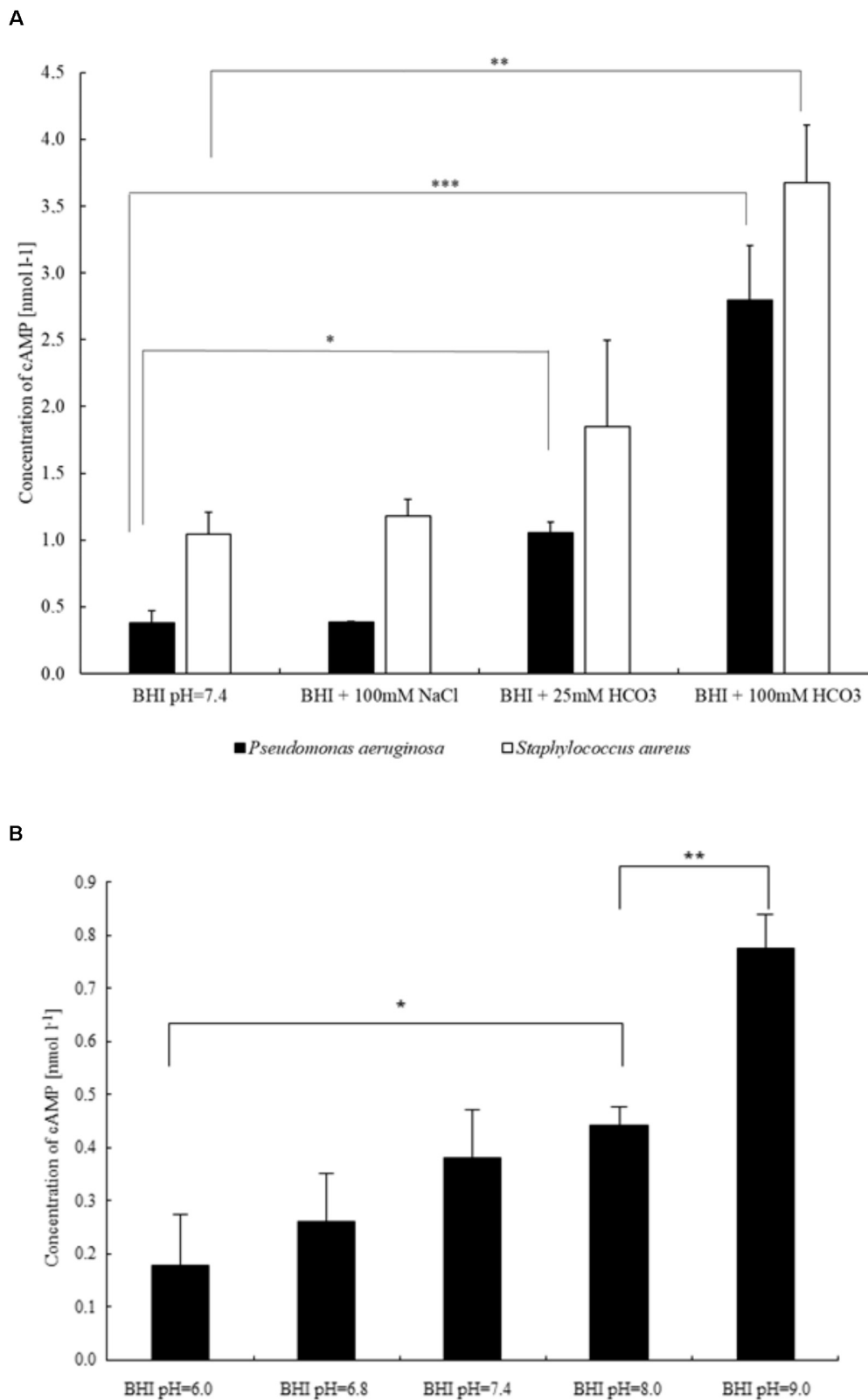


FIGURE 5 | Differences in intracellular cAMP production of bacteria influenced by **(A)** sodium chloride and two different concentrations of sodium bicarbonate (*P. aeruginosa* and *S. aureus*), and **(B)** external pH (*P. aeruginosa*). * $P < 0.05$, ** $P < 0.01$, *** $P < 0.001$.

growth *S. aureus* decreased, whereas *P. aeruginosa* increased the pH of the medium. These data suggest that HCO_3^- , rather than pH shifts, suppressed bacterial growth. In *P. aeruginosa* these observations were confirmed in HCO_3^- -containing media without CO_2 equilibration where despite the increase in the pH of the media, the growth rate was similar to that detected with CO_2 equilibration. Extending the incubation to 24 h clearly demonstrated that the effects of HCO_3^- were bacteriostatic rather than bactericidal. Furthermore, in the absence of CO_2 a critically high pH (>9.2) occurred with a reduced growth rate.

Recurrent lung infections caused by long-term colonization of biofilm-forming bacteria are a significant threat for CF patients (Høiby et al., 2017). Importantly, NaHCO_3 disrupts oral biofilms *in vitro* (Pratten et al., 2016). NaHCO_3 in combination with sodium metaperiodate and sodium dodecyl sulfate also suppressed the formation of *P. aeruginosa* biofilms (Gawande et al., 2008). We also confirmed these observations as NaHCO_3 prevented biofilm formation at 100 mmol l^{-1} and inhibited the planktonic growth of bacteria. Since the administration of equimolar NaCl (100 mmol l^{-1}) had no effect and lower concentrations of NaHCO_3 only partially blocked biofilm formation, we concluded that in our experimental model HCO_3^- suppresses bacterial conversion to biofilms as a function of concentration. These observations may be therapeutically promising as our unpublished data suggest that 100 mmol l^{-1} NaHCO_3 does not have toxic effects on airway epithelial cells *in vitro*.

Biofilm formation requires coordination between cAMP and c-di-GMP signaling in several bacteria. In *P. aeruginosa* increased levels of c-di-GMP suppress signaling from the cAMP-virulence factor regulator pathway and the expression of virulence factors that favor a persistent biofilm state (Almblad et al., 2015). On the other hand, cAMP stimulates the production of acute virulence factors, but inhibits biofilm formation in *Vibrio cholerae* (McDonough and Rodriguez, 2011). Likewise, HCO_3^- also activates virulence gene expression in *V. cholerae* (Iwanaga and Yamamoto, 1985; Abuaita and Withey, 2009). In the intestinal lumen, HCO_3^- apparently suppresses the bile-mediated induction of c-di-GMP that inhibits biofilm formation (Koestler and Waters, 2014b). Based on the above observations, we speculated that HCO_3^- should increase bacterial cAMP levels. In fact, our data show that NaHCO_3 stimulates intracellular cAMP concentrations in both *P. aeruginosa* and *S. aureus*. The stimulatory effect was not observed in the presence of equivalent NaCl concentrations indicating a specific role for HCO_3^- . Interestingly, however, cAMP production was dependent on external pH in the range between 6.0 and 9.0. These results are consistent with the findings that sAC is regulated by various environmental signals such as calcium and $\text{CO}_2/\text{HCO}_3^-/\text{pH}$ (McDonough and Rodriguez, 2011; Rahman et al., 2013). Chen et al. (2000) previously demonstrated that sAC functions as a HCO_3^- sensor in many biological systems. More recently, HCO_3^- has been shown to increase cAMP production via sAC stimulation in corals (Barott et al., 2013). Thus, we surmise that reduced HCO_3^- secretion from CF lung epithelial cells results in decreased luminal pH, which leads to decreased levels of cAMP production in bacterial cells. Low bacterial cAMP

levels reduce virulence factor production, and thus, fail to alert the innate host immune systems, allowing for more favorable conditions for biofilm formation. Parallel to these events, elevated concentrations of c-di-GMP may also support biofilm formation, making eradication of bacteria from the airways difficult.

CONCLUSION

Since we found that increased HCO_3^- impedes the growth and biofilm formation of several pulmonary bacterial pathogens, we expect that increasing HCO_3^- in the airways may reduce infection, inflammation, and a consequent tissue damage in the lungs. We assume that the inhalation of aerosolized HCO_3^- could prove therapeutic against bacteria such as *S. aureus* and *P. aeruginosa*, which are among the most relevant pathogens in lung infections in CF. Although inhalation therapy is inherently episodic and therefore the concentration of HCO_3^- on the airways is certain to dissipate between inhalation intervals, the therapy may offer significant benefits even with only acute changes in the airway surface liquid composition by depressing bacterial growth repetitively and by increasing the ability of the innate immune system to reduce or clear the infection load. However, caution should be taken with treatments that may affect intracellular cAMP levels because increasing cAMP may enhance the expression of virulence factors and lead to acute exacerbation in CF patients with chronic bacterial infections (Coggan and Wolfgang, 2012). Routinely, CF patients are treated repeatedly with different courses of antibiotics in spite of growing concerns over antibiotic side effects. Although antagonistic effects of HCO_3^- have been reported for tobramycin efficacy (Kaushik et al., 2016), our unpublished preliminary data suggest that the efficacy of both erythromycin and imipenem increases in an alkaline environment. Based on these observations, HCO_3^- , inhaled regularly, may reduce use of antibiotics.

AUTHOR CONTRIBUTIONS

OD, KL, BS, AK, BB, AT, SK, PJ, KR, and ÁZ were involved in lab experiments. PQ, ÁZ, and DO designed the study. ÁZ, DO, KL, and BS analyzed the data. ÁZ wrote the manuscript. PQ reviewed and critically revised the manuscript.

FUNDING

This work was supported by the Hungarian National Scientific Research Fund (Grant No. OTKA K108631) and by the Hungarian Human Resources Development Operational Program (Grant No. EFOP-3.6.2-16-2017-00006).

ACKNOWLEDGMENTS

We thank Dr. Katalin Kristóf for providing clinical bacterial isolates.

REFERENCES

- Abou Alaiwa, M. H., Reznikov, L. R., Gansemer, N. D., Sheets, K. A., Horswill, A. R., Stoltz, D. A., et al. (2014). pH modulates the activity and synergism of the airway surface liquid antimicrobials β -defensin-3 and LL-37. *Proc. Natl. Acad. Sci. U.S.A.* 111, 18703–18708. doi: 10.1073/pnas.1422091112
- Abuaita, B. H., and Withey, J. H. (2009). Bicarbonate induces *Vibrio cholerae* virulence gene expression by enhancing ToxT activity. *Infect. Immun.* 77, 4111–4120. doi: 10.1128/IAI.00409-09
- Almblad, H., Harrison, J. J., Rybtke, M., Groizeleau, J., Givskov, M., Parsek, M. R., et al. (2015). The cyclic AMP-Vfr signaling pathway in *Pseudomonas aeruginosa* is inhibited by cyclic di-GMP. *J. Bacteriol.* 197, 2190–2200. doi: 10.1128/JB.00193-15
- Barott, K. L., Helman, Y., Haramaty, L., Barron, M. E., Hess, K. C., Buck, J., et al. (2013). High adenylyl cyclase activity and in vivo cAMP fluctuations in corals suggest central physiological role. *Sci. Rep.* 3:1379. doi: 10.1038/srep01379
- Birket, S. E., Chu, K. K., Liu, L., Houser, G. H., Diephuis, B. J., Wilsterman, E. J., et al. (2014). A functional anatomic defect of the cystic fibrosis airway. *Am. J. Respir. Crit. Care Med.* 190, 421–432. doi: 10.1164/rccm.201404-0670OC
- Bosse, G. M. (1994). Nebulized sodium bicarbonate in the treatment of chlorine gas inhalation. *J. Toxicol. Clin. Toxicol.* 32, 233–241. doi: 10.3109/15563659409017956
- Chen, Y., Cann, M. J., Litvin, T. N., Iourgenko, V., Sinclair, M. L., Levin, L. R., et al. (2000). Soluble adenylyl cyclase as an evolutionarily conserved bicarbonate sensor. *Science* 289, 625–628. doi: 10.1126/science.289.5479.625
- Coggan, K. A., and Wolfgang, M. C. (2012). Global regulatory pathways and cross-talk control *Pseudomonas aeruginosa* environmental lifestyle and virulence phenotype. *Curr. Issues Mol. Biol.* 14, 47–70.
- Dorschner, R. A., Lopez-Garcia, B., Peschel, A., Kraus, D., Morikawa, K., Nizet, V., et al. (2006). The mammalian ionic environment dictates microbial susceptibility to antimicrobial defense peptides. *FASEB J.* 20, 35–42. doi: 10.1096/fj.05-4406com
- Drake, D. R., Vargas, K., Cardenzana, A., and Srikantha, R. (1995). Enhanced bactericidal activity of arm and hammer dental care. *Am. J. Dent.* 8, 308–312.
- Garcia, M. A., Yang, N., and Quinton, P. M. (2009). Normal mouse intestinal mucus release requires cystic fibrosis transmembrane regulator-dependent bicarbonate secretion. *J. Clin. Invest.* 119, 2613–2622. doi: 10.1172/JCI38662
- Gawande, P. V., LoVetri, K., Yakandawala, N., Romeo, T., Zhanel, G. G., Cvitkovitch, D. G., et al. (2008). Antibiofilm activity of sodium bicarbonate, sodium metaperiodate and SDS combination against dental unit waterline-associated bacteria and yeast. *J. Appl. Microbiol.* 105, 986–992. doi: 10.1111/j.1365-2672.2008.03823.x
- Gustafsson, J. K., Ermund, A., Ambort, D., Johansson, M. E., Nilsson, H. E., Thorell, K., et al. (2012). Bicarbonate and functional CFTR channel are required for proper mucin secretion and link cystic fibrosis with its mucus phenotype. *J. Exp. Med.* 209, 1263–1272. doi: 10.1084/jem.20120562
- Hammer, A., Hodgson, D. R., and Cann, M. J. (2006). Regulation of prokaryotic adenylyl cyclases by CO₂. *Biochem. J.* 396, 215–218. doi: 10.1042/BJ20060372
- Hoffman, L. R., and Ramsey, B. W. (2013). Cystic fibrosis therapeutics: the road ahead. *Chest* 143, 207–213. doi: 10.1378/chest.12-1639
- Høiby, N., Bjørnsholt, T., Moser, C., Jensen, P., Kolpen, M., Qvist, T., et al. (2017). Diagnosis of biofilm infections in cystic fibrosis patients. *APMIS* 125, 339–343. doi: 10.1111/apm.12689
- Horváth, A., Dobay, O., Kardos, S., Ghidán, Á., Tóth, Á., Pászti, J., et al. (2012). Varying fitness cost associated with resistance to fluoroquinolones governs clonal dynamic of methicillin-resistant *Staphylococcus aureus*. *Eur. J. Clin. Microbiol. Infect. Dis.* 31, 2029–2036. doi: 10.1007/s10096-011-1536-z
- Huynh, T. T., McDougald, D., Klebensberger, J., Al Qarni, B., Barraud, N., Rice, S. A., et al. (2012). Glucose starvation-induced dispersal of *Pseudomonas aeruginosa* biofilms is cAMP and energy dependent. *PLoS One* 7:e42874. doi: 10.1371/journal.pone.0042874
- Iwanaga, M., and Yamamoto, K. (1985). New medium for the production of cholera toxin by *Vibrio cholerae* O1 biotype El Tor. *J. Clin. Microbiol.* 22, 405–408.
- Kaushik, K. S., Stolhandske, J., Shindell, O., Smyth, H. D., and Gordon, V. D. (2016). Tobramycin and bicarbonate synergise to kill planktonic *Pseudomonas aeruginosa*, but antagonise to promote biofilm survival. *NPJ Biofilms Microbiomes* 2:16006. doi: 10.1038/nnpjbiofilms.2016.6
- Koestler, B. J., and Waters, C. M. (2014a). Bile acids and bicarbonate inversely regulate intracellular cyclic di-GMP in *Vibrio cholerae*. *Infect. Immun.* 82, 3002–3014. doi: 10.1128/IAI.01664-14
- Koestler, B. J., and Waters, C. M. (2014b). Intestinal GPS: bile and bicarbonate control cyclic di-GMP to provide *Vibrio cholerae* spatial cues within the small intestine. *Gut Microbes* 5, 775–780. doi: 10.4161/19490976.2014.985989
- Lee, M. C., Penland, C. M., Widdicombe, J. H., and Wine, J. J. (1998). Evidence that Calu-3 human airway cells secrete bicarbonate. *Am. J. Physiol.* 274, L450–L453. doi: 10.1152/ajplung.1998.274.3.L450
- Li, X., Tang, X. X., Vargas Buonfiglio, L. G., Comellas, A. P., Thornell, I. M., Ramachandran, S., et al. (2016). Electrolyte transport properties in distal small airways from cystic fibrosis pigs with implications for host defense. *Am. J. Physiol. Lung Cell. Mol. Physiol.* 310, L670–L679. doi: 10.1152/ajplung.00422.2015
- Linsdell, P., Tabcharani, J. A., Rommens, J. M., Hou, Y. X., Chang, X. B., Tsui, L. C., et al. (1997). Permeability of wild-type and mutant cystic fibrosis transmembrane conductance regulator chloride channels to polyatomic anions. *J. Gen. Physiol.* 110, 355–364. doi: 10.1085/jgp.110.4.355
- Mall, M. A., and Hartl, D. (2014). CFTR: cystic fibrosis and beyond. *Eur. Respir. J.* 44, 1042–1054. doi: 10.1183/09031936.00228013
- Maurer, L. M., Yohannes, E., Bondurant, S. S., Radmacher, M., and Slonczewski, J. L. (2005). pH regulates genes for flagellar motility, catabolism, and oxidative stress in *Escherichia coli* K-12. *J. Bacteriol.* 187, 304–319. doi: 10.1128/JB.187.1.304-319.2005
- McDonough, K. A., and Rodriguez, A. (2011). The myriad roles of cyclic AMP in microbial pathogens: from signal to sword. *Nat. Rev. Microbiol.* 10, 27–38. doi: 10.1038/nrmicro2688
- Merritt, J. H., Kadouri, D. E., and O'Toole, G. A. (2011). Growing and analyzing static biofilms. *Curr. Protoc. Microbiol.* S22, 1B.1.1–1B.1.17. doi: 10.1002/9780471729259.mc01b01s22
- Montgomerie, J. Z., Kalmanson, G. M., Hubert, E. G., and Guze, L. B. (1972). Osmotic stability and sodium and potassium content of L-forms of *Streptococcus faecalis*. *J. Bacteriol.* 110, 624–627.
- Newbrun, J. R., Hoover, C. I., and Ryder, M. I. (1984). Bactericidal action of bicarbonate ion on selected periodontal pathogenic microorganisms. *J. Periodontol.* 55, 658–667. doi: 10.1902/jop.1984.55.11.658
- Padan, E., Bibi, E., Ito, M., and Krulwich, T. A. (2005). Alkaline pH homeostasis in bacteria: new insights. *Biochim. Biophys. Acta* 1717, 67–88. doi: 10.1016/j.bbame.2005.09.010
- Pezzulo, A. A., Tang, X. X., Hoegger, M. J., Abou Alaiwa, M. H., Ramachandran, S., Moninger, T. O., et al. (2012). Reduced airway surface pH impairs bacterial killing in the porcine cystic fibrosis lung. *Nature* 487, 109–113. doi: 10.1038/nature11130
- Pratten, J., Wiecek, J., Mordan, N., Lomax, A., Patel, N., Spratt, D., et al. (2016). Physical disruption of oral biofilms by sodium bicarbonate: an in vitro study. *Int. J. Dent. Hyg.* 14, 209–214. doi: 10.1111/idh.12162
- Quinton, P. M. (2007a). Cystic fibrosis: lessons from the sweat gland. *Physiology* 22, 212–225. doi: 10.1152/physiol.00041.2006
- Quinton, P. M. (2007b). Too much salt, too little soda: cystic fibrosis. *Acta Physiol. Sin.* 59, 397–415.
- Quinton, P. M. (2008). Cystic fibrosis: impaired bicarbonate secretion and mucoviscidosis. *Lancet* 372, 415–417. doi: 10.1016/S0140-6736(08)61162-9
- Quinton, P. M. (2010). Role of epithelial HCO₃⁻ transport in mucin secretion: lessons from cystic fibrosis. *Am. J. Physiol. Cell Physiol.* 299, C1222–C1233. doi: 10.1152/ajpcell.00362.2010
- Rahman, N., Buck, J., and Levin, L. R. (2013). pH sensing via bicarbonate-regulated “soluble” adenylyl cyclase (sAC). *Front. Physiol.* 4:343. doi: 10.3389/fphys.2013.00343
- Reddy, M. M., and Quinton, P. M. (2003). Control of dynamic CFTR selectivity by glutamate and ATP in epithelial cells. *Nature* 423, 756–760. doi: 10.1038/nature01694
- Riordan, J. R., Rommens, J. M., Kerem, B. S., Alon, N., Rozmahel, R., Grzelczak, Z., et al. (1989). Identification of the cystic fibrosis gene: cloning and characterization of complementary DNA. *Science* 245, 1066–1073. doi: 10.1126/science.2475911
- Rogers, G. B., Hoffman, L. R., and Doering, G. (2011). Novel concepts in evaluating antimicrobial therapy for bacterial lung infections in patients with cystic fibrosis. *J. Cyst. Fibros.* 10, 387–400. doi: 10.1016/j.jcf.2011.06.014

- Rutala, W. A., Barbee, S. L., Aguiar, N. C., Sobsey, M. D., and Weber, D. J. (2000). Antimicrobial activity of home disinfectants and natural products against potential human pathogens. *Infect. Control Hosp. Epidemiol.* 21, 33–38. doi: 10.1086/501694
- Shah, V. S., Ernst, S., Tang, X. X., Karp, P. H., Parker, C. P., Ostedgaard, L. S., et al. (2016a). Relationships among CFTR expression, HCO₃⁻ secretion, and host defense may inform gene- and cell-based cystic fibrosis therapies. *Proc. Natl. Acad. Sci. U.S.A.* 113, 5382–5387. doi: 10.1073/pnas.1604905113
- Shah, V. S., Meyerholz, D. K., Tang, X. X., Reznikov, L. R., Abou Alaiwa, M. H., Ernst, S. E., et al. (2016b). Airway acidification initiates host defense abnormalities in cystic fibrosis mice. *Science* 351, 503–507. doi: 10.1126/science.aad5589
- Shamsuddin, A. K., and Quinton, P. M. (2014). Native small airways secrete bicarbonate. *Am. J. Respir. Cell. Mol. Biol.* 50, 796–804. doi: 10.1165/rcmb.2013-0418OC
- Stewart, P. S., and Costerton, J. W. (2001). Antibiotic resistance of bacteria in biofilms. *Lancet* 358, 135–138. doi: 10.1016/S0140-6736(01)05321-1
- Story, D. A. (2004). Bench-to-bedside review: a brief history of clinical acid-base. *Crit. Care* 8, 253–258. doi: 10.1186/cc2861
- Tang, X. X., Fok, K. L., Chen, H., Chan, K. S., Tsang, L. L., Rowlands, D. K., et al. (2012). Lymphocyte CFTR promotes epithelial bicarbonate secretion for bacterial killing. *J. Cell. Physiol.* 227, 3887–3894. doi: 10.1002/jcp.24101
- Thompson, K. D., Welykyj, S., and Massa, M. C. (1993). Antibacterial activity of lidocaine in combination with a bicarbonate buffer. *J. Dermatol. Surg. Oncol.* 19, 216–220. doi: 10.1111/j.1524-4725.1993.tb00339.x
- Valentini, M., and Filloux, A. (2016). Biofilms and cyclic di-GMP (c-di-GMP) signaling: lessons from *Pseudomonas aeruginosa* and other bacteria. *J. Biol. Chem.* 291, 12547–12555. doi: 10.1074/jbc.R115.711507
- Vanhautehem, D., Janssens, G. P., Lauwaerts, A., Sys, S., Boyen, F., Cox, E., et al. (2013). Exposure to the proton scavenger glycine under alkaline conditions induces *Escherichia coli* viability loss. *PLoS One* 8:e60328. doi: 10.1371/journal.pone.0060328
- Venkatesan, N., Perumal, G., and Doble, M. (2015). Bacterial resistance in biofilm-associated bacteria. *Future Microbiol.* 10, 1743–1750. doi: 10.2217/fmb.15.69
- Xie, C., Tang, X., Xu, W., Diaio, R., Cai, Z., and Chan, H. C. (2010). A host defense mechanism involving CFTR-mediated bicarbonate secretion in bacterial prostatitis. *PLoS One* 5:e15255. doi: 10.1371/journal.pone.0015255

Conflict of Interest Statement: The authors declare that the research was conducted in the absence of any commercial or financial relationships that could be construed as a potential conflict of interest.

Copyright © 2018 Dobay, Laub, Stercz, Kéri, Balázs, Tóthpál, Kardos, Jaikumpun, Ruksakiet, Quinton and Zsembery. This is an open-access article distributed under the terms of the Creative Commons Attribution License (CC BY). The use, distribution or reproduction in other forums is permitted, provided the original author(s) and the copyright owner(s) are credited and that the original publication in this journal is cited, in accordance with accepted academic practice. No use, distribution or reproduction is permitted which does not comply with these terms.